Aspects of Perturbative Open String Field Theory and Models of Antigravity Backgrounds

Albin James

▶ **To cite this version:**

Albin James. Aspects of Perturbative Open String Field Theory and Models of Antigravity Backgrounds. High Energy Physics - Theory [hep-th]. University of Southern California, Los Angeles, 2017. English. NNT : . tel-02139928

HAL Id: tel-02139928
https://hal.science/tel-02139928v1

Submitted on 26 May 2019

HAL is a multi-disciplinary open access archive for the deposit and dissemination of scientific research documents, whether they are published or not. The documents may come from teaching and research institutions in France or abroad, or from public or private research centers.

L'archive ouverte pluridisciplinaire **HAL**, est destinée au dépôt et à la diffusion de documents scientifiques de niveau recherche, publiés ou non, émanant des établissements d'enseignement et de recherche français ou étrangers, des laboratoires publics ou privés.

Aspects of Perturbative Open String Field Theory and Models of Antigravity Backgrounds

by
Albin James
University of Southern California,
Los Angeles, CA 90089, USA

A dissertation presented to the
University of Southern California Graduate School
in partial fulfillment of the
requirements for the degree of
Doctor of Philosophy, Physics

Committee Members: Prof. Stephan Haas (Chair)
Prof. Itzhak Bars
Prof. Nicholas Warner
Prof. Clifford Johnson
Prof. Fedor Malikov

Date of defence: 5th Dec 2017

Abstract

This thesis examines two aspects of gauge field theories: The first concerns the perturbative structure of bosonic open string field theory at the one-loop level, and the second considers geodesical completion of Einstein gravity with a local scale symmetry, predicting the existence of spacetime regions beyond singularities where gravity is repulsive.

In the first part, we evaluate the ghost contribution to the one-loop integrands in open string field theory (OSFT) using the Moyal representation of the star product. We primarily focus on the open string tadpole integrand, which is an intrinsically off-shell quantity. Due to the closed string tachyon, the full amplitude is badly divergent from the closed string degeneration region $t \to 0^+$ of the Schwinger parameter. We obtain expansions for the finite factors from the squeezed state matrix $\mathbf{R}(t)$ characterizing the pure ghost part of the tadpole in Siegel gauge. We demonstrate that the analytic structure of the integrands in the Moyal approach, as a function of the Schwinger parameter, captures the correct linear order behaviour near both the closed and open string degeneration limits. Using a geometric series for the matrix inverse, we obtain successive approximations for the even parity matrix elements. We employ an expansion based on results from the oscillator basis to construct Padé approximants to further analyse hints of non-analyticity near this limit. We also briefly discuss the evaluation of ghost integrands for the four string diagrams contributing to the one-loop 2-point function in OSFT.

In the second part of this thesis, we look at the scenario where the effective gravitational coupling becomes negative beyond singularities, starting from a local scale (Weyl) symmetric theory of gravity. This relative negative sign has non-trivial consequences for the dynamics of fields and particles propagating in these geometries. The resulting negative energy is unfamiliar and requires interpretation. As a first step in studying this issue, we consider Hamiltonians for particles, fields and strings whose kinetic terms flip signs in a non-analytic manner owing to a $\mathrm{sgn}(|x^0| - \Delta/2)$ factor. We show that the models capture the essential physics of such backgrounds: The new physics is primarily encoded in the structure of the propagator and the transition amplitudes, which we show are regular and have no physical problems. We thus resolve some important consistency questions pertaining to system stability. Lastly, we probe the modified Schwarzschild geometry where the beyond singularity region comprises antigravity. We show that one can connect geodesics across the spacelike singularity and then describe the radial trajectories in terms of the global Kruskal-Szekeres parametrization.

Acknowledgements

I am grateful to my advisor Prof. Itzhak Bars for his guidance and wish to thank him for sharing his knowledge of the subject and his willingness to devote his time and energy toward helping me. I also appreciate the warmth and deep friendliness he offered me, and for having me over for Thanksgiving dinners with his wonderful family. I wish to express my gratitude to the committee chair Prof. Stephan Haas and other members for their willingness. I also thank the faculty members of the high energy theory group Profs. Nicholas Warner, Krzysztof Pilch, Clifford Johnson, and Dennis Nemeschansky for their expertise and enthusiasm for the discipline. I wish to thank the laboratory director Dr. Gökhan Esirgen for his kindness, and the staff members Betty Byers and Mary Beth Hicks for their kind assistance during the programme.

I was fortunate to be around many friendly folks in my group and I wish to thank Dr. Ignacio Araya, Dr. Scott MacDonald, Alexander Tyukov, Robert Walker, and all the current and past students whom I have interacted with. I also thank my bestie from afar, Dr. Anirudh Kulkarni, for gentle encouragements, guidance, and for his patience and insights. I wish to thank my colleagues I have met at workshops and schools, especially Dr. Toru Masuda san and Dr. Hiroaki Matsunaga kun for inspiration. I am happy to thank my friends at Vidushak improv group at USC for some fond memories.

I must express my deep sense of gratitude to my parents James Skaria and Mollykutty V. M. and to my sister Dr. Joice James for their loving-kindness and affection. My parents have been the bedrock of support during every step of my academic journey and am indebted to them for their sacrifices, thoughtfulness, prayers, and strong encouragements at the expense of their time and energy. I feel thankful for their unwavering support combined with their sense of humour that lifted me up and kept me going during hardships. Finally, I also take this opportunity to thank all my well-wishers and past teachers.

Contents

List of Figures

To Appa and Amma. . . .

Overview

This thesis consists of two parts. Gauge symmetry is a common thread that ties together the structures arising in both discussions. This has been a guiding principle of fundamental importance in theoretical physics for several decades. Our current understanding of particle physics and gravity can be to a large extent uniquely determined by the requirement of gauge symmetries. The resulting consistency conditions at the quantum level put severe restrictions on the admissible mathematical structures; the Standard Model and Einstein gravity keep getting verified at particle accelerators such as the LHC, and through astrophysical observations. The spell of the gauge principle [1] continues to be felt also in the unified framework furnished by superstring theories. The present work [2–4] has attempted to expand our understanding of two such facets of gauge field theories.

The first part examines the one-loop structure of open string field theory (OSFT)—which possesses a huge spacetime gauge symmetry at the classical level. We study the integrands for the one-loop corrections to the tadpole and the string propagator using the Moyal representation of the $*$ (star) product, and demonstrate its utility [2] in improving upon the existing results from the oscillator and Boundary Conformal Field Theory (BCFT) methods. Since the loop amplitudes in OSFT necessarily receive contributions from internal propagation of closed string states, they can serve as useful probes of closed string physics. The second part is devoted to an exploration of the possible consequences of a modification of general relativity augmented with a local scale (Weyl) symmetry, that is motivated from gauge symmetries in phase space. It tests some simple models for studying the effects of antigravity and dynamical string tension, and addresses the question of negative kinetic energy [3] and geodesics [4] in blackhole backgrounds.

We begin part I with a review of OSFT and a summary of our results that provide context for the discussions that follow. The original work done in this dissertation from [2] is presented next, where we use an algebraic method in terms of explicit matrix representations to evaluate the one-loop integrands in the Moyal representation, while focussing on the ghost sector. We develop methods to successively approximate the resulting squeezed state matrix using a geometric series. We also perform several consistency checks and manage to extract algebraic data using analytical and numerical methods.

In part II, we set forth with a description of the aforementioned modification to general relativity in order to complete it geodesically. As a first step in studying implications of negative energy states for geometrical backgrounds, we examine some models where the

kinetic term switches signs discontinuously. It is conceivable that these serve as models for more physical systems which involve curvature singularities of the cosmological type or more localized ones from the black hole family, in this reformulated theory. Next, we describe radial geodesics in the modified Schwarzschild background that connect the gravity and the antigravity patches.

We conclude each part with a summary of the results and avenues for future research. Chapters are in part verbatim reproduction of the content from the work in [2–4]; nonetheless, any oversights may be solely ascribed to the author.

Part I

Moyal Structures in Open String Field Theory at the One-Loop Level

Chapter 1

Introduction and summary

Superstring theories seek to provide a quantum mechanically consistent framework for understanding the fundamental interactions in nature. The unification of the Standard Model forces with gravity necessitates the study of these one-dimensional extended objects—which can be closed or open—and all the consistency requirements emanating from them. These theories can be studied in the first quantized approach as a perturbative expansion for the string S-matrix involving various asymptotic states (represented by the so called vertex operators). Powerful Riemann surface techniques in the language of two dimensional superconformal field theory [5] have been exploited to expand our knowledge of superstring perturbation theory.

Since the days of the dual resonance models in the 1970s it has been known that closed string states (Pomeranchukons) are a necessary ingredient (see Ref. [6] and references therein) of open string theories for insuring (perturbative) unitarity, factorization, etc. The existence of graviton states has by now been firmly established with the direct detection of the gravitational wave signal GW150914 [7] by LIGO, which was followed by several other detections. Since the worldsheet path integral of superstring theory is currently the only machinery that computes a sensible S-matrix involving gravitons, which are described by closed string excitations, it is perennially important that we learn as much about the structures underlying this theory.

String field theories provide an off-shell formulation of string theory that is conceptually simple and very similar in structure to conventional gauge field theories. By construction [8–11], these furnish a field theory of strings with a spacetime action, and aspire to describe different regions of the parameter space of string theory using a universal set of degrees of freedom, encoded in the string field $|\Phi\rangle$. They thus provide a more conservative route to the problem of quantum string vacua, which being a second quantized formulation allows for understanding such off-shell string physics. The best understood covariant string field theory is the bosonic open string field theory (OSFT) with Witten type [8] cubic vertices. Remarkably, starting from a few axioms, this OSFT defines an interacting theory for an *infinite* number of fields by virtue of the underlying worldsheet conformal symmetry—which is closely tied to its spacetime gauge invariance.

In this first part, we revisit the perturbative structure of OSFT [12–16] at the one-loop level, with only one or two external states. Since the loop amplitudes receive contributions from internal propagation of closed strings, they can serve as useful probes of closed string physics. This requires evaluating the one-loop 1-point function (tadpole) and the one-loop 2-point function (string propagator). The latter receives contributions from four diagrams—three planar and one non-planar—due to the rigid nature of the Witten vertex. We have made analytical and numerical progress primarily on the ghost sector contribution to the tadpole integrand, which also appears as a subdiagram in two of the planar one-loop 2-point functions, and is an intrinsically off-shell quantity.

In [14], Ellwood et al. carry out a careful study of the (open string) tadpole state using boundary conformal field theory (BCFT) and oscillator methods. In the Siegel gauge $b_0|\Phi\rangle = 0$ that we shall be working in, the integrand is expressible as a function of the Schwinger parameter t (the length of the propagator loop in Fig. 3.1) and exhibits essential singularities at its limiting values, namely 0 and ∞. Physically, these divergent pieces may be understood in terms of degenerating string diagrams from the boundary of moduli space [10, 13] and arise from the open string tachyon ($t \to \infty$), the closed string tachyon, and massless closed string states ($t \to 0$) propagating in the loop.

One method to study the tadpole diagram near $t = 0$ is to approximate it by using an appropriate *boundary state* $|\mathcal{B}\rangle$ in a BCFT analysis. This explicitly includes the closed string oscillators $c_n, \tilde{c}_n, b_n, \tilde{b}_n$, a_n, $\tilde{a}_n$ and can be organized into levels. The chain of conformal maps employed reproduce the correct divergence structure; we refer the interested reader to [14, §3] where the leading divergence (for the D25 brane case) was carefully derived to be:

$$|\mathcal{T}(t)\rangle \sim \frac{e^{+2\pi^2/t}}{t^6} \exp\left[-\frac{1}{2}a_n^\dagger C_{nm} a_m^\dagger - c_n^\dagger C_{nm} b_m^\dagger\right] \hat{c}_0|\hat{\Omega}\rangle. \tag{1.1}$$

Here, the ket state on the RHS is the Shapiro-Thorn closed string tachyon state that arose in the work of [13] and later analyzed in detail in [10, 14, 15] and C is the twist matrix $(-)^n\,\delta_{nm}$. As discussed in [14, appendix A] (see also [12, 17]), it also contributes to a BRST anomaly $Q_B|\mathcal{T}\rangle \neq 0$, that is also present in the bosonic OSFTs based on the lower dimensional (unstable) Dp-branes. For a generic value of the parameter t, however, the expressions could only be represented in terms of implicit line integrals (which may however be inverted numerically). See also the earlier treatment in [13] using off-shell conformal theory. Additionally, as described in [14] there is operator mixing induced by conformal transformations, since the boundary state is *not* a conformal primary, and this leads to mixing of divergences from the massless and tachyon sectors.

In the oscillator construction of the 3-vertex, using squeezed state methods for inner products [18], the state was shown to be [14, §4]

$$|\mathcal{T}\rangle = \int_0^\infty dt\, e^t \frac{\det(1-S\widetilde{X})}{(Q\det(1-S\widetilde{V}))^{13}}\ \exp\left[-\frac{1}{2}a^\dagger \mathbf{M} a^\dagger - c^\dagger \mathbf{R} b^\dagger\right]\hat{c}_0|\hat{\Omega}\rangle, \tag{1.2}$$

where the constituent matrices are expressible in terms of Neumann matrices, as we shall describe later in §2.3. The determinant and the e^t factors contribute to divergences in the $t \to 0$ and the $t \to \infty$ limits respectively. There are also additional subleading IR divergences from the massless fields. The somewhat complicated nature of the Neumann matrices makes analytic study of the matrix $\mathbf{R}(t)$ difficult; it also suffers from an order of limits issue while considering expansions around $t = 0$ (see [14, appendix B] or §2.3) which leads to factor of 2 difference for the leading term from the correct BCFT prediction.

In contrast to the above, we will use Bars's Moyal star approach [19–24, 26], which a very different formulation of string field theory, as the only method of computation. Although Witten's formulation of OSFT is very elegant and only requires a cubic interaction, explicit calculations are made difficult by the somewhat complicated structure of the 3-string vertex that encodes the gluing condition of strings. By choosing a convenient diagonal basis (x_{2n}, p_{2n}), with $n = 1, 2, 3, \cdots$, for the degrees of freedom (matter + ghosts), Bars's formalism redefines the interactions in terms of the simple "Moyal product" [19, 25] between string fields. The string field is then valued in the noncommutative space defined by the direct product of the Moyal planes $\xi_i \coloneqq (x_2, x_4, x_6, \cdots, p_2, p_4, p_6, \cdots)$ and the midpoint coordinate $\bar{x}$, and would be denoted by $A(\bar{x}, \xi)$.

The Moyal formulation presents new and alternative computational tools [20, 26] for studying OSFT and which leads to simpler manipulations. As also suggested by Ellwood et al. in [14], it would therefore be interesting to explore the analytic structure of the tadpole state in the Moyal/diagonal basis, where the interaction term simplifies.

Although the BCFT analysis in [14] reveals a lot of information about the structure of the state $|\mathcal{T}\rangle$, it is also a useful exercice to understand it purely from the open string perspective as we do in the somewhat algebraic approach here. Another motivation for our work has been to test the validity of the Moyal representation at the one-loop level by extending the off-shell tree level results [20, 21, 26] and the computation of Neumann coefficients [20, 26]. As we shall explain below, the Moyal approach of Bars provides more analytic control over the infinite matrices arising at one-loop, using which we were able to improve our understanding of the matrix $\mathbf{R}(t)$ (in (1.2) above) near the two boundaries of moduli space: $t = 0$ and $t = \infty$. In particular, we were able to demonstrate the utility of the formalism by correctly capturing the linear order behaviour (3.63) near $t = 0$, which precisely coincides with the BCFT prediction [14], without any extra factors of 2

(as happened in the oscillator case). However, we are now able to see this purely from the OSFT perspective without employing explicit closed string operators.

Since the tachyonic divergences are artefacts of the bosonic theory, we shall limit our attention in this work to the finite factors from the squeezed state matrix $\mathbf{R}(t)$ characterizing the Fock space state in the ghost sector (1.2). Its matrix elements may be extracted by taking inner products with pure ghost excited states:

$$\langle\hat{\Omega}|\hat{c}_m\hat{b}_n|\mathcal{T}(t)\rangle = -\mathbf{R}_{nm}(t) \times S_0(t), \tag{1.3}$$

where $S_0(t)$ would be a scalar piece, dependent on the Dp brane system. We will be interested in hints of non-analyticities in $\mathbf{R}_{nm}(t)$, such as the exponentially suppressed sub-leading terms from (4.23) that are expected from closed string physics. Furthermore, in Siegel gauge, it is consistent to restrict to twist even and $SU(1,1)$ singlets [27] for the test states, which translates to

$$\mathbf{R}_{2n,2m-1} = 0, \qquad m\,\mathbf{R}_{nm} = n\,\mathbf{R}_{mn}. \tag{1.4}$$

The Feynman rules in non-commutative ξ space (§2.2.4) may be used for summing over a complete set of states $e^{i\xi^\top\eta-\xi^{gh\top}\eta^{gh}}$. The evaluation in the Moyal basis then involves transforming certain coefficient matrices having substructure in terms of some simple matrices—which in turn obey a set of rather simple relations (See [20] or §2.2). This has produced alternate expressions for the integrands that we have used as the starting point for an independent analysis. The calculations are simplified due to a monoid subalgebra [20], which is significantly easier to handle in the Moyal approach than the operator algebra used in the oscillator analysis. It is noteworthy that since the matrix relations are satisfied even at finite level, we have a *consistent truncation* for numerical checks, although we lack gauge invariance and are limited to machine precision due to the size of the constituent matrices and their substructure. Since gravity is an inconvenience, we shall concern ourselves with only the flat D25 brane background.

We show that the formal expressions involving matrix inverses correctly capture the linear order behaviour near both limits $t \to 0$ and $t \to \infty$ of $\mathbf{R}(t)$. The qualitative difference near the closed string region between the Moyal and oscillator expressions is that, in case of the oscillators an intermediate matrix becomes singular but in the Moyal case the matrix becomes singular trivially due to the whole matrix vanishing. Interestingly enough, the peculiar nature of the Virasoro operator L_0 in the diagonal basis (3.9) leads to a pole-zero cancellation and results in

$$\mathbf{R}_{nm}(t) = C_{nm} - n\,C_{nm}\,t + \mathcal{O}(t^2), \tag{1.5}$$

whose linear term carries information about the conformal mappings used for the incoming external states in the BCFT prescription, and serves as a consistency check on the expansions that follow. Again, the monoid algebra renders the treatment of excited states more tractable and allows one to extend the existing (very detailed) results from the tachyon case [13], at least numerically. Somewhat surprisingly, associativity is also seen to hold to this order §3.4.

Using a geometric series, we are able to expand the matrix $\mathbf{R}(t)$ in terms of special functions owing to the simple nature of the constituent matrices. This leads to a discussion of vanishing but non-analytic contributions at $t = 0$, such as $t^k \log(t)$. By going to the continuous κ-basis, we also verify the correct linear behaviour in $q := e^{-t}$ close to zero or $t \to \infty$, that matches with the oscillator construction. In order to probe for hints of non-analyticity in the complex q plane, we use the oscillator expression (2.76) to obtain the coefficients of the general matrix element $\mathbf{R}_{nm}(q)$ till q^{18} using the *NCAlgebra* [28] package. We move onto construct the associated Padé and Borel-Padé approximants and perform various consistency checks.

Quite a lot of work (see [15, 17] and references therein) has been done to understand the one-loop structure of the theory since the work in Refs. [12–14]. An analysis was also done using open-closed string field theory of Zwiebach [29] in [14] where it was shown that it naturally incorporates the shift in the closed string background—just like in gauge field theories. In this regard, we must mention the somewhat recent work of Sachs et al. [17] where the quantum (in)consistency of OSFT has been precisely characterized in the language of QOCHA (quantum open-closed homotopy algebras).

We must also mention in passing another more recent gauge choice called the Schnabl gauge, where tree amplitudes (and loop amplitudes to some extent) simplify immensely; both the kinetic term and the interaction terms become more tractable in this conformal frame. This gauge was originally chosen while constructing the non-perturbative tachyon vacuum solution of OSFT in terms of surface states called wedge states [30]. Additionally, at the one-loop level new interesting geometrical structures arise [31] which may help with computations in the more physical open superstring field theories where the tachyon would be projected out, but the gauge structure is much more intricate.

We however continue to choose the Siegel gauge since the computational techniques are more readily available in this frame. Due to the severe divergences from the closed string tachyon (and the absence of winding states, etc. See the discussion by Okawa in [11, §5]), the Witten type OSFT is truly inconsistent at the quantum level when one starts considering loop diagrams. Hence, the quantization procedure is necessarily formal but one can hope that the divergences are just an artefact of the bosonic theory and we can still learn helpful lessons from this kind of exercices. We refer the interested reader to the seminal work of Thorn [10, 12] and the construction of quantum effective actions using the Batalin-Vilkovisky (BV) machinery [9, 12] therein. Since we have been unable

to connect our analysis to the one in terms of the effective action, we do not discuss the role of these subtle boundary contributions to the one-loop tadpole graph, which is calculated "from scratch" in the work by Thorn. See also [14, §6.3] for a discussion of the issue of gauge invariance at the one-loop level and some comments on possible mismatch with the earlier analysis [10] in the Siegel gauge.

The rest of this Part is organized as follows: In chapter 2, we first review some essential aspects of perturbative OSFT and the Moyal representation. This is followed by a description of some known results from the oscillator analysis of the tadpole and a summary of our notations for quick reference. In chapter 3, we apply the Feynman rules in Moyal space to the tadpole and present algebraic expressions for the integrand, with focus on the ghost sector. The main calculational tools would be the monoid subalgebra §2.2.3 relations (2.59) and the transformation rule for a monoid element under e^{-tL_0} operator (3.10). We shall be quite explicit throughout the discussions since we are also seeking to clarify a minor mismatch with the oscillator construction, and because most of the operations are elementary block matrix multiplications or Gaussian integrations. Next, we analyse the squeezed state matrix $\mathbf{R}(t)$ in chapter 4 using a geometric series expansion and present some illustrations of the procedure. We compare various approximation methods near limiting cases numerically. These two chapters contain the main results of this Part. Several discussions and intermediate steps may be skipped altogether and the attention be restricted to the final form of the expressions. Due to the rigid nature of the Witten vertex, we have four diagrams contributing to the 2-point function and their ghost sector is discussed briefly in chapter 5. Finally, we close this part by making some comments in relation to our results and directions for future work in chapter 6.

Chapter 2

Algebraic structure of perturbative OSFT

In this chapter, we review some essential aspects of open string field theory that provides context for the subsequent discussions and also in order to set the notations. For the general structure of the theory, we follow closely the very excellent lectures by Zwiebach and Taylor [11]. See also [11, 16] for modern developments and [10, 12, 33] for classic treatments of the subject. We shall then review the Moyal representation of the $*$ product [19, 20, 25] using which most of the calculations in this part are done. The discrete Moyal basis would be reviewed in which the joining operation of strings simplifies. The monoid subalgebra and the Feynman rules in Moyal space would be discussed which are essential for describing perturbative scattering processes in our framework, and which lead to the analytic expressions for the one-loop tadpole and the string propagator we derive in the following chapters. Next, we recall some results [14] from the closely related oscillator formalism, where alternate expressions can be written down for the physical quantities we study, and which we seek to improve upon. We close this chapter by collecting together some oft used notations and slight modifications from prior conventions for quick reference.

2.1 Gauge choice and quantization

String field theories are spacetime formulations for interacting strings that are similar in spirit to the quantum field theories. Two essential requirements demanded from such theories are that a) the kinetic term should lead to the correct physical states , and b) the interacting action must reproduce the S-matrix elements of the Polyakov first quantized string theory by providing a single cover of the associated moduli space. A very useful toy model to study is the open string field theory for bosonic strings and where these statements have been rigorously proven [32].

2.1.1 Basic ingredients of OSFT

Open string field theory is a second-quantized formulation of bosonic open string theory that has as its dynamical variable the classical *string field* Φ, which may be represented as an element of the state space of a matter-ghost boundary conformal field theory (BCFT):

$$|\Phi\rangle \in \mathcal{H}_{\text{BCFT}} = \mathcal{H}_{matter} \otimes \mathcal{H}_{ghost}, \tag{2.1}$$

and contains a component field for every state in the first quantized string Fock space. An elegant covariant formulation of this theory has been given by Witten with the following classical action:

$$S_{cl}[\Phi] = -\frac{1}{2}\langle \Phi, Q_B \Phi \rangle_{\text{bpz}} - \frac{g_o}{3}\langle \Phi, \Phi * \Phi \rangle_{\text{bpz}}, \tag{2.2}$$

which has the general structure of a Chern-Simons theory. It employs the BRST quantization procedure which ensures that the underlying worldsheet theory is physically equivalent to the one in covariant quantization. The string field may also be thought of as being valued in a graded algebra $\mathcal{A}$ which is chosen as the space of string functionals of the embedding coordinates (matter) and the reparametrization ghost field arising from fixing the worldsheet metric to conformal gauge ($\gamma_{ab} \sim \delta_{ab}$), i.e.

$$\mathcal{A} = \{\Phi[X^\mu(\sigma); c(\sigma)]\}, \tag{2.3}$$

where $\sigma \in [0, \pi]$ denotes the canonical worldsheet parameter of the open string. We shall be focussing on the ghost sector primarily and hence discuss it in more detail in §2.2.2 and appendix 3.2.1 below. Additionally, we shall take the underlying boundary conformal field theory (BCFT) to be that of the flat D25 brane theory, although OSFTs may be defined for any matter system with $c = 26$.

The basic ingredients[1] of the above action are the first-quantized BRST operator Q_B, the BPZ inner product $\langle .,. \rangle_{\text{bpz}}$ (or the $\int$ operation), and an associative but non-commutative $*$ product between the string fields subject to the following "Witten axioms":

Grading: The string fields are subject to a $\mathbb{Z}$ grading for the ghost number, G_Φ and $\mathbb{Z}_2$ for Grassmannality. The c ghost and the b anti-ghost are assigned ghost number charges of $+1$ and -1 respectively, and are Grassmann odd. The classical string field $|\Phi\rangle \in \mathcal{H}_{\text{BCFT}}$ at ghost number $+1$ and is also Grassmann odd.

Differential: The BRST operator $Q_B = \oint \frac{dz}{2\pi i} j_B(z)$ defines a map $Q_B : \Lambda^n \mapsto \Lambda^{n+1}$, i.e. it's a degree one operator under the grading. It is nilpotent: $Q_B^2 \equiv 0$, and satisfies

[1] See [9] for a precise treatment of these algebraic structures. In recent formulations that have proven useful, this would define a differential graded algebra (DGA), which encodes the maps [17]. The requirement of associativity may be relaxed to obtain a *homotopy associative algebra* or a cyclic A_∞ structure [16, 17].

the derivation property:

$$Q_B(\Phi_1 * \Phi_2) = (Q_B\Phi_1) * \Phi_2 + (-)^{G_{\Phi_1}}\Phi_1 * (Q_B\Phi_2).$$

Associativity: The binary $*$ product is assumed to satisfy: $(\Phi_1 * \Phi_2) * \Phi_3 = \Phi_1 * (\Phi_2 * \Phi_3)$.

BPZ inner product: This is an invariant, bilinear form of ghost number -3 that is graded-symmetric. In terms of the $\int$ operation it induces a map $\int : \mathcal{A} \to \mathbb{C}$ that respects the following relations: $\int Q_B\Phi = 0$, $\int \Phi = 0$ if $G_\Phi \neq +3$, and cyclicity:

$$\int \Phi_1 * \Phi_2 = (-)^{G_{\Phi_1}G_{\Phi_2}} \int \Phi_2 * \Phi_1.$$

These axioms uniquely determine the action by the requirement of extending the gauge symmetry from the free theory to the interacting case.

This field theory reproduces a single covering of the moduli space of Riemann surfaces generated by the underlying matter-ghost boundary conformal field theory (BCFT). Hence, all on-shell scattering amplitudes are guaranteed to be generated through a Feynman diagrammatic expansion. It also encodes rich non-perturbative string physics even at the classical level, as has been shown in the study of tachyon condensation [11, 30] and the computation of gauge invariant observables, called Ellwood invariants [15], for example.

Next, let us turn towards the $*$ product which is one of the central aspects of Witten's OSFT.

2.1.2 The $*$ product operation

The interaction between open strings is implemented by using the $*$ product which endows the state space $\mathcal{H}_{\text{BCFT}}$ with the structure of a non-commutative algebra [8]. For the matter functionals, this can be imagined as by imposing delta function overlap between the two halves of each string: the right half of the first string matches with the left half of the second string, as depicted in Fig. 2.1. This leads to the following connection conditions:

$$X^{(r)}(\sigma) - X^{(r-1)}(\pi - \sigma) = 0, \qquad P^{(r)}(\sigma) + P^{(r-1)}(\pi - \sigma) = 0, \tag{2.4}$$

for the matter sector and in the ghost sector:

$$c^{\pm(r)}(\sigma) + c^{\pm(r-1)}(\pi - \sigma) = 0, \qquad b^{\pm(r)}(\sigma) - b^{\pm(r-1)}(\pi - \sigma) = 0, \tag{2.5}$$

where now the parameter σ is restricted to $0 \leq \sigma \leq \pi/2$ and $r = 1, 2, 3$. See [34] (and references therein) for a careful treatment of the ghost sector and of the general N-string vertex case. It is worth mentioning that in concrete calculations, the delta

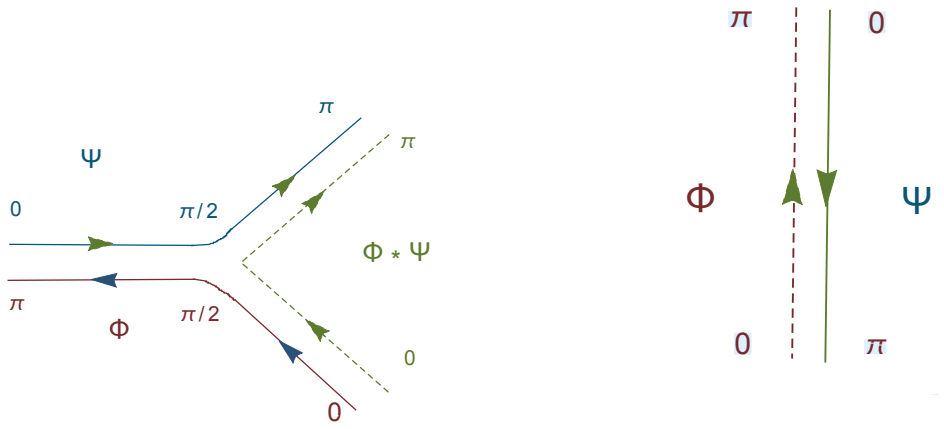

(a) (b)

Figure 2.1: (a) The Witten style gluing of two string fields Φ and Ψ to give the new string $\Phi * \Psi$. (b) The BPZ inner product or the $\int \Phi * \Psi$ operation among string fields.

function overlap above is implemented by evaluating correlation functions of the BCFT on canonical domains such as the upper half plane (UHP) where the Neumann functions may be constructed explicitly. In particular, the three half-discs corresponding to the three open string worldsheets can be glued together consistently using conformal maps discussed in [11] (See in particular Ohmori's helpful discussion in §2.3 from the set) to obtain the 3-vertex.

A wealth of information has been gained about the structure of the theory using powerful Riemann surface theory employing elegant conformal mapping techniques. To appreciate how non-trivial the construction of the interacting SFTs is, even for the bosonic open string is, it is necessary and instructive to understand the geometry of the conformal frame dictated by the underlying worldsheet theory. However in this work which focusses on the algebraic approach, it suffices to remark that since the conformal frame has a somewhat complicated geometry, it introduces non-trivial conformal factors and branch-cut structure in both the matter and the ghost sectors. This makes explicit study of the string diagrams highly non-trivial in general, especially for loop amplitudes requiring constructions involving higher genus Riemann surfaces [13].

2.1.3 Siegel gauge

From the resemblance of Witten type OSFT to the Chern-Simons action and p-forms, one can infer that the classical action in (2.2) is invariant under the following gauge

transformation, once the Witten axioms are satisfied:

$$\delta_\Lambda \Phi = Q_B \Lambda + \Phi * \Lambda - \Lambda * \Phi, \tag{2.6}$$

where Λ is a ghost number zero, Grassmann even string field. Conversely, the cubic action is the unique action allowed by extending the linear gauge symmetry ($\delta_\Lambda \Phi = Q_B \Lambda$) to the non-linear level.

Because of this huge gauge symmetry, we must first fix a gauge before deriving the Feynman rules of this theory. A venerable gauge choice is the *Siegel gauge* where the kinetic term $\langle \Phi, Q_B \Phi \rangle$ simplifies drastically. This is obtained by dictating that[2] the string field satisfies:

$$b_0 |\Phi\rangle = 0, \tag{2.7}$$

where b_0 is the anti-ghost zero mode. Then we can rewrite Φ as $\Phi = b_0 c_0 \Phi$ by virtue of the anti-commutation relation $\{b_0, c_0\} = 1$. Now, the kinetic term can be rewritten in terms of the total matter + ghost Virasoro zero mode:

$$\hat{L}_0 = \hat{L}_0^X + \hat{L}_0^{gh} \tag{2.8}$$

by making use of the relation $\{Q_B, b_0\} = L_0$ as

$$S_{\text{kin}} = \langle \Phi | \hat{c}_0 (\hat{L}_0 - 1) | \Phi \rangle \tag{2.9}$$

where we revert to the first quantized operator language for convenience. Now, one may express the propagator in terms of a Schwinger parameter as:

$$\alpha' b_0 (L_0 - 1)^{-1} = \alpha' b_0 \int_0^\infty dt\, e^t\, e^{-t L_0}, \tag{2.10}$$

where we assume that the integral exists. We can interpret the action of the operator e^{-tL_0} as to create a rectangular worldsheet strip of length t and width π, the canonical range for σ. The cubic term representing the $*$ product now results in a Riemann surface or *string configuration* constructed out of three such rectangular strips, which is flat everywhere, except for a curvature singularity at the common joining point. The external states in a given interaction can now be placed as vertex operators on the appropriate semi-infinite strips to evaluate the correlators [33]. We shall return to this procedure for OSFT perturbation theory later in §2.2.4 in the Moyal framework.

[2]This can be accomplished by a gauge transformation, at least at the linear level [10, 11].

2.2 Moyal representation of the star product

The operator formalism [34] in terms of explicit matter-ghost oscillators, $\hat{\alpha}_n^\mu, \hat{b}_n, \hat{c}_n$ for a given BCFT, provides another concrete realization of the Witten type overlap relations (in addition to the one based on worldsheet path integrals above). The correlation functions on the canonical domains are now expressed in terms of the nine Neumann matrices, which are infinite matrices derived from the *Neumann functions* for the corresponding domain. These come with state space and mode number labels. Since these are quite challenging to handle analytically, the interactions were difficult to analyze in this language for hand-calculations.

In [19] a basis for the open string degrees of freedom was introduced by Bars which diagonalizes the cubic interaction vertex, and makes the connection to non-commutative geometry as originally proposed by Witten rather manifest. The $*$ product was implemented as the Moyal product in the phase space of *even* string modes.

It is the qualitatively the same associative, non-commutative product between phase space functions for Quantum Mechanics [35] that arose in the context of deformation quantization and which coincides with the operator products, and also appears naturally in non-commutative field theories[36]. This development could also explain the spectroscopy of the Neumann matrices studied in [24]. These algebraic transformations correspond to diagonalizing the reparametrization operator K_1 (see §4.3.2) which fixes the special mid-point $\sigma = \pi/2$ or $z = +i$ (in the canonical half-disc coordinates) as may be expected from the geometric picture—this procedure in turn leads to a reduction in the effective number of Neumann matrices.

2.2.1 The discrete Moyal basis for OSFT in the matter sector

We now discuss the discrete Moyal formalism, extensively developed in [20, 22, 23, 26] by Bars et al, which will be the primary computational method used in this part. We first consider the matter sector before turning to the treatment of ghosts (which is quite similar structurally) and shall follow the discussion in [21, 26] closely. In Appendix A, we provide further background on the Moyal product in the context of a finite number of phase space coordinates.

Let us consider the mode expansion for the embedding coordinates and momenta for an open string with Neumann boundary conditions ($\partial_\sigma x^\mu|_{\sigma=0,\pi} = 0$) for a fixed worldsheet time ($\tau = 0$, say):

$$x^\mu(\sigma) = x_0^\mu + \sqrt{2}\sum_{n\in\mathbb{Z}_+} x_n^\mu \cos n\sigma, \qquad p^\mu(\sigma) = \frac{1}{\pi}\left(p_0^\mu + \sqrt{2}\sum_{n\in\mathbb{Z}_+} p_n^\mu \cos n\sigma\right), \tag{2.11}$$

where $x_0^\mu = \frac{1}{\pi}\int d\sigma\, x^\mu(\sigma)$ and p_0^μ denote the centre of mass position and momenta respectively (zero modes), and x_n^μ and p_n^μ with $n \in \mathbb{Z}_+$ correspond to the constituent Fourier modes for the excited string states. In this subsection, we shall suppress the dependence on the c ghost and the Lorentz indices (μ, ν) for simplicity.

Half-Fourier transform to Moyal space

Now, let us consider the open string field $|\Phi\rangle$ as a functional of the $x^\mu(\sigma)$ degrees of freedom, i.e. as a position space functional denoted by $\Phi(x_0, x_{2n}, x_{2n-1})$, where we have separated the even (e) and odd (o) modes. This can be made explicit by going to the oscillator representation of the position state bra $\langle x|$ and writing $\Phi(x_0, x_e, x_o) = \langle x|\Phi\rangle$ as the Fock space bra-ket product. The bra $\langle x|$ is now given in terms of the matter oscillators α_n as follows:

$$\langle x| = \langle x_0| \exp \sum_{n\geq 1} \left(\frac{1}{2\kappa_n}\alpha_n^2 + \frac{i\sqrt{2}x_n}{l_s}\alpha_n - \frac{\kappa_n}{2l_s^2} \right) \prod_{n\geq 1} \left(\frac{\kappa_n}{\pi l_s^2} \right)^{d/4}, \tag{2.12}$$

where we have denoted the oscillator frequencies by κ_n and $l_s = \sqrt{2\alpha'}$ is the string length, that would be later set to $\sqrt{2}$. As we shall discuss below, *the number of oscillators can be taken to be finite* in this framework consistent with the algebraic properties we wish to retain, and hence the sums above may be taken for a cut-off that we call $2N$. Then, the frequencies κ_n could be arbitrary functions of n instead of the usual integer values $\kappa_e = e = 2n, \kappa_o = o = 2n-1$, which we must restore while taking the open string limit $N \to \infty$.

The Moyal string field A is then obtained by taking a Fourier transform with respect to "half" of the degrees of freedom (we choose the odd modes x_o) to convert the string field $\Phi(x_0, x_e, x_o)$ defined in coordinate space to Moyal space $A(\bar{x}, x_e, p_e)$:

$$A(\bar{x}, x_e, p_e) = \det(2T)^{d/2} \prod_{o>0} \int dx_o^\mu \, \exp\left[-\frac{2i}{\theta}\eta_{\mu\nu} \sum_{e>0} p_e^\mu T_{eo} x_o^\nu \right] \Phi(x_0, x_e, x_o). \tag{2.13}$$

Here, the matrix T_{eo} expresses the relevant Fourier variables p_o in terms of new variables with even labels using a linear transformation:

$$p_o = \sum_{e>0} \frac{2}{\theta}\, p_e T_{eo}, \tag{2.14}$$

and θ is a parameter that absorbs dimensions and would be set to 1 later for convenience. The maps between the even (e) and odd (o) modded subspaces are thus implemented by

the matrices:

$$T : \mathcal{H}_o \mapsto \mathcal{H}_e, \qquad \text{and its inverse} \qquad R : \mathcal{H}_e \mapsto \mathcal{H}_o. \tag{2.15}$$

We will later discuss some of the infinite matrices related to T that arise naturally in this transformation to phase space variables.

The matrix T_{eo} with mixed labels appeared in the split string formalism (see [34, 37–39]) that was used as an intermediate step in the original derivation by Bars [19] to which we refer the reader for much more details and results. Additionally, the string field depends on the midpoint coordinate $\bar{x} \coloneqq x(\pi/2)$. This variable is related to the centre of mass variable x_0 used earlier through the mode expansions(2.11):

$$\bar{x} = x_0 - \sum_{e>0} w_e x_e \tag{2.16}$$

where the (infinite) vector w_e is another essential ingredient in the formalism. The expressions for T, R and w in the infinite and the finite (cut-off) cases are given below in (2.36), (2.38) and (2.52). These matrices will be crucial for the evaluation of string diagrams attempted in this part.

By a similar procedure, the position space basis state $\langle x|$ can be mapped to its Moyal image that we denote by:

$$\langle \bar{x}, \xi| \coloneqq \langle \bar{x}, x_e, p_e| = \langle \bar{x}|\ e^{\sum\left(\frac{\alpha_e^2}{2\kappa_e} - \frac{\alpha_o^2}{2\kappa_o}\right)} e^{-\sum_{ij}\xi_i (M_0)_{ij}\xi_j - \sum_i \xi_i \lambda_i} \det\left(4\kappa_e^{1/2} T \kappa_o^{-1/2}\right)^{d/2}, \tag{2.17}$$

where the ingredients M_0 and λ^μ are given in component form as:

$$M_0 = \begin{pmatrix} \kappa_e & 0 \\ 0 & \frac{2l_s^2}{\theta^2} T \kappa_o^{-1} T^\top \end{pmatrix}, \qquad \lambda^\mu = \begin{pmatrix} -\frac{i\sqrt{2}}{l_s}\alpha_e^\mu - i p_0^\mu w_e \\ -\frac{2\sqrt{2}l_s}{\theta}\sum_{o>0} T_{eo}\kappa_o^{-1}\alpha_o^\mu \end{pmatrix}, \tag{2.18}$$

and we have used $(\cdots)^\top$ for the matrix transpose. The phase space doublet with even labels (x_e^μ, p_e^μ) is denoted by ξ^μ i.e.

$$\xi_i^\mu = (x_2^\mu, x_4^\mu, \cdots, p_2^\mu, p_4^\mu, \cdots)^\top, \tag{2.19}$$

which we shall often use for brevity. Here, we remark that the $\langle x_0|$ appearing in (2.12) above and $\langle \bar{x}|$ are related by a translation:

$$\langle \bar{x}| = \langle x_0| \exp\left(-i p_0 \sum_{e>0} w_e x_e\right). \tag{2.20}$$

Henceforth, we shall often suppress the midpoint dependence and write $\langle \bar{x}, \xi|$ as $\langle \xi|$ for the bra defining the Moyal basis and also use p^μ for the momentum zero mode after dropping the 0 subscript. Then, the Moyal field obtained from the Fourier transform procedure

above and the Fock space state $|\Phi\rangle$ are equivalently associated by:

$$A(\xi) = \langle \xi | \Phi \rangle. \tag{2.21}$$

The $*$ product in the Moyal basis

After this change of basis, the $*$ product of Witten becomes *diagonal* in the half-phase space i.e. is applied independently for each mode label e. Additionally, the product is local in the midpoint coordinate $\bar{x}$ (and the ξ_0 variable corresponding to the b_0 dependence for the ghost sector) as is the case with the original $*$ product. This non-commutative but associative product is represented as the exponential of a differential operator defined through:

$$\boxed{(A * B)(\bar{x}, \xi) = A(\bar{x}, \xi) \exp\left[\frac{1}{2}\eta^{\mu\nu} \overleftarrow{\partial}^{i}_{\mu} \sigma_{ij} \overrightarrow{\partial}^{j}_{\nu}\right] B(\bar{x}, \xi)} \tag{2.22}$$

where the matrix σ is the off-block diagonal matrix

$$\sigma = i\theta \begin{pmatrix} \mathbb{0} & \mathbb{1}_e \\ -\mathbb{1}_e & \mathbb{0} \end{pmatrix} = -\theta \sigma_2 \otimes \mathbb{1}_e. \tag{2.23}$$

Here θ is the common non-commutativity parameter which appeared above in (2.13), σ_2 is the second Pauli matrix, and $\mathbb{1}_e$ represents the ($N \times N$ dimensional for the cut-off case) identity matrix with even labels. Let us also note the resulting canonical $*$ commutator in Moyal space:

$$[\xi^{\mu}_i, \xi^{\nu}_j]_* = \eta^{\mu\nu} \sigma_{ij}, \tag{2.24}$$

which is identical to the Heisenberg algebra.

We must emphasize here that before applying the derivatives to the string fields, *one must express the dependence on x_0 in terms of $\bar{x}$ and x_e* using (2.16) above and then carefully take the derivatives with respect to x_e, p_e.

The L_0 operator which defines the kinetic term in the Siegel gauge becomes non-diagonal in this basis and is represented by the differential operator:

$$L_0^X = \frac{1}{2}\beta_0^2 - \frac{d}{2}\,\mathrm{Tr}(\tilde{\kappa}) - \frac{1}{4} D_\xi^\top (M_0^{-1}\tilde{\kappa}) D_\xi - \xi^\top (\tilde{\kappa} M_0) \xi \tag{2.25}$$

for the matter sector. Here $\beta_0 = -il_s \dfrac{\partial}{\partial \bar{x}}, D_\xi = \left(\left(\dfrac{\partial}{\partial x_e} - i\dfrac{\beta_0}{l_s} w_e\right), \dfrac{\partial}{\partial p_e}\right)$, and the block matrices $\tilde{\kappa}$ and M_0 (identical to the one in (2.18) depend on the string spectrum κ_n through:

$$\tilde{\kappa} = \begin{pmatrix} \kappa_e & \mathbb{0} \\ \mathbb{0} & T\kappa_o R \end{pmatrix}, \qquad M_0 = \begin{pmatrix} \kappa_e & \mathbb{0} \\ \mathbb{0} & \frac{2l_s^2}{\theta^2} T \kappa_o^{-1} T^\top \end{pmatrix}. \tag{2.26}$$

The action of L_0 on Moyal fields is required for many physical applications, such as the computation of Feynman diagrams—which we outline in §2.2.4 below—for learning about the perturbative structure of OSFT.

Although the Moyal map employs infinite linear combinations in string mode space and hence is defined formally in the open string limit, it captures several aspects of the physics of OSFT including subtle contributions from the midpoint [22, 23]. It provides a concrete realization of the split-string picture [34, 37–39] while giving one prescription for treating the midpoint anomalies by providing a consistent truncation [20, 22, 26]. This regularization (briefly outlined in §2.2.3) is crucial for correctly reproducing the correct string spectrum from the one-loop vacuum amplitude [21, Eq. 47], [20, Eq. 4.20] and the 3-tachyon and 4-tachyon tree level amplitudes [20, 26]. For the reduced star product [34] in Siegel gauge, the ghost and matter Witten vertices are thus equivalent to the discrete Moyal star representation; this has also been shown from the fact that the formalism correctly reproduces the Neumann matrices (from the oscillator representation) and by making many algebraic relations among them manifest[20, 26]. It is one of the aims of this work to further test the applicability of this basis at the one-loop level when there are also external states involved.

Since we are mostly interested in the ghost contributions in this work, we have only illustrated the general idea in the matter sector—which was developed first historically, see [19, 26]. Some relevant matter contribution to the one-loop open string tadpole would be presented in Appendix B. The continuous κ basis would be briefly reviewed in §4.3.2. Another continuous basis called the σ basis which uses integral kernels was developed in [40]; see also the discussion in [19, §3] and [23, §2] concerning this basis.

Next, we move onto the ghost sector of the theory. In many calculations, it is convenient to work with fermionic ghosts instead of the bosonized ghosts (see for example, [19, 21]. This was carefully developed in [20] by Bars, Kishimoto and Matsuo, to which we refer the reader for more details. As expressed earlier in (2.5), the b anti-ghost, which is analogous to the embedding coordinate, satisfies overlapping conditions and the c ghost, which is similar to the momenta, satisfies *anti-overlapping* conditions. In terms of modes, the c ghost comes with cosine modes and the b anti-ghost comes with sine modes. Hence, we can expect some slight asymmetry between the two sets (see (2.28)) of odd Moyal coordinates (x_o, p_o) and (y_o, q_o) needed for describing the bc system.

2.2.2 The fermionic Moyal product

The bc ghost system

In the BRST formulation of the bosonic string, the worldsheet ghosts are introduced as part of the gauge-fixing procedure analogous to the Faddeev-Popov ghosts in gauge field theories. In the first quantized theory, the worldsheet ghost and the anti-ghost are

denoted by $c(z)$ and $b(z)$ respectively[3]. These are anti-commuting fields with conformal weights -1 and $+2$.

After setting the time coordinate τ of the underlying worldsheet theory to 0, we can have the mode expansion for these fields as follows:

$$b_{\pm\pm}(\sigma) = \sum_{n\in\mathbb{Z}} \hat{b}_n e^{\pm in\sigma} = \pi_c(\sigma) \mp ib(\sigma), \qquad c^{\pm}(\sigma) = \sum_{n\in\mathbb{Z}} \hat{c}_n e^{\pm in\sigma} = c(\sigma) \pm i\pi_b(\sigma). \tag{2.27}$$

Analogous to the matter sector, we can have "positions" and "momenta" linear combinations [20, §2.2] that we denote by $\hat{x}_n, \hat{p}_n, \hat{y}_n$ and $\hat{q}_n$ as follows:

$$\hat{x}_n = \frac{i}{\sqrt{2}}(\hat{b}_n - \hat{b}_{-n}), \quad \hat{p}_n = \frac{i}{\sqrt{2}}(\hat{c}_n - \hat{c}_{-n}), \quad \hat{y}_n = \frac{1}{\sqrt{2}}(\hat{c}_n + \hat{c}_{-n}), \quad \hat{q}_n = \frac{1}{\sqrt{2}}(\hat{b}_n + \hat{b}_n) \tag{2.28}$$

so that we may write:

$$\begin{aligned} b(\sigma) &= i\sqrt{2}\sum_{n\in\mathbb{Z}_+} \hat{x}_n \sin n\sigma, & \pi_b(\sigma) &= -i\sqrt{2}\sum_{n\in\mathbb{Z}_+} \hat{p}_n \sin n\sigma, \\ c(\sigma) &= \hat{c}_0 + \sqrt{2}\sum_{n\in\mathbb{Z}_+} \hat{y}_n \cos n\sigma, & \pi_c(\sigma) &= \hat{b}_0 + \sqrt{2}\sum_{n\in\mathbb{Z}_+} q_n \cos n\sigma. \end{aligned} \tag{2.29}$$

Schematically, we may represent [23] this as:

$$\begin{aligned} b \to x, \quad c \to y \oplus c_0 \\ \pi_b \to p, \quad \pi_c \to q \oplus b_0 \end{aligned} \tag{2.30}$$

After choosing the Siegel gauge, we take the physical string field to be dependent only on the c_0 mode. Here we understand that the b_0 factor has been explicitly "factored" out. By virtue of the canonical (anti-)commutation relations

$$\{\hat{c}_n, \hat{b}_m\} = \delta_{n+m,0}, \qquad n, m \in \mathbb{Z},$$

we have the corresponding structure:

$$\{\hat{x}_n, \hat{p}_m\} = \delta_{nm}, \qquad \{\hat{y}_n, \hat{q}_m\} = \delta_{nm}, \qquad \text{but now } n, m \in \mathbb{Z}_+. \tag{2.31}$$

At this point, it is essential to introduce the $SL(2,\mathbb{R})$/conformal vacuum and the associated ghost vacua constructed out of it. The conformal vacuum $|\Omega\rangle$ is the vacuum invariant under the global conformal group generated by the $L_{0,\pm}$ Virasoro generators. Because of the two ghost zero modes $\hat{c}_0$ and $\hat{b}_0$, we can have the two fold degenerate vacua $|\pm\rangle$ on

[3] We follow Polchinski conventions [41] for the bc ghost CFT.

top of this:

$$|-\rangle = \hat{c}_1|\Omega\rangle, \qquad |+\rangle = \hat{c}_0\hat{c}_1|\Omega\rangle, \tag{2.32}$$

at ghost numbers +1 and +2 respectively. One has the freedom to work with either of these two vacua and henceforth we define *states* by using the $|-\rangle$ vacuum, conventionally denoted as $|\hat{\Omega}\rangle$ or sometimes $|\hat{0}\rangle$.

From the underlying BCFT based on worldsheet path integrals, we require three ghost insertions to account for the conformal killing vectors (CKVs) for the disc (tree level) amplitudes. In the Fock space language, this translates to the additional normalization condition [4] on the vacua:

$$\langle +|-\rangle = 1 \qquad \Longleftrightarrow \qquad \langle \hat{c}_{-1}\hat{c}_0\hat{c}_1\rangle = 1. \tag{2.33}$$

Thus, in every non-vanishing inner product, it is assumed that the ghost number requirement is saturated to +3 in this form.[5]

Moyal fields

To go from the string field $|\Phi\rangle$ defined in Fock space of (b, c) ghosts to Moyal space, one performs a Fourier transform over half the number of degrees of freedom as done in the matter sector. Now, however, the x_e, y_e modes are integrated out (as opposed to the x_o matter modes earlier) resulting in a string field dependent on odd modded Moyal coordinates:

$$\begin{aligned}
&\hat{A}(\xi_0, x_o, y_o, p_o, q_o) \\
&= \int d\bar{c}\, e^{-\xi_0\bar{c}} A(\bar{c}, x_o, -p_o/\theta', y_o, -q_o/\theta') \\
&= 2^{-2N}(1 + w^\top w)^{-\frac{1}{4}} \int dc_0 \prod_{e>0}^{2N} (-i dx_e dy_e)\, e^{-\xi_0 c_0 + \xi_0 w^\top y_e + \frac{2}{\theta'} p_o S^\top x_e + \frac{2}{\theta'} q_o R y_e} \Phi(c_0, x_n, y_n),
\end{aligned} \tag{2.34}$$

where ξ_0 is a fermionic object encoding the zero mode dependence, and θ' is the common non-commutativity parameter in ghost space. the matrices T, R, S, and w would be defined below.

As explained in [20], we find that it is more convenient to work with objects having *even* labels instead of the *odd* parity elements that appear naturally in the ghost sector. This results in further similarity to the matter sector. We emphasize that these are *not*

[4] We thus set the total spacetime volume to 1 through this normalization, which may be accomplished by a toroidal compactification of all 26 bosonic coordinates, including the timelike direction. In general, for Dp branes, the tangential/longitudinal directions may be compactified.

[5] The ghost number assignments are understood to be for the vertex operators as per modern conventions.

the original even degrees of freedom but special (infinite) linear combinations:

$$\boxed{x^c_e = T_{eo} y_o, \qquad p^c_e = R^\top_{eo} q_o, \qquad x^b_e = \kappa_e^{-1} S_{eo} x_o, \text{ and} \qquad p^b_e = \kappa_e S_{eo} p_o}, \tag{2.35}$$

where

$$T_{eo} = \frac{4}{\pi}\int_0^{\frac{\pi}{2}} d\sigma\, \cos e\sigma \cos o\sigma = \frac{4o\, i^{o-e+1}}{\pi(e^2-o^2)}, \text{ and its inverse} \tag{2.36a}$$

$$R_{oe} = \frac{4}{\pi}\int_0^{\frac{\pi}{2}} d\sigma\, \cos o\sigma \left(\cos e\sigma - \cos\frac{e\pi}{2}\right) = \frac{4e^2\, i^{o-e+1}}{\pi o(e^2-o^2)}, \text{ and} \tag{2.36b}$$

$$S_{eo} = \frac{4}{\pi}\int_0^{\frac{\pi}{2}} d\sigma\, \sin e\sigma \sin o\sigma = \frac{4i^{o-e+1}e}{\pi(e^2-o^2)}, \tag{2.36c}$$

with mixed parity labels, in the open string limit $N \to \infty$. These matrices satisfy the relations:

$$T\,R = \mathbb{1}_e, \qquad R\,T = \mathbb{1}_o, \qquad S\,S^\top = \mathbb{1}_e, \qquad S^\top S = \mathbb{1}_o, \tag{2.37}$$

along with many more useful relations which we partially collect below in §2.4 and in §2.2.3. Here we remind the reader that $(\ )^\top$ refers to the matrix transpose which differs from the $(^-)$ notation used in [20]. The infinite vectors w, v are given by:

$$w_e = \sqrt{2} i^{-e+2}, \qquad v_o = \frac{2\sqrt{2} i^{o-1}}{\pi o} = \frac{1}{\sqrt{2}} T_{0o}. \tag{2.38}$$

Their finite N versions would be presented in §2.2.3 along with certain helpful algebraic properties they satisfy. See [20, §2.1.3, Appendix B] and [22] for derivations and a careful presentation of many more relations.

After this preparation, the $*$ product among string fields valued in Moyal space with even labels is implemented by the exponential of a bi-differential operator as follows:

$$\boxed{(A*B)(x^b_e, p^b_e, x^c_e, p^c_e) = A \exp\left(\frac{\theta'}{2}\sum_{e>0}\left[\frac{\overleftarrow{\partial}}{\partial x^b_e}\frac{\overrightarrow{\partial}}{\partial p^b_e} + \frac{\overleftarrow{\partial}}{\partial x^c_e}\frac{\overrightarrow{\partial}}{\partial p^c_e} + \frac{\overleftarrow{\partial}}{\partial p^b_e}\frac{\overrightarrow{\partial}}{\partial x^b_e} + \frac{\overleftarrow{\partial}}{\partial p^c_e}\frac{\overrightarrow{\partial}}{\partial x^c_e}\right]\right) B} \tag{2.39}$$

where $\overleftarrow{\partial}$ and $\overrightarrow{\partial}$ are respectively the left right and left fermionic derivatives obeying the standard anti-commutation rules, and θ' is the non-commutativity parameters for ghosts.

Metric in ghost space

In [20, 42], the ghost Moyal coordinates were combined into a single $4N \times 1$ vector $\xi^{gh} = (x^b_e, p^b_e, x^c_e, p^c_e)^\top$ for the cut-off theory. This results in a few structural differences with the matter sector, which we assume to have Lorentz symmetry. As suggested and exploited in [26], we can combine the ghost (non-zero) modes instead into the two doublet

vectors[6]

$$\xi^1 = \begin{pmatrix} x_e^b \\ -p_e^c \end{pmatrix} \qquad \text{and} \qquad \xi^2 = \begin{pmatrix} x_e^c \\ p_e^b \end{pmatrix} \tag{2.40}$$

which we denote together again by ξ^{gh}. This is done in order to use an $Sp(2)$ metric $+i\varepsilon_{ab}$ (with $\varepsilon_{12} = -1 = -\varepsilon^{12}, \varepsilon_{11} = 0 = \varepsilon_{22}$) in the (b, c) ghost phase space and to make the $SU(1,1)$ symmetry [27] [20, Appendix H] manifest whenever applicable; the metric $i\varepsilon_{ab}$ is the analogue of $\eta_{\mu\nu}$.

Since the signs and factors of i were somewhat important in our calculations, we briefly spell them out here. Under an $SO(4)$ rotation to the new basis,

$$\xi^{gh} = \begin{bmatrix} x_e^b \\ p_e^b \\ x_e^c \\ p_e^c \end{bmatrix} \to \qquad \xi^1 = \begin{bmatrix} x_e^b \\ -p_e^c \end{bmatrix}, \qquad \xi^2 = \begin{bmatrix} x_e^c \\ +p_e^b \end{bmatrix}$$

we find that the block matrices transform as:

$$\begin{aligned} &\varepsilon \otimes \alpha \to -i\varepsilon \otimes i\alpha, && \varepsilon \otimes \beta \to I_2 \otimes -\sigma_3\beta, \\ &I_2 \otimes \alpha \to I_2 \otimes \alpha, && I_2 \otimes \beta \to -i\varepsilon \otimes i\sigma_3\beta, \end{aligned} \tag{2.41}$$

where α is block diagonal and β is off block diagonal i.e.

$$\alpha = \begin{pmatrix} \alpha_1 & \mathbb{0} \\ \mathbb{0} & \alpha_2 \end{pmatrix}, \qquad \beta = \begin{pmatrix} \mathbb{0} & \beta_1 \\ \beta_2 & \mathbb{0} \end{pmatrix} \tag{2.42}$$

for $N \times N$ matrices $\alpha_1, \alpha_2, \beta_1$ and β_2, which can satisfy additional symmetry properties depending on the string configurations. The presentation now becomes slightly cleaner due to the similarity of the algebraic expressions with the matter sector, such as for the $*$ product for a monoid subalgebra (2.59) and propagator transformation rules (3.10). This makes the derivations of full matter+ghost integrands such as for the tadpole case below (3.23) a bit more straightforward than earlier.

Notice that we now have the canonical $*$ anti-commutator in the ghost Moyal plane:

$$\{\xi_i^n, \xi_j^m\}_* = -i\varepsilon^{nm}\sigma_{ij} \tag{2.43}$$

Hence, it is consistent to impose an $-i\varepsilon\otimes$ tensor product factor while defining dot products. *In all fermionic bilinears and quadratic terms, this metric factor would be understood to be present.*

[6] upto some factors from [26] we have chosen for convenience.

Expression for the Moyal basis bra $\langle \xi_0, \xi^{gh}|$

Including the ghost sector, the string field shall now be denoted by $\hat{A}(\bar{x}, \xi, \xi_0, \xi^{gh})$. Similar to the purely matter sector, the operation of going to Moyal space from the usual Fock space may also be implemented by taking an inner product with a bra $\langle \xi, \bar{x}, \xi^{gh}, \xi_0|$ defining the Moyal basis. Since the matter and ghost sectors factorize for considerations of the basis states, let us use $\langle \xi_0, \xi^{gh}|$ while restricting to the pure ghost sector and write

$$\hat{A}(\xi_0, \xi^{gh}) \coloneqq \langle \xi_0, \xi^{gh}|\Phi\rangle. \tag{2.44}$$

The result of the Fourier transform applied to the ghost "position space" basis is:

$$\langle \xi_0, \xi^{gh}| = -2^{-2N} \left(1 + w^\top w\right)^{-\frac{1}{4}} \langle \Omega|\hat{c}_{-1} e^{-\xi_0(\hat{c}_0 - \sqrt{2} w^\top \hat{c}_e)} e^{-\xi^{gh\top} M_0^{gh} \xi^{gh} - \xi^{gh\top} \lambda^{gh}}, \tag{2.45}$$

where M_0^{gh} is the analogue of M_0 above in the matter sector, and appears in the definition of the perturbative vacuum (2.61), and we have the vectors carrying $Sp(2)$ indices

$$\lambda_1^{gh} = \begin{pmatrix} \sqrt{2} R^\top \hat{b}_o \\ -2\sqrt{2}\kappa_e^{-1} \hat{b}_e + 2\kappa_e^{-1} w \xi_0 \end{pmatrix}, \qquad \lambda_2^{gh} = \begin{pmatrix} \sqrt{2} R^\top \kappa_o \hat{c}_o \\ 2\sqrt{2} i \hat{c}_e \end{pmatrix}, \tag{2.46}$$

which carries the positively modded oscillators $\hat{c}_n, \hat{b}_n$. Here we have transformed to the *even* basis the expression given in [20] by utilizing some simple algebraic relations satisfied by the relevant matrices.

In the Siegel gauge $b_0|\Phi\rangle = 0$, one can factor out the ghost zero mode dependence as $\hat{A}(\bar{x}, \xi, \xi_0, \xi^{gh}) = \xi_0 A(\bar{x}, \xi, \xi^{gh})$, and we shall often use the symbols $\langle \xi^{gh}|$ and $A(\xi^{gh})$ while referring to the ghost sector. We shall also set the non-commutativity parameters $\theta' = +1 = \theta$ by a choice of units. This sets the $2N \times 2N$ off-block diagonal matrix defined in (2.23) $\sigma = -\sigma_2 \otimes \mathbb{1}_e$, labelled by even integers. Thus, excluding the matter sector and the zero mode, we can now write the Moyal star product between two fields as:

$$\boxed{\big(A * B\big)(\xi^{gh}) = A(\xi^{gh}) \exp\left(\frac{1}{2} \frac{\overleftarrow{\partial}}{\partial \xi^{gh}} \Sigma \frac{\overrightarrow{\partial}}{\partial \xi^{gh}}\right) B(\xi^{gh}); \qquad \text{where now} \quad \Sigma \coloneqq -i\varepsilon \otimes \sigma} \tag{2.47}$$

where the matrix $\varepsilon = i\sigma_2$ in the outer product is part of the $Sp(2)$ metric above.

The trace operation

In order to discuss the string field theory action later in §2.2.4 and the normalization of string fields, we must now consider the trace operation that is analogous to the $\int$

operation in Witten's formulation. The trace[7] of the $*$ product of n Moyal string fields implements the joining of n strings and finally folding the string and gluing the half-strings. This is associated with the n string interaction vertex $|V_n\rangle$ in the Fock space language

$$\mathrm{Tr}\left(\hat{A}_1 * \cdots * \hat{A}_n\right) \sim {}_1\langle\Phi_1| \otimes \cdots \otimes {}_n\langle\Phi_n|V_n\rangle, \tag{2.49}$$

upto constant factors. This correspondence was used in the successful evaluation and study of Neumann coefficients in [20],[26, ref 1].

The trace above is simply represented as integration over Moyal (phase) space ξ, ξ^{gh} with the appropriate measure:

$$\mathrm{Tr} := \frac{\det \sigma'}{|\det(2\pi\sigma)|^{d/2}} \int (d\xi)\,(d\xi^{gh}) \tag{2.50}$$

where one can restore θ', θ for generality, by defining $\sigma' := \theta'\sigma_1 \otimes \mathbb{1}_e, \sigma = -\theta\sigma_2 \otimes \mathbb{1}_e$. It turns out that the integrals in this formalism would all be Gaussians and hence can be expressed in terms of determinants and inverse of matrices.

2.2.3 Regularization and the monoid subalgebra

Regularized matrices for finite N

A very interesting feature of the discrete Moyal basis is the consistent regularization developed in [22] by Bars and Matsuo, involving a cutoff prescription in the number of string modes $2N$ defining the phase space doublet. It allows for a *deformation of the string spectrum* from the frequencies valued in the non-negative integers, $0 \leq n < \infty$, to a sufficiently reasonable finite set[8] of frequencies κ_n, as functions of n with $1 \leq n \leq 2N$. The finite versions of the $N \times N$ matrices T, R, S and $N \times 1$ vectors w_e, v_o from (2.36) are in general dependent on all the frequencies κ_n. These are uniquely solved for by requiring that the following relations are satisfied:

$$R = \kappa_o^{-2} T^\top \kappa_e^2, \qquad R = T^\top + v w^\top, \qquad v = T^\top w, \qquad w = R^\top v \tag{2.51}$$

along with a few more general relations for the ghost sector [20]. The explicit finite forms thus obtained in [22, 26] (see also [20, Appendix B]) are given by:

$$T_{eo} = \frac{w_e v_o \kappa_o^2}{\kappa_e^2 - \kappa_o^2}, \qquad R_{oe} = \frac{w_e v_o \kappa_e^2}{\kappa_e^2 - \kappa_o^2},$$

[7] Although we do not use the zero mode dependence, it is instructive to mention the structure here in the normalization using the odd modes

$$\int d\xi_0\, \mathrm{Tr}\left(\hat{A}(\xi_0,\xi)^\dagger * \left(\frac{\partial}{\partial\xi_0} - \frac{\theta'}{2} v^\top \frac{\partial}{\partial q_0}\right) \hat{A}(\xi_0,\xi)\right) = \langle\Phi|\hat{c}_0|\Phi\rangle = 1. \tag{2.48}$$

[8] It is somewhat interesting to compare this to the spectrum of the so called fractal strings [43].

$$w_e = i^{2-e}\frac{\prod_{o'}|\kappa_e^2/\kappa_{o'}^2-1|^{\frac{1}{2}}}{\prod_{e'\neq e}|\kappa_e^2/\kappa_{e'}^2-1|^{\frac{1}{2}}}, \qquad v_o = i^{o-1}\frac{\prod_{e'}|1-\kappa_o^2/\kappa_{e'}^2|^{\frac{1}{2}}}{\prod_{o'\neq o}|1-\kappa_o^2/\kappa_{o'}^2|^{\frac{1}{2}}}. \tag{2.52}$$

in terms of the κ_n. The matrix S appearing in the ghost sector can be expresses as $S = \kappa_e T \kappa_o^{-1}$. In appendix B we shall use these for numerical checks towards the overall robustness of the regularization.

The T, R, w, v matrices were also shown to satisfy the following algebraic relations starting from (2.51):

$$\begin{aligned} &T\,R = \mathbb{1}_e, \qquad R\,T = \mathbb{1}_o, \qquad R^\top R = \mathbb{1}_e + w^\top w, \qquad T^\top T = \mathbb{1}_o - vv^\top, \\ &TT^\top = \mathbb{1} - \frac{ww^\top}{1+w^\top w}, \qquad Tv = \frac{w}{1+w^\top w}, \qquad v^\top v = \frac{w^\top w}{1+w^\top w}, \\ &Rw = v(1+w^\top w), \qquad RR^\top = \mathbb{1}_o + vv^\top(1+w^\top w). \end{aligned} \tag{2.53}$$

As mentioned earlier, many more relations are carefully derived in [20, §2] that also involve the matrix S and allowing for negatively indexed matrices .

This deformation results in a *preservation of associativity* while taking double sums. This can be seen as follows. From (2.38) for the infinite N limit expressions for the w, v vectors, we find that $w^\top w \to \infty$ as $N \to \infty$. Then from the relation $Tv = w/(1+w^\top w)$ above, we conclude that v is a zero mode of the T vector in the open string limit. Hence, marginally convergent infinite sums can become ill-defined by becoming dependent on the order of summations. For instance, in the open string limit, we could obtain two distinct results $R(Tv) = R \cdot \mathbb{0} = 0$ or $(RT)v = \mathbb{1}_o v = v$. However, looking at the relation $Rw = v(1+w^\top w)$, we infer a cancellation between an infinite and a vanishing factor taking place, leading to an unambiguous result $RTv = v$. Therefore, associativity anomalies of the above kind can be removed by working with the finite N expressions above (2.52) till the end of a computation and then taking the open string limit in a controllable manner.

We remark that the regularization essentially removes the null elements of the algebra by hand and hence is topologically different from the string field algebra, even in the open string limit. It would therefore be very interesting to study this structure on its own and because it correctly captures many aspects of perturbative OSFT as shown in [21, 26] and as we shall see in the following.

Monoid subalgebra relations

The regularization also leads to a (Moyal) star subalgebra constructed out of *finite* number of modes.[9] This subalgebra was originally derived for the infinite N case in [19, ref 1]

[9] In the full open string field theory, all star subalgebras necessarily contain an infinite number of modes for consistency with the Witten axioms. Here we are only considering the deformed theory. We can relegate the subtleties of the closure of sub-algebras in string field theory by working at a finite value of N, which is somewhat similar to level truncation, and hence amounts to imposing a UV cut-off.

but the relations naturally carry over to the finite N case and the ghost sector (see [26, §3, Appendix A] and also [20, §3.1] for an alternate derivation). The elements of this subalgebra are string configurations corresponding to quadratic exponentials defined in Moyal space:

$$A_{\mathcal{N},M,\lambda,k}(\xi) \coloneqq \mathcal{N} e^{-\xi^\top M \xi - \xi^\top \lambda + ik\bar{x}}, \qquad \mathrm{Tr}(A^\dagger A) = 1. \tag{2.54}$$

Here, the string configuration (for the matter sector) is parametrized by $2N \times 2N$ complex symmetric matrices M, a $2N \times 1$ complex vector λ, the d dimensional momentum k^μ, and a normalization factor $\mathcal{N}$ (which is independent of the ξ but may depend on $\bar{x}$ depending on the Dp-brane system), set by the (matter) trace (2.50)

$$\mathrm{Tr}(A_{\mathcal{N},M,\lambda,k}) = \frac{\mathcal{N} e^{ik\bar{x}} e^{\frac{1}{4}\lambda^\top M^{-1}\lambda}}{\det(2M\sigma)^{d/2}} \tag{2.55}$$

which shall be taken to exist formally for the purpose of intermediate calculations.

The interesting result is that these shifted Gaussians when star multiplied retain their structure in the sense that:

$$\mathcal{N}_1 e^{-\xi^\top M_1 \xi - \xi^\top \lambda_1 + ik_1\bar{x}} * \mathcal{N}_2 e^{-\xi^\top M_2 \xi - \xi^\top \lambda_2 + ik_2\bar{x}} = \mathcal{N}_{12} e^{-\xi^\top M_{12} \xi - \xi^\top \lambda_{12}}\, e^{i(k_1+k_2)\bar{x}}. \tag{2.56}$$

i.e. they define a closed algebraic structure under the Moyal star product:

$$A_{\mathcal{N}_1,M_1,\lambda_1,k_1} * A_{\mathcal{N}_2,M_2,\lambda_2,k_2} = A_{\mathcal{N}_{12},M_{12},\lambda_{12},k_{12}}. \tag{2.57}$$

Here k_{12} simply equals $k_1 + k_2$ by momentum conservation. The off-block diagonal anti-symmetric matrix σ appearing in the definition of the $*$ product (2.22) makes it convenient to define the matrices $m_i \coloneqq M_i\sigma$ so that we have:

$$m_1 = M_1\sigma, \qquad m_2 = M_2\sigma, \qquad \text{and } m_{12} = M_{12}\sigma. \tag{2.58}$$

Then the parameters for the product are fixed by the relations below:

$$m_{12} = (m_1 + m_2 m_1)(1 + m_2 m_1)^{-1} + (m_2 - m_1 m_2)(1 + m_1 m_2)^{-1}, \tag{2.59a}$$

$$\lambda_{12} = (1 - m_1)(1 + m_2 m_1)^{-1}\lambda_2 + (1 + m_2)(1 + m_1 m_2)^{-1}\lambda_1, \tag{2.59b}$$

$$\mathcal{N}_{12} = \mathcal{N}_1\mathcal{N}_2 \det(1 + m_2 m_1) \exp\Big[+ \frac{1}{4}\lambda^{gh\top}_\alpha \sigma K_{\alpha\beta} \lambda^{gh}_\beta \Big] \text{ where,} \tag{2.59c}$$

$$K_{\alpha\beta} = \begin{bmatrix} (m_1 + m_2^{-1})^{-1} & (1 + m_2 m_1)^{-1} \\ -(1 + m_1 m_2)^{-1} & (m_2 + m_1^{-1})^{-1} \end{bmatrix}; \qquad m_i \coloneqq M_i\sigma. \tag{2.59d}$$

Although this regularization cannot realize the Virasoro algebra and breaks the gauge invariance, it does preserve the *non-linear Gross-Jevicki* matrix identities [34] (see also (2.79) below) satisfied by the infinite Neumann matrices. This is because the fundamental matrices continue to satisfy the same relations as their infinite N counter-parts (whenever they are regular) even after the deformation.

We remark that with the choice of basis (2.40) we shall use, the relations in the ghost sector becomes identical including the signs, after the $Sp(2)$ metric factor $-i\varepsilon$ from (2.43) is inserted appropriately.

These shifted Gaussians form a monoid (essentially a group without the requirement of inverses) or a semi-group structure by virtue of the following properties:

1. It is closed under the $*$ product operation.
2. It is endowed with an *associative* product structure.
3. It has a unique unit element[10] which is the number 1.
4. Although the generic elements do have inverse images, not every element need have one (for example, the projectors satisfying $A_P * A_P = A_P$, $\mathrm{Tr}(A_P) = 1$ lack an inverse, as may be readily verified).

It is in general non-commutative just like a group. Thus being just short of forming a group structure due to the lack of an inverse, it is a monoid or a semi-group containing many interesting string configurations useful for calculations.

In particular, the perturbative vacuum state for the ghost sector (in the Siegel gauge) that we shall be using frequently, belongs to this class and is given by the monoid element:

$$\hat{A}_0^{gh}(\xi^{gh}) = \xi_0 \mathcal{N}_0^{gh} \exp\left[-\xi^{gh\top} M_0^{gh} \xi^{gh}\right], \tag{2.60}$$

where the matrix M_0^{gh} takes a block diagonal form in the purely even basis:

$$\begin{aligned} M_0^{gh} &= -\begin{bmatrix} \frac{1}{2}R^\top \kappa_o R & 0 \\ 0 & 2\kappa_e^{-1} \end{bmatrix}, \qquad \lambda^{gh} = 0, \qquad \text{and} \\ \mathcal{N}_0^{gh} &= 2^{-2N}(1 + w^\top w)^{-\frac{1}{4}} \end{aligned} \tag{2.61}$$

is a normalization factor determined from the $\mathrm{Tr}(A_0^\dagger A_0) = 1$ condition. We also provide the expression for the perturbative tachyon state $\hat{c}_1|p;\Omega\rangle$, with a momentum p [20, §4] which is employed in Appendix B for numerical checks requiring both the matter and ghost contributions:

$$A_p(\xi, \xi^{gh}) = 2^{N(d-2)}(1 + w^\top w)^{-\frac{d+2}{8}}\, e^{ip\bar{x}} e^{-\xi^\top M_0 \xi + ipw_e x_e} e^{-\xi^{gh\top} M_0^{gh} \xi^{gh}}, \tag{2.62}$$

where again the normalization is set by $\mathrm{Tr}(A_p^\dagger A_p) = 1$, M_0 is given in (2.26), and $d = 26$ for criticality.

As we shall see, the shifted Gaussians serve as generating functionals for describing scattering processes which can involve perturbative (and non-perturbative) excited string

[10] corresponding to the identity state $|\tilde{I}\rangle$ under the *reduced* star product studied in [34].

states in addition to the tachyon. To this end, let us consider again a general monoid element:

$$A_{\mathcal{N}M,\lambda,p,M^{gh},\lambda^{gh}} = \mathcal{N} e^{ip\bar{x}} e^{-\xi^\top M \xi - \xi^\top \lambda} e^{-\xi^{gh\top} M^{gh} \xi^{gh} - \xi^{gh\top} \lambda^{gh}}, \tag{2.63}$$

and for the purpose of string diagrams with perturbative external states, restrict to the class with $M = M_0$ and $M^{gh} = M_0^{gh}$, while keeping the rest of the parameters general. The excited states are represented by polynomials in ξ, ξ^{gh} multiplying the tachyon state $A_p(\xi, \xi^{gh})$ above, i.e. we have:

$$A_e(\xi, \xi^{gh}) = \wp(\xi, \xi^{gh}) A_p(\xi, \xi^{gh}) \tag{2.64}$$

These are the analogues of the Gaussian string states multiplied by Hermite polynomials in the functional formalism but now defined in the non-commutative Moyal space. The required polynomial factor can be prepared by differentiating the monoid $A_p(\xi, \xi^{gh}) e^{-\xi^\top \lambda - \xi^{gh\top} \lambda^{gh}}$ with respect to general matrix parameters λ, λ^{gh} to bring down "powers" of ξ, ξ^{gh}, taking the needed linear combinations, and at the end setting $\lambda = (-i w_e p_e, 0)$ and $\lambda^{gh} = 0$.

Hence, equivalently it would be possible to perform computations with general monoids $A_\alpha \coloneqq A_p(\xi, \xi^{gh})\, e^{-\xi^\top \lambda_\alpha - \xi^{gh\top} \lambda_\alpha^{gh}}$ while utilizing the monoid algebra relations to obtain a functional that depends on a set of $\lambda_\alpha, \lambda_\alpha^{gh}$ for each external state labelled by α, and then differentiate this functional to recover the original amplitude. Thus, we see that the subalgebra is a helpful structure for explicitly evaluating string diagrams, to which we turn next. We shall be mainly exploiting these rules while evaluating the tadpole and string propagator diagrams in the rest of this part.

2.2.4 Procedure for evaluating string diagrams

In order to study string diagrams using this formalism, we require the gauge fixed string field theory action written in Moyal space [20, 21]:

$$S_{\text{GF}} = -\int d^d\bar{x}\ \text{Tr}\left(\frac{1}{2\alpha'} A(\bar{x},\xi) * (L_0 - 1) A(\bar{x},\xi) + \frac{g_o}{3} A(\bar{x},\xi) * A(\bar{x},\xi) * A(\bar{x},\xi)\right), \tag{2.65}$$

where $A(\bar{x},\xi)$ contains only the non-zero ghost modes and the full string field has the explicit zero-mode dependence $\hat{A}(\bar{x},\xi_0,\xi) = \xi_0 A(\bar{x},\xi)$ in Siegel gauge. We remark that this form of the action is also applicable for the finite N truncations.

Let us recall from §2.1.3, that the $L_0 = L_0^X + L_0^{gh}$ operator appearing above is the worldsheet Hamiltonian and therefore the operator e^{-tL_0} generates worldsheet strips of length t and width π. This operator arises in the Schwinger parametrization (2.10) for the inverse of the kinetic operator above, i.e. $(L_0 - 1)^{-1}$, which is the propagator. The propagator is the other ingredient needed while constructing string diagrams using SFTs, in addition to the vertices, which is given by the $*$ product interaction in case of OSFT.

Due to the interplay between kinetic term and the interaction term in OSFT, the propagator becomes complicated in ξ space and involves a potential term (2.25), (3.9). Hence, we expect to have a non-trivial action of e^{-tL_0} on string fields, which can however be expressed in closed form in terms of hyperbolic functions. Let us look at the "t-evolved" monoid element in the matter sector:

$$A(t,\xi) \coloneqq e^{-tL_0^X}\left(\mathcal{N}e^{-\xi^\top M\xi-\xi^\top\lambda}\,e^{ip\bar{x}}\right) = \mathcal{N}(t)e^{-\xi^\top M(t)\xi-\xi^\top\lambda(t)}\,e^{ip\bar{x}} \tag{2.66}$$

The transformed parameters are given by the rules:

$$M(t) = \left[\sinh\,t\tilde{\kappa} + (\sinh\,t\tilde{\kappa} + M_0^X M^{-1}\cosh\,(t\tilde{\kappa}))^{-1}\right](\cosh\,(t\tilde{\kappa}))^{-1}M_0^X, \tag{2.67a}$$

$$\lambda(t) = \left[(\cosh\,(t\tilde{\kappa}) + MM_0^{X-1}\sinh\,t\tilde{\kappa})^{-1}(\lambda + iwp)\right] - iwp, \tag{2.67b}$$

$$\mathcal{N}(t) = \frac{\mathcal{N}e^{-p^2t}\exp\left[\frac{1}{4}(\lambda+ipw)^\top(M+\coth t\tilde{\kappa}M_0^X)^{-1}(\lambda+iwp)\right]}{\det\left(\frac{1}{2}(1+MM_0^{X-1}) + \frac{1}{2}(1-MM_0^{X-1})e^{-2t\tilde{\kappa}}\right)^{d/2}}. \tag{2.67c}$$

There are arrived at in [21] by using the fact that $A(t,\xi)$ is in the kernel of the Schrödinger operator $(\partial_t + L_0)$ or by transforming to Fourier space as done in [20, §4.2] for the ghost sector. The ghost sector rules would be provided later in (3.10) when needed. Here we recall that M_0^X (2.18) i is the matrix that appears in the perturbative vacuum $A_0(\xi)$ (2.62) and $\tilde{\kappa}$ (2.26) is a natural "spectral" matrix.

The monoid subalgebra [20, 26] (2.59) and the propagator rules thus allow for one straightforward way of formally writing down the integrands for Feynman graphs in the non-commutative ξ space. Now let us briefly consider how these are applied to general string diagrams. See [20, 21, 26] for more details and examples.

Tree diagrams

The procedure for evaluation of evaluation of tree diagrams can be outlined as follows:

1. The external states are represented by monoid elements $A_i(\bar{x},\xi,\xi^{gh})$ appropriate for the (primary or non-primary) operator insertions on the semi-infinite strips.

2. Two external legs A_i and A_j meeting at a vertex are joined together using the $*$ product rules (2.59) to give the resulting string field $A_{ij} = A_i * A_j$.

3. The intermediate string fields are propagated using the operators $q_a^{L_0} \coloneqq e^{-t_aL_0}$ (see (2.10)) using the transformation rules just described (2.67). These are then star multiplied at vertices and depending on the topology of the string diagram may be further propagated while accounting for all the string fields.

4. The final trace operation (Gaussian integration over ξ, ξ^{gh}) (2.50) implements the folding of the two halves of the resulting string.[11]

Here the variables $q_a = e^{-t_a}$ encode the modular parameters of the intermediate strips t_a; the string diagrams are therefore evaluated at fixed t_a. The combined matter + ghost integrand would then need to be integrated with the appropriate $dt_a\, e^{t_a}$ measure (see (2.10)) over the moduli space given by $t_a \in [0, \infty)$ (or equivalently $q_a \in (0, 1]$ with dq_a/q_a^2 measure factor), which is a simple enough geometrical object.[12]

For illustration, let us consider the tree level 4-point function in OSFT which was studied using the Moyal formalism in detail for tachyonic external states in [26, ref 2] by Bars and Park, and in [20, 21]. This requires the evaluation of the s-channel and the t-channel diagrams shown in Fig. 2.2 (and their permutations).

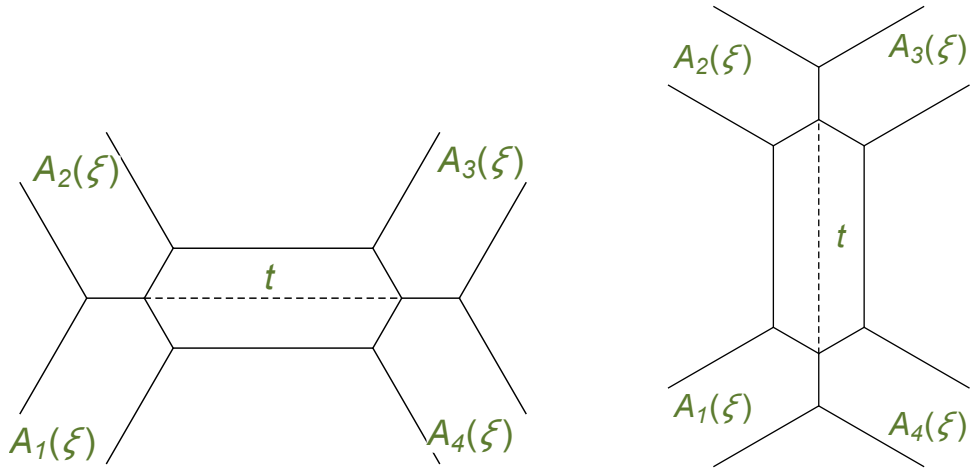

(a) (b)

Figure 2.2: (a) The s-channel diagram ${}_{12}A_{34}(t)$ and (b) the t-channel diagram ${}_{41}A_{23}(t)$ contributing to the OSFT 4-point function at a fixed modular parameter t. Here the external string fields are denoted by the monoid elements $A_i(\xi), i = 1, 2, 3, 4$, carrying momenta p_i^μ which could be taken off-shell. The t-channel is related to the s-channel by a cyclic permutation (colour ordering) and by interchanging the Mandelstam variables: $s \leftrightarrow t$. Further permutations give lead to identical dependence on s, t at the end.

For the s-channel, the starting expression as per the above procedure for Moyal space would be:

$$ {}_{12}A_{34}(q) = \int d^d\bar{x}\, \mathrm{Tr}\left[q^{L_0}(A_1 * A_2) * A_3 * A_4\right]. \tag{2.68} $$

[11] The last $*$ product may be omitted since it reduces to the ordinary commutative product under the trace by virtue of integration by parts.

[12] There are further change of variables and careful orderings needed for simplifications and for arranging identical expressions for the various string diagrams contributing to an amplitude. See [13, 26] and references therein.

In words, the external states represented by the monoids A_1 and A_2 are first star multiplied (2.59) to given an intermediate string field $A_{12} = A_1 * A_2$, which is also of the monoid type. The q^{L_0} then evolves it to the element $A_{12}(q)$ as per (2.67). The remaining vertex star multiplies $A_{12}(q), A_3$, and A_4 with the correct cyclic ordering, and implements the trace. It is convenient to first multiply A_3 and A_4 to give A_{34} and then drop the $*$ product between $A_{12}(q)$ and A_{34}. The $\bar{x}$ integral simply leads to a momentum conserving delta function $(2\pi)^d\delta^d(p_1 + p_2 + p_3 + p_4)$.

Using the same method, the t-channel expression is given by:

$$_{41}A_{23}(q) = \int d^d\bar{x}\, \mathrm{Tr}\left[q^{L_0}(A_4 * A_1) * A_2 * A_3\right]. \tag{2.69}$$

The off-shell integrands for 4 tachyonic external states were computed in [26, ref 2],[20, 21] in terms of the relevant Mandelstam variables $s = -(p_1 + p_2)^2, t = -(p_1 + p_4)^2$, and were shown to lead to the Veneziano amplitude directly, without recourse to conformal mapping techniques. Additionally, the formalism also produced detailed information on the relevant "off-shell factor" than was previously available. See the references mentioned for more details on the computations and analysis.

We shall be using the structure of the s and t channel diagrams above while writing down the one-loop 2-point function later in chapter 5. Let us now turn to loop diagrams whose simplest cases we analyze in the rest of this Part.

Loop diagrams

In case of diagrams with loops, one also needs to perform a state sum which is the analogue of the integral over loop momenta for a single scalar field. One can augment the procedure for tree diagrams to write down loop integrands as follows:

1. One can imagine a single loop as formed by identifying two legs of an off-shell tree amplitude, which can be obtained by cutting the loop. We can label the two fields by the monoids A_i and A_j as before.

2. Next, we replace these by

$$A_i \mapsto q_a^{L_0}\left(e^{+i\xi^\top\eta_i + ip_i\bar{x}}\, e^{-\xi^{gh\top}\eta^{gh}{}_i}\right), \qquad A_j \mapsto e^{-i\xi^\top\eta_i - ip_i\bar{x}}\, e^{+\xi^{gh\top}\eta^{gh}{}_i} \tag{2.70}$$

   If we consider the contribution only from the ordinary ghosts, we can insert a (normalized) Fourier basis $e^{+i\xi^\top\eta + ip\bar{x}}\, e^{-\xi^{gh\top}\eta^{gh}}$ which furnishes a complete set of states.[13] The states are propagated using $q_a^{L_0}$ as before.

3. A $(d\eta_i)$ and a d^dp_i integration at the end then implement the state sum we seek.

[13] These are to be understood in the form of a distribution due to the singular normalization involved and the vanishing quadratic term in the exponents.

Once again, the integrations over the moduli of the propagators t_a needs to be performed with the appropriate measure $\int_0^\infty dt_a\, e^{t_a} = \int_0^1 dq_a/q_a^2$.

The simplest one-loop diagram is the one-loop vacuum integrand without any external legs shown in Fig. 2.3. This is the annulus diagram which leads to the partition function and hence the open string spectrum. Applying the rules, we can write it as:

$$\mathcal{I}_0(t) = \int d^d\bar{x} \int \frac{d^dp}{(2\pi)^d} \frac{d\eta}{(2\pi)^{2dN}} \mathrm{Tr}\left[e^{-i\xi^\top\eta - ip\bar{x}} * e^{-tL_0^X}\left(e^{+i\xi^\top\eta + ip\bar{x}}\right)\right], \tag{2.71}$$

which can be obtained starting from the 2-point vertex $\mathrm{Tr}(A_1 * A_2)$. The result of the

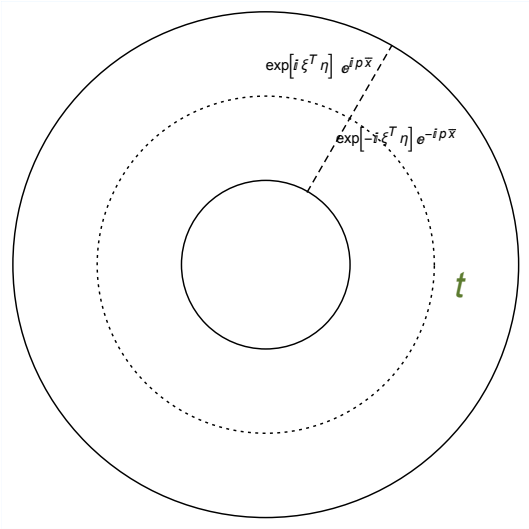

Figure 2.3: The one-loop vacuum diagram in OSFT at a fixed modular parameter t in the matter sector. The Fourier basis for taking the state sum are represented by $e^{\pm i\xi^\top\eta}\, e^{\pm ip\bar{x}}$. One state is propagated using e^{-tL_0} before taking the overlap; the integrals for state sum are over η, p.

calculation after taking into account the ghost contribution as presented in [20, §4.2] by Bars et al. is

$$\mathcal{I}_0(t) = (2\pi)^{d/2} l_s^{-d} t^{-d/2}\, e^t \prod_{e>0}(1-e^{-t\kappa_e})^{-(d-2)} \prod_{o>0}(1-e^{-t\kappa_o})^{-(d-2)} \tag{2.72}$$

This contains the correct open string spectrum with all the non-negative integer frequencies and coincides with the first quantized result. This calculation highlighted the importance of the finite N regularization limit prescription of taking the open string limit at the end of a calculation, without which the odd frequencies $\kappa_o = 2n-1$ would disappear. We shall also make use of this expression later in §4.3.3 while performing a simple consistency check using factorization [44] in the $t \to \infty$ limit for the tadpole result obtained in the next chapter.

The same method holds for loop diagrams with external states involved. For instance, the tadpole diagram Fig. 3.1 that we will be focussing on in §3.1 can be obtained by joining two legs of the off-shell 3-vertex $\mathrm{Tr}(A_1 * A_2 * A_3)$ to form a loop and inserting a complete set of states.

As is clear, there are many formally equivalent ways of doing a computation—some of which owe to associativity, cyclicity, etc. and others from interchanging $(d\eta_i), (d\xi)$ integrations. Thus the Moyal expressions can also lead to interesting algebraic relations. We note that for the purpose of numerical calculations, it is also useful to consider the Feynman rules in the Fourier basis given in [20, 21] and briefly described later in §3.4 while examining associativity for the tadpole calculation.

2.3 Results from the oscillator basis

In the oscillator construction [34], the Fock space of open (bosonic) string fields is constructed by acting with the creation operators $\alpha^{\mu}_{-k}, b_{-n}, c_{-m}$ on the vacuum $|\hat{\Omega}\rangle$. The star product is then implemented by using n-vertices belonging to the tensor product of the dual spaces $\mathcal{H}^{(i)*}$. In particular, we have the three-vertex $\langle V_3|$ and the two-vertex $\langle V_2|$ whose explicit structure encodes the Witten-style overlapping conditions (see [11, 34] and references therein). The 3-string vertex fixes all the interactions that may arise in the theory. For the purpose of this work, we provide only the relevant ghost part [34, 45] appearing in the combined vertex:

$$\begin{aligned} \langle V_3| &= {}^{X}\langle V_3| \otimes {}^{gh}\langle V_3|, \\ {}^{gh}\langle V_3| &\sim {}_{123}\langle \Omega| \exp(-E_3^{gh}), \end{aligned} \tag{2.73}$$

where E_3^{gh} is a quadratic form coupling the ghosts involving the ghost Neumann matrices X^{rs}_{nm}:

$$E_3^{gh} = \sum_{r,s=1}^{3} \sum_{\substack{n=1 \\ m=0}}^{\infty} c_n^{(r)} X^{rs}_{nm} b_m^{(s)}. \tag{2.74}$$

Furthermore only the coefficient matrices for the non-zero modes (in the Siegel gauge) would concern us. These are the ghost Neumann matrices denoted by X^{rs}_{nm}, with $r, s \in \{1, 2, 3\}$ and by their symmetry and cyclicity properties, we can restrict to $X^{11} = X^{(0)}, X^{12} = X^{(+)}$ and $X^{21} = X^{(-)}$. They are algebraic valued and can be obtained efficiently from CFT using contour integral representations [11, 34].

The one-loop tadpole can be represented as a ket (or more properly as a bra) which involves an exponential purely quadratic in the creation operators. These special states

then belong to the class of squeezed states in the Hilbert space.

$$|\mathcal{T}\rangle = \int_0^\infty dt\, e^t \frac{\det(1-S\widetilde{X})}{(Q\det(1-S\widetilde{V}))^{13}}\ \exp\left(-\frac{1}{2}a^\dagger \mathbf{M} a^\dagger - c^\dagger \mathbf{R} b^\dagger\right)\hat{c}_0|\hat{\Omega}\rangle. \tag{2.75}$$

where the t dependence in Q and the infinite matrices $\mathbf{M}, \mathbf{R}, \widetilde{X}$, and $\widetilde{V}$ are understood. The relevant inner product involving reflector $\langle V_2|, |V_3\rangle, \hat{L}_0$, etc. is presented in (3.65).

We quote the following form for $\mathbf{R}(t)$ derived in [14, §4] using squeezed state methods presented in [18]:

$$\mathbf{R}(t) = X^{11} + \begin{bmatrix} \hat{X}^{12}(0,t) & \hat{X}^{21}(0,t) \end{bmatrix} \frac{1}{\mathbb{1}-S\widetilde{X}} S \begin{bmatrix} \hat{X}^{21}(t,0) \\ \hat{X}^{12}(t,0) \end{bmatrix} \tag{2.76}$$

The "hatted" matrices are simply the Neumann matrices dressed with the t dependent propagator factors of the following form:

$$\hat{X}^{i_k j_l}_{nm}(t_k, t_l) \coloneqq e^{-nt_k/2} X^{i_k j_l}_{nm} e^{-mt_l/2}. \tag{2.77}$$

In terms of these, the infinite matrix $\widetilde{X}$ is given by

$$\widetilde{X}(t) = \begin{bmatrix} \hat{X}^{11}(t,t) & \hat{X}^{12}(t,t) \\ \hat{X}^{21}(t,t) & \hat{X}^{11}(t,t) \end{bmatrix}, \tag{2.78}$$

and $S = \mathbb{1}_2 \otimes C$, where again $C_{nm} = (-)^n \delta_{nm}$ is the twist matrix, that arises from the specific overlap conditions imposed by the Witten type vertex in the matter and ghost sectors. The above matrices become $2L \times 2L$ dimensional in an oscillator level truncation, which roughly corresponds to using $4N \times 4N$ dimensional matrices in the discrete Moyal representation for finite N.

Expansion around $t = 0$

As observed in [14], the infinite matrix $\mathbf{R}(t)$ cannot be reliably expanded around the point $t = 0$ (or $q \coloneqq e^{-t} = 1$) that we are interested in. This is because an intermediate matrix to be inverted, $\mathbb{1} - S\widetilde{X}(0)$, for the expansion point becomes singular due to a subset of the Gross-Jevicki non-linear relations satisfied by the unhatted matrices $\mathcal{M}_{0,\pm} \coloneqq -CX^{0,\pm}$ in the ghost sector:

$$\mathcal{M}_0 + \mathcal{M}_+ + \mathcal{M}_- = \mathbb{1}, \qquad \mathcal{M}_+\mathcal{M}_- = \mathcal{M}_0^2 - \mathcal{M}_0, \tag{2.79a}$$

$$\mathcal{M}_0^2 + \mathcal{M}_+^2 + \mathcal{M}_-^2 = \mathbb{1}, \qquad \mathcal{M}_0\mathcal{M}_+ + \mathcal{M}_+\mathcal{M}_- + \mathcal{M}_-\mathcal{M}_+ = 0, \tag{2.79b}$$

$$\mathcal{M}_\pm^2 - \mathcal{M}_\pm = \mathcal{M}_0\mathcal{M}_\mp. \tag{2.79c}$$

These are mutually commuting matrices and in the limit $t \to 0$, when we have

$$\mathbb{1} - S\widetilde{X}|_{t=0} = \begin{bmatrix} \mathbb{1} - \mathcal{M}_- & -\mathcal{M}_0 \\ -\mathcal{M}_0 & \mathbb{1} - \mathcal{M}_+ \end{bmatrix}, \tag{2.80}$$

this allows us to express the determinant in terms of the constituent blocks by the usual formula for 2×2 matrices:

$$\begin{aligned} \det(\mathbb{1} - S\widetilde{X})|_{t=0} &= \det(\mathbb{1} + \mathcal{M}_-\mathcal{M}_+ - \mathcal{M}_- - \mathcal{M}_+ - \mathcal{M}_0^2) \\ &= \det\left(\mathcal{M}_0 - \mathcal{M}_0^2 + \mathcal{M}_-\mathcal{M}_+\right) \\ &= \det(\mathbb{0}) = 0, \end{aligned} \tag{2.81}$$

which makes the Taylor series ill-defined. This fact is also carefully pointed out in [14, appendix B]. The authors study these expressions numerically and comment on why a level truncated analysis would differ from the correct numerical behaviour which matches with a BCFT based expansion (3.63) as the level is increased. Since the identities only hold in the infinite L limit, the problem does not arise at finite level, which effectively acts as a UV cutoff for $t = 0$.

Thus, the order of limits $t \to 0$ and the level $L \to \infty$ do *not* commute and subsequently the infinite level result gives a factor of $-2n$ for the linear term instead of $-n$ as confirmed by numerical studies at finite level. As we shall see in §3.3, the Moyal expressions do not suffer from this order of limits issue (at least at the leading order) and leads to the correct linear coefficients. In the consistent Moyal truncation we use, something similar happens with the inverse, but this time the full matrix to be inverted vanishes at $t = 0$ even for finite N thus altering the UV behaviour.

2.4 Summary of notations for Moyal space calculations

Here we collect some of the notations and conventions that will be used in the rest of this part.

Phase space basis vectors ξ, ξ^{gh}: The string field $A(\bar{x}, \xi, \xi^{gh})$ is valued in the non-commutative phase space $\xi_i^\mu = (x_2^\mu, \ldots . x_{2N}^\mu, p_2^\mu, \ldots p_{2N}^\mu), {\xi^{gh}}_i = (\xi_{2n}^1, \xi_{2n}^2)$ labelled by even integers. The doublet structure (x, p) would be understood in the following which for ghosts is in (2.40). The zero mode dependence is factored out in Siegel gauge through $\hat{A} = \xi_0 A(\xi^{gh})$. We shall suppress the Lorentz indices unless required.

The integration or the BPZ inner product is mapped to the trace in this phase space. Also, we shall denote $(d\xi), (d\eta)$, etc. for integration over the Moyal space

modes[14] $d^d\xi_1 \dots d^d\xi_{2N}$, $d^d\eta_1 \dots d^d\eta_{2N}$, and suppress the measure factors of $\frac{1}{2\pi i}$ unless necessary.

Constant matrices: The spectrum is denoted by a $2N \times 2N$ diagonal matrix κ, which in the parity basis is $\kappa = \mathrm{Diag}\{\kappa_e, \kappa_o\}$ and the labels e, o refer to the even and odd integer mode numbers. In the open string limit $N \to \infty$, we shall set $\kappa_{2n} = 2n$ and $\kappa_{2n-1} = 2n-1$, corresponding to the perturbative spectrum. A useful matrix which naturally appears in the ghost sector is given by a similarity transformation of κ:

$$\tilde{\kappa}^{gh} = \begin{bmatrix} R^\top \kappa_o T^\top & 0 \\ 0 & \kappa_e \end{bmatrix}. \tag{2.82}$$

The linear transformations to go to the discrete diagonal basis requires the use of certain (constant) infinite matrices whose elements are simple functions of the mode labels e and o. In the regulated theory, these have their finite dimensional analogues which in general depend on the frequency matrices κ_e and κ_o. The infinite N limit of the matrices is sufficient to see their fall off behaviour at large mode numbers in infinite sums:

$$T_{eo} = \frac{4}{\pi}\frac{o\, i^{o-e+1}}{e^2-o^2}, \qquad R_{oe} = \frac{4}{\pi}\frac{e^2\, i^{o-e+1}}{o(e^2-o^2)}, \qquad w_e = \sqrt{2} i^{2-e}, \qquad v_o = \frac{2\sqrt{2}}{\pi}\frac{i^{o-1}}{o}. \tag{2.83}$$

these satisfy the relations presented in [20] of which we mainly use:

$$T\,R = \mathbb{1}_e, \qquad R\,T = \mathbb{1}_o, \qquad R = \kappa_o^{-2}\, T^\top\, \kappa_e^2, \qquad T\,T^\top = \mathbb{1}_e - \frac{w w^\top}{1 + w^\top w}, \tag{2.84}$$

where the last one is among the finite N relations (2.53) and which turned out to be crucial for insuring associativity consistent with gauge invariance and the correct string spectrum.

Monoid elements: We shall be primarily using the monoid subalgebra §2.2.3 for our calculations. These are shifted Gaussian functionals of the form

$$A(\xi) = \mathcal{N} e^{-\xi^\top M \xi - \xi^\top \lambda + i k \bar{x}}.$$

For the perturbative ghost vacuum $\hat{A}_0^{gh} = \xi_0 A_0^{gh}$, where A_0^{gh} has parameters $\mathcal{N}_0^{gh} = 2^{-2N}(1 + w^\top w)^{-\frac{1}{4}}$ and $M = M_0^{gh}$ (2.61). For external states built on the perturbative vacuum, it is sufficient to consider a generating functional with $M^X = M_0^X$ and $M^{gh} = -i\varepsilon \otimes M_0^{gh}$ with a general λ^X, λ^{gh} and construct states as polynomials $\wp(\xi, \xi^{gh})$.

[14] The η, ξ here are (unfortunately) unrelated to the $\eta(z), \xi(z)$ conformal fields defined by FMS [5] and in the recent developments in open superstring field theories.

We shall assume that the interchanging functional operations as usually done in QFT can be performed here as well, although it does not seem that straightforward.

Normalization factor: The Witten type vertex and the Moyal vertex are related by a (divergent) factor. By using the regularized theory, it leads to a renormalization of the bare coupling g_0 to the physical g_T when considering the D25 brane reference BCFT. The two vertices are related as:

$$\langle \Phi_1 | \Phi_2 * \Phi_3 \rangle = \mu_3^{-1} \mathrm{Tr}\left[A_1 * A_2 * A_3 \right] \tag{2.85}$$

where we have chosen the Siegel gauge and $A_i(\xi) \coloneqq \langle \xi | \Phi_i \rangle$ and

$$\mu_3 = -2^{2N(d-2)} (1 + w^\top w)^{-\frac{d-6}{8}} \left(\det(3 + tt^\top) \right)^{-d} \left(\det(1 + 3tt^\top) \right)^2 . \tag{2.86}$$

Modular parameters: We use the variable t for the worldsheet lengths so as to match the usual convention for the nome $q = e^{2\pi i \tau}$. This requires that $\tau \mapsto it/2\pi$.

$$q = e^{-t}, \qquad q_1 = e^{-t_1}, \qquad q_2 = e^{-t_2}, \quad \text{etc.} \tag{2.87}$$

Some simple matrix functions that would be convenient for writing down integrands can then be defined in terms of q and the mode label n as $f_i(n;q)$ $(i = 1, 2, 3, 4)$ to be given in (3.16) and some auxiliary functions $h_i(n;q)$ and $g_i(n;q)$ in (4.1).

We shall be quite explicit in the following, since we are seeking to resolve the minor mismatch in the oscillator construction and since many of the steps are simple block matrix multiplications or Gaussian integrations. The reader can skip these intermediate steps and essentially consider the final form of the expressions if desired. We shall also retain the "gh" superscript although it is usually clear from the context when the quantities refer to the ghost contribution. When the superscript is not used, it refers to the matter sector which we shall sometimes denote by an "X" superscript.

In the next chapter, we shall apply the Feynman rules in Moyal space (described in §2.2.4) to write down the formal analytic expression for the tadpole integrand that will serve as the starting point for our analysis of the one-loop structure of open string field theory.

Chapter 3

One-loop tadpole integrand

In this chapter, we write down the one-loop tadpole integrand in the Moyal representation while focussing on the ghost contribution. This diagram represents the next simplest probe of the one-loop structure of OSFT after the one-loop vacuum amplitude (the annulus diagram which gives the partition function and hence the string spectrum). The open string tadpole has a single external leg, and it receives contributions from the internal propagation of closed string states. It thus encodes the coupling between the closed string background and open strings. In usual field theories, the tadpole contributes to a term linear in the field to the action, and can be chosen to vanish by a shift in the field value. As analysed using the open-closed SFT of Zwiebach [29] in [14, §5] by Ellwood et al, the shift in the closed string background is reflected in the open string tadpole as well.

We shall be using the Moyal method to further understand the structure of this interesting object and consider certain finite factors. These can then serve as a starting expression for examining the non-analyticities in the ghost sector, as a function of the modular parameter t. For prior treatments using the CFT and oscillator methods and for discussions on the divergences in the diagram, we refer to [10, 12, 14, 46] and references therein.

3.1 Ghost sector expressions in the Moyal basis

We wish to obtain an expression for the one-loop contribution to the tadpole graph in bosonic open string theory. Since this is an intrinsically off-shell quantity, we need to work in the framework of a string field theory and we choose the Witten type OSFT reviewed in the previous section. The string diagram for this process is depicted in Fig.3.1 where an open string state at zero momentum ($p_e = 0$) in a D25-brane background appears from vacuum, splits into two open strings and then annihilate each other, just like in QFT. It is parametrized by a single modular parameter associated with the length of the internal propagator. The corresponding integrand at a fixed modular parameter t, may be obtained by identifying two legs of an off-shell 3-point diagram and integrating over a complete set of (normalized) quantum states $e^{+i\xi^\top\eta+ip\bar{x}}\, e^{-\xi^{gh\top}\eta^{gh}}$ as described in §2.2.4.

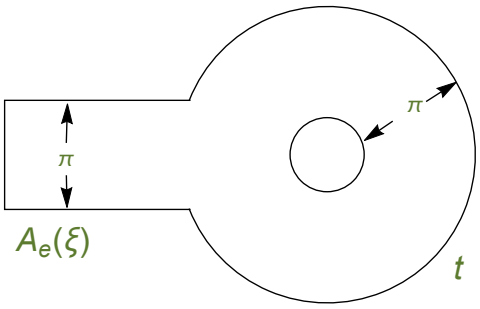

Figure 3.1: The open string tadpole diagram at a given modular parameter t for an external state $A_e(\xi)$ in Moyal space. The width of each strip is fixed to π and the curvature singularities are suppressed.

Following the Feynman rules for OSFT perturbation theory in Moyal space outlined in §2.2.4, we can formally write down the unintegrated amplitude corresponding to an external state $A_e(\xi)$ as follows:

$$\mathcal{I}_e(t) = -\frac{g_o}{3}\int d^d\bar{x}\,\frac{d^dp}{(2\pi)^d}\,\frac{(d\eta)}{(2\pi)^{2dN}}\,(d\eta^{gh})\,\mathrm{Tr}\left[A_e * \left(e^{-i\xi^\top\eta+\xi^{gh\top}\eta^{gh}}e^{-ip\cdot\bar{x}}\right) * \left(e^{-t(L_0-1)}\left(e^{i\xi^\top\eta-\xi^{gh\top}\eta^{gh}}e^{ip\cdot\bar{x}}\right)\right)\right]. \tag{3.1}$$

This will be the starting point for most of our analysis and it follows directly from the gauge fixed action in the Moyal approach (2.65) after choosing the Feynman-Siegel (FS) gauge, and is structurally distinct from the starting expressions in other methods. Here Tr denotes ξ integrations (2.50), $L_0 = L_0^X + L_0^{gh}$ is the total propagator and we have evolved one of the basis states using the e^{-tL_0} operator before taking the overlap implemented by the trace operation.

We have set $l_s = \sqrt{2}$ so that $\alpha' = 1$. Additionally as mentioned in the previous chapter, in the discrete Moyal formalism we may be allowed to rescale the modes appearing in the matter and ghost degrees of freedom in order to set the non-commutativity parameters $\theta = 1 = \theta'$.

The ghost number saturation condition for the Witten vertex dictates a total of $+3$ ghost number charge at each vertex. Since we restrict to off-shell states of ghost number 1, this then leads to the projection onto ghost number $(3-1)/2 = +1$ states for all the states propagating in the loop. Hence, the Fourier basis we chose would be sufficient, with the additional insertion of the ghost zero mode $-\xi_0$ which is always understood to be present.

The expressions for the ghost sector contributions are naturally simpler compared to the matter sector due to the absence of the ghost zero mode c_0 (in the Feynman-Siegel gauge). Additionally, the ghost contribution is in a sense universal. Hence, we restrict to pure ghost external states in this section and consider the matter contribution later in appendix

B. As discussed in §2.2.3, the fields we consider would now be of the form $\wp(\xi^{gh})A_0^{gh}(\xi^{gh})$, where $\wp(\xi^{gh})$ represents a polynomial in ξ^{gh} and A_0^{gh} is the vacuum monoid defined in (2.61):

$$A_0^{gh} = \mathcal{N}_0 \exp\left[-\xi^{gh\top} M_0^{gh} \xi^{gh} - \xi^{gh\top} \lambda^{gh}\right] \tag{3.2}$$

These integrands may therefore be obtained by evaluating from a generating functional $\mathcal{W}(\lambda^{gh}, t)$ dependent on an element valued in the monoid subalgebra

$$A_1(\xi^{gh}) = \mathcal{N} \exp\left[-\xi^{gh\top} M_0^{gh} \xi^{gh} - \xi^{gh\top} \lambda^{gh}\right], \tag{3.3}$$

differentiating with respect to this parameter λ^{gh} appropriately and then setting it to zero at the end of a calculation:

$$\wp(\xi^{gh})A_0^{gh} = \left(\wp\left(-\frac{\vec{\partial}}{\partial\lambda^{gh}}\right) A_1\right)\Big|_{\lambda^{gh}=0}, \tag{3.4}$$

as done in usual quantum field theory calculations. Hence, it would be sufficient to analyse the class of monoids of the form $A_1(\xi^{gh})$. Furthermore, we restrict $A_e(\xi^{gh})$ to be in the $SU(1,1)$ singlet sector [27][20, Appendix H] of twist even pure ghost excitations, since the tadpole state is a twist even singlet.

Method of evaluation

Interchanging the order of integration (between η and ξ) in (3.1) and using associativity of the $*$ product allows us to obtain various formally equivalent expressions:

(a) $A_1 * A_2 \to A_{12}[\eta, \xi] \to A_{12}A_3(t) \to \mathrm{Tr} \to \int d\eta$

(b) $A_2 * A_3(t) \to A_{23}[\eta, \xi, t] \to \int d\eta \to A_1 A'_{23}[\xi, t] \to \mathrm{Tr}$

(c) $A_2 * A_3(t) \to A_{23}[\eta, \xi, t] \to A_1 A_{23} \to \mathrm{Tr} \to \int d\eta$,

(d) $A_3(t) * A_1 \to A_{31}[\eta, \xi, t] \to A_{31}A_2 \to \mathrm{Tr} \to \int d\eta$, and

(e) $A_3(t) * A_1 \to A_{31}[\eta, \xi, t] \to A_{31}A_2 \to \int d\eta \to \mathrm{Tr}$,

where the last two are possible due to the cyclicity of the trace.

We choose the first sequence due to its relative simplicity. The second one allows us to identify the Fock space state by integrating $A'_{23}(\xi)$ with $|\xi\rangle$ but it involves a somewhat complicated inverse nested inside another inverse which makes direct evaluations difficult. It does lead to the correct behaviour near $t = 0$ as we shall mention in §3.4 while examining associativity. The remaining forms result in awkward expressions that turn out to be rather unwieldy for our purposes.

If one employs the finite N regularization from §2.2.3 and makes the assumption that all physical quantities appear as Cauchy sequences in N, one can ensure uniform convergence of the integrand as a function of t. Perhaps this could justify some of the algebraic manipulations we use, but in general one cannot avoid subtleties associated with order of limits, namely the non-analyticities from closed string physics may be extracted only in the open string limit. We shall return to this point in the later sections.

3.1.1 Overlap amplitude in Moyal space

After this preparation, let us list the three monoid elements appearing in the amplitude along with their parameters:

$$A_1^{gh} = \mathcal{N}_0 \exp\left[-\xi^{gh\top} M_0^{gh} \xi^{gh} - \xi^{gh\top} \lambda^{gh}\right], \quad M_1 = M_0^{gh}, \quad \lambda_1 = \lambda^{gh}, \quad \mathcal{N}_1 = \mathcal{N}_0^{gh}, \tag{3.5a}$$

$$A_2^{gh} = e^{+\xi^{gh\top}\eta^{gh}}, \qquad M_2 = 0, \qquad \lambda_2 = -\eta^{gh}, \quad \mathcal{N}_2 = 1, \tag{3.5b}$$

$$A_3^{gh} = e^{-\xi^{gh\top}\eta^{gh}}, \qquad M_3 = 0, \qquad \lambda_3 = +\eta^{gh}, \quad \mathcal{N}_3 = 1. \tag{3.5c}$$

Here we recall that M_0^{gh} is a symmetric matrix but the metric in ghost space is set to be $+i\varepsilon_{ab}$ (with $\varepsilon_{12} = -1 = -\varepsilon_{21}$) and hence the full structure of the matrix for the quadratic term is of the form $-i\varepsilon \otimes M_0^{gh}$. This makes the combination an anti-symmetric matrix, as required for anti-commuting degrees of freedom. Additionally, we have suppressed a metric factor in the linear term $\xi^{gh\top}\lambda^{gh}$, whose explicit form is $\xi^{gh\top}(-i\varepsilon \otimes \mathbb{1}_{2N})\lambda^{gh}$.
To commence evaluation, we first take the $*$ product of A_1 and A_2 to obtain:

$$A_{\mathcal{N}_{12}, M_{12}, \lambda_{12}} \coloneqq A_{\mathcal{N}_1, M_1, \lambda_1} * A_{\mathcal{N}_2, M_2, \lambda_2} \tag{3.6}$$

This can be written down by applying the monoid algebra relations given in [19, 20, 26] by Bars et al. and mentioned briefly in in §2.2.3. Given two monoid elements in Moyal space, $A_1(\xi)$ and $A_2(\xi)$ from the class of shifted Gaussians (quadratic exponentials with a linear term), the string field obtained through the $*$ operation is parametrized by [19, 26] which we provide here again for convenience:

$$m_{12} = (m_1 + m_2 m_1)(1 + m_2 m_1)^{-1} + (m_2 - m_1 m_2)(1 + m_1 m_2)^{-1}, \tag{3.7a}$$

$$\lambda_{12} = (1 - m_1)(1 + m_2 m_1)^{-1}\lambda_2 + (1 + m_2)(1 + m_1 m_2)^{-1}\lambda_1, \tag{3.7b}$$

$$\mathcal{N}_{12} = \mathcal{N}_1 \mathcal{N}_2 \det(1 + m_2 m_1) \exp\left[+\frac{1}{4}\lambda_\alpha^{gh\top} \sigma K_{\alpha\beta} \lambda_\beta^{gh}\right] \text{ where,} \tag{3.7c}$$

$$K_{\alpha\beta} = \begin{bmatrix} (m_1 + m_2^{-1})^{-1} & (1 + m_2 m_1)^{-1} \\ -(1 + m_1 m_2)^{-1} & (m_2 + m_1^{-1})^{-1} \end{bmatrix}, \qquad m_i \coloneqq M_i \sigma. \tag{3.7d}$$

Applying this rule to the two string fields for our case in (3.6) immediately leads to the parameters:

$$\begin{aligned} A_{12}(\xi^{gh}) &\coloneqq \mathcal{N}_{12}\exp(-\xi^{gh\top}M_{12}^{gh}\xi^{gh}-\xi^{gh\top}\lambda_{12}),\ \text{where}\\ M_{12} &= M_0^{gh},\quad \lambda_{12} = -(1-m_0^{gh})\eta^{gh}+\lambda^{gh},\\ \mathcal{N}_{12} &= \mathcal{N}_0\exp\left(\frac{1}{4}\eta^{gh\top}\sigma m_0^{gh}\eta^{gh}-\frac{1}{2}\lambda^{gh\top}\sigma\eta^{gh}\right). \end{aligned} \tag{3.8}$$

where we have used $K_{11}=0, K_{12}=1=-K_{21}$ and $K_{22}=m_0^{gh}$ and once again the ghost space metric is implicit.

Next, we need the t evolved monoid element $A_3(\xi^{gh},\eta^{gh},t)$, for which we use the action of L_0^{gh} on a general monoid element $\mathcal{N}e^{-\xi^{gh\top}M^{gh}\xi^{gh}-\xi^{gh\top}\lambda^{gh}}$. Unfortunately, the Virasoro operator L_0^{gh} is no longer diagonal in this basis:

$$L_0^{gh} = \mathrm{Tr}\tilde{\kappa}^{gh} - \frac{1}{4}\left(\frac{\partial}{\partial\xi^{gh}}\right)^{\top} M_0^{gh-1}\tilde{\kappa}^{gh}\left(\frac{\partial}{\partial\xi^{gh}}\right) + \xi^{gh\top}\tilde{\kappa}^{gh}M_0^{gh}\xi^{gh} \tag{3.9}$$

unlike the oscillator case: The simplicity in the interaction term has made the kinetic term complicated. Hence L_0^{X+gh} has a non-trivial action on the string fields, which can however be written down in closed form. This leads to the following transformation rules [20] in terms of hyperbolic functions of the "spectral matrix" $\tilde{\kappa}^{gh}$ (2.82):

$$A(t) \coloneqq e^{-tL_0^{gh}}A_{\mathcal{N}^{gh},M^{gh},\lambda^{gh}}(\xi^{gh}) = \mathcal{N}(t)\exp\left(-\xi^{gh\top}M^{gh}(t)\xi^{gh}-\xi^{gh\top}\lambda^{gh}(t)\right),\quad \text{where} \tag{3.10a}$$

$$M^{gh}(t) = \left[\sinh t\tilde{\kappa}^{gh} + \left(\sinh t\tilde{\kappa}^{gh} + M_0^{gh}M^{gh-1}\cosh t\tilde{\kappa}^{gh}\right)^{-1}\right]\mathrm{sech}\, t\tilde{\kappa}^{gh}M_0^{gh}, \tag{3.10b}$$

$$\lambda^{gh}(t) = \left[\cosh t\tilde{\kappa}^{gh} + M^{gh}M_0^{gh-1}\sinh t\tilde{\kappa}^{gh}\right]^{-1}\lambda^{gh}, \tag{3.10c}$$

$$\begin{aligned} \mathcal{N}^{gh}(t) = \mathcal{N}^{gh}&\exp\left[+\frac{1}{4}\lambda^{gh\top}(M^{gh}+\coth t\tilde{\kappa}^{gh})^{-1}\lambda^{gh}\right]\\ &\times\det\left[\frac{1}{2}(1+M^{gh}M_0^{gh-1})+\frac{1}{2}(1-M^{gh}M_0^{gh-1})e^{-2t\tilde{\kappa}^{gh}}\right], \end{aligned} \tag{3.10d}$$

a very similar expression to the one in matter sector (2.67) §B, except for the extra dependence on the zero mode momentum p^μ and the vector w for the matter case. Notice that the correct boundary conditions for $t=0$ and $t=\infty$ are taken into account in the above rules.

Now, applying this transformation on (3.5c), for which the matrix of parameters M_0^{gh} vanishes, we readily obtain the string field:

$$A_3(t) = \mathcal{N}_3(t)\exp\left(-\xi^{gh\top}M_3(t)\xi^{gh}-\xi^{gh\top}\lambda_3(t)\right),\quad \text{with parameters}$$

$$M_3(t) = \tanh t\tilde{\kappa}^{gh} M_0^{gh}, \quad \lambda_3(t) = +\mathrm{sech}(t\tilde{\kappa}^{gh})\ \eta^{gh},$$
$$\mathcal{N}_3(t) = 2^{-2N}\prod_{n=1}^{2N}(1+e^{-2tn})\exp\left(\frac{1}{4}\eta^{gh\top}M_0^{gh-1}\tanh t\tilde{\kappa}^{gh}\eta^{gh}\right). \tag{3.11}$$

We can now use the property that the remaining $*$ product between A_{12} and $A_3(t)$ may be dropped as total derivative pieces contribute only to boundary terms under a trace (ξ integration with appropriate measure factors inserted). We therefore define a new string field configuration $A_{12}A_3(t) =: A_{123}^{gh}(t)$, under the ordinary (local) product in function space, with parameters:

$$\begin{aligned} M_{123}(t) &= M_{12} + M_3(t), \\ \lambda_{123}(t) &= \lambda_{12} + \lambda_3(t), \\ \mathcal{N}_{123}(t) &= \mathcal{N}_{12}\cdot\mathcal{N}_3(t). \end{aligned} \tag{3.12}$$

Hence, the trace in (3.1) simply results in

$$\begin{aligned} \mathrm{Tr}[A_{123}(t)] &= \mathcal{N}_{123}\det(2M_{123}(t))\exp\left[+\frac{1}{4}\lambda_{123}^{\top}M_{123}^{-1}\lambda_{123}\right] \\ &=: \mathcal{C}_\eta \exp\left[-\eta^{gh\top}\mathcal{Q}_\eta\eta^{gh} + \lambda^{gh\top}\mathcal{L}_\eta^{\top}\eta^{gh}\right]. \end{aligned} \tag{3.13}$$

In order to perform the remaining Gaussian integration over η^{gh}, we have separated the quadratic, linear and zero degree terms in η^{gh} by collecting the contributions from $\mathcal{N}_{123}$ and the argument of the exponential in the first line of (3.13) above. In terms of the matrices that are used in the Moyal representation §2.4, these are given by:

$$\begin{aligned} \mathcal{Q}_\eta(t) = -\frac{1}{4}\Big[&\sigma m_0^{gh} + \sigma m_0^{gh-1}\tanh t\tilde{\kappa}^{gh} \\ &+ (m_0^{gh\top} + \mathrm{sech}t\tilde{\kappa}^{gh\top} - 1)\sigma m_0^{gh-1}(1+\tanh t\tilde{\kappa}^{gh})^{-1}(m_0^{gh} + \mathrm{sech}\, t\tilde{\kappa}^{gh} - 1)\Big], \end{aligned} \tag{3.14a}$$

$$\mathcal{L}_\eta^{\top}(t) = -\frac{1}{2}\sigma\left[1 + m_0^{gh-1}(1+\tanh t\tilde{\kappa}^{gh})^{-1}(1 - m_0^{gh} - \mathrm{sech}\, t\tilde{\kappa}^{gh})\right], \tag{3.14b}$$

$$\begin{aligned} \mathcal{C}_\eta(t) &= \mathcal{N}_0\det(2M_0)\exp\left[+\frac{1}{4}\lambda^{gh\top}M_{123}^{-1}\lambda^{gh}\right] \\ &= \det(M_0)^{\frac{1}{2}}\exp\left[+\frac{1}{4}\lambda^{gh\top}M_0^{-1}(1+\tanh t\tilde{\kappa}^{gh})^{-1}\lambda^{gh}\right]. \end{aligned} \tag{3.14c}$$

where we have used the subscript η to specify the variable in the quadratic form, a convention we shall be following from now onwards[1].

[1]Here we point out that the $+ve$ sign in the exponential factor in the first line of (3.13) is different from the usual $-ve$ sign for Grassmannian Gaussian integral, since the antisymmetric metric factor ε

At this point it is convenient to introduce the (Euclidean) nome $q = e^{+2\pi i\tau} = e^{-t}$ and the functions:

$$\begin{aligned} f_1(n;q) &= (1-q^n)^2, & f_2(n;q) &= 1+q^{2n}, \\ f_3(n;q) &= 1-q^{2n}, & f_4(n;q) &= (1-q^n)(3-q^n) = \frac{f_1^2+2f_3}{f_2}, \end{aligned} \tag{3.16}$$

in order to convert the hyperbolic functions to exponentials for typographical simplicity. We can then rewrite the coefficient matrices obtained above in terms of the matrix functions $f_i(\tilde{\kappa}^{gh};q)$. These have block diagonal structure but contain non-diagonal matrices in the upper block. Additionally, they do *not* commute with matrices such as m_0^{gh} and M_0^{gh}. However, using matrix relations such as

$$\tilde{\kappa}^{gh\top} = (M_0^{gh})^{-1}\tilde{\kappa}^{gh}M_0^{gh}, \quad m_0^{gh\top} = -\sigma M_0^{gh}, \text{ and } \qquad \sigma\begin{bmatrix}\alpha_1 & 0\\ 0 & \alpha_2\end{bmatrix}\sigma = \begin{bmatrix}\alpha_2 & 0\\ 0 & \alpha_1\end{bmatrix} \tag{3.17}$$

for block diagonal matrices, one can simplify the above expressions for η^{gh} coefficients as

$$\begin{aligned} \mathcal{Q}_\eta(q) &= -\frac{1}{4}\left(\sigma M_0^{gh}\sigma + M_0^{gh-1}\frac{f_3(q)}{f_2(q)}\right) - \frac{1}{8}\left(M_0^{gh-1}\frac{f_1^2(q)}{f_2(q)} - \sigma f_2(q)M_0^{gh}\sigma + \sigma f_1(q) - f_1(q)^\top\sigma\right) \\ &= -\frac{1}{8}\big(\sigma f_3(q)M_0^{gh}\sigma + M_0^{-1}f_4(q) + \sigma f_1(q) - f_1(q)^\top\sigma\big), \end{aligned} \tag{3.18}$$

$$\mathcal{L}_\eta(q) = \frac{1}{4}\sigma f_3(q) - \frac{1}{4}f_1(q)^\top M_0^{gh-1}, \tag{3.19}$$

where we have dropped one argument of $f_i(q;\tilde{\kappa}^{gh})$ as shall be done in other places as well for typographical simplicity.

Let us also mention that these functions simply appear through intermediate expressions[2]of the form

$$(1+\tanh t\tilde{\kappa}^{gh})^{-1} = e^{-t\tilde{\kappa}^{gh}}\cosh t\tilde{\kappa}^{gh} = \frac{1}{2}f_2, \tag{3.20a}$$

$$1-\operatorname{sech} t\tilde{\kappa}^{gh} = \frac{f_1}{f_2}, \tag{3.20b}$$

$$e^{-t\tilde{\kappa}^{gh}}\big(\cosh t\tilde{\kappa}^{gh} + \operatorname{sech} t\tilde{\kappa}^{gh} - 2\big) = \frac{f_1^2}{2f_2}. \tag{3.20c}$$

adjoining λ_{123} produces an extra -ve sign upon taking a transpose. Explicitly, we have the following signs:

$$(-i\varepsilon)^\top(-i\varepsilon)^{-1}(-i\varepsilon) = -(-i\varepsilon). \tag{3.15}$$

Since we insist on using an $-i\varepsilon$ metric in ghost space, there is the extra $-ve$ sign which makes the exponential part in the Gaussian integral identical to the matter sector.

[2]Yet another useful relation is

$$f_1^2 + f_3^2 = 2f_1f_2.$$

Additionally, we can obtain the half-angle relations by noting that $f_3(n;q) = f_2(n;\sqrt{q})\, f_3(n;\sqrt{q})$. Finally, we perform the integration over η^{gh} (3.13) to obtain a purely quadratic functional dependence on λ^{gh} in the exponential of the form $+\frac{1}{4}\lambda^{gh\top}\mathcal{F}\lambda^{gh}$, where the matrix $\mathcal{F}$ in the ghost sector can be written as

$$\mathcal{F}(t) = M_{123}^{-1}(t) + \mathcal{L}_\eta^\top \mathcal{Q}_\eta^{-1}\mathcal{L}_\eta. \tag{3.21}$$

Here, the first term M_{123}^{-1} arises from the η^{gh} independent overall factor $\mathcal{C}_\eta(t)$ in (3.14c) defined above.

Collecting all the factors together, the ghost contribution to the generating functional $W[\lambda, \lambda^{gh}, t]$ is given by:

$$\mathcal{W}[\lambda^{gh}, t] = (1 + w^\top w)^{\frac{1}{4}} \det(2\mathcal{Q}_\eta^{gh}) \exp\left[+\frac{1}{4}\lambda^{gh\top}\mathcal{F}\lambda^{gh}\right]. \tag{3.22}$$

We shall include the matter sector contribution from appendix B, which is obtained through a very similar computation—with the only difference being the integration over the zero mode momenta p^μ along the Neumann directions, and the use of a different set of constant matrices for defining the monoid elements. The matter contribution to the generating functional serves to provide a consistency check for our analytical expressions. Only the determinant factors need be included in numerical checks when considering overlap with the perturbative vacuum state $|\hat{\Omega}\rangle = \hat{c}_1|\Omega\rangle$. And for purely ghost excitations, we use this scalar piece for the matter sector—it contributes to the measure factor and does not affect the structure of the $\mathbf{R}_{nm}(q)$ factors in (2.75), that we are primarily interested in.

Finally, the total matter+ghost generating functional has the structure:

$$\mathcal{W}[\lambda^X, \lambda^{gh}, t] = \left(1 + ww^\top\right)^{\frac{d+2}{8}} e^t \frac{\det(2\mathcal{Q}_\eta)}{|\det(2\mathcal{Q}_\psi)|^{d/2}} \exp\left[\frac{1}{4}\left(\lambda^{X\top}\mathcal{F}_X\lambda^X + \lambda^{gh\top}\mathcal{F}_{gh}\lambda^{gh}\right)\right] \tag{3.23}$$

where X denotes the matter part from the embedding coordinates $X^\mu(z)$, have combined the conjugate variables η^X and p into a single "vector"

$$\psi := \begin{pmatrix} \eta^X \\ p \end{pmatrix}$$

and denoted the matter coefficient matrix $\mathcal{Q}$ with the subscript ψ.

3.1.2 Block matrices

Next, we can consider the block structure of the matrices $\mathcal{Q}_\eta, \mathcal{L}_\eta$, and $\mathcal{F}_{gh}$. To this end, we recall that the matrices M_0^{gh} and $\tilde{\kappa}^{gh}$ (given in §2.4) take the block diagonal form:

$$M_0^{gh} = -\frac{1}{2}\begin{bmatrix} R^\top \kappa_o R & 0 \\ 0 & 4\kappa_e^{-1} \end{bmatrix}, \qquad \tilde{\kappa}^{gh} = \begin{bmatrix} R^\top \kappa_o T^\top & 0 \\ 0 & \kappa_e \end{bmatrix}. \tag{3.24}$$

We remark that the M_0^{gh} above is given by $i \times M_0^{gh}$ as compared to the one given in [20] whereas the matrix $\tilde{\kappa}^{gh}$ remains the same. Then the $2N \times 2N$ coefficient matrices have the explicit constituent block structure:

$$\begin{aligned} \mathcal{Q}_\eta(q) &= +\frac{1}{4}\begin{bmatrix} \kappa_e^{-1} f_3(\kappa_e) + T\kappa_o^{-1} f_4(\kappa_o) T^\top & -\frac{i}{2}\left[f_1(\kappa_e) - T f_1(\kappa_o) R\right] \\ -\frac{i}{2}\left[f_1(\kappa_e) - R^\top f_1(\kappa_o) T^\top\right] & \frac{1}{4}\left[\kappa_e f_4(\kappa_e) + R^\top \kappa_o f_3(\kappa_o) R\right] \end{bmatrix}, \text{ and} \\ \mathcal{L}_\eta(q) &= \frac{1}{2}\begin{bmatrix} T\kappa_o^{-1} f_1(\kappa_o) T^\top & \frac{i}{2} f_3(\kappa_e) \\ -\frac{i}{2} R^\top f_3(\kappa_o) T^\top & \frac{1}{4}\kappa_e f_1(\kappa_e) \end{bmatrix}, \end{aligned} \tag{3.25}$$

where again the blocks are labelled by half-phase space degrees of freedom $(x_e^{c,b}, p_e^{c,b})$.

Let us observe that the infinite sums over the odd integers κ_o in all the four blocks of $\mathcal{Q}_\eta$ diverge badly for $t < 0$ since the functions f_1, f_3, and f_4 are unbounded as κ_o increases. Hence, these matrix elements are not analytic in a neighbourhood of 0. Only the $t \to 0^+$ limit is well-defined for which the matrix $\mathcal{Q}_\eta$ vanishes due to the zeroes of the functions f_1, f_3 and f_4 at that point (as we shall discuss below). Strictly speaking, this prevents the expansion we seek involving $\mathcal{Q}_\eta^{-1}$. However, the matrix $\mathcal{L}(t)$ also vanishes at $t = 0$ due to the zeroes in f_1 and f_3. Hence, the combination $\mathcal{L}(t)^\top \mathcal{Q}(t)^{-1} \mathcal{L}(t)$ in $\mathcal{F}(t)$—which does involve infinite sums—can be taken to vanish at $t = 0$ for the purpose of this work. This behaviour signals that the expansion we obtain may be asymptotic and not a convergent expansion, owing to this non C^∞ nature.

Additionally, we notice that in the open string limit $N \to \infty$, the order of the pole from the combined determinant factors, $\mathcal{Q}_\eta$ and $\mathcal{Q}_\psi$ in (3.23), becomes infinite as well. This is consistent with our expectations of an essential singularity at $t = 0$ associated with the Shapiro-Thorn closed string tachyon state in (1.1).

In general, due to the relatively simple structure of the T matrix, we can expect combinations of the generalized hypergeometric functions, ${}_JF_{J-1}$, to arise from the infinite sums in $\mathcal{Q}_\eta$. The non-analyticity in $\mathcal{Q}_\eta$ matrix elements would then be a log branch cut. The non-diagonal terms, with $n \neq m$ are of the form:

$$\begin{aligned} \mathcal{Q}^{xx}_{2n,2m} = \frac{(-1)^{m+n}}{4\pi^2(m^2-n^2)} \Bigg\{ q\Bigg(q\Bigg(\Phi\left(q^4, 1, \frac{1}{2} - m\right) - \Phi\left(q^4, 1, \frac{1}{2} - n\right) + \Phi\left(q^4, 1, m + \frac{1}{2}\right) \\ - \Phi\left(q^4, 1, n + \frac{1}{2}\right)\Bigg) - 4\Phi\left(q^2, 1, \frac{1}{2} - m\right) + 4\Phi\left(q^2, 1, \frac{1}{2} - n\right) - 4\Phi\left(q^2, 1, m + \frac{1}{2}\right) \end{aligned}$$

$$+4\Phi\left(q^2,1,n+\frac{1}{2}\right)\Big)-3\psi^{(0)}\left(m+\frac{1}{2}\right)-3\psi^{(0)}\left(\frac{1}{2}-m\right)$$
$$+3\psi^{(0)}\left(n+\frac{1}{2}\right)+3\psi^{(0)}\left(\frac{1}{2}-n\right)\Big\}, \tag{3.26a}$$

$$\mathcal{Q}^{xp}_{2n,2m}=\frac{-i(-1)^{n+m}mq}{4\pi^2n(m^2-n^2)}\Big\{-nq\Phi\left(q^4,1,\frac{1}{2}-m\right)+mq\Phi\left(q^4,1,\frac{1}{2}-n\right)+2n\Phi\left(q^2,1,\frac{1}{2}-m\right)$$
$$-2m\Phi\left(q^2,1,\frac{1}{2}-n\right)+nq\Phi\left(q^4,1,m+\frac{1}{2}\right)-mq\Phi\left(q^4,1,n+\frac{1}{2}\right)$$
$$-2n\Phi\left(q^2,1,m+\frac{1}{2}\right)+2m\Phi\left(q^2,1,n+\frac{1}{2}\right)\Big\}, \tag{3.26b}$$

$$\mathcal{Q}^{pp}_{2n,2m}=\frac{(-1)^{n+m}}{4\pi^2(m^2-n^2)}\Big\{m^2\left(H_{-n-\frac{1}{2}}+H_{n-\frac{1}{2}}\right)-n^2\left(H_{-m-\frac{1}{2}}+H_{m-\frac{1}{2}}\right)$$
$$+q^2m^2\left(\Phi\left(q^4,1,\frac{1}{2}-n\right)+\Phi\left(q^4,1,n+\frac{1}{2}\right)-q^2n^2\left(\Phi\left(q^4,1,\frac{1}{2}-m\right)+\Phi\left(q^4,1,m+\frac{1}{2}\right)\right)\right)$$
$$+4\left(n^2-m^2\right)\tanh^{-1}\left(q^2\right)+4\log(2)(m^2-n^2)\Big\} \tag{3.26c}$$

while the diagonal matrix elements are given by:

$$\mathcal{Q}^{xx}_{2n,2n}=\frac{1}{8\pi^2n}\Big\{q\left(q\Phi\left(q^4,2,\frac{1}{2}-n\right)-4\Phi\left(q^2,2,\frac{1}{2}-n\right)-q\Phi\left(q^4,2,n+\frac{1}{2}\right)+4\Phi\left(q^2,2,n+\frac{1}{2}\right)\right)$$
$$-\pi^2\left(q^{4n}-1\right)+3\psi^{(1)}\left(\frac{1}{2}-n\right)-3\psi^{(1)}\left(n+\frac{1}{2}\right)\Big\}, \tag{3.27a}$$

$$\mathcal{Q}^{xp}_{2n,2n}=\frac{i}{8\pi^2n}\Big\{q\left(-q\Phi\left(q^4,1,\frac{1}{2}-n\right)+nq\Phi\left(q^4,2,\frac{1}{2}-n\right)+2\Phi\left(q^2,1,\frac{1}{2}-n\right)\right.$$
$$-2n\Phi\left(q^2,2,\frac{1}{2}-n\right)+q\Phi\left(q^4,1,n+\frac{1}{2}\right)+nq\Phi\left(q^4,2,n+\frac{1}{2}\right)-2\Phi\left(q^2,1,n+\frac{1}{2}\right)$$
$$\left.-2n\Phi\left(q^2,2,n+\frac{1}{2}\right)\right)-\pi^2nq^{2n}\left(q^{2n}-2\right)\Big\}, \tag{3.27b}$$

$$\mathcal{Q}^{pp}_{2n,2n}=\frac{1}{8\pi^2}\Big\{2H_{-n-\frac{1}{2}}+2H_{n-\frac{1}{2}}+2q^2\Phi\left(q^4,1,\frac{1}{2}-n\right)-nq^2\Phi\left(q^4,2,\frac{1}{2}-n\right)$$
$$+2q^2\Phi\left(q^4,1,n+\frac{1}{2}\right)+nq^2\Phi\left(q^4,2,n+\frac{1}{2}\right)+\pi^2n\left(-4q^{2n}+q^{4n}+3\right)$$
$$+n\psi^{(1)}\left(\frac{1}{2}-n\right)-n\psi^{(1)}\left(n+\frac{1}{2}\right)-8\tanh^{-1}\left(q^2\right)+8\log(2)\Big\}. \tag{3.27c}$$

In this case, the ${}_JF_{J-1}$ functions get further expressed in terms of Lerch transcendents $\Phi(z,s,a)$, a generalization of the zeta and the polylog functions, defined classically [47] by the infinite series representation:

$$\Phi(z,s,a)=\sum_{n=0}^{\infty}\frac{z^n}{(n+a)^s}. \tag{3.28}$$

In all of the above, the Φ functions with the argument $\Re(a)<0$ is chosen to be the analytic continuation Hurwitz-Lerch Transcendents, which has by definition, an identical

analytic expression[3].

We can now examine some series expansions to notice that these are functions having a leading logarithmic branch cut $t^4 \log t$ for the blocks $\mathcal{Q}^{xx}$ and $\mathcal{Q}^{pp}$, and $t^3 \log(t)$ for the blocks $\mathcal{Q}^{xp} = \mathcal{Q}^{px\top}$:

$$\begin{aligned}
\mathcal{Q}^{pp}_{88} &= 16t - \frac{6612992t^2}{11025\pi^2} + \frac{512t^3}{3} + t^4\left(\frac{4096\log(t)}{3\pi^2} - \frac{365923328}{33075\pi^2} + 1024\right) + O\left(t^5\right), \\
\mathcal{Q}^{xp}_{24} &= -\frac{8it^3(18\log(t) + 19 + 6\log(2))}{9\pi^2} - \frac{2it^5(360\log(t) + 151 + 24\log(2))}{9\pi^2} + O\left(t^6\right). \qquad (3.30)
\end{aligned}$$

Since the three functions $f_{1,3,4}(t)$ have first order zeroes at $t = 0$ (or $q = 1$), and because the single sum over the odd frequencies κ_o still retain the *same order* of zero for both finite and infinite N, we can factor out this zero. Hence, in the open-string limit, corresponding to $N \to \infty$, we can simply[4] divide out by t in order to expand the inverse. The physically correct order of operations would be to consider the expansion only in the open string limit. However, one can also attempt an expansion for the deformed theory defined at finite N, and see where it leads us; since both have similar formal structure. The oscillator counterpart of this issue with order of limits, namely level $L \to \infty$ followed by $t \to 0$ and its reverse, is discussed in [14] (and was reviewed earlier in §2.3) where it was found that the result does differ from BCFT[5] by a factor of 2 already at the leading correction in t.

Let us therefore factor out the parameter $t = -\ln q$ and introduce the two matrices:

$$\mathcal{Z}(q) \coloneqq -\frac{4\mathcal{Q}_\eta(q)}{\ln q}, \quad \mathcal{Y}(q) \coloneqq -\frac{2\mathcal{L}_\eta(q)}{\ln q} \qquad (3.31)$$

in order to rewrite the matrix $\mathcal{F}(q)$ in (3.21) as below:

$$\boxed{\mathcal{F}(q) = \frac{1}{2}(M_0^{gh})^{-1} f_2(q) - \ln q\, \mathcal{Y}(q)^\top \mathcal{Z}(q)^{-1} \mathcal{Y}(q).} \qquad (3.32)$$

This form will turn out to be convenient when we study the behaviour of the matrix $\mathbf{R}(t)$ in the limit $t \to 0^+$ directly in the modular parameter t later in §4.1. The matrix $\mathcal{F}$ has component blocks which would be labelled as $\mathcal{F}^{xx}, \mathcal{F}^{xp} = \mathcal{F}^{px\top}$ and $\mathcal{F}^{pp}$ in terms of the phase space doublet indices (x, p) as usual.

[3]This would differ from the representation in terms of the original Lerch functions, which take the form

$$\Phi^*(z, s, a) = \sum_{n=0}^{\infty} \frac{z^n}{[(n+a)^2]^{s/2}}. \qquad (3.29)$$

for $\Re(a) < 0$, where we omit any term with $n + a = 0$.

[4]We do however expect to miss some of the very interesting non-analyticities of the form $e^{-2j\pi^2/t} = e^{+\frac{2j\pi^2}{\ln q}}$ in our analysis.

[5]Although the oscillator and Moyal representations are formally isomorphic, there are subtle differences due to the special nature of the Witten type vertex. See [22, 23] for a careful discussion of these matters and for a detailed analysis of midpoint issues.

The matrix $\mathcal{Z}(q)$ as it appears above is bounded at $t = 0$ and hence would still be amenable to an expansion. However, the resulting expression for $\mathcal{F}$ need not be analytic because the matrix inverse $\mathcal{Z}(t)^{-1}$ allows for infinite sums that alter the pole-zero structure. Furthermore, there are double infinite sums involved when this is sandwiched between $\mathcal{Y}^\top$ and $\mathcal{Y}$. Perhaps these non-analyticities may be relatable to the closed string states arising in this degeneration limit geometrically. In order to simplify the analysis, we shall restrict to the case when the $\mathcal{Y}$s contribute only diagonal matrices—corresponding to even parity elements—thus eliminating some of the multiple summations. We hope to look at the other cases in more detail when occasion offers itself.

3.1.3 Remarks on determinant factors

In this work, we are primarily interested in the analytic behaviour of the squeezed state matrix $\mathbf{R}(t)$ or equivalently $\mathcal{F}(t)$ in the limit $t \to 0^+$, but as a check on the correctness of our expressions, we shall study the determinant factor numerically in appendix B using similar methods as in [14]. The determinant part corresponds to the overlap with the *perturbative* vacuum state, i.e $|A_e\rangle = |\hat{\Omega}\rangle$: the open string tachyon at zero momentum, and has interesting divergence structure of its own. However, as encountered in [14], it is awkward to study this factor analytically due to the essential singularity at $t = 0$.

The full matrix element contributing to the ghost sector does not lend itself to an expansion because in general each of the matrices whose determinant would be required would appear as a power series starting at degree 0 (constant term). As the minimal degree does not decrease or increase along a row or a column, this form of the determinant proves unwieldy for a systematic expansion. We therefore do not perform a series based analysis of the determinant using the diagonal basis in this work and instead focus on the finite factor from the $\mathbf{R}$ matrix:

$$\langle\hat{\Omega}|\hat{c}_n\hat{b}_m|\mathcal{T}(t)\rangle \sim \mathbf{R}_{nm}(t) \times \det(\cdots; t) \tag{3.33}$$

Additionally, as part of a series of papers on *off-shell* conformal field theory (see [13] and references therein), the N-tachyon scattering case has been studied in great detail by Samuel et al. and addresses these questions much more directly using advanced Riemann surface theory upto the one-loop level. In this approach, the measure factors corresponding to the matter + ghost determinants are evaluated in terms of line integrals involving rational combinations of elliptic functions and their derivatives. It may be possible to extend some of their results to the overlap with a general Fock space state other than the tachyon case considered there.

3.2 Squeezed state matrix elements

In the Siegel gauge, the ghost contribution to the tadpole *state* can be expressed in terms of Fock space kets and Moyal fields as:

$$|\mathcal{T}(t)\rangle = \int d\xi^{gh} \mathcal{T}(\xi^{gh}, t) |\xi^{gh}\rangle. \tag{3.34}$$

Comparing to (3.1), we have the Moyal string field

$$\mathcal{T}(\xi^{gh}, t) \sim \int (d\eta^{gh}) \left[e^{+\xi^\top \eta^{gh}} * (e^{-tL_0^{gh}} e^{-\xi^\top \eta^{gh}}) \right], \tag{3.35}$$

where again we have left the overall sign unfixed and we note that this particular form is only given in the Moyal basis. We transform the expression for $\langle \xi^{gh}|$ in the odd basis given in [20] to the basis labelled by *even* integers, that we use, and write this as a bra:

$$\langle \xi^{gh}| = -2^{-2N} \left(1 + w^\top w\right)^{-\frac{1}{4}} \langle \Omega | \hat{c}_{-1} e^{-\xi_0 (\hat{c}_0 - \sqrt{2} w^\top \hat{c}_e)} e^{-\xi^{gh\top} M_0^{gh} \xi^{gh} - \xi^{gh\top} \lambda^{gh}}, \tag{3.36}$$

as we wrote in (3.36) earlier and where we have the vectors

$$\lambda_1^{gh} = \begin{pmatrix} \sqrt{2} R^\top \hat{b}_o \\ -2\sqrt{2} \kappa_e^{-1} \hat{b}_e + 2\kappa_e^{-1} w \xi_0 \end{pmatrix}, \qquad \lambda_2^{gh} = \begin{pmatrix} \sqrt{2} R^\top \kappa_o \hat{c}_o \\ 2\sqrt{2} i \hat{c}_e \end{pmatrix}, \tag{3.37}$$

and M_0^{gh} is the matrix defining the perturbative ghost vacuum A_0^{gh}:

$$M_0^{gh} = -\frac{1}{2} \mathrm{Diag}\{R^\top \kappa_o R, 4\kappa_e^{-1}\}.$$

We remind the reader of the metric convention we have been using—where the $-i\varepsilon$ factor is implicit—and hence $\xi^{gh\top} M_0^{gh} \xi^{gh} = -2i \xi^{1\top} M_0^{gh} \xi^2$ as well as $\xi^{gh\top} \lambda^{gh} = -i(\xi^{1\top} \lambda^2 - \xi^{2\top} \lambda_1)$.

To probe the structure of the state $|\mathcal{T}(t)\rangle$, one usually finds its overlap with various Fock space basis states $\langle \varphi|$. Hence, we must consider the corresponding overlap amplitudes in Moyal space and then transform back to Fock space.

In order to convert the amplitude written in Moyal space, (3.1) to the one in terms of Fock space states, we need to construct the appropriate perturbative string fields $A_e(\xi)$. To this end, we give the corresponding expressions[6] in the oscillator formalism:

$$\langle A_e | \mathcal{T}(t) \rangle \sim \int d\xi \, \langle A_e | \xi^{gh} \rangle \langle \xi^{gh} | \mathcal{T}(t) \rangle, \tag{3.38}$$

where we have denoted the external state by $|A_e\rangle$ and introduced a complete set of states $\langle \xi^{gh}|$—the appropriately normalized bra defining the Moyal basis in ghost space to be

[6] Upto a t independent normalization factor to which we return in §4.3.3.

given below in (3.36).

We recall that we can restrict to the $SU(1,1)$ symmetric [27] combination of pure ghost external states, since the tadpole state is a singlet under this symmetry. In particular, the matrix $\mathbf{R}_{nm}$ defining the quadratic form in the exponential of the squeezed state satisfies:

$$m\,\mathbf{R}_{nm} = n\,\mathbf{R}_{mn}, \tag{3.39}$$

i.e $\mathbf{R}\,\kappa$ is a symmetric matrix. This does not demand the full $SU(1,1)$ but can be achieved by restricting to the discrete $\mathbb{Z}_4$ subgroup.

3.2.1 $\hat{\beta}$ oscillators

The relation between the matrix elements $\mathcal{F}_{nm}$ corresponding to the half-phase space degrees of freedom ξ^{gh} and the usual Fock space matrix elements $\mathbf{R}_{nm}(t)$ can be obtained by using the form of the $\hat{c}_n, \hat{b}_n$ oscillators in the diagonal basis. To this end, we must employ the action of the linear maps between the two bases on these operators. The Moyal images of the Fock space states can be obtained by acting on the vacuum monoid with the so-called $\hat{\beta}$ oscillators:

$$\hat{c}_n \mapsto \hat{\beta}^c_n, \qquad \hat{b}_n \mapsto \hat{\beta}^b_n, \qquad \text{where } \ \hat{\beta}_{\mathcal{O}} A(\xi) \coloneqq \langle \xi | \hat{\mathcal{O}} | \psi \rangle. \tag{3.40}$$

These are thus simply the counterparts for $\hat{c}_n, \hat{b}_n$ and the usual $\hat{\alpha}$ oscillators (in the matter sector) used in bosonic string theory and may be expressed either as *differential operators* or phase space *fields* with left and right $*$ action on the string field in the ξ basis. We choose the differential operator representation in our discussion that follows.

In [20], the oscillators are given for the *odd* parity degrees of freedom x^o, p^o, y^o and q^o, that can also be used to represent the *bc* ghost system in the Moyal language. We have applied the canonical transformation that takes the odd basis to the even basis (§2.2) to rewrite them as follows:

$$\begin{aligned}
\hat{\beta}^c_e &\coloneqq \frac{1}{\sqrt{2}}\left[-\frac{2i}{\theta'}\,\mathrm{sgn}(e)\kappa_e^{-1} p^b_{|e|} + \frac{\theta'}{2}\frac{\partial}{\partial p^c_{|e|}}\right], & \hat{\beta}^c_o &\coloneqq \frac{1}{\sqrt{2}}\left[R_{|o|e} x^c_e - i\,\mathrm{sgn}(o) S^{\top}_{|o|e}\kappa_e^{-1}\frac{\partial}{\partial x^b_e}\right],\\
\hat{\beta}^b_e &\coloneqq \frac{1}{\sqrt{2}}\left[\frac{2}{\theta'} p^c_{|e|} - i\,\mathrm{sgn}(e)\frac{\theta'}{2}\kappa_e\frac{\partial}{\partial p^b_{|e|}}\right], & \hat{\beta}^b_o &\coloneqq \frac{1}{\sqrt{2}}\left[-i\,\mathrm{sgn}(o) S^{\top}_{|o|e}\kappa_e x^b_e + T^{\top}_{|o|e}\frac{\partial}{\partial x^c_e}\right],
\end{aligned} \tag{3.41}$$

where we have restored the non-commutativity parameter θ' for the ghost sector and the summations over repeated indices are restricted to only the positively modded variables.[7]

[7] We only give the ghost parts without the zero-mode contribution since once we have chosen the Siegel gauge, only this form would be relevant to the discussion that follows.

We remind the reader that the matrix S_{eo} arises naturally while defining the Moyal product in the ghost sector and simply equals $S_{eo} = \kappa_e T_{eo} \kappa_o^{-1}$. It also satisfies $SS^\top = \mathbb{1}_e, S^\top S = \mathbb{1}_o$, which can be proven from the properties of the T and R matrices.

3.2.2 The ghost sector matrix $\mathbf{R}(t)$

The $\hat{\beta}^{c,b}_{e,o}, \hat{\beta}^{X}_{e,o}$ oscillators can now be directly used to construct the perturbative string fields $A_e(\xi, \xi^{gh})$ that correspond to the matrix elements $\mathbf{R}_{nm}(t)$ (and $\mathbf{M}_{nm}(t)$ in the matter sector) when written in terms of Fock space states. The pure ghost fields would be of the form

$$\wp(\xi^{gh}) A_0^{gh}(\xi^{gh})$$

where $\wp(\xi^{gh})$ is an appropriately normalized polynomial, which would be the analogue of Hermite polynomials acting on Gaussians in a representation in terms of position space functionals $\Phi[X^\mu(\sigma), c(\sigma)]$.

In terms of these, the relevant matrix elements get mapped to the following Moyal polynomials with ghost bilinear pieces:

$$\mathbf{R}_{ee'} \leftarrow -\delta_{ee'} + \frac{8i}{\kappa_{e'}} p^c_e p^b_{e'}, \tag{3.42a}$$

$$\mathbf{R}_{oo'} \leftarrow \delta_{oo'} + 2i(\kappa_o R x^b x^{c\top} R^\top)_{oo'}, \tag{3.42b}$$

$$i\mathbf{R}_{eo} \leftarrow -4i(p^c x^{c\top} R^\top)_{eo}, \tag{3.42c}$$

$$i\mathbf{R}_{oe} \leftarrow +4i(\kappa_o R x^b p^{b\top})_{oe}. \tag{3.42d}$$

acting on the perturbative vacuum field (as an ordinary product). We know that the mixed parity cases $\mathbf{R}_{eo}, \mathbf{R}_{oe}$ terms[8] vanish identically which reflects the *twist* symmetry of the tadpole state $|\mathcal{T}\rangle$. This can also be seen numerically as we have verified. We remark in passing that we can also obtain the matrix elements for the matter part by using the oscillators given in [26] as:

$$\mathbf{M}_{ee'} \leftarrow -\big(\kappa_e \delta_{ee'} - \kappa_e \kappa_{e'} x_e x_{e'}\big) \tag{3.43a}$$

$$i\mathbf{M}_{eo} = i\mathbf{M}_{oe} \leftarrow \big(4\kappa_e x_e (p^\top T)_o\big) \tag{3.43b}$$

$$\mathbf{M}_{oo\prime} \leftarrow \big(\kappa_o \delta_{oo'} - 16(p^\top T)_o (p^\top T)_{o'}\big) \tag{3.43c}$$

which may be useful for future applications.

Now that we know the required form of the polynomials, we can proceed to construct them starting from the generating string field $A_1(\xi^{gh}, \lambda^{gh})$ given in (3.3) using

[8] In the above, we have inserted extra factors of i in the mixed parity cases to make the string fields real.

$$\wp(\xi^{gh})A_0 = \left(\wp\left(-\frac{\vec{\partial}}{\partial\lambda^{gh}}\right)A_1\right)\Big|_{\lambda^{gh}=0} \tag{3.44}$$

while taking into account the implicit $-i\varepsilon\otimes\mathbb{1}_{2N}$ metric factors everywhere, including the linear term. Explicitly, we make the replacements:

$$\wp\left(x^c, p^c, x^b, p^b\right) \mapsto \wp\left(+i\frac{\partial}{\partial\lambda_{x^b}}, -i\frac{\partial}{\partial\lambda_{p^b}}, -i\frac{\partial}{\partial\lambda_{x^c}}, +i\frac{\partial}{\partial\lambda_{p^c}}\right). \tag{3.45}$$

Once we have the matrix $\mathcal{F}(t)$ defining the quadratic form in λ^{gh} in the exponential of the generating functional $\mathcal{W}(\lambda^{gh}, t)$ for the integrand (3.22), we can plug it in the above map which produces the Fock space amplitudes from the ones in Moyal space. Then we can rewrite the matrix element $\mathbf{R}_{nm}(t)$ corresponding to $\langle\hat{\Omega}|\hat{c}_m\hat{b}_n|\mathcal{T}(t)\rangle$ (or equivalently the perturbative monoid element $p^b_{2n}p^c_{2m}A_0^{gh}$ for the purely even parity case, etc.) as follows:

$$\mathbf{R}_{2n,2m} = -\left(\delta_{nm} + \frac{4}{2m}\mathcal{F}^{pp}_{2n,2m}\right) \tag{3.46a}$$

$$\mathbf{R}_{2n-1,2m-1} = \delta_{nm} + (2n-1)(R\mathcal{F}^{xx}R^\top)_{2n-1,2m-1}, \tag{3.46b}$$

$$\mathbf{R}_{2n,2m-1} = -2i(R\mathcal{F}^{xp})^\top_{2n,2m-1}, \tag{3.46c}$$

$$\mathbf{R}_{2n-1,2m} = -2i(\kappa_o R\mathcal{F}^{xp})_{2n-1,2m}. \tag{3.46d}$$

where the upper indices on $\mathcal{F}$ refer to the $N\times N$ blocks in the $2N\times 2N$ matrix $\mathcal{F}(t)$ belonging to the phase space representation used, namely "momenta" p^cp^b, "position" x^cx^b and the mixed cases. The negative sign in the first equation (and implicit in the following) is due to the particular way the ghost zero mode ξ_0 is incorporated in the Moyal basis. This gives a normalization constant $(-\mu_3^{-1})$ (§2.4) that absorbs the extra negative sign.

From the expression for $\mathcal{F}$, (3.32) , we notice that the matrix elements in the purely *momentum* sector, $\mathcal{F}^{pp}$ are particularly simple since the $N\times N$ block matrices in $\mathcal{Y}$ that contribute to the product are all *diagonal* matrices. Hence, the infinite summations are sidestepped. By using the above map, we find that these correspond to the purely even parity elements of the $\mathbf{R}$ matrix. In §4.1, we shall study the behaviour of these class of matrix elements more closely by taking advantage of the simple forms for the T, R matrices(in the infinite N limit).

Because of the twist symmetry of the Witten type vertex $\langle V_3|$ and the reflector $\langle\widetilde{V}_2|$, we have vanishing of the mixed parity elements $\mathbf{R}_{eo} = 0 = \mathbf{R}_{oe}$. This requires that block $\mathcal{F}^{xp} = 0$, which then translates to a linear constraint relating the three blocks[9] in $\mathcal{Q}_\eta^{-1}$,

$$\mathcal{L}_\eta^{\top x\alpha}(\mathcal{Q}_\eta^{-1})^{\alpha\beta}\mathcal{L}_\eta^{\beta p} = \mathbb{0}. \tag{3.47}$$

[9]Since $\mathcal{Q}_\eta$ is symmetric and $(M_0^{gh})^{-1}f_2(q)$ is already block diagonal, it suffices to consider only three independent blocks.

We can now express the relation (3.46) as:

$$\begin{aligned}\mathbf{R} &= -C + \sigma \begin{bmatrix} \kappa_o R & \mathbb{0} \\ \mathbb{0} & \mathbb{1} \end{bmatrix} \mathcal{F} \begin{bmatrix} R^\top & \mathbb{0} \\ \mathbb{0} & -4\kappa_e^{-1} \end{bmatrix} \sigma \\ &= -C + C + \begin{bmatrix} q^{2\kappa_e} & \mathbb{0} \\ \mathbb{0} & -q^{2\kappa_o} \end{bmatrix} + \sigma \begin{bmatrix} \kappa_o R & \mathbb{0} \\ \mathbb{0} & \mathbb{1} \end{bmatrix} \mathcal{L}_\eta^\top \mathcal{Q}_\eta^{-1} \mathcal{L}_\eta \begin{bmatrix} R^\top & \mathbb{0} \\ \mathbb{0} & -4\kappa_e^{-1} \end{bmatrix} \sigma \\ &= \begin{bmatrix} q^{2\kappa_e} & \mathbb{0} \\ \mathbb{0} & -q^{2\kappa_o} \end{bmatrix} + \frac{1}{4}\sigma \begin{bmatrix} f_1(\kappa_o)T^\top & -\frac{i}{2}\kappa_o f_3(\kappa_o) R \\ \frac{i}{2} f_3(\kappa_e) & \frac{1}{4}\kappa_e f_1(\kappa_e) \end{bmatrix} \mathcal{Q}_\eta^{-1} \begin{bmatrix} T\kappa_o^{-1} f_1(\kappa_o) & -2i\kappa_e^{-1} f_3(\kappa_e) \\ -\frac{i}{2} R^\top f_3(\kappa_o) & -f_1(\kappa_e) \end{bmatrix}. \end{aligned} \tag{3.48}$$

Here, we have inserted the σ matrices simply to interchange the two blocks on the diagonal in order to match our conventions for the parity basis. We have written the above to show that the the $\mathcal{L}_\eta$ matrices do not result in two more infinite sums—but only one extra infinite sum—which gets simplified by using the $TR = \mathbb{1}_e$, $RT = \mathbb{1}_o$ relations after the matrix inverse is expanded as a formal operator series as we do in §4.1 for the purely even parity case.

3.3 Matrix elements to linear order

One of the interesting results from our analysis is that our starting expressions correctly reproduce the linear order behaviour of the matrices $\mathbf{R}_{nm}(t)$ and $\mathbf{M}_{nm}(t)$ that appear in the definition of the one-loop tadpole state in (2.75) as expected from BCFT. The oscillator and the Moyal formalism are formally isomorphic but this is one of the instances where the subtleties in the definition of the propagator and level truncation result in different forms. It is difficult to say where exactly the isomorphism breaks down but it may be attributable to the level truncation which breaks the gauge symmetry of OSFT and the peculiar nature of the Virasoro zero mode operator $\hat{L}_0$ in the Moyal basis[23, §7]. It is interesting[10] that the difference for the linear correction term from the two methods is only a factor of 2.

Verification of the linear behaviour

Zeroth Order

For $t = 0$, the matrix $\mathcal{F}$ becomes simply

$$\begin{aligned}\mathcal{F}|_{t=0} &= \frac{1}{2} M_0^{gh-1} f_2(\tilde{\kappa}^{gh}; q)|_{q=1} \\ &= -\begin{bmatrix} T\kappa_o^{-1} T^\top & \mathbb{0} \\ \mathbb{0} & \frac{1}{4}\kappa_e \end{bmatrix} \times \begin{bmatrix} R^\top (1+1) T^\top & \mathbb{0} \\ \mathbb{0} & 2 \end{bmatrix}\end{aligned}$$

[10] Due to non-associativity, a factor of 2 issue arises also in the computation of the closed string tachyon mass [48] through the Ellwood-Hashimoto-Itzhaki-Zwiebach invariant.

$$= - \begin{bmatrix} 2T\kappa_o^{-1}T^\top & \mathbb{0} \\ \mathbb{0} & \frac{1}{2}\kappa_e \end{bmatrix}, \tag{3.49}$$

by quickly noting that $f_2(n;1) = 2, T\,R = \mathbb{1}_e$ and $R\,T = \mathbb{1}_o$. This when substituted into (3.46) gives the t independent piece to be

$$\mathbf{R}_{nm}|_{t=0} = (-1)^n \delta_{nm} = C_{nm} \tag{3.50}$$

and by a similar short calculation, we can show that

$$\mathbf{M}_{nm}|_{t=0} = (-1)^{nm} \delta_{nm} = C_{nm} \tag{3.51}$$

for the matter sector. Here we recall that C is the twist matrix which is crucial in defining the reflector vertex $\langle \tilde{V}_2|$ and arises from BPZ conjugation and the Witten style overlapping conditions. These precisely correspond to the closed string tachyon state (1.1) which dominates due to the divergence structure arising from the determinant factor near $t = 0$.

Here, we have assumed that there are no extra poles from the infinite summations in $\mathcal{Y}^\top(t)\mathcal{Z}(t)^{-1}\mathcal{Y}(t)$ that cancels the single power of t multiplying it. This will certainly be true for $\mathbf{R}_{2n,2m}$ associated with the diagonal blocks in $\mathcal{Y}(t)$ but can also be seen to hold for $\mathbf{R}_{2n-1,2m-1}$ by examining the block structure in (3.48). But more importantly, we can take this as the correct prescription since it matches with the BCFT prediction for the structure of $|\mathcal{T}(t)\rangle$!

First Order

Interchanging the order of summation over κ_o (odd integers) and the non-negative integers defining the exponentials e^{-t} of $f_i(n;t)$, appearing in the various blocks in $\mathcal{Q}_\eta$ and $\mathcal{L}_\eta$ given in (3.25), we can expand them to the lowest order in the parameter t:

$$\begin{aligned} \mathcal{Q}_\eta &= \frac{t}{4} \begin{bmatrix} 2(\mathbb{1} + TT^\top) & \mathbb{0} \\ \mathbb{0} & \frac{1}{4}4\kappa_e^2 \end{bmatrix} + \mathcal{O}(t^2) \\ &= t \begin{bmatrix} \mathbb{1} - \frac{1}{2}\frac{ww^\top}{1+w^\top w} & \mathbb{0} \\ \mathbb{0} & \frac{1}{4}\kappa_e^2 \end{bmatrix} + \mathcal{O}(t^2), \end{aligned} \tag{3.52}$$

$$\mathcal{L}_\eta = \frac{t}{2} \begin{bmatrix} \mathbb{0} & i\kappa_e \\ -iR^\top \kappa_o T^\top & \mathbb{0} \end{bmatrix} + \mathcal{O}(t^2), \tag{3.53}$$

where we have used the relations:

$$TT^\top = \mathbb{1} - \frac{ww^\top}{1 + w^\top w}, \qquad R = \kappa_o^{-2} T^\top \kappa_e^2, \tag{3.54}$$

and the off-block diagonal elements in $\mathcal{Q}_\eta$ do not contribute since $f_1(n;t)$ starts at $\mathcal{O}(t^2)$.

The quantity $w^\top w$ diverges linearly as $\mathcal{O}(N)$ and expressions involving it should be treated with care to avoid inconsistencies. Hence, we shall keep the $\mathcal{O}(1/N)$ term and argue when it may be dropped. The matrix

$$\mathbb{V} \coloneqq \mathbb{1} - \frac{1}{2}\frac{ww^\top}{1+w^\top w} \tag{3.55}$$

appearing in the first block of $\mathcal{Q}_\eta$ above can be readily inverted using a Taylor series in $1/\bar{w}w < 1$ when $N \geq 1$. We make the following ansatz involving a function $\mu(z)$:

$$\mathbb{V}^{-1}_{2n,2m} = \delta_{nm} + \mu(w^\top w)\; w_{2n}(w^\top)_{2m} \tag{3.56}$$

and require $\mathbb{V}\mathbb{V}^{-1} = \mathbb{1} = \mathbb{V}^{-1}\mathbb{V}$ to find

$$\mathbb{W} \coloneqq \mathbb{V}^{-1} = \mathbb{1} + \frac{ww^\top}{2+w^\top w}, \tag{3.57}$$

which may then be verified by a direct substitution. Then we find that

$$\mathcal{Q}_\eta^{-1} = \frac{1}{t}\begin{bmatrix} \mathbb{W} & \mathbb{0} \\ \mathbb{0} & 4\,\kappa_e^{-2} \end{bmatrix} + \text{ finite} + \text{ subleading}, \tag{3.58}$$

showing that:

$$\begin{aligned}
\mathcal{L}_\eta^\top \mathcal{Q}_\eta^{-1}\mathcal{L}_\eta &= -\frac{t}{4}\begin{bmatrix} 4T\kappa_o R\kappa_e^{-2}R^\top\kappa_o T^\top & \mathbb{0} \\ \mathbb{0} & \kappa_e\mathbb{W}\kappa_e \end{bmatrix} + \mathcal{O}(t^2) \\
&= -t\begin{bmatrix} TT^\top & \mathbb{0} \\ \mathbb{0} & \frac{1}{4}\kappa_e\mathbb{W}\kappa_e \end{bmatrix} + \mathcal{O}(t^2) \\
&= -t\begin{bmatrix} \mathbb{1} - \frac{ww^\top}{1+w^\top w} & \mathbb{0} \\ \mathbb{0} & \frac{1}{4}\left(\kappa_e^2 + \frac{\kappa_e ww^\top \kappa_e}{2+w^\top w}\right) \end{bmatrix} + \mathcal{O}(t^2).
\end{aligned} \tag{3.59}$$

Now we can consider the open string limit for the second block since there are no divergent terms in this expansion, while we retain the $TT^\top$ form for the first block. Isolating the linear term from $\frac{1}{2}(M_0^{gh})^{-1}f_2(q)$, we obtain

$$+t\begin{bmatrix} 2\,T\,T^\top & \mathbb{0} \\ \mathbb{0} & \frac{1}{2}\kappa_e^2 \end{bmatrix}$$

This when substituted into (3.32) leads to:

$$\mathcal{F} = -\begin{bmatrix} 2T\kappa_o^{-1}T^\top - t\,TT^\top & \mathbb{0} \\ \mathbb{0} & \frac{1}{2}\kappa_e - \frac{t}{4}\,\kappa_e^2 \end{bmatrix} + \mathcal{O}(t^2). \tag{3.60}$$

Consequently, we can readily write down the squeezed state matrix $\mathbf{R}_{nm}$ to this order using (3.46):

$$\begin{aligned}\mathbf{R}_{2n,2m} &= -\delta_{nm} - \frac{4}{2m} \times -\frac{1}{2} 2n\delta_{nm} - \frac{4t}{2m} \times \frac{1}{4} 4n^2 \delta_{nm} \\ &= \delta_{nm} - 2nt\,\delta_{nm} + \mathcal{O}(t^2), \qquad (3.61) \\ \mathbf{R}_{2n-1,2m-1} &= \delta_{nm} + (2n-1)\left[R\left(-2T\kappa_o^{-1}T^\top + tTT^\top\right)R^\top\right]_{2n-1,2m-1} \\ &= -\delta_{nm} + (2n-1)t\,\delta_{nm} + \mathcal{O}(t^2). \qquad (3.62)\end{aligned}$$

The mixed parity cases $\mathbf{R}_{2n,2m-1}$ vanishes identically as we have argued before. This enables us to express the general matrix element as:

$$\mathbf{R}^{(\mathrm{Moy})}_{nm} = C_{nm} - n\,C_{nm}\,t + \mathcal{O}(t^2) \qquad (3.63)$$

As shown in [14], the linear correction in t is completely generated from the conformal transformation of the external Fock space state, and is determined from a BCFT analysis of the conformal map done near $t = 0$.

It precisely coincides with the above form, whereas a Taylor expansion based on the oscillator expressions gives a linear coefficient off by a factor of 2:

$$\mathbf{R}^{(\mathrm{osc})}_{nm} = C_{nm} - \underline{2}n\,C_{nm}\,t + \mathcal{O}(t^2). \qquad (3.64)$$

As explained carefully in [14], the two limits involving the level (size of the matrices) and the modular parameter, $L \to \infty$ and $t \to 0$ do not commute in the oscillator case but holds in the Moyal case at least to the order that we have analysed. As inferred earlier in this thesis, the difference in the propagator structure could account for this subtle breakdown of the isomorphism. Hence, the peculiar structure of the propagator in Moyal space merits further investigation. See also the interesting discussion in [23, §7].

Additionally, let us remark here that the Moyal approach, including the method of regularization, has worked extremely well to produce the most advanced analytic results for the off-shell 4-point function for tachyonic states [26] as mentioned in the introduction. Hence there is ample reason to trust the Moyal method, that has already been tested in that context.

One may also verify this behaviour numerically by repeating the analysis done in [14] for finding a numerical fit near $t = 0$. Here we have used the finite N versions of the matrices (2.52) which ensure that the star algebra relations are satisfied. For $N = 84$ (requiring inversion of 168×168 matrices) and t varying from 10^{-4} to 16×10^{-4} in steps of 10^{-4}, we obtain the linear fit given in Table 3.1. We emphasize that the higher order terms starting at t^2 are the ones that really encode any effects of the Shapiro-Thorn massless closed-string states. Unfortunately, our algebraic approach only allows to successively

$\mathbf{R}_{11}^{(lin)}$	$-(0.99999974 - 0.99912772 \times t)$
$\mathbf{R}_{22}^{(lin)}$	$+(0.99999858 - 0.99010797 \times 2t)$
$\mathbf{R}_{33}^{(lin)}$	$-(0.99999768 - 0.99743118 \times 3t)$
$\mathbf{R}_{44}^{(lin)}$	$+(0.99999516 - 0.98843886 \times 4t)$

Table 3.1: Linear behaviour of the matrix elements $\mathbf{R}_{nm}$ near $t = 0$ based on numerical evaluation of 168×168 size matrices. The fit reinforces the agreement between the Moyal and the BCFT predictions for the structure of $\mathbf{R}(t)$.

approximate these coefficients (as we do in §4.1) but not exactly. It does clarify the discrepancy noticed in the oscillator case and is in that sense an improvement. However, we remark that in the geometric approach based on a BCFT analysis, it is difficult to isolate their effects as well due to operator mixing under a conformal transformation of non-primary operators.

3.4 Associativity at linear order

The various orders for evaluating the overlap mentioned in §3.1 could differ if associativity is not strictly satisfied, as is possible if one is expanding directly in the $N = \infty$ open string limit, and not applying the controlled limit prescription which guarantees associativity but can miss non-analyticities. The alternate order $A_2 * A_3 \to A_{23}(\eta, \xi) \to \int d\eta \to A_1 A'_{23}(\xi) \to \mathrm{Tr}$ corresponds to the manner in which the amplitude would be evaluated in the oscillator method (see §2.3) where the tadpole state is evaluatedt as:

$$|\mathcal{T}\rangle = -g_T\, K^3 \int_0^\infty dt\ {}_{1,2}\langle \widetilde{V}_2 | b_0^{(2)} e^{-\frac{1}{2}t(L_0^{(1)}+L_0^{(2)})} |V_3\rangle_{1,2,3}. \tag{3.65}$$

and the amplitude is obtained by taking the inner product with an external state $\langle A_e|$. Here the superscripts refer to the string Hilbert spaces in the first quantized formalism.

The corresponding matrix $\mathcal{F}(t)$ defining the quadratic form in λ^{gh} towards the generating functional, $\mathcal{W}(\lambda^{gh}, t)$ in this particular order of evaluation is then

$$\mathcal{F}(t) = (M'_{123})^{-1},\ \text{with}$$
$$M'_{123} = \frac{2}{f_2(q)} M_0^{gh} + \left(\frac{f_1}{f_2} + \frac{f_3}{f_2} m_0^{gh}\right) \left(M_0^{-1} \frac{f_3}{f_2} + \sigma \frac{f_3}{f_2} M_0^{gh} \sigma - 2\sigma \frac{q^{\tilde{\kappa}^{gh}}}{f_2(q)} + 2 \left(\frac{q^{\tilde{\kappa}^{gh}}}{f_2}\right)^\top \sigma \right)^{-1}$$
$$\left(\frac{f_1}{f_2} + \frac{f_3}{f_2} m_0^{gh}\right)^\top \tag{3.66}$$

A quick inspection of the above structure reveals that similar to the earlier evaluation order, the matrix to be inverted in M'_{123} *vanishes* at $t = 0$. Collecting the linear order terms after some simple algebra results in an identical expression for the linear correction term, namely:

$$\mathbf{R}_{nm} = C_{nm} - nC_{nm}t + \mathcal{O}(t^2), \tag{3.67}$$

and hence we conclude that the order of limits problem does not arise in this order of evaluation either. However, further expansions are made awkward by the somewhat complicated form of the above expression, which requires two matrix inverse operations nested one inside the other.

Hence, from the above exercice we can infer that constructing the tadpole state out of the Fourier basis and then combining their contribution to the overlap amplitude (by the η^{gh} integration as we have done earlier) would be preferred over considering the overlap with the state itself, which may be somewhat counter-intuitive. Of course, just the linear order behaviour does not fix a prescription uniquely or prove the correctness of these expressions. Nonetheless, this is an encouraging result showing the subtleties in the map between Moyal space and Fock space.

It would have been more interesting if associativity was indeed violated in this calculation, which could display the similarity to the oscillator inner product directly. Hence, we have not been able to clarify the order of limits issue completely.

Fourier Basis

We must remark that the issue encountered in the oscillator basis also arises if one attempts to expand the amplitude in Fourier space defined by the conjugate variable η^{gh}. The Feynman rules in Fourier space were studied and given in detail in Refs. [20, 21] by Bars et al. The propagator and vertex take of the form:

$$\Delta(\eta^{gh}, \eta'^{gh}, t) \sim \exp\left[\eta^{gh\top} F^{gh} \eta^{gh} + \eta'^{gh\top} F^{gh}(t) \eta'^{gh\top} - 2\eta'^{gh\top} G^{gh}(t) \eta^{gh}\right], \text{ and} \tag{3.68}$$

$$\mathrm{Tr}\left(e^{-\xi^{gh\top}\eta_1^{gh}} * \cdots * e^{-\xi^{gh\top}\eta_n^{gh}}\right) \sim \exp\left[-\frac{1}{2}\sum_{i<j} \eta_i^{gh\top} \sigma \eta_j^{gh}\right] \delta\left(\eta^{gh}{}_1 + \cdots + \eta^{gh}{}_n\right), \tag{3.69}$$

respectively, where we are now using the $2N \times 2N$ basis with implicit $-i\varepsilon$ metric and

$$F^{gh}(t) = -\frac{1}{4} M_0^{gh-1} \frac{f_2(q)}{f_3(q)}, \qquad G^{gh}(t) = -\frac{1}{2} M_0^{gh-1} \frac{q^{\tilde{\kappa}^{gh}}}{f_3(q)} \tag{3.70}$$

One may again write down an amplitude formally and as $t \to 0$, the matrix to be inverted becomes singular simply due to the linear dependence of the blocks

$$\mathcal{Q}(t) \sim \frac{1}{t} \begin{bmatrix} 1 & 1 \\ 1 & 1 \end{bmatrix} \otimes M_0^{gh-1} \tag{3.71}$$

where the first block has vanishing determinant. Hence this form cannot be used as the starting point for a systematic series expansion around $t = 0$. However, we remark that for numerical purposes, the Fourier basis provides quicker analytic expressions since the $*$ products are already taken care of. The disadvantage is numerical instability due to using much bigger sized matrices as compared to the ξ basis.
Thus in summary, we have demonstrated in this section that the expected behaviour from BCFT is correctly reproduced by the Moyal expressions in ξ space. For showing the validity of the relations, we have used the map (3.41) from th oscillators as operators in Fock space to differential operators in Moyal space. One really interesting aspect is the non-analyticity of these matrix elements already seen at the quadratic stage: the higher order terms come with factors of $\log(t)$ as we shall show later in §4.1. Hence, even the expansion in BCFT can at best be asymptotic and thus allows for explicitly including the closed-string states in the form of exponentially suppressed subleading tails in the form of $e^{-2\pi^2 n/t}$.

3.5 The twisted ghost butterfly case

It is an interesting exercice to consider the overlap with the twisted ghost butterfly state instead of the perturbative vacuum. This is one of the simplest star algebra projectors (those string fields satisfying $\Phi * \Phi = \Phi$) and is defined by the following state in Fock space:

$$|\psi_B\rangle = \exp\left[-\frac{1}{2}L'_{-2}\right]|\Omega'\rangle, \tag{3.72}$$

where the prime refers to the twisted ghost conformal field theory studied by Gaiotto, Rastelli, Sen, and Zwiebach (GRSZ) [49](see also [20, 50]). It is conceivable that the full twisted butterfly captures some of the physics of the tachyon vacuum solution (closed string vacuum) OSFT owing to its role in projector based solutions [51].

Because the (total) stress tensor on the canonical strip coordinate w is twisted as:

$$T'(w) = T(w) - \partial j_g(w), \tag{3.73}$$

where $j_g = c\,b$ is th ghost number current in the original CFT, (and similarly for the anti-holomorphic component), the new Virasoro operator above is given by

$$L'_{-2} = L_{-2} - 2j_{-2}. \tag{3.74}$$

In Moyal space, the ghost part of this state is represented by the twist even and $SU(1,1)$ symmetric string field [20, Appendix E]

$$\hat{A}'_B = \xi_0\,\mathcal{N}_B e^{-\xi^{gh\top} M_B \xi^{gh}}, \tag{3.75}$$

where now the normalization and the coefficient matrix are:

$$\mathcal{N}_B = 2^{-2N}, \qquad M_B = -\frac{1}{2}\begin{bmatrix} \kappa_e & \mathbb{0} \\ \mathbb{0} & 4\kappa_e^{-1} \end{bmatrix}. \tag{3.76}$$

We remark that this string field satisfies

$$\beta_e^b * \hat{A}'_B = \beta_e^c * \hat{A}'_B = \hat{A}'_B * \beta_{-e}^b = \hat{A}'_B * \beta_{-e}^c = 0, \forall e > 0, \tag{3.77}$$

where now the $\beta_e^{b,c}$ are *fields* in Moyal space instead of differential operators:

$$\beta_e^b = p_{|e|}^c - \frac{i}{2}\,\mathrm{sgn}(e)\kappa_e x_{|e|}^b, \qquad \beta_e^c = \frac{1}{2}x_{|e|}^c - i\,\mathrm{sgn}(e)\kappa_e^{-1}p_{|e|}^b. \tag{3.78}$$

Moving on, let us write $M_B =: \chi M_0^{gh}$, where we introduce the matrix

$$\chi = \begin{bmatrix} \Gamma^\top & \mathbb{0} \\ \mathbb{0} & \mathbb{1} \end{bmatrix}, \text{ with } \Gamma \coloneqq T\kappa_o^{-1}T^\top\kappa_e. \tag{3.79}$$

We mention that the matrix elements of $\Gamma^\top$ can be evaluated exactly in the infinite N limit and are given by:

$$\Gamma^\top_{2n,2m} = (-)^{n+m+1}\frac{2n}{\pi^2(n^2-m^2)}\left[\psi\left(\frac{1}{2}+n\right)+\psi\left(\frac{1}{2}-n\right)-\psi\left(\frac{1}{2}+m\right)-\psi\left(\frac{1}{2}-m\right)\right]. \tag{3.80}$$

Then, we have $M_B(M_0^{gh})^{-1} = \chi$. Now, let us consider the monoid defined by

$$\hat{A}'_B * e^{\xi^{gh\top}\eta^{gh}} \cdot (q^{L_0}e^{-\xi^{gh\top}\eta^{gh}}).$$

This has the parameters:

$$\begin{aligned} M_{123} &= M_B + \frac{f_3(q)}{f_2(q)}M_0^{gh} = \left[\chi + \frac{f_3(q)}{f_2(q)}\right]M_0^{gh}, \\ \lambda_{123} &= \left[m_B - \frac{f_1(q)}{f_2(q)}\right]\eta = \left[\chi m_0^{gh} - \frac{f_1(q)}{f_2(q)}\right]\eta, \text{ and} \\ \mathcal{N}_{123} &= 4^{-2N}\det(f_2(q))\exp\left[\frac{1}{4}\eta^{gh\top}\left((M_0^{gh})^{-1}\frac{f_3(q)}{f_2(q)} + \sigma\chi M_0^{gh}\sigma\right)\eta^{gh}\right]. \end{aligned} \tag{3.81}$$

As for the perturbative vacuum state, we can next take the trace over ξ^{gh} and then perform the Gaussian integral over η^{gh}. This time, we set $\lambda^{gh} = 0$ and have the non-vanishing coefficient matrices as follows:

$$\mathcal{Q}_\eta^B = \frac{1}{4}\left[(M_0^{gh})^{-1}\frac{f_1(q)}{f_2(q)} + \sigma\chi\right]\left[\chi + \frac{f_3(q)}{f_2(q)}\right]^{-1}\left[\frac{f_1(q)}{f_2(q)} - \chi M_0^{gh}\sigma\right]$$

$$+\frac{1}{4}\sigma\chi M_0^{gh}\sigma+\frac{1}{4}(M_0^{gh})^{-1}\frac{f_3(q)}{f_2(q)}, \tag{3.82a}$$

$$\mathcal{C}_\eta^B=2^{-2N}(1+w^\top w)^{1/2}\det\left(f_2(q)\chi+f_3(q)\right). \tag{3.82b}$$

Finally, the Gaussian integration results in $\mathcal{C}_\eta^B\det(2\mathcal{Q}_\eta^B)$ which may be looked at numerically. Here, we can also consider excitations on top of this state by having a general λ^{gh} but keeping in mind that the state already contains excitations created by the odd oscillator modes $\hat{c}_{-o},\hat{b}_{-o}$. Since it is annihilated by all the even oscillators $\hat{c}_e,\hat{b}_e$, we notice that for excitations created by the corresponding creation operators, we recover the same even parity matrix elements $\mathbf{R}_{2n,2m}$ as in the earlier analysis.

Chapter 4

Expansions for squeezed state matrix elements

In this chapter, we wish to study the behaviour of the matrix element factor $\mathbf{R}_{nm}$—defining the squeezed state in the (ghost) exponential factor of the integrand as appearing in (2.75)—as $t \to 0^+$ using expansions in various basis functions. The exponential is quadratic in the creation operators, and the coefficient matrix $\mathbf{R}$ can serve as a probe of closed string physics since it describes the resulting field configuration. The region near $t = 0$ would be of most interest in this direction, as may be seen from Fig. 3.1 in a conformal frame appropriate for closed strings. Naturally, one can find an absolutely convergent expansion in the nome $q \coloneqq e^{-t}$ for $|q| < 1$, corresponding to open string degrees of freedom. Because of the essential singularity at $t = 0$ coming from the massive closed string states, the expansion in other basis functions such as $\{t^s, \ln t\}$ or equivalently $\{(-\ln q)^s, \ln(-\ln q)\}$ would not be a convergent expansion, but could at best be an asymptotic expansion. This is consistent with our understanding of the *quantum inconsistency* of bosonic OSFT (or any open bosonic string theory) at the loop level.

In the following, we shall explore the utility of the Moyal formulation to directly learn about the structure of the integrand as a function of the parameter t. We learn that the expressions we obtained in §3.1 do have the correct qualitative features near $t = 0$ and we found that it reproduces the correct zeroth and linear order coefficients, which is somewhat non-trivial. Furthermore, we can develop a series expansion involving special functions to successively approximate the true analytic form for $\mathbf{R}_{nm}(t)$ by our method.

4.1 Even parity matrix elements as $t \to 0^+$

In order to perform an expansion in t, let us introduce the following auxiliary functions derived from the functions f_1, f_2, f_3 and f_4 employed earlier (3.16)

$$h_i(n;t) \coloneqq \frac{f_i(n;t)}{t}, \qquad g_i(n;t) \coloneqq h_i(n;t) - h_i(n;0) = \frac{f_i(n;t)}{t} - f_i^{(1)}(0), \quad \text{giving explicitly}$$

$$
\begin{aligned}
h_1(n;t) &= \frac{(1-e^{-nt})^2}{t}, \qquad & h_2(n;t) &= \frac{1+e^{-2nt}}{t}, \\
h_3(n;t) &= \frac{1-e^{-2nt}}{t}, \qquad & h_4(n;t) &= \frac{3-4e^{-nt}+e^{-2nt}}{t}, \quad \text{and} \\
g_1(n;t) &= \frac{(1-e^{-tn})^2}{t}, \qquad & g_2(n;t) &= \frac{1+e^{-2nt}}{t} + 2n, \\
g_3(n;t) &= \frac{1-e^{-2nt}}{t} - 2n, \quad & g_4(n;t) &= \frac{3-4e^{-nt}+e^{-2nt}}{t} - 2n.
\end{aligned} \tag{4.1}
$$

These can be thought of as certain basis functions with a well-defined asymptotic behaviour. Also, we notice that $|g_i(n;t)| < 2n$ for $i = 1, 3, 4$; a boundedness property which we will use later.

We remark at this juncture that the functions $\tanh t$ and $\operatorname{sech} t$ which appear in the original form of the block matrices (3.14) may be Taylor expanded in terms of the Bernoulli numbers B_{2n} and the Euler numbers E_{2n} around the point $t = 0$. However, reorganizing the multiple sums and products followed by applying any identities involving them quickly becomes challenging. Therefore, we continue to use the much more straightforward (and uniform) representation in terms of exponential functions in our analysis.

Moving on, we illustrate this expansion scheme for the case of even parity matrix elements, $\mathbf{R}_{2n,2m}$, for convenience. Since its expression involves the inverse of a matrix function, which is difficult to obtain analytically (at least in the discrete diagonal basis), we employ a formal series to represent the inverse[1]. After this step, one can find expansions around the point $t = 0$ although the sub-matrices do lead to more terms without any apparent patterns for resummations. To this end, we split the matrix to be inverted $\mathcal{Z}(t)$, which appeared in (3.31) as follows:

$$
\begin{aligned}
\mathcal{Z}(t) &= \mathcal{Z}_0 + \delta\mathcal{Z}(t), \quad \text{so that we may write} \\
\mathcal{Z}(t)^{-1} &= (1 + \mathcal{Z}_0^{-1}\delta\mathcal{Z}(t))^{-1}\mathcal{Z}_0^{-1} \\
&\coloneqq (1 + \mathbf{M}(t))^{-1}\mathcal{Z}_0^{-1} \\
&= \sum_{s=0}^{\infty}(-1)^s\mathbf{M}^s(t) \times \mathcal{Z}_0^{-1}.
\end{aligned} \tag{4.2}
$$

where we have defined a matrix function $\mathbf{M}(t) \coloneqq \mathcal{Z}_0^{-1}\delta\mathcal{Z}(t)$. Here we recall that $\mathcal{Z}_0$ must be defined as the limit $\lim\limits_{t\to 0^+} \dfrac{\mathcal{Q}_\eta(t)}{t}$ but note that the matrix $\mathcal{Q}_\eta(t)$ in (3.25) is not analytic at $t = 0$ due to the insufficient fall-off behaviours of the $T_{2n,2m-1}$ matrix elements as n, m increases

$$
T^{\infty}_{2n,2m-1} = (-)^{n+m}\frac{4(2m-1)}{\pi(4n^2-(2m-1)^2)} \tag{4.3}
$$

[1]This is justified because the domains of analyticity of the two maps overlap.

which behave like $\dfrac{1}{2m-1}$ in sums for large m.

We also remind the reader of the block matrix forms from (3.57)

$$\mathcal{Z}_0 = \begin{bmatrix} 4\mathbb{V} & \mathbb{0} \\ \mathbb{0} & \kappa_e^2 \end{bmatrix}, \mathbb{V} \coloneqq \mathbb{1} - \frac{1}{2}\frac{ww^\top}{1+w^\top w}, \text{ and } \qquad \mathbb{W} \coloneqq \mathbb{V}^{-1} = \mathbb{1} + \frac{ww^\top}{2+w^\top w}, \tag{4.4}$$

giving

$$\mathcal{Z}_0^{-1} = \begin{bmatrix} \frac{1}{4}\mathbb{W} & 0 \\ 0 & \kappa_e^{-2} \end{bmatrix}. \tag{4.5}$$

The matrix $\delta\mathcal{Z}(t)$ is then expressed in terms of functions g_1, g_3 and g_4 in a form very similar to $\mathcal{Z}(t)$:

$$\begin{aligned} \delta\mathcal{Z}(t) &= \begin{bmatrix} \kappa_e^{-1}g_3(\kappa_e) + T\kappa_o^{-1}g_4(\kappa_o)T^\top & -\frac{i}{2}\left(g_1(\kappa_e) - Tg_1(\kappa_o)R\right) \\ -\frac{i}{2}\left(g_1(\kappa_e) - R^\top g_1(\kappa_o)T^\top\right) & \frac{1}{4}\left(\kappa_e g_4(\kappa_e) + R^\top\kappa_o g_3(\kappa_o)R\right) \end{bmatrix} \\ \Rightarrow \mathbf{M}(t) &= \begin{bmatrix} \frac{1}{4}\mathbb{W}\left(\kappa_e^{-1}g_3(\kappa_e) + T\kappa_o^{-1}g_4(\kappa_o)T^\top\right) & -\frac{i}{8}\mathbb{W}\left(g_1(\kappa_e) - T\kappa_o^{-2}g_1(\kappa_o)T^\top\right) \\ -\frac{i}{2}\left(\kappa_e^{-2}g_1(\kappa_e) - T\kappa_o^{-2}g_1(\kappa_o)T^\top\right) & \frac{1}{4}(\kappa_e^{-1}g_4(\kappa_e) + T\kappa_o^{-3}g_3(\kappa_o)T^\top\kappa_e^2) \end{bmatrix}, \end{aligned} \tag{4.6}$$

where we remind the reader that *each matrix element* is in general an infinite sum — owing to the matrix products — and we have used the relation $R = \kappa_o^{-2}T^\top\kappa_e^2$ for rewriting the structure using only the T and κ matrices. However, in taking powers of the matrix $\mathbf{M}$ symbolically it is more helpful to keep the matrix R since then we can readily apply relations such as $RT = \mathbb{1}_o$ and $TR = \mathbb{1}_e$ in order to reduce the number of terms.

Note that although the individual blocks in $\mathbf{M}(t)$ have at least a first order zero at $t = 0$, the products of these blocks still *retain only a first order zero* due to the higher order poles arising from the infinite sums. This is because we are interchanging the order of summation in double sums which are not absolutely convergent. Therefore all the higher matrix powers $(\mathbf{M}(t))^s$ continue to contribute to the t^2 term in $\mathbf{R}_{nm}(t)$ in our expansion scheme and consequently these coefficients cannot be obtained exactly by the above series. This drawback is again due to the infinite dimensional nature of the problem.

Because of the logarithmic branch points, the terms for various s are not analytic, although they vanish at $t = 0$ as remarked above. However, we expect that the contributions fall off with increasing values of s (as seen from the tractable $s = 0, 1, 2$ cases) and must converge since the full function only has a removable singularity as $t \to 0^+$. The matrix $\mathcal{Y}(q)$ presented in (3.31) is now written in terms of the functions $h_1(n;q)$ and $h_3(n;q)$ as follows:

$$\mathcal{Y}(q) = \begin{bmatrix} T\kappa_o^{-1}h_1(\kappa_o)T^\top & \frac{i}{2}h_3(\kappa_e) \\ -\frac{i}{2}R^\top h_3(\kappa_o)T^\top & \frac{1}{4}\kappa_e h_1(\kappa_e) \end{bmatrix}. \tag{4.7}$$

We shall now try to investigate the effect of working with a finite size truncation for the matrices vs directly using the infinite N versions of the expressions. Because the functions involved in the infinite sums satisfy the *boundedness* property: $|g_i(n;t)| < 2n$ for $i = 1, 3, 4$, we find that on examining the structure of the matrix powers $\mathbf{M}^s$, the contribution from the extra term $\dfrac{ww^\top}{2 + w^\top w}$ in $\mathbb{W}$ remains subleading and always goes as N^{-p} for some $p \geq 1$. Since we only work with the partial sums for defining the series representation of the inverse, i.e $s = 0, 1, \ldots, S$, say, these terms do not add up to give extra finite N corrections. Consequently, we can drop these $\mathcal{O}(1/N^p)$ extra terms from our calculations and effectively set $\mathbb{W} = \mathbb{1}$ to do the relevant infinite sums over odd/even integers. In other words, we have made a choice of order of limits that allows us to use the infinite N expressions consistently.

Now, in order to study these partial sums using a series representation in t, we shall now comment on their analytic structure. As the functions arising from the infinite sums over the *odd/even* parity indices are uniformly convergent only for $\Re(t) > 0$, term by term differentiation is not justified. Such mathematical niceties would have existed if we kept $N < \infty$ but then one misses the nice non-analytic behaviour expected in the quantum theory which signals the inconsistency attributed to closed string states. In the following, we therefore work directly in the open string limit. In addition, as we are expecting only an asymptotic expansion due to physical reasons, it may be possible to justify sending $N \to \infty$ at this stage of the calculation for practical reasons.

In concrete terms, the above procedure would result in an expansion of the form:

$$\mathbf{R}_{nm}(t) = \sum_{r=0}^{\infty} (\Lambda_r + \log(t)\tilde{\Lambda}_r) t^r \tag{4.8}$$

where the coefficients Λ_r and $\tilde{\Lambda}_r$ receive contributions from the partial sums over s and the $\log(t)$ piece will be shown to result from the non-analytic behaviour of the special functions that arise.

There are more non-analytic terms than the simple $\log(t)$ dependence that can be admitted (see (4.23)) since we do not have absolute convergence and hence the individual coefficients Λ_r and $\tilde{\Lambda}_r$ may not all exist. We are at this point only looking for hints of non-analytic behaviour and cannot rigorously account for any missing subleading terms.

After these digressions, let us return to the series expansion at hand. In the following we illustrate the general procedure and also display some coefficients that contribute to the final matrix elements. We shall denote the expansion for $\mathbf{R}(t)$ in terms of the matrix products by a sequence of functions

$$\mathbf{R}(t) = \sum_{s=0}^{\infty} \mathcal{R}^{(s)}(t), \tag{4.9}$$

where we have chosen $\mathcal{R}^{(0)}$ to match the linear order expansion we derived in §3.3. We emphasize that this sequence of functions constructed out of hypergeometric functions does *not* furnish an asymptotic basis as can be seen from the basic criteria for the gauge functions

$$\phi_{n+1}(z) = o(\phi_n(z)), \qquad \left(\text{as } \frac{1}{z} \to +\infty\right) \tag{4.10}$$

not being satisfied by these. Except the first two terms, the rest all contribute starting at $\mathcal{O}(t^2)$ and consequently these provide only an asymptotic approximation to the true function.

The simplest block to look at is the *purely even* block $\mathbf{R}_{2n,2m}$ given by (3.46) which we provide here again:

$$\mathbf{R}_{2n,2m} = -\left(\delta_{2n,2m} + \frac{4}{2m}\mathcal{F}^{pp}_{2n,2m}\right) \tag{4.11}$$

This is because it involves $\mathcal{Z}^{-1}$ sandwiched between $\mathcal{Y}^{xp}$ and $\mathcal{Y}^{pp}$ which are diagonal matrices and hence is easy to keep track of in a power series expansion. In block matrix form, the matrix $\mathcal{F}^{pp}$ from (3.32) corresponding to the even parity elements is given by:

$$\begin{aligned}
\mathcal{F}^{pp} &= -\frac{1}{4}\kappa_e f_2(\kappa_e) + t\,(\mathcal{Y}^\top \mathcal{Z}^{-1}\mathcal{Y})^{pp}, \quad \text{where we can expand} \\
(\mathcal{Y}^\top \mathcal{Z}^{-1}\mathcal{Y})^{pp} &= \mathcal{Y}^{\top px}(\mathcal{Z}^{-1})^{xx}\mathcal{Y}^{xp} + \mathcal{Y}^{\top px}(\mathcal{Z}^{-1})^{xp}\mathcal{Y}^{pp} + \mathcal{Y}^{\top pp}(\mathcal{Z}^{-1})^{px}\mathcal{Y}^{xp} + \mathcal{Y}^{\top pp}(\mathcal{Z}^{-1})^{pp}\mathcal{Y}^{pp} \\
&= -\frac{1}{4}h_3(\kappa_e)(\mathcal{Z}^{-1})^{xx}h_3(\kappa_e) + \frac{i}{8}h_3(\kappa_e)(\mathcal{Z}^{-1})^{xp}\kappa_e h_1(\kappa_e) \\
&\quad + \frac{i}{8}\kappa_e h_1(\kappa_e)(\mathcal{Z}^{-1})^{px}h_3(\kappa_e) + \frac{1}{16}\kappa_e h_1(\kappa_e)(\mathcal{Z}^{-1})^{pp}\kappa_e h_1(\kappa_e)
\end{aligned} \tag{4.12}$$

The matrix powers $\mathbf{M}, \mathbf{M}^2, \ldots$ required for implementing this procedure requires some block matrix multiplications. These can be performed using the *NCAlgebra* package [28] and recursively applying the relations satisfied by the T, R matrices such as

$$T\,R = \mathbb{1}_e, \qquad R\,T = \mathbb{1}_o, \qquad T^\top T = \mathbb{1}_o - vv^\top, \text{ etc.}$$

using the "NCReplace" series of commands[2].

We are not at this point able to explicitly resum the series and demonstrate that this converges but it is still instructive to look at the functional behaviour of each of these contributing terms separately.

[2]The *sth* power would give 2×2 blocks where each block is a sum of 2^{s-1} terms. Each such term is a product of s elements from the matrix $\mathbf{M}$ which in turn have sub-structure.

4.2 Illustrations for geometric series

We have therefore obtained a few lower order terms by this method when the expressions reduce to a sum of terms with infinite sum over a single index (the odd integers). At higher values of s, there are many terms which still involve only a single infinite sum but the few remaining terms involving double and triple sums (over both even and odd integers) lead to computational problems.

In the following, the integer in the superscript corresponds to the power s in the series expansion for the inverse.

$s = 0$ term

The first term in the expansion corresponding to $s = 0$ is given by:

$$\begin{aligned}\mathcal{R}^{(0)}_{2n,2m} &= -\delta_{nm} - \frac{4}{2m}\left[-\frac{1}{4}2nf_2(2n;t)\delta_{nm} + \frac{t}{16}\left(h_1(2n;t)^2 - h_3(2n;t)^2\right)\delta_{nm}\right] \\ &= \left(\frac{e^{-4nt}(nt-1)}{nt} + \frac{e^{-6nt}}{2nt} + \frac{e^{-2nt}}{2nt}\right)\delta_{nm} \\ &= \left(1 - 2nt + 6n^3t^3 - \frac{40n^4t^4}{3} + \mathcal{O}\left(t^5\right)\right)\delta_{nm} \end{aligned} \tag{4.13}$$

which contributes to the leading behaviour in the even sector, namely, $C_{nm} - nC_{nm}t + \mathcal{O}(t^2)$. The coefficients increase rapidly initially but then decrease as expected due to the factorial suppression.

$s = 1$ term

For $s = 1$, the infinite sums arising from the matrix products over the *odd* integers can be performed using *Mathematica*.

$$\mathcal{R}^{(1)}_{2n,2m} = -\frac{4}{2m} \times -t\left[\mathcal{Y}^{\top}\mathbf{M}\mathcal{Z}_0^{-1}\mathcal{Y}\right]^{pp} \tag{4.14}$$

Since the matrices $T_{2n,2m-1}$ and $R_{2n-1,2m}$ have a relatively simple structure expressible in terms of integers, we expect these to be in general in terms of hypergeometric functions ${}_JF_{J-1}$ with arguments of the form $q^k;\ k \in \mathbb{Z}_+$.[3]

For the diagonal matrix elements, we obtain:

$$\begin{aligned}\mathcal{R}^{(1)}_{2n,2n} = \frac{\left(q^{2n}-1\right)^2}{64\pi^2 n^3 \log^2(q)}\Bigg\{&-4q^{2n+2}\Phi\left(q^4,1,\frac{1}{2}-n\right) + 2nq^{2n+2}\Phi\left(q^4,2,\frac{1}{2}-n\right) \\ &+nq^{4n+2}\Phi\left(q^4,2,\frac{1}{2}-n\right) + 4q\left(q^{4n}-1\right)\Phi\left(q^2,1,\frac{1}{2}-n\right) \\ &-4nq\left(q^{4n}-1\right)\Phi\left(q^2,2,\frac{1}{2}-n\right) + 4q^2\Phi\left(q^4,1,\frac{1}{2}-n\right)\end{aligned}$$

[3] For the $s = 1$ case, which is very similar to the original matrix $\mathcal{Z}(q)$((3.26a), (3.27a)), these functions reduce to the Lerch transcendent representations and the appropriate analytic continuations—see (3.28).

$$
\begin{aligned}
&-3nq^2\Phi\left(q^4,2,\frac{1}{2}-n\right)+4q\Phi\left(q^2,1,n+\frac{1}{2}\right)+4nq\Phi\left(q^2,2,n+\frac{1}{2}\right)\\
&-4q^{2n+2}\Phi\left(q^4,1,n+\frac{1}{2}\right)-2nq^{2n+2}\Phi\left(q^4,2,n+\frac{1}{2}\right)+4q^{4n+2}\Phi\left(q^4,1,n+\frac{1}{2}\right)\\
&+3nq^{4n+2}\Phi\left(q^4,2,n+\frac{1}{2}\right)-4q^{4n+1}\Phi\left(q^2,1,n+\frac{1}{2}\right)-4nq^{4n+1}\Phi\left(q^2,2,n+\frac{1}{2}\right)\\
&-nq^2\Phi\left(q^4,2,n+\frac{1}{2}\right)-16\pi^2n^2q^{2n}\log(q)-16\pi^2nq^{2n}-8\gamma q^{2n}+14\pi^2nq^{4n}+4\gamma q^{4n}\\
&+8\log(2)\left(q^{2n}-1\right)^2+2\left(q^{2n}-1\right)^2\psi^{(0)}\left(\frac{1}{2}-n\right)(2n\log(q)+1)\\
&-2\left(q^{2n}-1\right)^2\psi^{(0)}\left(n+\frac{1}{2}\right)(2n\log(q)-1)\\
&-n\psi^{(1)}\left(\frac{1}{2}-n\right)\left(-5q^{4n}-2q^{6n}+q^{8n}+4q^{2n}(4n\log(q)+1)+2\right)\\
&+n\psi^{(1)}\left(n+\frac{1}{2}\right)\left(4q^{2n}-5q^{4n}-2q^{6n}+q^{8n}+8n\left(q^{4n}+1\right)\log(q)+2\right)\\
&+16q^{2n}\tanh^{-1}\left(q^2\right)-8q^{4n}\tanh^{-1}\left(q^2\right)+2\pi^2n-8\tanh^{-1}\left(q^2\right)+4\gamma\Bigg\}. \qquad (4.15)
\end{aligned}
$$

The above expression would simplify for particular integer values n. A very useful series representation for understanding these special functions is given by Erdélyi [47], which is valid for $|\log(z)|<2\pi$, $s=2,3,\ldots$ and $a\neq 0,-1,-2,\ldots$

$$
\Phi[z,s,a]=z^{-a}\left\{\sum_{\substack{k=0\\k\neq s-1}}^{\infty}\zeta(s-k,a)\frac{\log^k(z)}{k!}+[\psi(s)-\psi(a)-\log(-\log(z))]\frac{\log^{s-1}(z)}{(s-1)!}\right\} \qquad (4.16)
$$

where $\zeta(s,a)=\Phi(1,s,a)$ is the Hurwitz zeta function. Substituting this into the *Mathematica* output would give us the $\log(t)$ dependence we wanted (as $z=e^{-\#t}$ in our case). The resulting expression can be truncated at a finite k to obtain an expansion in t and $\log t$ as for instance:

$$
\begin{aligned}
\mathcal{R}_{22}^{(1)}&=\log t\left[\frac{16t^4}{\pi^2}-\frac{64t^5}{\pi^2}+\mathcal{O}\left(t^6\right)\right]\\
&+\left[2t^2+\frac{32}{3}\left(\frac{1}{\pi^2}-1\right)t^3-\frac{4t^4\left(34-21\pi^2+4\log(2)\right)}{3\pi^2}+\frac{4t^5\left(1408-589\pi^2+240\log(2)\right)}{45\pi^2}+\mathcal{O}\left(t^6\right)\right].
\end{aligned} \qquad (4.17)
$$

For $\Re(a)>0$, the two functions defined by Lerch Transcendents and Hurwitz Lerch transcendent coincide and one can simply replace the former with the latter. This is useful since *Mathematica* is able to expand Hurwitz Lerch functions with arguments $e^{\#t}$ arguments near $t=0$. This is another way to obtain the series expansions, although it is sightly less computationally efficient.

Similarly, the non-diagonal elements ($n \neq m$) are expressed as:

$$\begin{aligned}
\mathcal{R}^{(1)}_{2n,2m} = \frac{(-)^{n+m}}{32\pi^2 m(n^2-m^2)\log^2(q)} \Bigg\{ & \frac{\left(q^{2m}-1\right)^2\left(q^{2n}-1\right)^2}{nm}\Bigg[-m^2q^2\Phi\left(q^4,1,\frac{1}{2}-n\right) \\
& +n^2q^2\Phi\left(q^4,1,\frac{1}{2}-m\right)-m^2q^2\Phi\left(q^4,1,n+\frac{1}{2}\right)+n^2q^2\Phi\left(q^4,1,m+\frac{1}{2}\right) \\
& -4m^2n\psi^{(0)}\left(\frac{1}{2}-n\right)\log(q)+4m^2n\psi^{(0)}\left(n+\frac{1}{2}\right)\log(q)-m^2\psi^{(0)}\left(\frac{1}{2}-n\right) \\
& -m^2\psi^{(0)}\left(n+\frac{1}{2}\right)+4m^2\tanh^{-1}\left(q^2\right)+2m^2\psi^{(0)}\left(\frac{1}{2}\right)+4mn^2\psi^{(0)}\left(\frac{1}{2}-m\right)\log(q) \\
& -4mn^2\psi^{(0)}\left(m+\frac{1}{2}\right)\log(q)+n^2\psi^{(0)}\left(\frac{1}{2}-m\right)+n^2\psi^{(0)}\left(m+\frac{1}{2}\right)-4n^2\tanh^{-1}\left(q^2\right) \\
& -2n^2\psi^{(0)}\left(\frac{1}{2}\right)\Bigg]+\frac{\left(q^{2m}-1\right)\left(q^{2n}-1\right)}{nm}\left(n\left(q^{2m}+1\right)\left(q^{2n}-1\right)+m\left(q^{2m}-1\right)\left(q^{2n}+1\right)\right) \\
& \times\Bigg[2nq\Phi\left(q^2,1,\frac{1}{2}-m\right)-2mq\Phi\left(q^2,1,\frac{1}{2}-n\right)-nq^2\Phi\left(q^4,1,\frac{1}{2}-m\right) \\
& +mq^2\Phi\left(q^4,1,\frac{1}{2}-n\right)-2nq\Phi\left(q^2,1,m+\frac{1}{2}\right)+2mq\Phi\left(q^2,1,n+\frac{1}{2}\right) \\
& +nq^2\Phi\left(q^4,1,m+\frac{1}{2}\right)-mq^2\Phi\left(q^4,1,n+\frac{1}{2}\right)+n\psi^{(0)}\left(\frac{1}{2}-m\right)-n\psi^{(0)}\left(m+\frac{1}{2}\right) \\
& -m\psi^{(0)}\left(\frac{1}{2}-n\right)+m\psi^{(0)}\left(n+\frac{1}{2}\right)\Bigg]+\left(q^{4m}-1\right)\left(q^{4n}-1\right)\Bigg[-4q\Phi\left(q^2,1,\frac{1}{2}-m\right) \\
& +q^2\Phi\left(q^4,1,\frac{1}{2}-m\right)+4q\Phi\left(q^2,1,\frac{1}{2}-n\right)-q^2\Phi\left(q^4,1,\frac{1}{2}-n\right)-4q\Phi\left(q^2,1,m+\frac{1}{2}\right) \\
& +q^2\Phi\left(q^4,1,m+\frac{1}{2}\right)+4q\Phi\left(q^2,1,n+\frac{1}{2}\right)-q^2\Phi\left(q^4,1,n+\frac{1}{2}\right) \\
& -4m\psi^{(0)}\left(\frac{1}{2}-m\right)\log(q)+4m\psi^{(0)}\left(m+\frac{1}{2}\right)\log(q)-3\psi^{(0)}\left(\frac{1}{2}-m\right)-3\psi^{(0)}\left(m+\frac{1}{2}\right) \\
& +4n\psi^{(0)}\left(\frac{1}{2}-n\right)\log(q)-4n\psi^{(0)}\left(n+\frac{1}{2}\right)\log(q)+3\psi^{(0)}\left(\frac{1}{2}-n\right)+3\psi^{(0)}\left(n+\frac{1}{2}\right)\Bigg]\Bigg\}
\end{aligned} \tag{4.18}$$

By construction, these non-diagonal elements all satisfy the $SU(1,1)$ condition [27]

$$\mathbf{R}_{nm}\ m = \mathbf{R}_{mn}\ n \tag{4.19}$$

order by order in s. For specific values of n, m, the above expressions do simplify, for instance:

$$\begin{aligned}
\mathcal{R}^{(1)}_{24} = \frac{\mathcal{R}^{(1)}_{42}}{2} = \frac{1}{288\pi^2q^4\log^2(q)} \Big\{ & (q-1)^4(q+1)^2\left(q^2+1\right)\Big(3(q+1)^2\left(q^4+4q^2+1\right)\left(q^2+1\right)^3\tanh^{-1}q^2 \\
& +(q-1)^2q\left(3q^8+9q^7+34q^6+65q^5+78q^4+65q^3+34q^2+9q+3\right)\Big) \\
& -3\left(q^4-1\right)^4\left(q^4+4q^2+1\right)\tanh^{-1}q\Big\}.
\end{aligned} \tag{4.20}$$

However, we find that after $\Phi(z,1,a)$ simplifies, the $\log t$ terms from those terms are

absent in a series expansion for the non-diagonal elements. For example, we find interestingly enough that:

$$\begin{aligned}
\mathcal{R}^{(1)}_{24} &= -\frac{8t^2\log(2)}{\pi^2} + \frac{48t^3\log(2)}{\pi^2} + \frac{t^4(31-512\log(2))}{3\pi^2} + \mathcal{O}\left(t^5\right) \\
\mathcal{R}^{(1)}_{46} &= -\frac{16t^2\log(2)}{\pi^2} + \frac{160t^3\log(2)}{\pi^2} - \frac{2t^4(1408\log(2)-79)}{3\pi^2} + \mathcal{O}\left(t^5\right) \\
\mathcal{R}^{(1)}_{26} &= \frac{8t^2\log(2)}{\pi^2} - \frac{64t^3\log(2)}{\pi^2} + \frac{t^4(928\log(2)-61)}{3\pi^2} + \mathcal{O}\left(t^5\right) \\
\mathcal{R}^{(1)}_{28} &= -\frac{8t^2\log(2)}{\pi^2} + \frac{80t^3\log(2)}{\pi^2} + \frac{t^4(103-1472\log(2))}{3\pi^2} + \mathcal{O}\left(t^5\right), \text{ etc.}
\end{aligned} \tag{4.21}$$

The log branch cuts from arctanh terms have cancelled after the sum over the block matrix indices (x, p). The individual infinite sums from $\mathbf{M}$ all diverge badly for $t < 0$ but they combine appropriately for the non-diagonal case to give a *log-free expansion* at this order in s.

$s = 2$ term

We are able to construct the matrix elements $\mathcal{R}^{(2)}_{2n,2m}$ for a general n, m although they are a longer combination of special functions, namely products of Hurwitz Lerch transcendents and Lerch transcendents which are not particularly illuminating. Hence, we only provide the series expansions for certain matrix elements to show the general numerical structure:

$$\begin{aligned}
\mathcal{R}^{(2)}_{22} = &\frac{2t^2(44\log(2)-27\log(3))}{3\pi^2} + t^3\left(2 - \frac{16\log^2(2)}{\pi^4} - \frac{304\log(2)}{3\pi^2} + \frac{72\log(3)}{\pi^2}\right) \\
&+ t^4\left(-\frac{32}{3} + \frac{71}{15\pi^2} + \frac{64\log^2(2)}{\pi^4} + \frac{9416\log(2)}{45\pi^2} - \frac{894\log(3)}{5\pi^2}\right) + \mathcal{O}\left(t^5\right),
\end{aligned} \tag{4.22a}$$

$$\begin{aligned}
\mathcal{R}^{(2)}_{24} = &\frac{2t^2(27\log(3)-44\log(2))}{3\pi^2} + t^3\left(\frac{16\log^2(2)}{\pi^4} - \frac{108\log(3)}{\pi^2} + \frac{76\log(4)}{\pi^2}\right) \\
&+ t^4\left(-\frac{34}{3\pi^2} - \frac{96\log^2(2)}{\pi^4} + \frac{411\log(3)}{\pi^2} - \frac{2162\log(4)}{9\pi^2}\right) + \mathcal{O}\left(t^5\right).
\end{aligned} \tag{4.22b}$$

Next, we can combine the contributions from these three terms and analyse how well they approximate the behaviour by comparing to a numerical evaluation of the same as we do in Fig. 4.1. However, from the open-closed correspondence we expect the above expansion in terms of the t^r and $\log(t)$ basis to be incomplete. The crucial point is that one cannot dictate that the summation over s and the Taylor series expansions over r above must commute. Hence, the summation over s can lead to the subleading terms[4]

[4]This physical input from the CFT picture can be taken into account explicitly by the formalism of *Hardy fields* employed in real asymptotics, which allows to amalgamate many "exponential scales". See chapter V, appendix 1 of [52] and chapters 3, 5 of [53] for details on the theory.

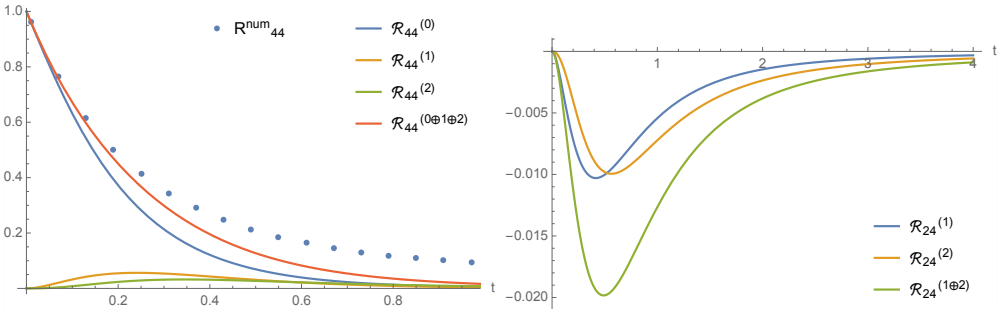

(a) (b)

Figure 4.1: The individual contributions from the various matrix powers $s = 0, 1, 2$ and their sum is plotted for two matrix elements (a) $\mathbf{R}_{44}(t)$ and (b) $\mathbf{R}_{24}(t)$. The numerical estimate for $N = 64$ is also plotted for the $\mathbf{R}_{44}$ case and is seen to closely follow the analytic sum. For $\mathbf{R}_{24}$, the fit is not quite good since it starts only at the quadratic order and more terms would be required to account for the small but comparable contributions.

from closed string states of the form:

$$\mathbf{R}_{nm}(t) = \sum_{k=0}^{\infty}\sum_{j=0}^{\infty}\sum_{s_1,s_2=0}^{\infty} c_{k|j|s_1s_2}(\log_{s_1}(t^{-1}))^{s_2}t^j e^{-\frac{2\pi^2 k}{t}} \tag{4.23}$$

where $c_{k|j|s_1s_2}$ are some specific (real) coefficients and we have suppressed the mode labels n, m for simplicity.

By adding the contributions from the higher matrix powers in s, one may obtain a subset of the above coefficients to higher accuracy, the ones corresponding to the $k = 0$ level in this expansion. The exponentially small parts from $k \geq 1$ are the ones of most interest to us and which encode information about the *on-shell* closed string states and it would be interesting to recover some information about those states.

In summary, we have provided a formal procedure for successively approximating the coefficients in an expansion near $t = 0$. We do not claim to the efficiency or numerical control resulting from this method. We must also acknowledge that this procedure does not extend in practice beyond the lowest orders due to some of the double sums (involving generalized hypergeometric functions) that arise from the block matrix multiplications. Because of the non-analytic behaviour—which has its physical origins in the worldsheet picture—it is intrinsically difficult to identify the divergences or the subleading terms in the algebraic method we have used. Nonetheless, we hope that it has augmented the knowledge levels on the algebraic structure of OSFT at the quantum level.

In the next subsection, we shall study the behaviour of these matrix elements near the other limit of the modular parameter, that is, $t \to +\infty$ by using an expansion in the variable $q = e^{-t}$ near $q = 0^+$. Since the oscillator based expressions are much more suited for this kind of an expansion, we only check till the linear order term for consistency. We will find that our expressions correctly reproduce the numbers that can be generated from

the oscillator based expansion.

4.3 Expansions near $t = \infty$ in the continuous κ-basis

In order to obtain the expansion for $\mathbf{R}_{nm}$ in the large t (or small q) limit, as a power series in $q = e^{-t}$, one goes to the continuous κ-basis [23, 24, 26] that we discuss later in §4.3.2. It corresponds to another basis for the same $j = 0$ representation of $SL(2, \mathbb{R})$ associated with the discrete basis defined in terms of mode number labels, that we have been using. We choose it to convert some of the infinite sums to integrals for the purpose of numerical evaluation of the series coefficients. In certain cases, one can correctly guess the exact algebraic numbers by using the *RootApproximant* command in *Mathematica* if they stabilize as the "WorkingPrecision" is increased.

4.3.1 Even parity elements till linear order in q

To commence the evaluation, let us define a matrix $\mathcal{S}$ in terms of purely the even frequencies κ_e as $\mathcal{S} \coloneqq \mathrm{diag}\{\kappa_e^{1/2}, \kappa_e^{-1/2}\}$. Then we can express the matrices $\mathcal{Q}_\eta$ and $\mathcal{L}_\eta$ that contribute to $\mathbf{R}(q)$ as:

$$\begin{aligned}
\mathcal{Q}_\eta &= \frac{1}{4}\mathcal{S}^{-1}\begin{bmatrix} f_3 + t f_4 t^\top & -\frac{i}{2}(f_1 - t f_1 r) \\ -\frac{i}{2}(f_1 - r^\top f_1 t^\top) & \frac{1}{4}(f_4 + r^\top f_3 r) \end{bmatrix}\mathcal{S}^{-1} =: \frac{1}{4}\mathcal{S}^{-1}\mathbf{Q}^\kappa\mathcal{S}^{-1}, \\
\mathcal{L}_\eta &= \frac{1}{2}\mathcal{S}^{-1}\begin{bmatrix} t f_1 t^\top & \frac{i}{2} f_3 \\ -\frac{i}{2} r^\top f_3 t^\top & \frac{1}{4} f_1 \end{bmatrix}\mathcal{S}^{-1} =: \frac{1}{2}\mathcal{S}^{-1}\mathbf{L}^\kappa\mathcal{S}^{-1},
\end{aligned} \tag{4.24}$$

where we have introduced the block matrices $\mathbf{Q}^\kappa$ and $\mathbf{L}^\kappa$ after absorbing the numerical factors. Here, we have employed the matrix $t \coloneqq \sqrt{\kappa_e}\, T \frac{1}{\sqrt{\kappa_o}}$ which is the operator [26] $\tanh\frac{\pi\hat{Q}_1}{2}$ which appears in the continuous Moyal basis[5] and r is the formal inverse of the matrix t, i.e. $r \coloneqq \sqrt{\kappa_o} R \frac{1}{\sqrt{\kappa_e}}$. Then we can rewrite the matrix which appears in the matrix $\mathcal{F}(q)$ (3.32) as:

$$\begin{aligned}
\mathcal{L}_\eta^\top \mathcal{Q}_\eta^{-1}\mathcal{L}_\eta &= \mathcal{S}^{-1}\mathbf{L}^{\kappa\top}(\mathbf{Q}^\kappa)^{-1}\mathbf{L}^\kappa\mathcal{S}^{-1} \\
&= \mathcal{S}^{-1}\begin{bmatrix} t f_1 t^\top & -\frac{i}{2} t f_3 r \\ \frac{i}{2} f_3 & \frac{1}{4} f_1 \end{bmatrix}\begin{bmatrix} f_3 + t f_4 t^\top & -\frac{i}{2}(f_1 - t f_1 r) \\ -\frac{i}{2}(f_1 - r^\top f_1 t^\top) & \frac{1}{4}(f_4 + r^\top f_3 r) \end{bmatrix}^{-1}\begin{bmatrix} t f_1 t^\top & \frac{i}{2} f_3 \\ -\frac{i}{2} r^\top f_3 t^\top & \frac{1}{4} f_1 \end{bmatrix}\mathcal{S}^{-1}
\end{aligned} \tag{4.25}$$

in block matrix form.

To obtain the inverse, once again we perform a geometric series expansion by separating the degree zero term through $\mathbf{Q}^\kappa(q) =: \mathbf{Q}_0^\kappa + \delta\mathbf{Q}^\kappa(q)$. Since as $q \to 0^+$, we have

[5] As we do not use the parameter $t = -\log q$ in this section, we hope the repeated use of the symbol wouldn't give rise to any ambiguities.

$f_1(q) \to 1^-, f_3(q) \to 1^-$ and $f_4(q) \to 3^-$,

$$(\mathbf{Q}_0^\kappa)^{-1} = \begin{bmatrix} \Lambda & 0 \\ 0 & 4\Omega \end{bmatrix}, \tag{4.26}$$

where we define the infinite matrices:

$$\Lambda \coloneqq \frac{1}{1+3tt^\top}, \qquad \Omega \coloneqq \frac{1}{3+r^\top r} = \frac{1}{3}(1-\Lambda). \tag{4.27}$$

Next, we insert the following binomial inverse series in order to obtain $\mathcal{F}(q)$ which in terms of these new matrices become:

$$\mathcal{F}(q) = \frac{1}{2} M_0^{gh-1} f_2(q) + \sum_{s=0}^{\infty} (-1)^s \mathcal{S}^{-1} \mathbf{L}^{\kappa\top} \left[(\mathbf{Q}_0^\kappa)^{-1} \delta \mathbf{Q}^\kappa \right]^s \cdot (\mathbf{Q}_0^\kappa)^{-1} \mathbf{L}^\kappa \mathcal{S}^{-1}. \tag{4.28}$$

We shall denote the expansion as:

$$\mathcal{F}(q) = \sum_{s=0}^{\infty} (-1)^s \mathcal{F}^{\kappa|s}(q), \text{ where we set} \tag{4.29}$$

$$\mathcal{F}^{\kappa|0}(q) = \frac{1}{2} M_0^{gh-1} f_2(q) + \mathcal{S}^{-1} \mathbf{L}^{\kappa\top}(q) (\mathbf{Q}_0^\kappa)^{-1} \mathbf{L}^\kappa(q) \mathcal{S}^{-1}. \tag{4.30}$$

Here as well, the simplest element to consider is the purely even block $\mathcal{F}^{pp}_{2n,2m}$, which contains the explicit term:

$$(\mathbf{L}^{\kappa\top}(\mathbf{Q}^\kappa)^{-1}\mathbf{L}^\kappa)^{pp} = \mathbf{L}^{\kappa\top}_{px}(\mathbf{Q}^\kappa)^{-1}_{xx}\mathbf{L}^\kappa_{xp} + \mathbf{L}^{\kappa\top}_{px}(\mathbf{Q}^\kappa)^{-1}_{xp}\mathbf{L}^\kappa_{pp} + \mathbf{L}^{\kappa\top}_{pp}(\mathbf{Q}^\kappa)^{-1}_{px}\mathbf{L}^\kappa_{xp} + \mathbf{L}^{\kappa\top}_{pp}(\mathbf{Q}^\kappa)^{-1}_{pp}\mathbf{L}^\kappa_{pp}, \tag{4.31}$$

where we have used the doublet indices x, p as subscripts for typographical convenience.

In the following, we simply restrict to the general structure of the lowest order $s = 0$ term since we are primarily interested in certain consistency checks in the $q \to 0^+$ limit. The oscillator expansion is much better suited for expansions near this limit and hence we return to that method in §4.4. We shall later collect the exact coefficients for q^0 and q^1 and verify that they match with the exact results from the oscillator expressions.
Upon inserting the constituent block matrices, the momentum block $\mathcal{F}^{\kappa pp|0}$ in (4.30) has the structure:

$$\begin{aligned}
\mathcal{F}^{\kappa pp|0}_{2n,2m}(q) &= -\frac{1}{4} \cdot 2n f_2(2n)\delta_{nm} + 2\sqrt{nm} \cdot \frac{1}{4} \left(f_1(2n) f_1(2m) \Omega_{2n,2m} - f_3(2n) f_3(2m) \Lambda_{2n,2m} \right) \\
&= -\frac{n}{2}\delta_{nm} + \frac{\sqrt{nm}}{2}(\Omega - \Lambda)_{2n,2m} \\
&\quad + \frac{\sqrt{nm}}{2} \left[-2\Omega_{2n,2m} q^{2n} - 2\Omega_{2n,2m} q^{2m} + \left(\Lambda_{2n,2m} + \Omega_{2n,2m} - \sqrt{\frac{n}{m}} \right) q^{4n} \right. \\
&\quad \left. + (\Omega + \Lambda)_{2n,2m} q^{4m} + 4\Omega_{2n,2m} q^{2n+2m} \right.
\end{aligned}$$

$$-2\Omega_{2n,2m}q^{2n+4m} - 2\Omega_{2n,2m}q^{4n+2m} + (\Omega-\Lambda)_{2n,2m}q^{4n+4m}\Big], \tag{4.32}$$

without any summations over repeated indices. The next term in the expansion becomes more tedious but starts contributing at q^1 (due to the infinite summations over the *odd* index).

To this end, it is worthwhile to note that the constant part of the matrix $\mathbf{L}^\kappa$ is of the form:

$$\mathbf{L}^\kappa(0) = \begin{bmatrix} tt^\top & \frac{i}{2} \\ -\frac{i}{2} & \frac{1}{4} \end{bmatrix} \tag{4.33}$$

This allows us to collect the coefficient of q^0 from

$$(\mathbf{L}^{\kappa\top}(\mathbf{Q}^\kappa)^{-1}\mathbf{L}^\kappa)^{(0)}_{pp} = -\frac{1}{4}\kappa_e - \frac{1}{4}\sqrt{\kappa_e}\frac{1-tt^\top}{1+3tt^\top}\sqrt{\kappa_e} \tag{4.34}$$

which when substituted into the expression for $\mathbf{R}_{2n,2m}$ in terms of $\mathcal{F}_{2n,2m}$ (3.46):

$$\begin{aligned}\mathbf{R}^{(0)}_{2n,2m} &= -\Big[\mathbb{1} - \mathbb{1} - \sqrt{\kappa_e}\frac{1-tt^\top}{1+3tt^\top}\frac{1}{\sqrt{\kappa_e}}\Big]_{2n,2m} \\ &= \sqrt{\frac{n}{m}}\left[\frac{1-tt^\top}{1+3tt^\top}\right]_{2n,2m},\end{aligned} \tag{4.35}$$

which is precisely the even parity elements of the Neumann matrix $X^{11}_{2n,2m}$ in (2.76) as was derived in the oscillator formalism.

Similarly, the coefficient of q^1 is given by the matrix:

$$\mathbf{R}^{(1)}_{2n,2m} = -2\sqrt{nm}\left[(\Lambda t)_{2n,1}(\Lambda t)_{2m,1} + \frac{1}{2}\Big((\Lambda t)_{2n,1}(\Omega r^\top)_{2m,1} + (n \leftrightarrow m)\Big)\right] \times \frac{-4}{2m} \tag{4.36}$$

by considering the $s=1$ power and noticing that the q^{4n}, q^{2n} terms do not contribute at this order for any n. Now, one can show that $\Omega r^\top = \Lambda t$; hence the above reduces to:

$$\mathbf{R}^{(1)}_{2n,2m} = 8\sqrt{\frac{n}{m}}(\Lambda t)_{2n,1}(\Lambda t)_{2m,1}. \tag{4.37}$$

4.3.2 Numerical evaluation in the continuous κ-basis

The matrix elements of the rational functions involving the t matrix such as

$$\Lambda t = \frac{1}{1+3tt^\top}t = t\frac{1}{1+3t^\top t}$$

can be obtained by numerical integration by going to the continuous Moyal basis[6], known as the κ-basis. The κ basis diagonalizes the operator $K_1 = (L_1 + L_{-1})$ of $SL(2,\mathbb{R})$ [23, 24, 26]:

$$K_1|\kappa\rangle = \kappa|\kappa\rangle \tag{4.38}$$

which commutes with the vertex, and is useful for performing analytic and numerical calculations.

The t matrix is diagonalized in the infinite N limit to give the eigenvalues[26]: $t_\kappa = \tanh(\pi\kappa/4)$. Then we have the integral representation for the matrix elements as

$$\begin{aligned} t_{2n,2m-1} &= \sqrt{2n}\; T_{2n-1,2m-1}\; \frac{1}{\sqrt{2m-1}} \\ &= \int_{-\infty}^{\infty} d\kappa\, v_{2n}(\kappa) \tanh(\pi\kappa/4) v_{2m-1}(\kappa) \end{aligned} \tag{4.39}$$

where we start[7] with defining the overlap functions

$$v_n(\kappa) = \langle\kappa|n\rangle = \frac{y_n(\kappa)}{\sqrt{n}\sqrt{\frac{2}{\kappa}\sinh\frac{\pi\kappa}{2}}} \tag{4.40}$$

which are a class of polynomials that arise naturally in the continuous basis and are analogous to the Hermite polynomials for the number operator. These are orthogonal with respect to the weight function

$$w(\kappa) = \left(\frac{2}{\kappa}\sinh\frac{\pi\kappa}{2}\right)^{-1} \tag{4.41}$$

A generating functional for these polynomials is given by:

$$\sum_{n\in\mathbb{Z}_+} \frac{z^n}{n} y_n(\kappa) = \frac{1}{\kappa}(1 - e^{-\kappa \arctan z}) = f_\kappa(z) \tag{4.42}$$

and they satisfy the recurrence relation:

$$y_{n+1}(\kappa) + y_{n-1}(\kappa) = -\frac{\kappa}{n} y_n(\kappa), \tag{4.43}$$

among many other relations listed in [23]. Setting $y_0(\kappa) = 0, y_1(\kappa) = 1$, leads to the polynomials:

$$\begin{aligned} y_1(\kappa) &= 1, & y_2(\kappa) &= -\kappa, \\ y_3(\kappa) &= \frac{1}{2}\kappa^2 - 1, & y_4(\kappa) &= -\frac{1}{6}\kappa^3 + \frac{4}{3}\kappa, \end{aligned}$$

[6]The notational conflict in using κ for the continuous basis and for the spectral matrix would be restricted to this subsubsection.

[7] The following properties are taken from App A of [23].

$$y_5(\kappa) = \frac{1}{24}\kappa^4 - \frac{5}{6}\kappa^2 + 1, \qquad y_6(\kappa) = -\frac{1}{120}\kappa^5 + \frac{1}{3}\kappa^3 - \frac{23}{15}\kappa, \tag{4.44}$$

and so on and so forth.

After this short exposition of these somewhat amusing polynomials, let us return to the evaluation of the matrix functions. In terms of the new continuous basis, we can express functions of the t matrices such as

$$\left(F(tt^\top)\right)_{2n,2m} = \int_{-\infty}^{\infty} d\kappa\, v_{2n}(\kappa) F\left(\tanh^2\left(\frac{\pi\kappa}{4}\right)\right) v_{2m}(\kappa), \tag{4.45a}$$

$$\left(tF(t^\top t)\right)_{2n,2m-1} = \int_{-\infty}^{\infty} d\kappa\, v_{2n}(\kappa) \tanh\left(\frac{\pi\kappa}{4}\right) F\left(\tanh^2\left(\frac{\pi\kappa}{4}\right)\right) v_{2m-1}(\kappa), \text{ etc.} \tag{4.45b}$$

using which we have evaluated (4.37) upto a WorkingPrecision of 16 in *Mathematica*. The resulting numbers for some matrix elements are listed in Table 4.1. Now, by using the

$\mathbf{R}_{nm}^{\text{Moy}\|1}$	2	4	6	8
2	0.325154	−0.0939333	0.0511147	−0.0338815
4	−0.187867	0.0542726	−0.0295329	0.0195760
6	0.153344	−0.0442994	0.0241059	−0.0159787
8	−0.135526	0.0391520	−0.0213049	0.0141220

Table 4.1: Numerical evaluation of the linear coefficient in a few even parity matrix elements $\mathbf{R}_{nm}(q)$ using the continuous κ basis for the Moyal $*$.

oscillator based expansion in (2.76) and (4.57), we obtain the linear coefficient to be in terms of the ghost Neumann matrices:

$$\mathbf{R}_{2n,2m}^{(1)|osc} = -\left(X_{2n,1}^{12} X_{1,2m}^{12} + X_{2n,1}^{21} X_{1,2m}^{21}\right). \tag{4.46}$$

These rational numbers are tabulated in Table 4.2 and found to be the stabilizing value as the WorkingPrecision for the numerical integrations above is increased. Indeed, we

$\mathbf{R}_{nm}^{\text{osc}\|1}$	2	4	6	8
2	$\frac{6400}{19683}$	$-\frac{16640}{177147}$	$\frac{244480}{4782969}$	$-\frac{13126400}{387420489}$
4	$-\frac{33280}{177147}$	$\frac{86528}{1594323}$	$-\frac{1271296}{43046721}$	$\frac{68257280}{3486784401}$
6	$\frac{244480}{1594323}$	$-\frac{635648}{14348907}$	$\frac{9339136}{387420489}$	$-\frac{501428480}{31381059609}$
8	$-\frac{52505600}{387420489}$	$\frac{136514560}{3486784401}$	$-\frac{2005713920}{94143178827}$	$\frac{107688985600}{7625597484987}$

Table 4.2: Exact linear coefficients in a few even parity matrix elements $\mathbf{R}_{nm}(q)$ obtained using the oscillator method in terms of Neumann coefficients.

may also express the Neumann matrices $X^{(\pm)}$ in terms of the matrix

$$\hat{m}_0^* := \begin{pmatrix} 0 & -S \\ -T^\top & 0 \end{pmatrix} \tag{4.47}$$

defined in [20] to analytically prove that both expressions for the linear term coincide. This expansion can thus result in interesting relations between the Neumann matrices and matrices arising from the Moyal structure which may be established by using the canonical way of expressing all the Neumann matrices in terms of the matrix t and the frequency matrices κ_e and κ_o [20].

Regarding studying the determinant factor in the integrand using a q expansion(see also 3.1.3), which is common for all matrix elements, we find that the lowest power of each matrix element *do not decrease along a row or a column* which is required for a systematic expansion. Essentially, one cannot separate the degree zero piece as there is no nice way to express $\det(1 + A^{-1}B)$ in terms of $\det A^{-1}B$.

Although one can include the higher powers $((\mathbf{Q}_0^\kappa)^{-1}\delta\mathbf{Q}^\kappa)^s$ to obtain the exact coefficients for a q series, this would necessitate many more numerical integrations arising from collecting powers together and results in numerical uncertainties. The oscillator basis on the other hand furnishes the exact coefficients since the Neumann matrices are known exactly from CFT. We therefore simply contend ourselves with the zeroth order and the linear coefficient using the κ basis and compare with the oscillator based expansion. This serves as a consistency check on the correctness of our expressions in the $t \to +\infty$ limit. Hence for the purpose of constructing a q-series, we employ the oscillator based expressions in (2.76) expressed in terms of Neumann matrices in the following subsection. This can then be used to search for some hints of the non-analyticities expected from the underlying geometrical picture.

4.3.3 Another consistency check using factorization

Let us pause for a moment and do a quick check on the overall determinant factors near the $t \to \infty$ or $q \to 0$ limit to make sure that the result is regulator independent. In this limit, we expect the integrand to factorize into the 3-point function, with two legs on-shell with $p^2 = 1 = -m^2$ for the "lightest" tachyon state and one off-shell tachyon state with $p = 0$, and a tachyon propagator[8] with $t \to \infty$. The off-shell 3-tachyon amplitude has been known[13, 34, 45] to be of the form:

$$g_{123}(k_i) = g_T K^3 \times K^{-(k_1^2+k_2^2+k_3^2)}, \tag{4.48}$$

[8]This may be read off from open string partition function.

where we recall that g_T is the on-shell 3-tachyon coupling (by definition) and $K = \dfrac{3\sqrt{3}}{4}$. Hence, we expect the leading asymptotics to be:

$$\frac{g_0}{3}\frac{(1+w^\top w)^{\frac{d+2}{2}}}{(2\pi)^{d(N+1/2)}}q^{-1}\frac{\det(2\mathcal{Q}_\eta^{gh})}{|\det(2\mathcal{Q}_\eta^X)|^{d/2}}(2\mathcal{Q}_p)^{-d/2} \to g_T K^3 \times K^{-2}\,\frac{q^{-1}(-2\log q)^{-d/2}}{(2\pi)^{d(N+1/2)}} \quad (4.49)$$

as $q \to 0$, when $d = 26$. The 2π factors arise from the η^X and p integrations and the manner in which the basis states $e^{i\xi^\top \eta}$ are normalized. We have also set $l_s = \sqrt{2}$ on the right hand side for consistency with our earlier conventions.

The factor $\mathcal{Q}_p$ arising from the momentum integration is dominated by $-\log q$ and hence we require:

$$\lim_{t\to\infty}\frac{g_0}{3}(1+w^\top w)^{\frac{d+2}{2}}\frac{\det(2\mathcal{Q}_\eta^{gh})}{|\det(2\mathcal{Q}_\eta^X)|^{d/2}} = g_T\,K \quad (4.50)$$

The determinant factors involve the block matrices (3.18), (B.11):

$$\begin{aligned}
\mathcal{Q}_\eta^{gh} &= +\frac{1}{4}\begin{bmatrix} \kappa_e^{-1}f_3(\kappa_e) + T\kappa_o^{-1}f_4(\kappa_o)T^\top & -\frac{i}{2}\left[f_1(\kappa_e) - Tf_1(\kappa_o)R\right] \\ -\frac{i}{2}\left[f_1(\kappa_e) - R^\top f_1(\kappa_o)T^\top\right] & \frac{1}{4}\left[\kappa_e f_4(\kappa_e) + R^\top\kappa_o f_3(\kappa_o)R\right]\end{bmatrix}, \\
\mathcal{Q}_\eta^{X} &= +\frac{1}{2}\begin{bmatrix} \kappa_e^{-1}f_4 + T\kappa_o^{-1}f_3(\kappa_o)T^\top & -\frac{i}{4}(f_1(\kappa_e) - Tf_1(\kappa_o)R) \\ -\frac{i}{4}(f_1(\kappa_e) - Tf_1(\kappa_o)R)^\top & \frac{1}{16}\left(\kappa_e f_3 + R^\top\kappa_o f_4 R\right)\end{bmatrix}
\end{aligned} \quad (4.51)$$

In the $q \to 0$ limit, we have $f_1 \to 1, f_3 \to 1$ and $f_4 \to 3$ and hence the ratio of the determinant factors above reduces to give:

$$\begin{aligned}
\det(2)_{2N}^{-1}\frac{\det(1+3tt^\top)\det\left(\frac{3+r^\top r}{4}\right)}{\det(3+tt^\top)^{d/2}\det\left(\frac{1+3r^\top r}{16}\right)^{d/2}} &= 2^{2N(d-2)}\frac{\det(1+3tt^\top)\det(3+r^\top r)}{\det(3+tt^\top)^{d/2}\det\left(1+3r^\top r\right)^{d/2}} \\
&= 2^{2N(d-2)}\det(1+3tt^\top)^2\det(3+tt^\top)^{-d}\det(tt^\top)^{\frac{d-2}{2}},
\end{aligned} \quad (4.52)$$

where $r \coloneqq t^{-1} = \kappa_o^{-1}t^\top\kappa_e$ and we have substituted $r^\top r = (tt^\top)^{-1}$. Multiplying with the remaining factors and using $\det(tt^\top) = (1+w^\top w)^{-1/2}$, we have:

$$\begin{aligned}
\frac{g_0}{3}(1+w^\top w)^{\frac{d+2}{2}} \times 2^{2N(d-2)}\frac{\det(1+3tt^\top)^2}{\det(3+tt^\top)^d}\det(tt^\top)^{\frac{d-2}{2}} &= 2^{2N(d-2)}\frac{g_0}{3}(1+w^\top w)^{-\frac{d}{8}+\frac{3}{4}}\frac{\det(1+3tt^\top)^2}{\det(3+tt^\top)^d}, \\
&= -\mu_3\frac{g_0}{3},
\end{aligned} \quad (4.53)$$

where μ_3 is the normalization factor (2.86) that relates the interaction term in the Moyal and the oscillator formalisms(§2.4), and which vanishes as $N \to \infty$. In terms of μ_3, the couplings are related as $g_T = -\mu_3 \times 2g_0K^{-3}$ [26, ref 2, Eq. 2.3] and hence the N dependence is removed. The LHS now becomes: $g_T/6\,K^3$ which is off from the expected result of g_TK by a factor of $\dfrac{1}{6}K^2 = 9/32 = 0.28125$. The 6 is because of the symmetry factor 3! for the 3-point function but no such factors would arise for the tadpole case. We

hope to return to this slight discrepancy when occasion offers itself.

Moving on, we can obtain the higher order terms more efficiently and exactly using the oscillator based expression, to which we turn next.

4.4 A convergent expansion in q using the oscillator expression

In this work, we have been mainly interested in the behaviour of the finite matrix elements as $t \to 0^+$. This corresponds to looking at the $q \to 1^-$ limit, and hence may also be indirectly inferred from a series expansion near $q = 0$ (the $t = +\infty$ limit) due to the expected non-analyticities. Physically, one would expect that the t evolved string field becomes ill-defined when $\Re(t) < 0$; the propagator would result in divergent sums while acting on a string field for $t < 0$. Thus, intuitively we would expect the matrix elements to be uniformly convergent for $|q| < 1$ and to have non-analytic behaviour everywhere on the unit circle $|q| = 1$ which obstructs an analytic continuation beyond the unit disc in the q plane.

We therefore proceed to directly use the oscillator expression given in [14] to probe the $q \to 1^-$ limit. The matrix elements $\mathbf{R}_{nm}(q)$, can be given a systematic expansion in powers of q as follows. The matrix whose powers are taken in the geometric series expansion has a minimal degree 1. Therefore, the matrix powers start contributing only from higher and higher powers onwards as the infinite sums in the matrix products would not alter the order of the zeroes. This allows us to obtain the exact coefficients by adding up the contribution from a *finite* number of matrix powers.

A q-series expansion

By a theorem of Sierpiński (see [54, §4.2]), there can exist power series which converges at a single point on the boundary (say $z = 1$) but diverges at every other point. In our particular case, we would have a series with radius of convergence 1, that converges at $q = 1$ to either $+1$ or -1 but exhibits discontinuous behaviour on the disc boundary.

The oscillator based expressions given in [14, §4] is naturally suited for systematically finding a q series expansion for $\mathbf{R}_{nm}(q)$ since the propagator is simple in this basis. Again, the ghost sector is relatively simpler as compared to the matter sector due to the absence of the momentum zero mode.

As the hatted matrices (2.77) appearing in (2.76) for $\mathbf{R}(q)$ do not seem to satisfy any nice identities unlike the $\mathcal{M}_{0,\pm}$ matrices, we resort to a geometric series for studying the matrix inverse $(\mathbb{1} - S\widetilde{X})^{-1}$. Inserting this formal expansion into (2.76), we have:

$$\mathbf{R}(t) = X^{11} + \begin{bmatrix} \hat{X}^{12}(0,t) & \hat{X}^{21}(0,t) \end{bmatrix} \sum_{s=0}^{\infty} (S\widetilde{X})^s S \begin{bmatrix} \hat{X}^{21}(t,0) \\ \hat{X}^{12}(t,0) \end{bmatrix} \tag{4.54}$$

and let us introduce the infinite matrices $\mathbf{R}^{(s)}_{nm}$ by rewriting:

$$\mathbf{R}_{nm}(q) = \sum_{s=0}^{\infty} \mathbf{R}^{(s)}_{nm}(q) \tag{4.55}$$

in terms of the variable q.

At the risk of further over-complicating the notation, let us also introduce a constant matrix $\mathfrak{X}$ as follows:

$$\mathfrak{X} \coloneqq \begin{bmatrix} X^{21} & X^{11} \\ X^{11} & X^{12} \end{bmatrix}, \tag{4.56}$$

which is essentially the $S\widetilde{X}(t)$ matrix stripped off the t dependent propagator pieces and the C matrices. The C matrices and the $q^{n/2}$ factors from the propagator effectively make the contribution from the sth power term into:

$$\begin{aligned} \mathbf{R}^{(s)}_{nm}(q) = \delta_{s,0}\; X^{11}_{nm} + \sum_{p=s+1}^{\infty} (-1)^p q^p \sum_{|\vec{\mu}|=p} \Big[& X^{12}_{n,\mu_1} \big(\underbrace{\mathfrak{X} \ldots \mathfrak{X}}_{\text{s terms}} \big)_{11|\mu_1\mu_{s+1}} X^{12}_{\mu_{s+1}m} \\ & + X^{12}_{n,\mu_1} \big(\underbrace{\mathfrak{X} \ldots \mathfrak{X}}_{\text{s terms}} \big)_{12|\mu_1\mu_{s+1}} X^{21}_{\mu_{s+1}m} \\ & + X^{21}_{n,\mu_1} \big(\underbrace{\mathfrak{X} \ldots \mathfrak{X}}_{\text{s terms}} \big)_{21|\mu_1\mu_{s+1}} X^{12}_{\mu_{s+1}m} \\ & + X^{21}_{n,\mu_1} \big(\underbrace{\mathfrak{X} \ldots \mathfrak{X}}_{\text{s terms}} \big)_{22|\mu_1\mu_{s+1}} X^{21}_{\mu_{s+1}m} \Big], \end{aligned} \tag{4.57}$$

where we are only summing over the set of integer partitions of the power p into $s+1$ terms:

$$|\vec{\mu}| = \mu_1 + \ldots + \mu_{s+1} = p,$$

and its permutations. For performing these block matrix computations we have again used the *NCAlgebra* package[9] [28] which among its many powerful features handles block matrices in a somewhat more reliable and easier manner as compared to *Mathematica*'s built-in functions. For instance, the block matrix powers which grow exponentially with the degree can be quickly evaluated as formal expressions using the "NCDot"/"MM" (MatrixMultiply) command. These can then be fed into a "module" for inserting the $X^{0,\pm}$ exact values. Essentially, the output of the *NCAlgebra* commands are used to construct *lists* and we apply the transformation rules on them to convert them to the coefficients.

For low values of s, one can use the "Permutations" and "IntegerPartitions" commands

[9] I would like to thank the UC San Diego Mathematics department for making available this package using which parts of the computations in this work were performed.

in *Mathematica* to insert the appropriate indices and perform the (constrained) summations[10]. Again, this becomes computationally challenging since the number of terms in each block grows exponentially with s as 2^{s-1} and we had to contend ourselves with $s \leq 17$ truncation due to time and energy constraints.

To obtain till the q^{18} coefficient exactly, one needs to include the $s = 0, \ldots, 17$ contributions (the $s = 18$ terms start only at q^{19}). Once we have an expansion in terms of exact coefficients, we can find the corresponding diagonal or near diagonal Padé approximant ($n \approx m$) and look at its pole-zero structure in the complex q plane as we do in appendix 4.5. This is a useful exercice in general, when the available data is limited due to a multitude of reasons.

We have obtained the coefficients till the q^{18} term for a *general matrix element* $\mathbf{R}_{nm}$ symbolically. For particular values of n, m, the expansions can then be readily obtained. We provide a few elements below for illustration:

$$\begin{aligned}
\mathbf{R}_{11}(q) &= -\frac{11}{3^3} - \frac{2^7}{3^6}q - \frac{2^7 \cdot 23}{3^8}q^2 + \frac{2^9 \cdot 7 \cdot 13}{3^{12}}q^3 - \frac{2^7 \cdot 13693}{3^{15}}q^4 + \frac{2^8 \cdot 54503}{3^{17}}q^5 \\
&\quad + \cdots + \frac{2^8 \cdot 53 \cdot 3469 \cdot 105251 \cdot 28802532911}{3^{53}}q^{17} + \frac{2^7 \cdot 20826099209 \cdot 1406808088061}{3^{56}}q^{18} + \mathcal{O}(q^{19}) \\
&\approx -0.407407 - 0.175583q - 0.448712q^2 + 0.0876711q^3 - 0.122149q^4 + 0.108044q^5 \\
&\quad - 0.0360726q^6 - 0.0321163q^7 + 0.0250613q^8 + 0.0228212q^9 - 0.0179066q^{10} \\
&\quad - 0.0218985q^{11} + 0.00985881q^{12} + 0.0211021q^{13} - 0.000638823q^{14} - 0.0163765q^{15} \\
&\quad - 0.00652212q^{16} + 0.00736123q^{17} + 0.00716576q^{18} + \mathcal{O}(q^{19}), \qquad (4.58) \\
\mathbf{R}_{22}(q) &= \frac{19}{3^5} + \frac{2^8 \cdot 5^2}{3^9}q + \frac{2^8 \cdot 269}{3^{11}}q^2 - \frac{2^{10} \cdot 569}{3^{14}}q^3 + \frac{2^8 \cdot 107 \cdot 2131}{3^{17}}q^4 - \frac{2^9 \cdot 7 \cdot 224617}{3^{20}}q^5 \\
&\quad + \cdots + \frac{2^8 \cdot 204248123 \cdot 1153179431133481}{3^{58}}q^{18} + \mathcal{O}(q^{19}) \\
&\approx 0.0781893 + 0.325154q + 0.388739q^2 - 0.121819q^3 + 0.452008q^4 - 0.23088q^5 \\
&\quad + 0.139741q^6 + 0.0208859q^7 - 0.0978634q^8 + 0.0156951q^9 + 0.0705072q^{10} \\
&\quad - 0.0118808q^{11} - 0.0591811q^{12} - 0.00238481q^{13} + 0.0496639q^{14} + 0.0171492q^{15} \\
&\quad - 0.0333904q^{16} - 0.0243469q^{17} + 0.0128015q^{18} + \mathcal{O}(q^{19}), \qquad (4.59)
\end{aligned}$$

and for two non-diagonal elements, we have:

$$\mathbf{R}_{24}(q) = -\frac{2^5 \cdot 5^2}{3^9} - \frac{2^8 \cdot 5 \cdot 13}{3^{11}}q + \frac{2^8 \cdot 5 \cdot 109}{3^{14}}q^2 + \frac{2^{10} \cdot 5 \cdot 67 \cdot 199}{3^{18}}q^3 + \frac{2^8 \cdot 5^2 \cdot 137 \cdot 181}{3^{20}}q^4$$

[10] One can also employ "If" conditionals to do these summations by brute-force for low enough s. The routine needs to check $\sum_{p=1}^{r}\sum_{s=1}^{p}(p-s+1)^s$ *If* conditionals and also perform multiplication and addition for the size of the Permutations of Integer Partitions to obtain the first $r+1$ coefficients exactly. This number grows very quickly.

$$
\begin{aligned}
&- \cdots + \frac{2^8 \cdot 5 \cdot 7^4 \cdot 181 \cdot 846389 \cdot 14954516415841}{3^{62}} q^{18} + \mathcal{O}(q^{19}) \\
&\approx -0.0406442 - 0.0939333q + 0.0291702q^2 + 0.176204q^3 + 0.0455149q^4 - 0.051438q^5 \\
&\quad - 0.00973223q^6 - 0.0752605q^7 - 0.0205626q^8 + 0.0851266q^9 - 0.023345q^{10} \\
&\quad - 0.0660465q^{11} + 0.032174q^{12} + 0.0440361q^{13} - 0.0130819q^{14} - 0.032953q^{15} \\
&\quad - 0.00765715q^{16} + 0.019743q^{17} + 0.0184546q^{18} + \mathcal{O}(q^{19}), \text{ and for} \qquad (4.60)
\end{aligned}
$$

$$
\begin{aligned}
\mathbf{R}_{26}(q) = &\frac{2^5 \cdot 5 \cdot 29}{3^{11}} + \frac{2^8 \cdot 5 \cdot 191}{3^{14}} q - \frac{2^8 \cdot 5 \cdot 199}{3^{15}} q^2 - \frac{2^{10} \cdot 5 \cdot 7 \cdot 37 \cdot 53}{3^{19}} q^3 - \frac{2^8 \cdot 5 \cdot 11 \cdot 7489}{3^{23}} q^4 \\
&- \cdots - \frac{2^8 \cdot 5 \cdot 7 \cdot 31 \cdot 18664747 \cdot 823481250069563}{3^{64}} q^{18} + \mathcal{O}(q^{19}) \\
&\approx 0.0785788 + 0.153344q - 0.0532556q^2 - 0.181411q^3 - 0.00336015q^4 - 0.0665607q^5 \\
&\quad - 0.157655q^6 + 0.0480861q^7 + 0.179151q^8 + 0.0564545q^9 - 0.119223q^{10} \\
&\quad + 0.0299126q^{11} + 0.132947q^{12} - 0.0913012q^{13} - 0.0771423q^{14} + 0.0626403q^{15} \\
&\quad + 0.028327q^{16} + 0.0115182q^{17} - 0.00372998q^{18} + \mathcal{O}(q^{19}). \qquad (4.61)
\end{aligned}
$$

It is interesting to note that the coefficients are all nice rational numbers given that the Neumann matrices are only algebraic valued. We observe that there is a (rather slow) non-monotonic fall-off of the coefficients as seen from Fig. 4.2. However, we can see from

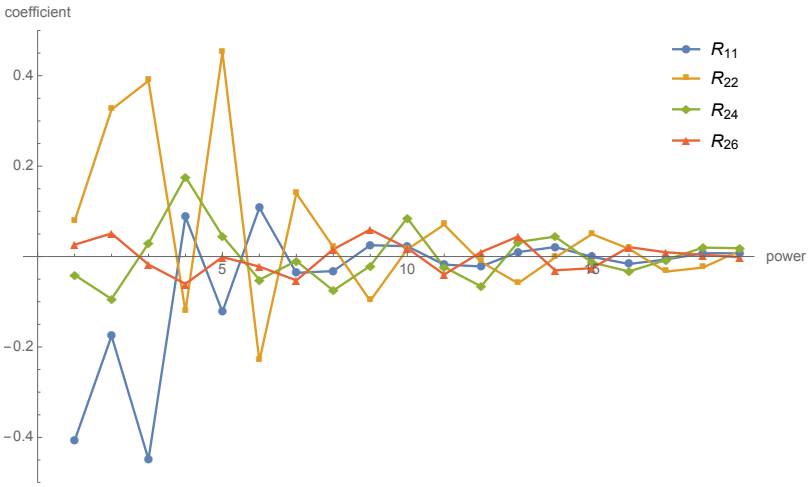

Figure 4.2: $\mathbf{R}_{11}, \mathbf{R}_{22}, \mathbf{R}_{24}, \mathbf{R}_{26}$ coefficients vs the corresponding powers of q

Table 4.3 below that for low n, m, they still approximate the function near $q = 1$. We expect these Taylor series expansions to correspond to certain special combinations of elliptic functions. As it is difficult to identify the form of the function from the series—and it varies for each matrix element—we tried to look up the numbers [11] in the OEIS [55]. Although we haven't found any match so far, it may be possible that one can

[11] It offers a feature to check rational sequences by searching for the numerator sequence and denominator sequence separately.

$\mathbf{R}^{series}_{2n,2m}(1)$	1	2	3	4
1	0.988788	0.0157688	0.00910705	−0.00146615
2	0.0315376	1.00062	−0.0204256	0.0336059
3	0.0273211	−0.0306384	1.07677	0.0259935
4	−0.0058646	0.0672117	0.034658	1.01014

Table 4.3: A few of the purely even parity matrix elements $\mathbf{R}_{2n,2m}$ evaluated at $q = 1$ or $t = 0$ using the oscillator based expansion till q^{18}. The diagonal elements are all consistent with being $+1$ with the off-diagonal ones vanishing, since the twist matrix $C_{nm} = (-)^n\delta_{nm}$ reduces to $+\delta_{nm}$ in the even sector. In the odd sector, we have checked that there is consistency with $-\delta_{nm}$ as well.

express these in terms of rational expressions[12] of elliptic functions and their derivatives, line integrals, etc. Once one obtains the expression in terms of elliptic functions, one can convert them to Jacobi Θ functions and then apply the Jacobi imaginary transform to obtain the closed string contributions explicitly, similar to [13].

Furthermore, it is interesting to compare this expansion to the one we obtained in §4.1 for the general even parity matrix elements directly in the t variable. We find that they do all follow each other sufficiently closely near the $t \to 0^+$ region (which maps to the $q \to 1^-$ region) as can be seen from some sample matrix elements plotted in Fig.4.3a; in the non-diagonal case there is a numerical difference since the true function is expected to vanish as $q \to 1^-$, but notice that the scales differ.

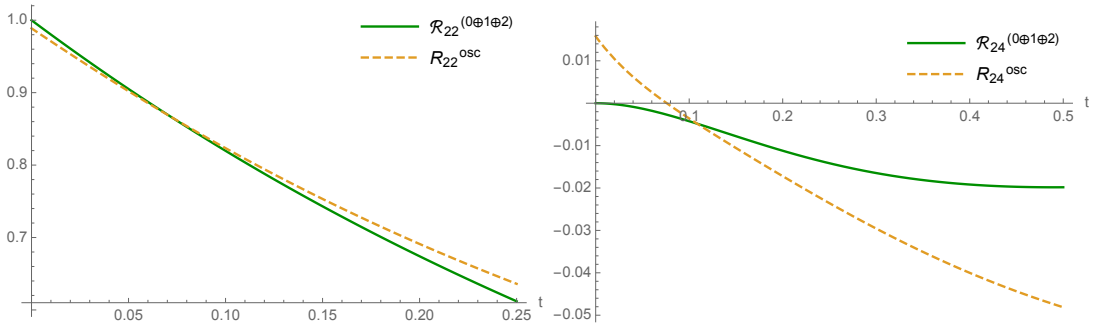

(a) (b)

Figure 4.3: A comparison of the behaviour of the matrix element $\mathbf{R}_{2n,2m}$ near $t = 0$ obtained using the first three terms ($s = 0, 1, 2$) in the Moyal basis (green) and using the first 19 terms (till $q^{18} = e^{-18t}$) in the oscillator basis (orange, dashed) plotted for (a)$\mathbf{R}_{22}(t)$ and (b)$\mathbf{R}_{24}(t)$. The two furnish very similar values for the diagonal case but differ for the non-diagonal case, which was expected given the vanishing behaviour near $t = 0$.

[12]This is expected the case as the Schottky double is a torus and elliptic functions are the natural doubly periodic functions should appear in any physical quantity[13, 14].

4.5 Padé approximants for $\mathbf{R}_{nm}(q)$

In this section, we shall try to infer the analytic properties of the functions represented by the expansions from §4.4 in the q plane by considerations of their *Padé approximants*. These are meromorphic functions of the expansion parameter that have identical Taylor series coefficients till the finite data generated for an unknown function (by using various computational techniques).

Specifically, the r/s Padé approximant till order N is a rational function, constructed as the quotient of two polynomials of degree r, s respectively such that $r + s = N$ and:

$$P_s^r(z) \coloneqq \frac{A_r(z)}{B_s(z)} = \frac{a_0 + a_1 z + \cdots + a_r z^r}{1 + b_1 z + \cdots + b_s z^s} = p_0 + p_1 z + \cdots + p_N z^N + R_N(z), \qquad (4.62)$$

where the expansion coefficients p_i, $(i = 0, \cdots, N)$ coincide with the series expansion at hand. Generally, the diagonal/symmetric case $r = s \approx \lfloor N/2 \rfloor$ captures the zeros and poles of the unknown function more accurately and provides the fastest convergence to the true function as N increases. One can estimate if the poles so obtained are spurious or not by roughly checking how much they overlap with the zeros in the complex z plane as the value of N increases. An accumulation of non-spurious poles could signal an essential singularity or a branch cut [56].

We have constructed the Padé approximants for a few matrix elements in Table 4.4 to demonstrate their utility and to show that these provide a better approximation compared to relying on the Taylor series as can be seen by comparing to Table 4.3 above. In order

k	$\mathbf{R}_{11}^P$	$\mathbf{R}_{22}^P$	$\mathbf{R}_{13}^P$	$\mathbf{R}_{24}^P$
6	-0.999853	1.00166	-0.00221739	0.0244735
7	-1.00018	1.00347	-0.0218953	-0.0581234
8	-0.999948	1.00009	0.000125679	0.00170096
9	-1.00003	1.00014	-0.000261842	-0.00459688

Table 4.4: The Padé approximant P_k^k evaluated at $q = 1$ for various matrix elements. The values are consistent with what one expects for the diagonal and non-diagonal elements, namely $(-)^n$ and 0 respectively, although the convergence as k increases is not uniform.

to look for hints of non-analyticity, we can study the poles and zeros of these rational functions as we do in Fig. 4.4 for two purely odd parity matrix elements. As can be observed from the plots, the poles do not appear to accumulate near the unit circle (or near $q = +1$ for that matter) at this order, and a few of them even seem to be somewhat spurious since they overlap a nearby zero. But notice that the poles are still consistent with being outside the unit disc. Let us therefore consider the absolute values of the corresponding residues at these poles to ascertain the relative strength of the poles. We

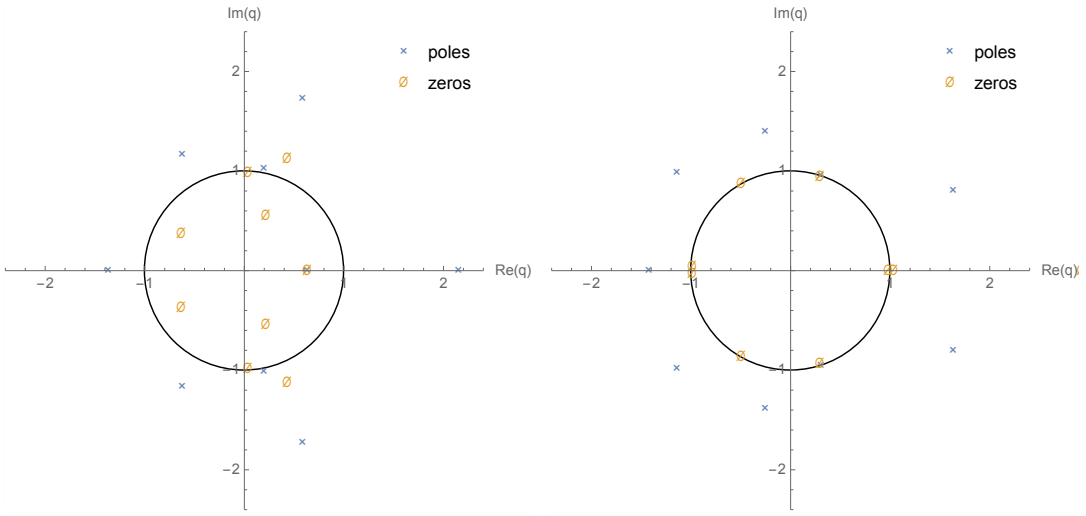

(a) (b)

Figure 4.4: The zeros and poles in the complex q plane of the 9/9 Padé approximant to the matrix elements (a) $\mathbf{R}_{33}(q)$ and (b) $\mathbf{R}_{13}(q)$ obtained using the oscillator expansions based on the exact Neumann matrices.

divide out by the constant terms in these expansions—which is always X^{11}_{nm} as can be seen immediately from (2.76)—in order to provide the numbers more intuitive. Furthermore, it is useful to consider the absolute values of the location of the poles to see if they are indeed approaching the boundary of the unit disc. We have performed these checks for several matrix elements and have presented the data in Table 4.5 corresponding to the $\mathbf{R}_{13}$ case above. Because the off-diagonal functions vanish at the point $t = 0$, we may expect to see stronger signals for these. Once again, we remark that with the current limited data there is not a robust behaviour that may be claimed to hold and also that the residues may not be representative of the (non)analytic structure due to possible rapid oscillations. To get a better idea of the strength of these poles, we can also consider a plot[13] of the absolute value (rescaled by X^{11}_{nm}) of these approximants in the complex q plane as in Fig. 4.5 below. Next, we have at our disposal another approximation scheme which is known to work better for low values of N: the Borel-Padé approximation. In this method, one combines Padé approximants with the Borel transform by first taking the Borel transform of the truncated series, then finding its Padé approximant and finally doing the inverse Borel transform.[14] The Borel transform of the truncated power series in q is obtained by replacing each coefficient p_k by $p_k/k!$, i.e:

$$\sum_{k=0}^{N} p_k q^k \to \sum_{k=0}^{N} \frac{p_k}{k!} q^k \tag{4.63}$$

[13]The code for generating this plot was taken from a *Mathematica* Stack Exchange page:`https://mathematica.stackexchange.com/questions/3458/plotting-complex-quantity-functions`.

[14]See the discussion in [57, §3.1] whose notation we shall try to follow.

q_i	$\lvert q_i\rvert$	Rescaled residue at q_i
-1.42723	1.42723	1.73178
$-1.14524 - 0.985928i$	1.51117	4.92979
$-1.14524 + 0.985928i$	1.51117	4.92979
$-0.259587 - 1.39047i$	1.4145	4.20125
$-0.259587 + 1.39047i$	1.4145	4.20125
$0.300928 - 0.953144i$	0.99952	0.0630495
$0.300928 + 0.953144i$	0.99952	0.0630495
$1.63103 - 0.80282i$	1.81791	1.96839
$1.63103 + 0.80282i$	1.81791	1.96839

Table 4.5: The location of the poles of the 9/9 Padé approximant to $\mathbf{R}_{13}$, their absolute values and the corresponding residues. For being more useful, we have rescaled all the residues with the constant term $X_{13}^{11} = \frac{80}{729} \approx 0.10974$.

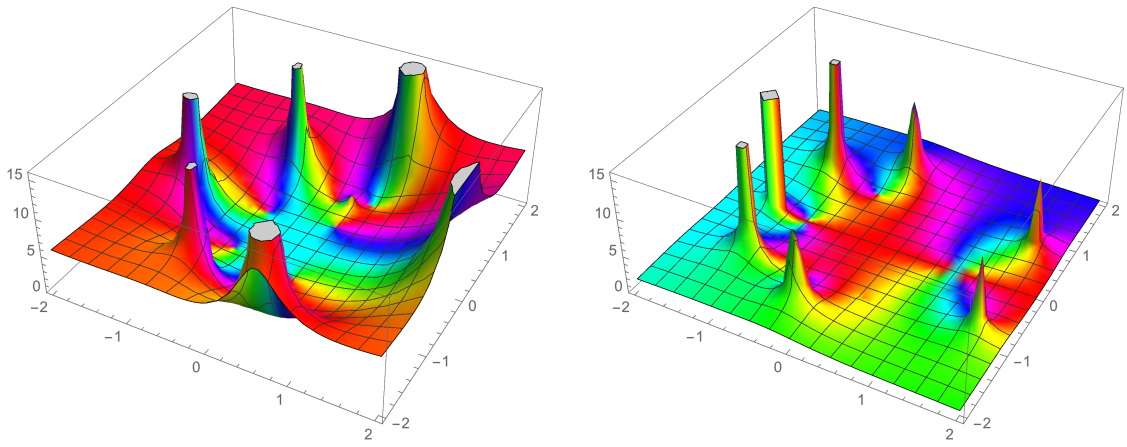

(a) (b)

Figure 4.5: A plot displaying the absolute value and phase for the 9/9 Padé approximants to (a) $\mathbf{R}_{33}$ and (b) $\mathbf{R}_{13}$ in the complex q plane. The "spikes" correspond to the location of the (simple)poles and the strength of the residues can be visually estimated by noticing how fast these are diverging. The phases are indicated using colours such that positive real numbers are assigned red, negative real numbers are assigned cyan, and the hue varies linearly. All the numbers for absolute values are rescaled by the constant piece X_{nm}^{11}.

whose Padé approximant $P_s^r(q)_{\text{Borel}}$ can be obtained in a similar manner as above.

The final step is to perform the inverse Borel transformation that involves an integration along the positive real axis:

$$\tilde{P}_s^r(q) = \int_0^\infty dt\, e^{-t}\, P_s^r(tq)_{\text{Borel}}. \tag{4.64}$$

The interesting case is when the integrand has poles on the positive real axis which can

correspond to ambiguities from subleading terms, not ordinarily seen in a power series expansion. Hence, we have analysed the pole structure of $P_s^r(q)_{\text{Borel}}$ but have found that although there appears to be poles at certain positive values of q, these are not stable as the order r/s is varied. For $\mathbf{R}_{33}$, for instance, we have in Table 4.6 but for many other

$\{r, s\}$	Pole of $(P_s^r)_{\text{Borel}}$ on $\mathbb{R}_+$
$\{8, 7\}$	none
$\{8, 8\}$	18.526252
$\{9, 8\}$	17.710812
$\{9, 9\}$	18.450791

Table 4.6: The location of the poles on the positive real axis for the Padé approximant to the Borel transform, $(P_s^r)_{\text{Borel}}$, as r, s is varied for $\mathbf{R}_{33}(q)$.

matrix elements we have checked, this behaviour is much less clear as the imaginary parts are not stable.

However, we have evaluated the above integral for $q = 1$ and have found the expected result of $C_{nm} = (-)^n \delta_{nm}$ to good enough accuracy. We have also examined the (scaled) residues of $P_s^r(q)_{\text{Borel}}$ towards this line of analysis. In short, the essential singularity expected for $q = +1$ and branch cuts due to $\log(-\log q)$ do not show up conclusively at this order, indicating the need for much higher order coefficients or some other underlying features of the functions.

Chapter 5

Comments on the string propagator in the ghost sector

In this chapter, we write down the ghost sector expressions for the corrections to open string propagator at the one-loop level ($N = 2, g = 1$). This corresponds to the self-energy diagram in QFTs and in case of the bosonic theory, the diagrams are similar[1] to the ϕ^3 theory. However, in OSFT there would be an infinite number of string states allowed in the loop and as remarked earlier, the propagator used (3.9) has an interesting structure involving an additional potential term. We shall be using a similar method employing state sums as done for the tadpole in chapter 3, and use only the Moyal star in ξ space for our analysis. We will begin by reviewing the covering of the bosonic moduli space using the four relevant string diagrams [13] in Fig.5.1 after some preliminary remarks concerning ghost charges. Notice that there are two bosonic moduli t_1 and t_2 each ranging from 0 to ∞ and the analytic structure becomes much more intricate (and interesting) consequently.

On ghost number assignments

Recall that for one-loop[2] diagrams, the perturbative quantization procedure dictates that states of all ghost number, $G_i \in \mathbb{Z}$, must propagate in the loop subject to the ghost number saturation condition for the corresponding genus by the Riemann-Roch theorem. These are the so called spacetime "ghost strings" which are different from the ordinary reparametrization bc ghosts [33] on the worldsheet.

Applying this rule for the one-loop 2-point function, we require that the vertex operators for the two states $|\Phi_1\rangle$ and $|\Phi_2\rangle$ corresponding to the two propagators of "length" $t_1 = -\ln q_1$ and $t_2 = -\ln q_2$ carry the ghost charges:

$$G_2 = 3 - 1 - G_1 = 2 - G_1, \tag{5.1}$$

[1] The extended nature of the world-sheet however also allows for "twisting" the internal propagators [6].

[2] To be precise, what we call "one-loop" here would correspond to the lowest order $\mathcal{O}(\hbar^{1/2})$ correction if the relation between the open string and the closed string coupling are taken into account and hence would actually be "half-loop" ($\sqrt{\hbar}$) level, as per standard Polchinski conventions.

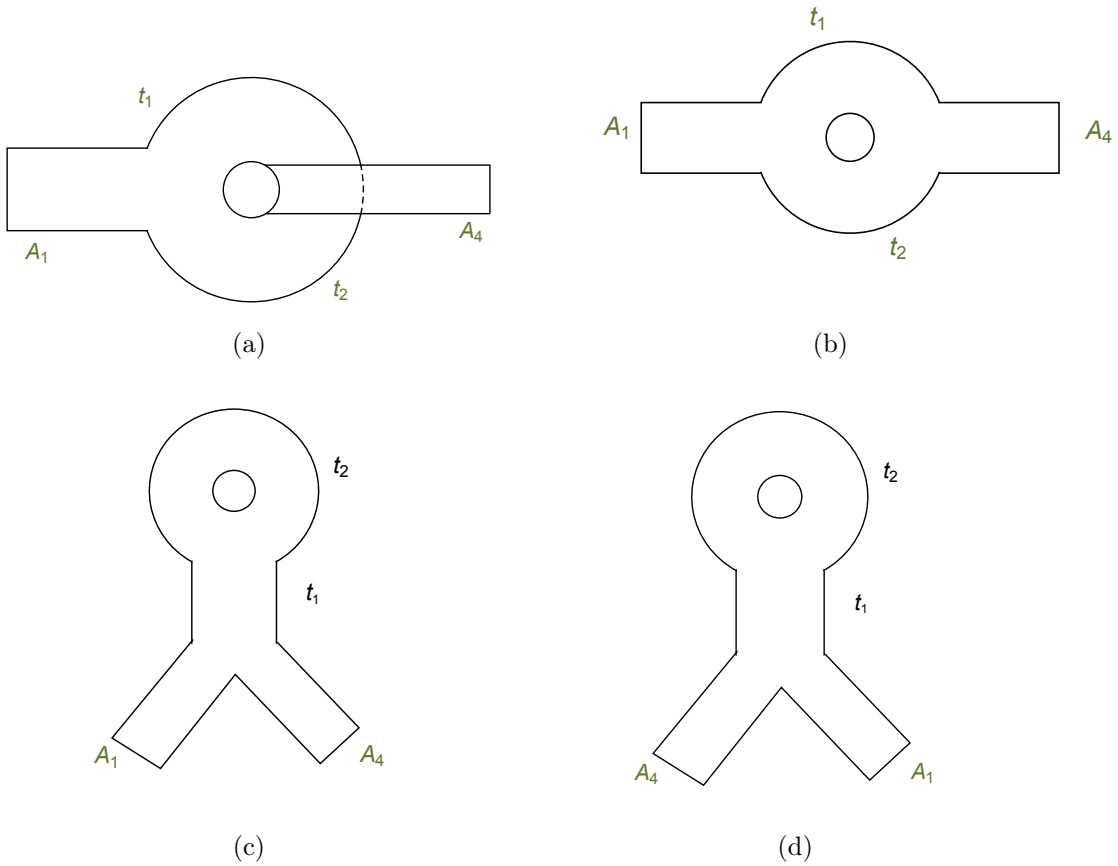

Figure 5.1: The four diagrams contributing to one-loop 2-point function. Diagrams (a) and (b) may be considered to arise from the s channel and the last two: (c) and (d), from the t channel.

when both external lines are connected to the loop but only $G_1 = 1 = G_2$ when only a single line is connected to the loop as in . This results from the requirement of total ghost number +3 for the Witten type vertex. For the first case, the condition requires that both states be of either even or odd ghost number which is true also for the Schnabl gauge analysis[31].

While considering the two diagrams of the first type, we will account for only the contribution from the ghost number +1 quantum states in this work. However, while constructing the quantum effective action it is essential that we remove this restriction. Hence, our analysis would necessarily be limited in its physical validity. The remaining two are not one particle irreducible and have the tadpole as a subgraph. Hence they share some of the structures. At the end, all the four diagrams should be added with equal weight (= +1) in order to match with the first quantized results on-shell [6].

Covering of moduli space

As expounded in [13, §5] by Samuel et al., the moduli space is covered by four string diagrams as depicted in Fig.5.1, of which one is *non-planar* and the rest three are planar.[3] Of these three planar cases, two have the one loop tadpole as a subdiagram and hence has zero momentum transfer. With the appropriate change of variables, these are guaranteed to have the same form of the integrand. These diagrams smoothly cross-over as the modular parameters are varied in order to provide a single covering of the moduli space (Ref.[13] clearly demonstrates this). Additionally, the ghost factors are no longer trivial as in the tree level cases.

We see that the last two diagrams differ by the way two legs of the *off-shell* four-point function are glued together to form a loop. The Witten vertex is cyclic but not permutation symmetric and hence we find these inequivalent diagrams for obtaining a single covering of moduli space as required by consistency with the Polyakov amplitudes on-shell. In the following, we consider only pure ghost external states for convenience. It was shown that in addition to the physical poles corresponding to an intermediate particle going on-shell, there are also *unphysical* poles in the off-shell amplitude[13]. Hence these diagrams contribute to very interesting off shell structure.

5.1 The non-planar integrand $\mathcal{I}^{(s)}_{12|43}$

The non-planar contribution to the open string propagator is given by:

$$\mathcal{A}^{(s)}_{12|43} = \int_0^\infty dt_1 \int_0^\infty dt_2\, \mathcal{I}^{(s)}_{12|43}(t_1,t_2) = \int_0^1 \frac{dq_1}{q_1} \int_0^1 \frac{dq_2}{q_2}\, \mathcal{I}^{(s)}_{12|43}(q_1,q_2), \tag{5.2}$$

where the legs 2 and 3 in Fig. 2.2a are identified, and the labels 2 and 3 are therefore redundant. The integrand (in the ghost sector) can be expressed as below (see also (2.68)):

$$\mathcal{I}^{(s)}_{12|43}(q_1,q_2) = \int d\eta^{gh} \mathrm{Tr}\left[A_{12}(q_1,\eta^{gh},\xi^{gh},\lambda_1^{gh}) * A_4(\xi^{gh},\lambda_4^{gh}) * A_3(q_2,\eta^{gh},\xi^{gh})\right], \tag{5.3}$$

and we have explicitly indicated the arguments for clarity. Here we have defined the monoids:

$$\begin{aligned} A_{12}(q_1,\eta^{gh},\xi^{gh},\lambda_1^{gh}) &= q_1^{L_0^{gh}}\left[A_1(\xi,\lambda_1^{gh}) * e^{+\xi^{gh\top}\eta^{gh}}\right] \\ A_3(q_2,\eta^{gh},\xi^{gh}) &= q_2^{L_0^{gh}}\left[e^{-\xi^{gh\top}\eta^{gh}}\right], \end{aligned} \tag{5.4}$$

[3] Planar is used in the sense of Feynman graphs; the string diagrams are still non-planar due to the unique structure of the Witten type vertex.

in terms of the simpler elements:

$$\begin{aligned}
A_1(\xi^{gh},\lambda_1^{gh}) &= \mathcal{N}_0 e^{-\xi^{gh\top}M_0^{gh}\xi^{gh}-\xi^{gh\top}\lambda_1^{gh}},\\
A_2(\eta^{gh},\xi^{gh}) &= e^{+\xi^{gh\top}\eta^{gh}},\\
A_3(\eta^{gh},\xi^{gh}) &= e^{-\xi^{gh\top}\eta^{gh}},\\
A_4(\xi^{gh},\lambda_4^{gh}) &= \mathcal{N}_0 e^{-\xi^{gh\top}M_0^{gh}\xi^{gh}-\xi^{gh\top}\lambda_4^{gh}}.
\end{aligned} \tag{5.5}$$

where as before, $\lambda_1^{gh},\lambda_4^{gh}$ are the sources which may be used to insert the specific asymptotic string states at the end of the calculations. Here again, we choose to remove the first $*$ product that appears between A_{12} and A_4 while evaluating the trace under the assumption of associativity. We apply the sub-algebra rules for the monoid and the propagator rules to write down the parameters for the resulting string fields below:

$A_{12}^{gh}(q_1)$:

$$\begin{aligned}
M_{12}(q_1) &= M_0^{gh}, \qquad \lambda_{12}^{gh}(t_1) = q_1^{\tilde{\kappa}^{gh}}(-(1-m_0^{gh})\eta^{gh}+\lambda_1^{gh}),\\
\mathcal{N}_{12}(q_1) &= \mathcal{C}_\eta^{(12)}\exp\left[-\eta^{gh\top}\mathcal{Q}_\eta^{(12)}\eta^{gh}+\lambda_1^{gh\top}\mathcal{L}_\eta^{(12)\top}\eta^{gh}\right],
\end{aligned} \tag{5.6}$$

where the coefficient matrices appearing in the normalization factor $\mathcal{N}_{12}$c are given by:

$$\mathcal{Q}_\eta^{(12)} = -\frac{1}{4}\sigma m_0^{gh} - \frac{1}{8}(1-m_0^{gh\top})M_0^{gh-1}f_3(q_1)(1-m_0^{gh}) \tag{5.7a}$$

$$\mathcal{L}_\eta^{(12)\top} = -\frac{1}{2}\left[\sigma+\frac{1}{2}M_0^{gh-1}f_3(q_1)\right] \tag{5.7b}$$

$$\mathcal{C}_\eta^{(12)} = \mathcal{N}_0\exp\left[\frac{1}{8}\lambda_1^{gh\top}M_0^{-1}f_3(q_1)\lambda_1^{gh}\right], \tag{5.7c}$$

and for the monoid

$A_3^{gh}(q_2)$:

$$\begin{aligned}
M_3(q_2) &= \frac{f_3(q_2)}{f_2(q_2)}M_0^{gh}, \qquad \lambda_3^{gh}(q_2) = \frac{2q_2^{\tilde{\kappa}^{gh}}}{f_2(q_2)}\eta^{gh}\\
\mathcal{N}_3(q_2) &= \det\left[\frac{1}{2}f_2(q_2)\right]\exp\left[+\frac{1}{4}\eta^{gh\top}M_0^{-1}\frac{f_3(q_2)}{f_2(q_2)}\eta^{gh}\right].
\end{aligned} \tag{5.8}$$

Now, let us proceed to evaluate the string field resulting from taking $A_4 * A_3(q_2) =: A_{43}(q_2)$. The parameters for the resulting expression are the following:

$$\begin{aligned}
m_{43}(q_2) = &\left[m_0^{gh}+\frac{f_3(q_2)}{f_2(q_2)}(m_0^{gh})^2\right]\left[1+\frac{f_3(q_2)}{f_2(q_2)}(m_0^{gh})^2\right]^{-1}\\
&+\left[\frac{f_3(q_2)}{f_2(q_2)}m_0^{gh}-m_0^{gh}\frac{f_3(q_2)}{f_2(q_2)}m_0^{gh}\right]\left[1+m_0^{gh}\frac{f_3(q_2)}{f_2(q_2)m_0^{gh}}\right]^{-1},
\end{aligned} \tag{5.9a}$$

$$\lambda_{43}(q_2) = 2[1-m_0^{gh}]\left[1+\frac{f_3(q_2)}{f_2(q_2)}(m_0^{gh})^2\right]^{-1}\frac{q_2^{\tilde{\kappa}^{gh}}}{f_2(q_2)}\eta^{gh} + \left[1+\frac{f_3(q_2)}{f_2(q_2)}m_0^{gh}\right]\left[1+m_0^{gh}\frac{f_3(q_2)}{f_2(q_2)}m_0^{gh}\right]^{-1}\lambda_4^{gh}, \tag{5.9b}$$

$$\mathcal{N}_{43} = \mathcal{N}_0\mathcal{N}_3(q_2)\det\left[1+\frac{f_3(q_2)}{f_2(q_2)}(m_0^{gh})^2\right]\exp\left[+\frac{1}{4}\lambda_\alpha^\top\sigma K_{\alpha\beta}\lambda_\beta\right], \tag{5.9c}$$

where in the last expression, we must substitute:

$$K_{44} = \left(m_0^{gh}+(m_0^{gh})^{-1}\frac{f_2(q_2)}{f_3(q_2)}\right)^{-1}, \qquad K_{43} = \left(1+\frac{f_3(q_2)}{f_2(q_2)}(m_0^{gh})^2\right)^{-1},$$
$$K_{34} = -\left(1+m_0^{gh}\frac{f_3(q_2)}{f_2(q_2)}m_0^{gh}\right)^{-1}, \text{ and} \qquad K_{33} = \left(\frac{f_3(q_2)}{f_2(q_2)}m_0^{gh}+(m_0^{gh})^{-1}\right)^{-1}. \tag{5.10}$$

Combining the two string fields by taking the ordinary product of functions and taking the ξ^{gh} trace, we are left with

$$\mathcal{C}_\eta^{(12|43)}\int(d\eta)\,\exp\left[-\eta^\top\mathcal{Q}_\eta^{(12|43)}\eta+\mathcal{L}_\eta^{(12|43)\top}\eta\right] \tag{5.11}$$

where the $\lambda_{1,4}$ dependences are implicit. Thus, the final contribution from the ghost sector becomes the following:

$$\det\left(2\mathcal{Q}_\eta^{(12|43)}\right)\exp\left[+\frac{1}{4}\mathcal{L}_\eta^{(12|43)\top}\mathcal{Q}_\eta^{(12|43)-1}\mathcal{L}_\eta^{(12|43)}\right]. \tag{5.12}$$

Here, the argument of the exponential mixes the components of the "vector"

$$\vec{\lambda} = \begin{pmatrix}\lambda_1^{gh}\\ \lambda_4^{gh}\end{pmatrix}$$

and for a general one-loop n-point function, we obtain an n component vector. This is similar in spirit to working in Fourier space but here we only work with $2N\times 2N$ matrices. In certain cases, we can use these formal expressions for numerical calculations; the advantage of this representation is the straightforward application of the transformation rules, although they involve several inverses of infinite matrices and intermediate matrix multiplications.

5.2 The planar graphs

One may observe that the planar amplitude with both external states on the same boundary of the annulus, $\mathcal{A}_{12|34}^{(s)}$, comes with a relative positive sign with respect to the amplitude above. Hence, the combined integrand can be written as

$$\mathcal{I}_{12|43}^{(s)}+\mathcal{I}_{12|34}^{(s)} = \int d\eta^{gh}\,\mathrm{Tr}\left[A_{12}(q_1,\eta^{gh},\lambda_1^{gh})\left\{A_4(\lambda_4^{gh}),A_3(q_2,\eta^{gh})\right\}_*\right]. \tag{5.13}$$

This is special for the 2-point function since for general diagrams, the permutation *non-invariance* of the Witten vertex requires that we treat such diagrams, with lines on different boundary components, as contributing to separate amplitudes in general (colour ordering). The anti-commutator structure in the amplitude allows for taking advantage of the partial twist symmetry of these monoid elements. Here, we simply remark that we can write:

$$\hat{A}_3 * \hat{A}_4 = (-)^2 \Omega \left(\Omega(\hat{A}_4) * \Omega(\hat{A}_3) \right), \tag{5.14}$$

where we have included the ghost zero modes ξ_0^i in the form of $\hat{A}_i = -\xi_0^{(i)} A_i$ for clarity. This leads to some partial simplifications and we hope to report in this direction in the future.

As mentioned earlier, the two remaining planar graphs have the one-loop tadpole as a subdiagram and are related by interchange of the external states labelled 1 and 4. We consider the integrand (see also (2.69))

$$\mathcal{I}^{(t)}_{41|23}(q_1, q_2) = \int d\eta^{gh} \, \mathrm{Tr} \left[A_{41}(q_1, \lambda_1^{gh}, \lambda_4^{gh}) * A_2(\eta^{gh}) * A_3(q_2, \eta^{gh}) \right]. \tag{5.15}$$

which one can think of as being obtained by identifying the 2 and 3 legs of a t channel diagram (see Figs. 5.1 and 2.2b again). One can again write down formal expressions for the parameters in the integrand in terms of lightcone like variables, although we are unable to simplify them for further analysis at this point.

Chapter 6

Concluding remarks

In this part, we have primarily focussed on the finite contributions from the squeezed state matrix elements $\mathbf{R}_{nm}(t)$ characterizing the tadpole state in the ghost sector of OSFT, and looked for hints of non-analyticity as a function of the modular parameter t. Using the Moyal representation of the star product, we were able to write down formal expressions for the generating functionals for correlators. Since all integrals in this formalism are of the Gaussian kind, we obtained these in terms of determinants and inverses of infinite matrices, which is one of the main difficulties with these methods.

Due to the partial analytic control we have over the infinite matrices, we were able to study the behaviour of $\mathbf{R}_{nm}(t)$ near the two boundaries of moduli space by employing expansions in t and in $q = e^{-t}$ for the matrix inverse—although conformal techniques become awkward in this basis. The matrix $\mathbf{R}$ carries information about excited string states and how they couple to closed string states arising in the $t \to 0^+$ limit. In particular, we were able to demonstrate the utility of the formalism by capturing the linear order behaviour (§3.3) near $t = 0$ which precisely matches with the correct BCFT prediction (3.63). However, we are now able to see this purely from the OSFT perspective. This is one of the newer results in this work. In the oscillator representation, this expansion becomes ill-defined and produced results that differed by a factor of 2. In the process of identifying the zeroth and linear order coefficients, we have thus uncovered a subtle difference between the Moyal and the oscillator methods, owing to the Fourier transform (2.34) and the resulting somewhat peculiar form of the propagator (3.9).

Ideally, one would like to see the signatures of the closed string states by generating an expansion involving the closed string variable $\hat{q} := e^{2\pi^2/\ln q}$, starting from a closed form expression in the q variables and doing the Jacobi imaginary transform. This way one could recover the off-shell physics associated with the closed string spectra. Unfortunately, the algebraic approach we employ in this work is not tailored for this endeavour and hence we have studied the effects of closed string physics only indirectly.

Nonetheless, we have performed consistency checks of our analytic expressions by examining various limiting regimes of interest and found general agreement with the

oscillator and BCFT results. Beyond the linear order, we are able to successively approximate the matrix elements of $\mathbf{R}_{nm}(t)$. However, the algebra becomes quite unwieldy as may be expected from the fact that the aforementioned infinite matrices are constructed out of non-commuting blocks. We have also employed the oscillator expression (2.76) to generate a series in q till the $18th$ degree (for general n, m) and used it to analyse hints of non-analyticity. We however, refrain from making any claims pertaining to the margin of errors or the efficiency yet, since these are much less clear.

To summarize, the present work makes a modest attempt at answering perturbative questions in OSFT using the Moyal formalism and complements the CFT and oscillator investigations. Due to the strong divergences from the closed string tachyon, the full amplitude is unphysical but still serves as a useful probe of the structure of this very special string field theory. Recently, more physical superstring field theories have been fully constructed which can describe the Ramond sector [9, 16, 58, 59]. The work in [60] has correctly reproduced the 4-point amplitude involving spacetime fermions. It would be of utmost interest to study quantization of this theory from which the tachyon is projected out.

One promising avenue would be extending the recent progress made in the direction of *partial gauge fixing* [61]. This still remains somewhat mysterious and a better understanding of the gauge algebra at the quantum level may also shed more light on how closed string degrees of freedom are encoded in open superstring field theories.

Part II

Models for Antigravity Backgrounds

Chapter 7

Local scale symmetry in spacetime

In this Part, we investigate several simple models for backgrounds accommodating regions of antigravity. The motivation for these originate from a formulation of Einstein gravity combined with the Standard Model, augmented with a local scale (Weyl) symmetry, as developed by Bars et al [62, 63]. This construction dictates that the theory only contains dimensionless parameters and in particular, the usual dimensionful gravitational coupling would be promoted to a field dependent quantity (See also [64–67]). The field dynamics hence determines the value of the effective Newton's constant which is now allowed to be negative. As shall be explained in more detail in the next chapter, this theory may be gauge fixed in a manner so as to identically reproduce the conventional Einstein gravity coupled to matter in familiar regions of spacetime, but in others that lie beyond singularities, with an opposite sign of the gravitational coupling, thus leading to antigravity.

This required relative negative sign has non-trivial consequences for the dynamics of fields and particles propagating in these backgrounds. In particular, the Hamiltonian comes with kinetic terms that can change signs. This negative kinetic energy requires interpretation: It was shown that unitarity is not violated, but there may be an instability associated with negative kinetic energies in the antigravity regions. As a first step in studying this issue, we consider Hamiltonians for particles, fields and strings in chapter 8 where the kinetic terms flip signs in an abrupt, non-analytic manner. This would be sufficient to capture some of the physics we are looking for—chapters 8 and 9 are mostly verbatim reproductions from the work in [3] and [4] respectively, which are mostly self-contained. In the current chapter, we briefly provide further context for this kind of probe analysis. Through examples we show that negative kinetic energy in antigravity presents no problems of principles but is an interesting topic for physical investigations of fundamental significance.

7.1 Conformal coupling

The Einstein-Hilbert action for pure gravity

$$S_{EH} = -\frac{1}{16\pi G_N}\int d^d x\,\sqrt{-g}\,[R+\Lambda] \tag{7.1}$$

in the bulk, is characterized by the Ricci scalar R which is a function of the metric $g_{\mu\nu}$ and its derivatives, the cosmological constant Λ, and a dimensionful coupling G_N which can be related to the d dimensional Planck length. Now let us consider coupling scalar fields to the background metric in a local scale (Weyl) invariant manner. In $d = 4$, we start with the dilaton $\phi(x)$ and the transformations:

$$g_{\mu\nu}(x) \to \Omega^{-2} g_{\mu\nu}(x), \qquad \phi(x) \to \Omega\phi(x), \tag{7.2}$$

where a smooth arbitrary function $\Omega(x)$ provides a local rescaling of fields. The canonical conformal coupling required for this gives rise to the two terms

$$\frac{1}{12}\phi^2 R + \frac{1}{2} g^{\mu\nu}\partial_\mu\phi\partial_\nu\phi, \tag{7.3}$$

which makes the field theory action invariant (the Lagrangian changes by a total derivative piece, see [68, §6]). The field ϕ acts as a Weyl *compensator* and is a gauge degree of freedom.

One can immediately notice that the kinetic term for the dilaton ϕ in (7.3) comes with the wrong sign as for ghosts, but since it is a redundant gauge degree of freedom, that by itself does not pose a problem. In fact, this negative sign leads to a relative sign structure when coupling to physical scalars and evades the restriction to non-negative Newton's constant.

Taking the metric as dynamical and dropping the Einstein-Hilbert term and the cosmological constant, let us now restrict to only the conformally invariant field theory; then we find that the effective Newton's constant becomes spacetime dependent from identifying $1/16\pi G_N = \phi^2/12$. Such theories have been of interest in modelling the large scale structure of the universe and also arise naturally in string compactifications to lower dimensions. As we shall describe next, by a suitable gauge fixing, the Weyl invariant theory above can be seen to be equivalent to the usual Einstein gravity. The cosmological constant can also be recovered from a potential term. But when more scalars are considered, we obtain new features such as geodesic completeness due to additional spacetime regions, that were absent in the ordinary general relativity.

2T-gravity

We must mention that this particular modification of Einstein gravity has its roots in 2T-physics, which postulates a local $Sp(2,R)$ gauge symmetry but now defined in *phase space* (See [69, 70] and references therein). In order for consistency and absence of ghosts, the theory naturally comes with one extra space and one extra time coordinate, i.e the 2T formulation of a d-dimensional theory must be $d+2$ dimensional. Nevertheless, the gauge invariant sector of the theory reduces to the Weyl invariant formalism described above. By embedding the system in this manner, the formalism makes phase space gauge symmetries manifest and many hidden symmetries and dualities in d dimensions would arise as natural predictions from $d+2$ dimensions in the process of getting rid of the extra $1+1$ dimensions. By suitable gauge conditions, the parent theory can thus be used to obtain several different looking systems from the perspective of 1T-physics, that share the same gauge invariant content with a different 1T-physics interpretation. These gauge invariant observables encode the physics of the equivalence class, whose members are called "shadows" and are related by canonical transformations—that change the meaning of time and Hamiltonian in 1T-physics—mapped by the local $Sp(2,R)$ gauge transformations.

In particular, 2T-gravity—the $d+2$ dimensional dynamical gravitational theory—equipped with the diffeomorphism group, when gauge fixed to d dimensions, in the so called "conformal gauge", predicts a remnant local scale symmetry. The Noether current for this symmetry vanishes identically [71], and hence its effect on dynamics becomes rather subtle. The 2T-gravity theory has a dilaton like field which descends to the dilaton field $\phi(x)$ and acts as the Weyl compensator. Hence, although this scalar couples to the Riemann curvature $R^{\mu}{}_{\nu\rho\sigma}$ directly, the usual Einstein gravity can be recovered by gauge fixing this field, with an effective minimal coupling. With more than one conformally coupled scalar field, however, we can expect some new non-trivial physics: The novelties include geodesic completion through additional spacetime sectors that are predicted to exist beyond the singularities of the traditional Einstein theory. Thus, the Weyl symmetry demanded by 2T-physics, provides a solution to the problem of geodesic incompleteness of the traditional general relativity coupled to the standard model of particle physics[62, 63].

7.2 Negative kinetic energy

Requiring all physical scalar fields to be conformally coupled implies that the additional scalars beyond ϕ contribute to the Lagrangian with the usual negative sign, leading to

$$\sqrt{-g}\left[\frac{1}{2}g^{\mu\nu}(\partial_\mu\phi\partial_\nu\phi-\partial_\mu s\partial_\nu s)+\frac{1}{2}(\phi^2-s^2)R\right]\subset\mathcal{L}_{\rm lcs} \tag{7.4}$$

in case of two scalars, for instance. We observe that the Ricci scalar is multiplied by a $\phi^2 - s^2$ factor, which is then proportional to the inverse gravitational coupling. The conventional general relativity is recovered in the so called "Einstein gauge" (E gauge) set by requiring the scalars to satisfy:

$$\frac{1}{12}\left(\phi_{E+}^2 - s_{E+}^2\right) = +\frac{1}{16\pi G_N} \tag{7.5}$$

where the + refers to the resulting usual positive sign for the gravitational constant (i. e. attractive gravity, see (8.4)). Following the dynamics of these fields, however, one must also consider field configurations where $(\phi^2 - s^2) < 0$. The additional spacetime regions where the sign is negative are required by the dynamics; their inclusion makes the theory geodesically complete. Then, the gauge condition restricting the coupling to positive values becomes ill-defined. The transition region where the coupling blows up or $\phi^2 - s^2$ vanishes[1] is associated with curvature singularities [72, 73].

In the case of cosmology, this has led to cyclic cosmologies that are geodesically complete [63, 74, 75]. Geodesic incompleteness is a signal of the breakdown of the spacetime description and predictability in both general relativity [76, §9, §12] and superstring field theories. Generically, these improved and geodesically complete cosmological solutions require that the universe pass through an antigravity phase. Classically, when the coupling diverges near $\phi^2 - s^2 \sim 0$, one can use the existence of an enhanced conformal symmetry to connect the field solutions on the gravity and antigravity patches [75]. Moreover, quantum mechanically, the behaviour is automatically regularized for the wavefunction of the universe as a solution of the Wheeler de Witt equation in the geodesically complete universe (see for example, §8.3.3).

One natural question pertains to the negative kinetic energy states allowed during the antigravity periods. Naively, it seems as if this could lead to severe instabilities from the usual physics intuitions for flat space perturbative processes. However, this is not at all true in this theory. To explain this in a soluble toy model that captures the essential mechanisms that make the theory work, we shall present in the next chapter various Hamiltonians having a kinetic term with an extra sign function factor $\mathrm{sgn}(x^0 - \Delta/2)$. By constructing the classical solutions as well as the quantum propagator for some cases, we find that the physics is regular and has an interesting interpretation at this order in perturbation theory. We also consider interaction terms by including a harmonic oscillator potential in §8.4.4. Terms of this nature occur naturally in the Wheeler deWitt equation (8.17) discussed in §8.3.3 due to spacial curvature. We find using some elegant $SL(2,\mathbb{R})$ representation theory techniques that the amplitudes (8.46) are bounded and nonsingular , and satisfy the expected orthonormality conditions.

[1] Another intriguing possibility is for the factor to change signs in a discontinuous manner from $+\infty$ to $-\infty$ whereby the coupling $G_N \to 0$.

We show that the apparent problems can be resolved with the interpretation of the theory from the perspective of observers strictly in the gravity region. Such observers cannot experience the negative kinetic energy in antigravity directly, but can only detect in and out signals that interact with the antigravity region. This is no different than a spacetime black box for which the information about its interior is encoded in scattering amplitudes for in/out states at its exterior.

Black hole backgrounds

In chapter 9 we consider modified black hole backgrounds in this theory, when the beyond singularity region included for geodesical completeness; the extra region automatically is a region of to have antigravity. We shall study the nature of this geometry in the classical limit by restricting to geodesic probes. The physics question of the effect of the antigravity patch is addressed by connecting the geodesics across the spacelike singularity. We proceed to present the geodesic completion of the Schwarzschild black hole in four dimensions which covers the entire space in the global (u, v) Kruskal-Szekeres coordinates. We remark that since the analysis is effectively two dimensional, similar results would follow for black hole backgrounds in other dimensions [77–80] as well.

Chapter 8

Physical interpretation of antigravity

In this chapter, we consider some simple models for probing spacetime regions with negative gravitational coupling. Their simplicity makes them interesting scenarios to ask physical questions about such geometries.

8.1 Why antigravity?

The Lagrangian for the geodesically complete version of the Standard Model coupled to General Relativity is [62]

$$\mathcal{L}(x) = \sqrt{-g} \begin{pmatrix} L_{\mathrm{SM}}\left(A_\mu^{\gamma,W,Z,g},\ \psi_{q,l},\ \nu_R,\ \chi\right) \\ +g^{\mu\nu}\left(\frac{1}{2}\partial_\mu\phi\partial_\nu\phi - D_\mu H^\dagger D_\nu H\right) \\ -\left(\frac{\lambda}{4}\left(H^\dagger H - \omega^2\phi^2\right)^2 + \frac{\lambda'}{4}\phi^4\right) \\ +\frac{1}{12}\left(\phi^2 - 2H^\dagger H\right)R(g) \end{pmatrix} \tag{8.1}$$

In the first line, L_{SM} contains all the familiar degrees of freedom in the properly extended conventional Standard Model, including gauge bosons ($A_\mu^{\gamma,W,Z,g}$), quarks & leptons ($\psi_{q,l}$), right-handed neutrinos ν_R, dark matter χ, and their SU(3) ×SU(2) ×U(1) gauge invariant interactions among themselves and with the spin-0 fields (H, ϕ), where H=electroweak Higgs doublet, ϕ = a singlet. In L_{SM} all fields are minimally coupled to gravity. The second and third lines describe the kinetic energy terms and interactions of the scalars among themselves. The last term is the unique *non-minimal coupling* of conformal scalars to the scalar curvature $R(g)$, that is required by invariance of the full $\mathcal{L}(x)$ under local rescaling (Weyl) with an arbitrary local parameter $\Omega(x)$

$$\begin{array}{c} g_{\mu\nu} \to \Omega^{-2} g_{\mu\nu},\ \phi \to \Omega\phi,\ H \to \Omega H \\ \psi_{q,l} \to \Omega^{3/2}\psi_{q,l},\ A_\mu^{\gamma,W,Z,g}\ \text{unchanged.} \end{array} \tag{8.2}$$

If dark matter χ is a spin-0 field, then lines 2-4 in (8.1) should be modified to treat χ as another conformally coupled scalar.

This theory has several pleasing features. There are no dimensionful parameters, so all of those arise from a unique source, namely the gauge fixing of the Weyl symmetry such as, $\phi(x) \to \phi_0$, where ϕ_0 is a dimensionful constant of the order of the Planck scale. Then the gravitational constant is $(16\pi G_N)^{-1} = \phi_0^2/12$, the electroweak scale is $\langle|H|\rangle = \omega\phi_0$, while dark energy, and masses for quarks, leptons, gauge bosons, neutrinos and dark matter arise from interactions with the scalars (ϕ, H). The hierarchy of mass scales is put in by hand through a hierarchy of dimensionless parameters. A deeper theory is needed to explain this hierarchy, but in the present effective theory it is at least possible to maintain it under renormalization since dimensionless constants receive only logarithmic quantum corrections (no need for low energy supersymmetry for the purpose of "naturalness"). To preserve the local scale symmetry in the quantum theory one must adopt a Weyl invariant renormalization scheme in which ϕ is the only renormalization scale, and consequently dimensionless constants receive only Weyl invariant logarithmic renormalizations of the form $\ln(H/\phi)$, etc. With such a renormalization scheme the scale anomaly of all matter cancels against the scale anomaly of ϕ [81], thus not spoiling the local symmetry. Then the unbroken Weyl symmetry in the renormalized theory may play a central role in explaining the smallness of dark energy. This also suggests a definite relation between the electroweak vacuum and dark energy – both of which fill the entire universe.

The presence of the scalar ϕ is compensated by the Weyl symmetry, so ϕ is not a true additional physical degree of freedom but, as a conformally coupled scalar, participates in an important structure of the Weyl symmetry that has further physical consequences involving antigravity spacetime regions in cosmology and black holes as will be discussed in the following sections. The structure of interest, that leads to the central discussion in the rest of this chapter, is the *relative minus sign* in $\left(\phi^2 - 2H^\dagger H\right) R$ and in the scalar kinetic terms in (8.1). These signs are compulsory and play an important role in the geodesic completeness of the theory. With the given sign patterns, H has the correct sign for its kinetic term but ϕ has the wrong sign. If ϕ had the same sign of kinetic energy as H, then the conformal coupling to R would become purely negative which would lead to a negative gravitational constant. So, to generate a positive gravitational constant, ϕ must come with the opposite sign to H. This makes ϕ a ghost field, but this is harmless since the Weyl symmetry can remove this ghost by means of gauge fixing.

This scheme has a straightforward generalization to supersymmetry/supergravity and grand unification, but all scalars $\vec{s}$ must be conformally coupled, $\left(\phi^2 - \vec{s}^2\right) R$, although some generalization is permitted as long as the geodesically complete feature (related to signs) is maintained [62]. Furthermore, we point out that in all supergravity theories, the curvature term has the form $(1 - K(\varphi_i, \bar{\varphi}_i)/3) R$, where K is the Kähler potential and 1 represents the Einstein-Hilbert term [82]. This is again of the form $(|\phi|^2 - |\vec{s}|^2)R$ with complex $(\phi, \vec{s})$, where a complex version of ϕ has been gauge fixed to 1 in a Weyl

invariant formulation of supergravity [74] (see also [83]). Finally we emphasize that the same relative minus sign occurs also in a Weyl invariant reformulation of the low energy limit of string theory, but now with a different interpretation of s related to the dilaton [84]. Hence the structure $\left(\phi^2 - \vec{s}^2\right) R$ is ubiquitous, but was overlooked because it was generally assumed that the gravitational constant, or an effective structure that replaces it, could not or should not become negative to avoid pathological behaviours.

At the outset of this approach in 2008 [69] the immediate question was whether the dynamics would allow $\left(\phi^2 - s^2\right)$ to remain always positive. It was eventually determined by Bars, Chen, Steinhardt and Turok, in a series of papers during 2010-2012 (summary in [72]), that the solutions of the field equations that do not switch sign for this quantity are *non-generic* and of measure zero in the phase space of initial conditions for the fields (ϕ, s). So, according to the dynamics, it is untenable to insist on a limited patch $|\phi| > |\vec{s}|$ of field space. By contrast, it was found that the theory becomes geodesically complete when all field configurations are included, thus solving generally the basic problem of geodesic incompleteness.

The other side of the coin is that solving geodesic incompleteness comes with the prediction that there would be antigravity sectors in the theory since the effective gravitational constant that is proportional to $\left(\phi^2(x) - s^2(x)\right)^{-1}$ would dynamically become negative in some spacetime regions. In view of the pleasing features of the theory outlined in the second paragraph above, these antigravity sectors must then be taken seriously and the corresponding new physics must be understood. In our investigations so far, we discovered that the antigravity sectors are geodesically connected to our own gravity sector through gravitational singularities, like the big bang/crunch or black holes, which occur precisely at the same spacetime points where $\left(\phi^2(x) - s^2(x)\right)$ vanishes or diverges. The related dynamical string tension [84]

$$T(\phi, s) \sim (\phi + s)^{2\frac{1+\sqrt{d-1}}{d-2}} (\phi - s)^{2\frac{1-\sqrt{d-1}}{d-2}}, \tag{8.3}$$

goes to zero or infinity simultaneously. So we need to figure out the physical effects that can be observed in our universe due to the presence of antigravity sectors behind cosmological [75] and black hole singularities [4]. After overcoming several conceptual as well as technical challenges we have been able to discuss some new physics problems and developed new cosmological scenarios that involve an antigravity period in the history of the universe [63, 85]. A remaining conceptual puzzle is an apparent possible instability in the antigravity sector that is addressed and resolved in the remainder of this chapter. Our conclusion is that there are no fundamental problems but only interesting physics which merits further study.

8.2 Geodesic completeness in the Einstein or string frames

The classical or quantum analysis of this theory is best conducted in a Weyl gauge we shall call the "γ-gauge"[62, 75, 84] which amounts to fixing $\det(-g) = 1$. This allows the $\text{sgn}\left(\phi^2 - s^2\right)$ to be determined by the dynamics. Note that the sign is *gauge invariant*, so if the sign switches dynamically in one gauge it has to also switch in all gauges. If one wishes to use the traditional "Einstein gauge" (E) or the "string gauge" (s) one may err by choosing an illegitimate gauge that corresponds to a geodesically incomplete patch, such as

$$\begin{array}{l} \text{E}^+\text{-gauge: } \frac{1}{12}\left(\phi_{E+}^2 - s_{E+}^2\right) = \frac{+1}{16\pi G_N}, \\ \text{s}^+\text{-gauge: } \frac{d-2}{8(d-1)}\left(\phi_{s+}^2 - s_{s+}^2\right) = \frac{+1}{2\kappa_d^2}e^{-2\Phi},\ \Phi = \text{dilaton}. \end{array} \tag{8.4}$$

Here, the E or s subscripts on the fields indicate the gauge fixed form of the corresponding field. If this were all, then there would be nothing new, and the Weyl symmetry could indeed be regarded as "fake" [71]. However, the fact is that conventional general relativity and string theory are geodesically incomplete because the gauge choices just shown are valid only in the field patch in which $|\phi| > |s|$. The dynamics contradict the assumption of gauge fixing to only the positive patch. In the negative regions one may choose again the Einstein or string gauge, but now with a negative gravitational constant, $\frac{1}{12}\left(\phi_{E-}^2 - s_{E-}^2\right) = \frac{-1}{16\pi G_N}$, or $\frac{d-2}{8(d-1)}\left(\phi_{s-}^2 - s_{s-}^2\right) = \frac{-1}{2\kappa_d^2}e^{-2\Phi}$. In those spacetime regions gravity is repulsive (antigravity).

The same situation arises in string theory. In the worldsheet formulation of string theory the string tension is now promoted to a background field $T(\phi, s)$ by connecting it directly to the features of the Weyl invariant low energy string theory [84]. Then the string tension $T(\phi, s)$ switches sign together with the corresponding gravitational constant [84]. Thus the Weyl symmetric (SM+GR) and string theory predict that, in the Einstein or string gauges, one should expect a *sudden sign switch* of the effective Planck mass $\frac{1}{12}\left(\phi^2 - s^2\right)$ at certain spacetime points that typically correspond to singularities (e.g. big bang, black holes) encountered in the Einstein or string frames.

One may choose better behaved Weyl gauges (e.g. "γ-gauge", choose $\det(-g) \to 1$, or "c-gauge", choose $\phi \to$ constant) that cover globally all the positive and negative patches in field space. Then the sign switch of the effective Planck mass $\frac{1}{12}\left(\phi^2 - s^2\right)$ is smooth rather than abrupt.

However, if one wishes to work in the more familiar Einstein or string frames, to recover the geodesically complete theory one must allow for the gravitational constant to switch sign at singularities, and *connect solutions* for fields across gravity/antigravity patches. In the $\pm$ Einstein gauges shown above, the last term in (8.1) becomes

$$\frac{\left(\phi_{E\pm}^2 - s_{E\pm}^2\right) R(g_{E\pm})}{12} = \frac{R(g_{E\pm})}{\pm 16\pi G_N} = \frac{R(\pm g_{E\pm})}{16\pi G_N}. \tag{8.5}$$

where the ± for the gravity/antigravity regions can be absorbed into a redefinition of the signature of the metric,

$$\hat{g}^E_{\mu\nu} = \pm g^{E\pm}_{\mu\nu}, . \tag{8.6}$$

Here we have denoted the *continuous* $\hat{g}^E_{\mu\nu}$ as the geometry in the *union* of the gravity/antigravity patches.

The same ± gauge choice is applied to every term in the SM+GR action in (8.1). Under the replacement $g^{E-}_{\mu\nu} \to -g^{E-}_{\mu\nu}$ in the *antigravity sector* certain terms in the action flip sign while some don't [86], e.g. $F_{\mu\nu}F^{\mu\nu}$ does not, but $R\,(g)$ does, as in (9.20). One may (quite rightfully) be concerned that the drastic sign switches of the gravitational constant or the string tension may lead to problems like unitarity or negative kinetic energy ghosts. We mention that [84] has already argued that there are no unitarity problems due to sign flips in field/string theories. There remains the question of possible instability due to negative kinetic energy in the antigravity region. We show in this chapter that its presence is not a problem of principle for observers localised in the gravity region and that those observers can detect interesting physical effects related to the geodesically connected regions of antigravity.

8.3 Unitarity and antigravity in cosmology

There is a general impression that negative kinetic energy in field or string theory implies ghosts associated with negative norm states. It is not generally appreciated that negative norms (hence negative probabilities) are automatically avoided by insisting on a strictly unitary quantization of the theory. This has been illustrated in the quantization of the relativistic harmonic oscillator [87] with a timelike direction that appears with the opposite sign to the spacelike directions, just like the ϕ field as compared to the H field in the SM+GR action in (8.1). Similar situations occur in the antigravity region where some fields may appear with the wrong sign as described after (9.20). The first duty in quantization should be maintaining sanity in the meaning of probability, as in [87], by avoiding a quantization procedure that introduces negative norm states. Of course, there exist successful cases, such as string theory in the "covariant quantization" procedure, that at first admits negative norms to later kill them by applying constraints that select the positive norm states. In principle, the relativistic oscillators in string theory could also be treated as in [87] and very likely still recover the same gauge invariant physical states without ever introducing negative norm states in string theory. It would be preferable to quantize without negative norm states at all from the very beginning.

When there is not enough gauge symmetry to remove a degree of freedom that has the wrong sign of kinetic energy, a unitary quantization procedure like [87] maintains unitarity. However, the effect of the negative kinetic energy is to cause an instability (not unlike a tachyonic mass term, or a bottomless potential, would), so that there may not

be a ground state for that degree of freedom while it propagates in the antigravity region. This is the negative kinetic energy issue in the antigravity sector. Perhaps some complete theory as a whole conspires to have a ground state even in antigravity. Although this would be reassuring, it appears that this is not necessary in order to make sense of the physics as detected by observers in the gravity sector. Such observers can verify that the same degree of freedom does have a ground state in the gravity region while they can never experience directly the negative kinetic energy in the antigravity sector. The only physics questions that make sense for those observers is what can be learned about the existence of antigravity through scattering experiments that involve in/out states as defined in the gravity region. For those questions the issue of whether there is a ground state in the antigravity region does not matter, but unitarity continues to matter. Therefore we point out how this works in the case of cosmology that admits an antigravity region.

8.3.1 WdW equation and unitarity in mini superspace

The Wheeler de Witt (WdW) equation is the quantum version of the $\mu = 0$ and $\nu = 0$ component of the Einstein equation, $(G_{00} - T_{00})\,\psi = 0$. This is a *constraint* applied on physical states in covariant quantization of general relativity [88]. The "mini superspace" consists of only time dependent (homogeneous) scalar fields $\left(\phi\left(x^0\right), s\left(x^0\right)\right)$ and the FRW metric, $ds^2 = a^2\left(x^0\right)\left(-\left(dx^0\right)^2 + \gamma_{ij}\left(x^0, \vec{x}\right) dx^i dx^j\right)$, with γ_{ij} describing spacial curvature and anisotropies, while T_{00} includes the radiation density, $\rho_r\left(x^0\right)/a^4\left(x^0\right)$. From the action in (8.1) we can derive a Wheeler de Witt equation that is invariant under Weyl rescalings $(\phi, s, a) \to \left(\Omega\phi, \Omega s, \Omega^{-1}a\right)$ with a time dependent $\Omega\left(x^0\right)$; this allows us to choose a gauge. To allow $\left(\phi^2 - s^2\right)$ to have any sign dynamically, we prefer the γ-gauge given by

$$(\phi, s, a) \to (\phi_\gamma, s_\gamma, 1)\,, \text{ or } a_\gamma\left(x^0\right) = 1. \tag{8.7}$$

We concentrate here on the simplest FRW geometry in the γ-gauge,

$$ds^2_\gamma = -\left(dx^0\right)^2 + \frac{dr^2}{1 - Kr^2} + r^2 d\Omega^2, \tag{8.8}$$

with no anisotropy or inhomogeneities, but with a positive constant spatial curvature $K > 0$. This is not realistic, but it is the easiest case to illustrate the unitarity properties of the quantum theory that includes antigravity regions (more degrees of freedom, and negative or zero K would be treated in a similar manner). The mini superspace is just (ϕ_γ, s_γ), while the constraint $(T_{00} - G_{00}) = 0$ derived from (8.1) is, $-\frac{1}{2}\dot{\phi}^2_\gamma + \frac{1}{2}\dot{s}^2_\gamma + \frac{1}{2}K\left(-\phi^2_\gamma + s^2_\gamma\right) + \rho_r = 0$. This is recognized as the Hamiltonian for the relativistic harmonic oscillator, $H = \frac{1}{2}\left(\dot{x}^2 + Kx^2\right)$, with $x^\mu(\tau) = \left(\phi_\gamma(\tau), s_\gamma(\tau)\right)$, subject to the constraint, $H + \rho_r = 0$, where ρ_r is a constant. Note that this Hamiltonian contains negative energy for the (time-like) ϕ_γ degree of freedom. Recall that we have already used up the Weyl symmetry so

this degree of freedom cannot be removed and its negative energy must be dealt with. The naive quantization of the relativistic harmonic oscillator would introduce negative norm states for the ϕ_γ degree of freedom (as in string theory), so it appears there may be trouble with unitarity. However, this is not the case, because this system (and similar cases) can be quantized by respecting unitarity without ever introducing negative norms as shown in [87]. This goes as follows: the quantum system obeys the constraint equation $(H+\rho_r)\,\Psi=0$. This is the WdW equation that takes the form

$$\left(\frac{1}{2}\partial_{\phi_\gamma}^2-\frac{1}{2}\partial_{s_\gamma}^2+\frac{K}{2}\left(-\phi_\gamma^2+s_\gamma^2\right)+\rho_r\right)\Psi\left(\phi_\gamma,s_\gamma\right)=0. \tag{8.9}$$

This is recognized as the Klein-Gordon equation for the quantized relativistic harmonic oscillator. The eigenstates and eigenvalues of the independent ϕ_γ and s_γ oscillators are

$$\begin{array}{l}\frac{1}{2}\left(-\partial_{\phi_\gamma}^2+K\phi_\gamma^2\right)\psi_{n_\phi}\left(\phi_\gamma\right)=\sqrt{K}\left(n_\phi+\frac{1}{2}\right)\psi_{n_\phi}\left(\phi_\gamma\right),\\ \frac{1}{2}\left(-\partial_{s_\gamma}^2+Ks_\gamma^2\right)\psi_{n_s}\left(s_\gamma\right)=\sqrt{K}\left(n_s+\frac{1}{2}\right)\psi_{n_s}\left(s_\gamma\right),\end{array} \tag{8.10}$$

where (n_ϕ,n_s) are positive integers, $0,1,2,3,\cdots$, and the explicit *positive norm* complete set of off-shell solutions are

$$\begin{array}{c}\Psi_{n_\phi n_s}\left(\phi_\gamma,s_\gamma\right)=\psi_{n_\phi}\left(\phi_\gamma\right)\psi_{n_s}\left(s_\gamma\right),\\ \psi_{n_\phi}\left(\phi_\gamma\right)=A_{n_\phi}e^{-\frac{1}{2}\sqrt{K}\phi_\gamma^2}H_{n_\phi}\left(\phi_\gamma\right),\\ \psi_{n_s}\left(s_\gamma\right)=A_{n_s}e^{-\frac{1}{2}\sqrt{K}s_\gamma^2}H_{n_s}\left(s_\gamma\right),\end{array} \tag{8.11}$$

where $H_n\left(z\right)$ are the Hermite polynomials and A_{n_ϕ},A_{n_s} are normalization constants. Then the WdW equation (8.9) is solved by constraining the eigenvalues, $\sqrt{K}\left(-n_\phi+n_s\right)+\rho_r=0$. Hence the complete on-shell basis that satisfies the constraint is

$$\Psi_n\left(\phi_\gamma,s_\gamma\right)=A_{n+r}A_ne^{-\frac{\sqrt{K}}{2}\left(\phi_\gamma^2+s_\gamma^2\right)}H_{n+r}\left(\phi_\gamma\right)H_n\left(s_\gamma\right), \tag{8.12}$$

with $n=0,1,2,\cdots$, where we defined

$$n_s\equiv n,\quad n_\phi\equiv n+r,\quad \text{and } \frac{\rho_r}{\sqrt{K}}\equiv r \text{ a fixed integer.} \tag{8.13}$$

If $\frac{\rho_r}{\sqrt{K}}$ is not an integer there is no solution to the constraint, hence radiation must be quantized for this system to be non-trivial at the quantum level. The general on-shell solution of the WdW equation is an arbitrary superposition of this basis

$$\Psi\left(\phi_\gamma,s_\gamma\right)=\sum_{n=0}^{\infty}c_n\Psi_n\left(\phi_\gamma,s_\gamma\right) \tag{8.14}$$

The complex coefficients c_n are chosen to insure that $\Psi\left(\phi_\gamma,s_\gamma\right)$ is properly normalized.

All quantum states have *positive norm* and unitarity is satisfied. $\Psi\left(\phi_\gamma, s_\gamma\right)$ is the probability amplitude for where the system is in the (ϕ_γ, s_γ) plane. The gravity/antigravity regions are $\phi_\gamma^2 \lesseqgtr s_\gamma^2$. Evidently there is no way of preventing the generic wavefunctions from being non-zero in the antigravity region, so the system generically evolves through both the gravity and antigravity regions.

We emphasize that the quantization method in [87] that we used to maintain unitarity is very different than the quantization of the relativistic oscillator used in string theory. In string theory one defines relativistic creation/annihilation operators $a_\mu, a_\mu^\dagger$ and a vacuum state that satisfies $a_\mu|0\rangle = 0$. Then the quantum states at level l are given by applying l creation operators, $a_{\mu_1}^\dagger a_{\mu_2}^\dagger \cdots a_{\mu_l}^\dagger|0\rangle$. The vacuum state is Lorentz invariant, while the states at level l form a collection of *finite dimensional* irreducible representations of the Lorentz group. All the states at level l have *positive energy*, $E_l = \sqrt{K}\,(l+1)$. The constraint $H + \rho_r = 0$ (WdW equation) can be satisfied only for negative quantized ρ_r at only one level $l = -1 + |\rho_r|/\sqrt{K}$. In position space the vacuum state takes the Lorentz invariant form $\psi_0\left(x^\mu\right) \sim e^{-\sqrt{K}x^2} = e^{-\sqrt{K}\left(-\phi_\gamma^2 + s^2\right)}$, while the the states at level l are of the form of a polynomial of x^μ of degree l multiplied by the same exponential $e^{-\sqrt{K}x^2}$.

A subset of the level-l states have negative norm because finite dimensional representations are *not* unitary representations of the Lorentz group, so this method of quantization gets into trouble with unitarity. We contrast this result to ours in (8.12) where we have displayed an infinite, rather than finite, number of states and a Gaussian factor $e^{-\sqrt{K}\left(\phi_\gamma^2 + s^2\right)}$ that converges in all directions, rather than the non-convergent Lorentz invariant form $e^{-\sqrt{K}\left(-\phi_\gamma^2 + s^2\right)}$. There is *no Lorentz invariant* vacuum state. As shown in [87], our states in (8.12) form an *infinite dimensional unitary representation* of the Lorentz group for which all the states have positive norm. Furthermore, those that satisfy the constraint have positive total energy, $H = \rho_r$, as long as ρ_r is positive. However, as seen in (8.11), there are *off-shell states* of positive as well as negative energy. These remarks make it clear that the price for maintaining unitarity (which is the first duty in quantization) is the presence of regions of spacetime with negative kinetic energy, which, in our case, amounts to regions of antigravity. Our task in this chapter is to explain that negative kinetic energy in the antigravity sector does not necessarily imply a problem by interpreting the physical significance of antigravity.

8.3.2 Feynman propagator in mini superspace

The Feynman propagator associated with this WdW equation is

$$G\left(\phi', s'; \phi, s\right) = \langle \phi', s'| \frac{i}{H + \rho_r + i\varepsilon} |\phi, s\rangle. \tag{8.15}$$

We can use the complete basis $|n_\phi, n_s\rangle$ to insert identity in terms of the eigenstates of the off-shell $H = -H_\phi + H_s$ operator without any constraints on the integers (n_ϕ, n_s). Then

we compute

$$\begin{aligned} G\left(\phi',s';\phi,s\right) &= i\sum_{n_\phi,n_s\geq 0}\frac{\langle\phi',s'|n_\phi,n_s\rangle\langle n_\phi,n_s|\phi,s\rangle}{-n_\phi+n_s+\rho_r+i\varepsilon} \\ &= i\sum_{n_\phi,n_s\geq 0}\psi_{n_\phi}\left(\phi'\right)\psi_{n_s}\left(s'\right)\psi^*_{n_\phi}\left(\phi\right)\psi^*_{n_s}\left(s\right)\left(-n_\phi+n_s+\rho_r+i\varepsilon\right)^{-1} \\ &= i\sum_{n_\phi,n_s\geq 0}\int_0^\infty d\tau\ \psi_{n_\phi}\left(\phi'\right)\psi_{n_s}\left(s'\right)\psi^*_{n_\phi}\left(\phi\right)\psi^*_{n_s}\left(s\right)\left(-i\ e^{i\tau\left(-n_\phi+n_s+\rho_r+i\varepsilon\right)}\right) \\ &= \int_0^\infty d\tau e^{i\tau(\rho_r+i\varepsilon)}\langle\phi'|e^{-i\tau H_\phi}|\phi\rangle\ \langle s'|e^{i\tau H_s}|s\rangle \\ &= \int_0^\infty d\tau\frac{\sqrt{K}\ e^{i\tau(\rho_r+i\varepsilon)}}{2\pi\sin\left(\sqrt{K}\tau\right)}\exp\left(\frac{-i\sqrt{K}}{2\sin\left(\sqrt{K}\tau\right)}\left[\left(x^2+x'^2\right)\cos\sqrt{K}\tau-2x\cdot x'\right]\right) \end{aligned} \tag{8.16}$$

In the last step we used the propagator $\langle\phi'|e^{-i\tau H_\phi}|\phi\rangle$ for the 1-dimensional harmonic oscillator, and then substituted $x^2=-\phi^2+s^2$ and $x\cdot x'=-\phi\phi'+ss'$. This quantum computation in the Hamiltonian formalism agrees with the path integral computation in [85].

The Feynman propagator is a measure of the probability that the system that starts in some initial state will be found in some final state. For observers outside of the antigravity region the initial and final states $|\phi,s\rangle,|\phi',s'\rangle$ are both in the gravity region, $|\phi|>|s|$ and $|\phi'|>|s'|$, although during the propagation from initial to final state the antigravity region is probed as seen from the sums over (n_ϕ,n_s) where both positive and negative energy states of the off-shell Hamiltonian $H=-H_\phi+H_s$ enter in the calculation. We see from the last expression in (8.16) that $G\left(\phi',s';\phi,s\right)$ is a perfectly reasonable function indicating that there are no issues with fundamental principles in this calculation which involves an intermediate period of antigravity in the evolution of the universe.

This was the case of a radiation dominated spatially curved spacetime which is far from being a generic configuration in the early universe close to the singularity. The generic dominant terms in the Einstein frame are the kinetic energy of the scalar and anisotropy (in the spatial metric) and the next non-leading term is radiation. The subdominant terms, including curvature, inhomogeneities, potential energy, dark energy, etc. are negligible near the singularity. The dominant generic behaviour near the singularity was computed classically in [75] where it was discovered that there *must* be an inescapable excursion into the antigravity regime before coming back to the gravity sector, as outlined in the previous paragraph. Hence, a similar computation to (8.16), by using the dominant terms in the WdW equation (instead of (8.9)) should replace our computation here. Unpublished work along these lines dating back to 2011 [72] indicate that the physical picture already obtained through classical solutions in [75] continues to hold in minisuperspace at the quantum level.

8.3.3 More general WdW equation

As mentioned in the previous paragraph, we can generalize the WdW equation above (8.9) by including the physical features that would make it more realistic for a description of

the early universe in terms of a mini superspace. This includes the kinetic energy for anisotropy degrees of freedom that cannot be neglected when $s^2/\phi^2 \simeq 1$ close to the singularity, and the potential energy terms for both the scalars and anisotropies that tend to become important when $\left|1 - s^2/\phi^2\right| \gtrsim 1$. The action for the mini-superspace that includes these features is given in (8) in [72]. The corresponding WdW equation in the γ-gauge modifies (8.9) as follows

$$\left(\begin{array}{c} \frac{1}{2}\partial^2_{\phi_\gamma} - \frac{1}{2}\partial^2_{s_\gamma} - \frac{1}{2}\frac{1}{\phi^2_\gamma - s^2_\gamma}\left(\partial^2_{\alpha_1} + \partial^2_{\alpha_2}\right) + \rho_r \\ +V\left(\phi_\gamma, s_\gamma\right) - \frac{1}{2}\left(\phi^2_\gamma - s^2_\gamma\right) v\left(\alpha_1, \alpha_2\right) \end{array} \right) \Psi\left(\phi_\gamma, s_\gamma, \alpha_1, \alpha_2\right) = 0. \tag{8.17}$$

The additional anisotropy degrees of freedom (α_1, α_2) are part of the 3-dimensional metrics of types Kasner, Bondi-VIII, and Bondi-IX, as shown in (7) of Ref.[72]. The term containing the anisotropy potential $v\left(\alpha_1, \alpha_2\right)$ above vanishes for the Kasner metric, while for Bondi-VIII and IX it simplifies to a constant, $v\left(\alpha_1, \alpha_2\right) \to K$, in the zero anisotropy limit (as in (8.9)). The details of the anisotropy potential $v\left(\alpha_1, \alpha_2\right)$ are given in (9) of Ref.[72].

With these additional features the WdW equation is no longer separable in the (ϕ_γ, s_γ) degrees of freedom. To make progress we make a change of variables by defining

$$z = \phi^2_\gamma - s^2_\gamma,\ \sigma = \frac{1}{2}\ln\left|\frac{\phi_\gamma + s_\gamma}{\phi_\gamma - s_\gamma}\right|. \tag{8.18}$$

Note that $z \gtrless 0$ corresponds to gravity/antigravity. These variables were used in the classical analysis of the same system in [75] where the classical equations that follow from the same action were studied. Weyl invariance requires $V\left(\phi, s\right)$ to be a homogeneous function of degree four, $V\left(t\phi, ts\right) = t^4 V\left(\phi, s\right)$, so without loss of generality we may write

$$V\left(\phi_\gamma, s_\gamma\right) = z^2 v\left(\sigma\right), \tag{8.19}$$

where $v\left(\sigma\right)$ is any function that is specified by some physical model. The WdW equation above takes the following form in the $z, \sigma, \alpha_1, \alpha_2$ basis

$$\left(\begin{array}{c} \partial^2_z + \frac{1}{4z^2}\left(-\partial^2_1 - \partial^2_2 - \partial^2_\sigma + 1\right) \\ +\frac{z}{2}v\left(\sigma\right) - \frac{1}{4}v\left(\alpha_1, \alpha_2\right) + \frac{\rho_r}{2z} \end{array} \right) \left(z^{1/2}\Psi\left(z, \sigma, \alpha_1, \alpha_2\right)\right) = 0. \tag{8.20}$$

Near the singularity, $z = 0$, assuming the potentials are neglected compared to the dominant and subdominant z^{-2}, z^{-1} terms, the wavefunction becomes separable in the form of a 3-dimensional plane wave, $\Psi = \exp\left(ip_1\alpha_1 + ip_2\alpha_2 + ip_3\sigma\right)\psi\left(z\right)$ with constant "momenta" $\left(p_1, p_2, p_3\right)$, thus reducing (8.20) to an ordinary second order differential equation

$$\left(\partial^2_z + \frac{1}{4z^2}\left(p^2_1 + p^2_2 + p^2_3 + 1\right) + \frac{\rho_r}{2z}\right)\left(z^{1/2}\psi\left(z\right)\right) \simeq 0. \tag{8.21}$$

This is recognized as a Hydrogen-atom type differential equation; its solutions are given analytically in terms of special functions related to the representations of $\mathrm{SL}(2,R)$ as discussed in [89]. From these wavefunctions we learn that the behaviour of the probability distributions near the singularity, $z \sim 0$ where the gravity/antigravity transition occurs, matches closely the behaviour of the unique analytic classical "attractor" solution that corresponds to the "antigravity loop" described in [75]. Namely, with a non-zero parameter, $p \equiv \sqrt{p_1^2 + p_2^2 + p_3^2}$, the cosmological evolution of the universe cannot avoid to pass temporarily though an antigravity sector, $z < 0$. Meanwhile, as seen here, the wavefunctions are normalizable and fully consistent with unitarity in both the gravity and antigravity sectors $z \gtrless 0$. This conclusion, in the presence of the dominant anisotropy terms, is in agreement with the lessons learned above with the simpler form of the WdW equation in (8.9).

As $|z|$ increases beyond the singularity and reaches $|z| \sim 1$, in either the gravity or antigravity sectors, the potentials $v(\sigma)$ and $v(\alpha_1, \alpha_2)$ can no longer be neglected. We may still reduce the 4-variable partial differential equation to a single-variable ordinary differential equation as follows. Define the wavefunctions $\Phi_n(\sigma)$ and $\xi_{m_1 m_2}(\alpha_1, \alpha_2)$ as follows

$$\begin{gathered} \left(-\partial_\sigma^2 + 2z^3 v(\sigma)\right) \Phi_n(\sigma) = E_n(z)\, \Phi_n(\sigma) \\ \left(-\partial_1^2 - \partial_2^2 - z^2 v(\alpha_1, \alpha_2)\right) \xi_{m_1 m_2}(\alpha_1, \alpha_2) = E_{m_1 m_2}(z)\, \xi_{m_1 m_2}(\alpha_1, \alpha_2) \end{gathered} \tag{8.22}$$

In solving these equations the parameter z is considered a constant parameter, but the eigenvalues $E_n(z)$ and $E_{m_1 m_2}(z)$ clearly depend on z. Then, writing the wavefunction in separable form,

$$\Psi(z, \sigma, \alpha_1, \alpha_2) \sim \Psi_{n,m_1,m_2}(z) \times \Phi_n(\sigma) \times \xi_{m_1 m_2}(\alpha_1, \alpha_2), \tag{8.23}$$

(8.20) reduces to

$$\left(\partial_z^2 + \frac{1}{4z^2}\left(E_n(z) + E_{m_1 m_2}(z) + 1\right) + \frac{\rho_r}{2z}\right)\left(z^{1/2} \Psi_{n,m_1,m_2}(z)\right) = 0. \tag{8.24}$$

while the general solution takes the form

$$\Psi(z, \sigma, \alpha_1, \alpha_2) = \sum_{n,m_1,m_2} c_{n,m_1,m_2} \Psi_{n,m_1,m_2}(z) \times \Phi_n(\sigma) \times \xi_{m_1 m_2}(\alpha_1, \alpha_2) \tag{8.25}$$

with arbitrary constant coefficients c_{n,m_1,m_2}.

As we saw above, when $v(\sigma), v(\alpha_1, \alpha_2)$ are zero, the corresponding energies tend to constants $E_n(z) \to p_3^2$ and $E_{m_1 m_2}(z) \to p_1^2 + p_2^2$, so this can be used as a guide to the role played by $E_n(z)$ and $E_{m_1 m_2}(z)$ in (8.24). Using simple models for $v(\sigma), v(\alpha_1, \alpha_2)$

to extract properties of $E_n(z)$ and $E_{m_1 m_2}(z)$ and also using semi-classical WKB approximation methods for more complicated cases, we may estimate the behaviour of $E_n(z) + E_{m_1 m_2}(z)$ for small as well as large z. This can then be used to discuss the behaviour of the quantum universe beyond the approximations described above. In such attempts, with non-trivial $v(\sigma), v(\alpha_1, \alpha_2)$, we find that $E_n(z), E_{m_1 m_2}(z)$ are generically not analytic near $z = 0$ in the complex z-plane (in the sense of cuts that extend to $z = 0$) so this complicates the use of analyticity methods [85] to extract information from these equations. We continue to investigate this approach and hope to report more results in the future.

To conclude this section, an important remark is that unitarity is maintained in the WdW treatment throughout gravity and antigravity, while the presence of negative energy during antigravity is not of concern regarding fundamental principles as already illustrated in the previous sections, especially with the simpler computation based on (8.9).

8.4 Negative energy in antigravity and observers in gravity

To develop a physical understanding of negative kinetic energy we shall discuss several toy models that will include the analog of a background gravitational field that switches sign between positive and negative kinetic energy. The physical question is, what do observers in the gravity region detect about the presence of a negative kinetic energy sector? Conceptually this is the analog of a black box being probed by in/out signals detected at the exterior of the box.

In the field theory or particle examples discussed below a simple sign function that is modeled after the "antigravity loop " in [75] captures the main effect of antigravity. This sign function is a simple device to answer questions that arose repeatedly on unitarity and possible instability and is not necessarily a solution to the gravitational field equations of some specific model. Rather, it is used here only to capture the main effect of an antigravity sector in a simple and solvable model. In the case of realistic applications one would need to use a self consistent solution of matter and gravitational equations (as in [75]) as long as it captures the main features of antigravity as in the simplified model background discussed here.

8.4.1 Particle with time dependent kinetic energy flips

A free particle with a relativistic (or non-relativistic) Hamiltonian that switches sign as a function of time provides an example of a system propagating in a background gravitational field that switches sign as in (8.6)

$$H = \varepsilon\left(|t| - \frac{\Delta}{2}\right) \times \sqrt{p^2 + m^2} \quad \text{or} \quad H = \varepsilon\left(|t| - \frac{\Delta}{2}\right) \times \frac{p^2}{2m}, \tag{8.26}$$

where $\varepsilon(u) \equiv \text{Sign}(u)$. Such a background captures some of the properties of the antigravity loop of Bars-Steinhardt-Turok [75]. The particle's phase space (x, p) can also represent more generally a typical generalized degree of freedom in field theories or string field theories (SFTs).

As per Hamilton's equations, the momentum p is conserved since H is independent of x, but the velocity $\dot{x} = \partial H/\partial p = \varepsilon\left(|t| - \frac{\Delta}{2}\right) \frac{p}{\sqrt{p^2+m^2}}$ alternates signs as shown below. The Hamiltonian is time dependent, so it is not conserved.

$t:$	$t < -\frac{\Delta}{2}$	$-\frac{\Delta}{2} < t < \frac{\Delta}{2}$	$t > \frac{\Delta}{2}$
$H_{\pm}:$	$\sqrt{p^2+m^2}$	$-\sqrt{p^2+m^2}$	$\sqrt{p^2+m^2}$
$x:$	$\dot{x} = \frac{p}{\sqrt{p^2+m^2}}$	$\dot{x} = -\frac{p}{\sqrt{p^2+m^2}}$	$\dot{x} = \frac{p}{\sqrt{p^2+m^2}}$

At the $t = \pm\Delta/2$ kinks the velocity vanishes if we define $\varepsilon(0) = 0$. It is possible to make other models of what happens to the velocity by replacing the sign function $\varepsilon(z)$ by other time dependent kinky or smooth models; for example, if we replace $\varepsilon(z)$ by $(\varepsilon(z))^{-1}$, then the velocity at the kinks changes sign at an infinite value rather than at zero, while the momentum remains a constant in all cases.

If the initial position before entering antigravity is $x_i(t_i)$, we compute the evolution at any time as follows (see Fig.1)

$$\begin{array}{rcl} t < -\frac{\Delta}{2} & : & x(t) = x_i(t_i) + \frac{p}{\sqrt{p^2+m^2}}(t - t_i) \\ -\frac{\Delta}{2} < t < \frac{\Delta}{2} & : & x(t) = x\left(-\frac{\Delta}{2}\right) - \frac{p}{\sqrt{p^2+m^2}}\left(t + \frac{\Delta}{2}\right) \\ t > \frac{\Delta}{2} & : & x(t) = x\left(\frac{\Delta}{2}\right) + \frac{p}{\sqrt{p^2+m^2}}\left(t - \frac{\Delta}{2}\right) \end{array} \tag{8.27}$$

where $x\left(-\frac{\Delta}{2}\right) = x_i(t_i) + \frac{p}{\sqrt{p^2+m^2}}\left(-\frac{\Delta}{2} - t_i\right)$, and $x\left(\frac{\Delta}{2}\right) = x_i(t_i) - \frac{p}{\sqrt{p^2+m^2}}(3\Delta/2 + t_i)$. The final position $x_f(t_f)$, at a time t_f after waiting long enough to exit from antigravity, $t_f > \Delta/2$, is

$$x_f(t_f) = x_i(t_i) + \frac{p}{\sqrt{p^2+m^2}}(t_f - t_i - 2\Delta). \tag{8.28}$$

The effect of antigravity during the interval, $-\frac{\Delta}{2} < t < \frac{\Delta}{2}$, is the backward excursion between the two kinks shown in Fig.8.1. For observers waiting for the arrival of the particle at some position $x_f(t_f)$, we see from (8.28) that antigravity causes a time delay by the amount of 2Δ as compared to the absence of antigravity. Hence there is a measurable signal, namely a time delay, as an observable effect in comparing the presence and absence of antigravity.

A similar problem is analyzed at the quantum level by computing the transition amplitude from an initial state $|x_i, t_i\rangle$ to a final state $|x_f, t_f\rangle$, requiring that the final observation is in the gravity period, *after* passing through the antigravity period. This is

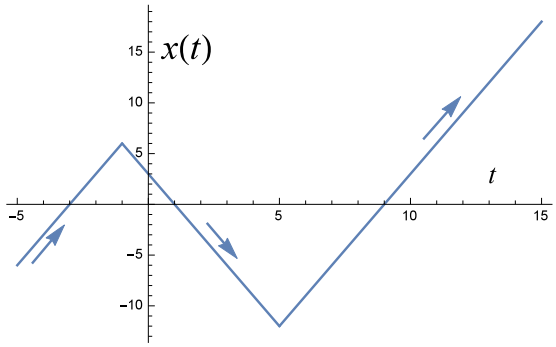

Figure 8.1: Propagation of a point particle probe through a region of antigravity.

given by

$$\begin{aligned} A_{fi} &= \langle x_f, t_f | e^{-\frac{i}{\hbar}H_+\left(t_f-\frac{\Delta}{2}\right)} e^{-\frac{i}{\hbar}H_-\left(\frac{\Delta}{2}-\frac{-\Delta}{2}\right)} e^{-\frac{i}{\hbar}H_+\left(\frac{-\Delta}{2}-t_i\right)} | x_i, t_i \rangle \\ &= \langle x_f, t_f | e^{-\frac{i}{\hbar}H\left(t_f-t_i-2\Delta\right)} | x_i, t_i \rangle \\ &= \sqrt{\frac{m}{2\pi i\hbar\left(t_f-t_i-2\Delta\right)}} \exp\left(\frac{i\ m\ \left(x_f-x_i-2\Delta\right)^2}{2\hbar\left(t_f-t_i-2\Delta\right)}\right) \end{aligned} \tag{8.29}$$

The last expression is for the case of a non-relativistic particle with $H_\pm = \pm H = \pm p^2/2m$. The exponentials involving $H_\pm$ are simplified because $H_\pm$ commute with each other, allowing the combination of the exponentials into a single exponential. Thus, the effect of the intermediate antigravity period is to cause only a time delay just as in the classical solution above. Note also that there are no unitarity problems; the evolution operator is unitary, and norms of states are positive, at all stages.

8.4.2 Particle with space dependent kinetic energy flips

Consider a non-relativistic particle with a total energy Hamiltonian that switches sign in different regions of space, for example

$$H = \varepsilon\left(|x| - \frac{\Delta}{2}\right) \times \left(\frac{p^2}{2m} + V\left(x\right)\right). \tag{8.30}$$

This is another example of a system propagating in a background gravitational field that switches sign as in (8.6). In this case energy is conserved since there is no explicit time dependence in H. Therefore at generic energies, $E = \left(\frac{p^2}{2m} + V\left(x\right)\right)$, the particle cannot cross the boundaries at $|x| = \frac{\Delta}{2}$ since the Hamiltonian would flip sign and this would contradict the energy conservation. Hence if the particle is in the the gravity region, $|x| > \frac{\Delta}{2}$, it stays there, and if it is in the antigravity region, $|x| < \frac{\Delta}{2}$, it stays there. However, the particle can cross from gravity to antigravity and back again to gravity at zero energy $\frac{p^2}{2m} + V\left(x\right) = 0$. This is similar to the geodesics in a black hole that cross from gravity to antigravity [4].

8.4.3 Free massless scalar field with sign flipping kinetic energy

Consider a free massless scalar field in flat space with a time dependent background field that causes sign flips of the kinetic energy as a function of time

$$S=-\frac{1}{2}\int d^4x\,\varepsilon\left(\left|x^0\right|-\frac{\Delta}{2}\right)\,\partial^\mu\phi\left(x\right)\partial_\mu\phi\left(x\right). \tag{8.31}$$

The factor $\varepsilon\left(\left|x^0\right|-\frac{\Delta}{2}\right)$ can be viewed as a gravitational background field of the form, $\sqrt{-g}g^{\mu\nu}\partial_\mu\phi\partial_\nu\phi$, with $g^{\mu\nu}\left(x\right)=\varepsilon\left(\left|x^0\right|-\frac{\Delta}{2}\right)\eta^{\mu\nu}$ and $\sqrt{-g}=1$. This sign flipping metric should be regarded as an example of a geometry that spans the union of the gravity and antigravity regions, as in (8.6). We proceed to analyze the time evolution of this system. Let the on-shell initial field configuration at time $x_i^0<(-\Delta/2)$ be defined by

$$\phi_i\left(\vec{x}_i,x_i^0\right)=\int\frac{d^3p}{\left(2\pi\right)^{3/2}2\left|p\right|}\left(a\left(\vec{p}\right)e^{-i\left|p\right|x_i^0+i\vec{p}\cdot\vec{x}_i}+\bar{a}\left(\vec{p}\right)e^{i\left|p\right|x_i^0-i\vec{p}\cdot\vec{x}_i}\right) \tag{8.32}$$

The general solution for $\phi\left(\vec{x},x^0\right)$ evolved up to a final time $x_f^0>\Delta/2$ is then given by (using the method in (8.27))

$$\phi_f\left(\vec{x}_f,x_f^0\right)=\int\frac{d^3p}{\left(2\pi\right)^{3/2}2\left|p\right|}\left(\begin{array}{l}a\left(\vec{p}\right)e^{-i\left|p\right|\left(x_f^0-x_i^0-2\Delta\right)+i\vec{p}\cdot\vec{x}_f}\\+\bar{a}\left(\vec{p}\right)e^{i\left|p\right|\left(x_f^0-x_i^0-2\Delta\right)-i\vec{p}\cdot\vec{x}_f}\end{array}\right). \tag{8.33}$$

This shows that for initial/final observations, that are strictly outside of the antigravity period, the effect of the antigravity period is only a time delay as compared to the complete absence of antigravity. The time evolution of the field in the interim period is just like the time evolution of the particle as shown in Fig.1. For more details on the classical evolution of the field in the interim period see the case of the massive field in section (8.4.5), and take the zero mass limit.

An important remark is that the multiparticle Hilbert space $\{|\vec{p}_1,\vec{p}_2\cdots\vec{p}_n\rangle\}$ is the Fock space constructed from the creation operators applied on the vacuum defined by $a\left(\vec{p}\right)|0\rangle=0$, namely $|\vec{p}_1,\vec{p}_2\cdots\vec{p}_n\rangle\equiv\bar{a}\left(\vec{p}_1\right)\bar{a}\left(\vec{p}_2\right)\cdots\bar{a}\left(\vec{p}_n\right)|0\rangle$. This time independent Fock space is the complete Hilbert space that can be used during gravity or antigravity. It is clearly unitary since it is the same Hilbert space that is independent of the existence of an antigravity period (i.e. same as the $\Delta=0$ case). This shows that there is no unitarity problem due to the presence of the antigravity period.

However, there is negative kinetic energy during antigravity, seen as follows. The time dependent Hamiltonian for this system is

$$H\left(x^0\right)=\left\{\begin{array}{l}+H,\text{ for }t<-\frac{\Delta}{2}\\-H,\text{ for }-\frac{\Delta}{2}<t<\frac{\Delta}{2}\\+H,\text{ for }t>\frac{\Delta}{2}\end{array}\right. \tag{8.34}$$

where H, which is constructed from the quantum creation-annihilation operators as usual, is time independent. So there seems to be a possible source of instability due to negative energy during antigravity. For freely propagating particles there are no transitions that alter the energy, so no questions arise, it is only when there are *interactions* that an effect may be observed due to transitions created by the negative energy sector. The effect of interactions, as observed by detectors in the gravity sector, is analogous to the case of a time dependent Hamiltonian as discussed in simple examples below in section (8.4.4). Hence, the presence of a sector with negative kinetic energy is not a fundamental problem in the quantum theory.

Nevertheless, the antigravity sector, with or without interactions, is the source of interesting physical signals for the observers in the gravity sectors. For example, in the absence of additional interactions, consider the quantum propagator that corresponds to initial/final states in the two gravity sectors $\left|x^0\right| > \Delta/2$. The transition amplitude from an initial state in gravity $\left(x_i^0 < -\Delta/2\right)$ to a final state in gravity $\left(x_f^0 > \Delta/2\right)$, after the field evolves through antigravity, is given by

$$\begin{aligned} A_{fi} &= \langle \phi_f\left(x_f\right) | e^{-\frac{i}{\hbar}H_+\left(t_f-\frac{\Delta}{2}\right)} e^{-\frac{i}{\hbar}H_-\left(\frac{\Delta}{2}-\frac{-\Delta}{2}\right)} e^{-\frac{i}{\hbar}H_+\left(\frac{-\Delta}{2}-t_i\right)} | \phi_i\left(x_i\right)\rangle \\ &= \langle \phi_f\left(\vec{x}_f, x_f^0\right) | e^{-\frac{i}{\hbar}H\left(t_f-t_i-2\Delta\right)} | \phi_i\left(\vec{x}_i, x_i^0\right)\rangle \end{aligned}$$

Here, $|\phi\left(x\right)\rangle$ is defined as the 1-particle state in the quantum theory which is created by applying the quantum field $\hat{\phi}\left(x\right)$ on the oscillator vacuum $a\left(\vec{p}\right)|0\rangle = 0$,

$$|\phi\left(\vec{x}, x^0\right)\rangle = \hat{\phi}\left(x\right)|0\rangle = \int d^3p \frac{e^{i|p|x^0 - i\vec{p}\cdot\vec{x}}}{\left(2\pi\right)^{3/2} 2\left|p\right|} \bar{a}\left(\vec{p}\right)|0\rangle. \tag{8.35}$$

Then we obtain

$$A_{fi} = \int d^3p \frac{e^{i|p|\left(x_f^0 - x_i^0 - 2\Delta\right) - i\vec{p}\cdot\left(\vec{x}_f - \vec{x}_i\right)}}{\left(2\pi\right)^{3/2} 2\left|p\right|}. \tag{8.36}$$

This is the propagator for a free massless particle. From this expression it is clear that the effect of antigravity on the result for the transition amplitude A_{fi} is only a time delay by an amount of 2Δ as compared to the same quantity in the complete absence of antigravity. The same general statement holds true for the transition amplitudes for multi-particle states. Clearly there is no particle production due to antigravity in the case of free massless particles. This will be contrasted with the case of massive particles in section (8.4.5).

Of course, if there are field interactions, there will be additional effects, but none of those are à priori problematic from the point of view of fundamental principles.

8.4.4 Particle with flipping kinetic energy while interacting in a potential

To learn more about the effects of antigravity we now add an interaction term that does not flip sign during antigravity. We first investigate the case of a single degree of freedom whose kinetic energy flips sign during antigravity. This phase space (x, p) should be thought of as a generalized coordinate associated with any single degree of freedom within local field theory or string field theory (after integrating out all other degrees of freedom), but in its simplest form it can be regarded as representing a particle moving in one dimension.

We discuss a simple model described by the Hamiltonian

$$H = \varepsilon\left(|t| - \frac{\Delta}{2}\right) \times \frac{p^2}{2m} + \frac{m\omega^2}{2}x^2. \tag{8.37}$$

This is a time dependent Hamiltonian that has two different forms, $H_\pm$, during different periods of time as follows

$t:$	$t < -\frac{\Delta}{2}$	$-\frac{\Delta}{2} < t < \frac{\Delta}{2}$	$t > \frac{\Delta}{2}$
$H_\pm:$	$\left(\frac{p^2}{2m} + \frac{m\omega^2 x^2}{2}\right)$	$\left(-\frac{p^2}{2m} + \frac{m\omega^2 x^2}{2}\right)$	$\left(\frac{p^2}{2m} + \frac{m\omega^2 x^2}{2}\right)$

(8.38)

During gravity, $|t| > \frac{\Delta}{2}$, the Hamiltonian H_+ is the familiar harmonic oscillator Hamiltonian with a well defined quantum state, so all energies are positive. But during antigravity, $-\frac{\Delta}{2} < t < \frac{\Delta}{2}$, the Hamiltonian H_- has no bottom, so all positive and negative energies are permitted. Does this pose an instability problem for the entire system? The answer is that, as in the simpler cases already illustrated above, there is no such problem from the perspective of the class of observers in gravity.

A complete basis for a unitary Hilbert space may be defined to be the positive norm complete Fock space associated with the usual harmonic oscillator Hamiltonian H_+ whose energy eigenvalues are strictly positive. The eigenstates of H_- are also positive norm and define another complete unitary basis. Clearly one complete basis may be expanded in terms of another complete basis, so the usual Fock space basis is sufficient to analyze the complete system, including its evolution through antigravity. This shows that the interacting problem that includes antigravity is an ordinary time dependent problem in quantum mechanics. There are no unitarity problems, and the presence of antigravity is analyzed below as a regular problem of a time dependent Hamiltonian, without encountering any fundamental problems of principles.

A technical remark may be useful: this model can be treated group theoretically by using the properties of $\mathrm{SL}(2, R)$ representations. Note that the three Hermitian quantum operators $\left(x^2, p^2, \frac{1}{2}(xp + px)\right)$ form the algebra of $\mathrm{SL}(2, R)$ under quantum commutation rules $[x, p] = i\hbar$. The Hamiltonian H_+ is proportional to the compact generator J_0 of

$\mathrm{SL}(2,R)$, while H_- is proportional to one of the non-compact generators J_1. The second non-compact generator J_2 appears in the commutator $[H_+, H_-]$. Explicitly,

$$J_0 \equiv \frac{1}{2\hbar\omega} H_+,\ J_1 \equiv \frac{1}{2\hbar\omega} H_-,\ J_2 = \frac{1}{4\hbar}(xp + px). \tag{8.39}$$

The (J_0, J_1, J_2) form the standard Lie algebra of $\mathrm{SL}(2,R)$. Since these $J_{0,1,,2}$ are Hermitian operators, the corresponding quantum states which are labelled as $|j,\mu\rangle$ form a unitary representation of $\mathrm{SL}(2,R)$. The quantum number μ is associated with the eigenvalues of J_0 (which is basically the eigenvalues of H_+) while $j(j+1)$ is associated with the eigenvalues of Casimir operator C_2 that commutes with all the generators, $C_2 \equiv J_0^2 - J_1^2 - J_2^2$. For the present construction, keeping track of the orders of operators (x,p) one finds that C_2 is a constant, $C_2 = -3/16 = j(j+1)$, which yields two solutions $j = -\frac{3}{4}$ or $j = -\frac{1}{4}$. Hence the spectrum of this theory, including the properties of $H_\pm$ can be thought of consisting of two infinite dimensional irreducible unitary representations of $\mathrm{SL}(2,R)$. For $j = -\frac{3}{4}$ or $j = -\frac{1}{4}$ these are positive discrete series representations. The allowed values of μ are given by $\mu = j + 1 + k$ where $k = 0, 1, 2, \cdots$ is an integer. We see that the two representations taken together correspond to the spectrum of H_+, which is the spectrum of the harmonic oscillator given by $E_n = \omega\left(n + \frac{1}{2}\right) \Leftrightarrow 2\omega\mu$, with even $n = 2k$ corresponding to $j = -3/4$ and odd $n = 2k+1$ corresponding to $j = -1/4$. Hence the basis $|j,\mu\rangle$ form a complete set of eigenstates for the observers in the gravity sector of the theory.

How about the antigravity sector? Since the corresponding Hamiltonian is H_-, a complete set of eigenstates corresponds to diagonalizing the non-compact generator J_1 instead of the compact generator J_0. Either way the Casimir operator is the same; hence diagonalizing $J_1 \to q$ provides another unitary basis $|j,q\rangle$ for the same unitary representations of $\mathrm{SL}(2,R)$. The spectrum of J_1, $J_1|j,q\rangle = q\ |j,q\rangle$, is continuous q on the real line since this is a non-compact generator of $\mathrm{SL}(2,R)$. This antigravity basis is also a complete unitary basis for this Hamiltonian that includes both sectors $H_\pm$. One basis can be expanded in terms of the other, $|j,q\rangle = \sum_{\mu=j+1}^{\infty} |j,\mu\rangle\langle j,\mu|j,q\rangle$, where the expansion coefficients $\langle j,\mu|j,q\rangle = U^{(j)}_{\mu,q}$ is a unitary transformation for each $j = -\frac{3}{4}$ or $-\frac{1}{4}$.

Therefore it doesn't matter which basis we use to analyze the quantum properties of this Hamiltonian. Using the discrete basis $|j,\mu\rangle$ which is more convenient to analyze the physics in the gravity sector, in no way excludes the antigravity sector from making its effects felt for observers in the gravity sector.

With this understanding of this simple quantum system, we now analyze the transition amplitudes A_{fi} for an initial state $|i\rangle$ to propagate to a final state both in the gravity sector. We define $|i\rangle, |f\rangle$ at the two edges of the antigravity sector, at times $t_i = -\Delta/2$ and $t_f = \Delta/2$. Moving t_i, t_f to other arbitrary times in the gravity sector is trivial since we can write $|i\rangle = e^{-iH_+(-\Delta/2 - t_i)}|i,t_i\rangle$ and $|f\rangle = e^{-iH_+\left(t_f - \Delta/2\right)}|f,t_f\rangle$ and we know how

H_+ acts on any linear combination of harmonic oscillator states $|i\rangle, |f\rangle$. Hence we have

$$A_{fi} = \langle f|e^{-\frac{i}{\hbar}\Delta H_-}|i\rangle \tag{8.40}$$

where $|i\rangle, |f\rangle$ are arbitrary states in the gravity sector. If we take any two states in the SL$(2,R)$ basis $|j,\mu\rangle$, this becomes

$$A_{fi} = \langle j,\mu_f|e^{-i\frac{\Delta}{2\omega}J_1}|j,\mu_i\rangle. \tag{8.41}$$

This is just the matrix representation of a group element of SL$(2,R)$ in a unitary representation labelled by $j = -\frac{3}{4}$ or $-\frac{1}{4}$. It must be the same j for both the initial and final states, i.e. there is a selection rule because there can be no transitions at all from $j = -\frac{3}{4}$ to $j = -\frac{1}{4}$ and vice-versa.

This quantity can be computed by using purely group theoretical means, but it is perhaps more instructive to use the standard harmonic oscillator creation/annihilation operators to evaluate it. Then we can write

$$H_+ = \hbar\omega\left(a^\dagger a + \frac{1}{2}\right), \quad H_- = \frac{\hbar\omega}{2}\left(a^{\dagger 2} + a^2\right). \tag{8.42}$$

We have used this form to compute the transition amplitude

$$A_{fi} = \langle f|e^{-\frac{i}{\hbar}\Delta H_-}|i\rangle = \langle f|e^{-i\frac{\omega\Delta}{2}\left(a^{\dagger 2}+a^2\right)}|i\rangle, \tag{8.43}$$

by taking initial/final states to be the number states or the coherent states of the harmonic oscillator. To perform the computation we use the following identity

$$e^{-i\frac{\omega\Delta}{2}\left(a^{\dagger 2}+a^2\right)} = e^{-\frac{i}{2}\tanh(\omega\Delta)a^{\dagger 2}}\left(\cosh(\omega\Delta)\right)^{-\left(a^\dagger a+\frac{1}{2}\right)}e^{-\frac{i}{2}\tanh(\omega\Delta)a^2}. \tag{8.44}$$

For initial/final coherent states, $|z_i\rangle$ & $|z_f\rangle$ for observers in gravity, we define the transition amplitude for normalized states as, $A(z_f,z_i) = \langle z_f|e^{-\frac{i}{\hbar}\Delta H_-}|z_i\rangle/\sqrt{\langle z_f|z_f\rangle\langle z_i|z_i\rangle}$, which yields

$$|A(z_f,z_i)|^2 = \frac{e^{-|z_f|^2-|z_i|^2+\frac{2\,\mathrm{Re}\left(z_i\bar{z}_f\right)}{\cosh(\omega\Delta)}}e^{\tanh(\omega\Delta)\,\mathrm{Im}\left(\bar{z}_f^2e^{-i\omega\Delta}+z_i^2e^{i\omega\Delta}\right)}}{\cosh(\omega\Delta)}. \tag{8.45}$$

This should be compared to the absence of antigravity when $\Delta = 0$, namely $|A(z_f,z_i)|^2 \overset{\Delta\to 0}{=} e^{-|z_f-z_i|^2}$.

Similarly, for initial/final number eigenstates $|n\rangle$ & $|m\rangle$ of the Hamiltonian $H_+ = \left(\frac{p^2}{2m}+\frac{m\omega^2x^2}{2}\right) = \hbar\omega\left(a^\dagger a+\frac{1}{2}\right)$ for observers in gravity, we obtain

$$A_{mn} = \sqrt{\frac{m!n!e^{i\omega\Delta(n+m+1)}}{\left(\cosh(\omega\Delta)\right)^{m+n+1}}}\sum_{k=0}^{\min(m,n)}\frac{\left(\frac{1}{2i}\sinh(\omega\Delta)\right)^{\frac{m+n}{2}-k}}{k!\left(\frac{m-k}{2}\right)!\left(\frac{n-k}{2}\right)!}, \tag{8.46}$$

where (m,n,k) are all even or all odd. This gives

$$|A_{mn}|^2 = \left(\begin{array}{c} \left({}_2F_1(-\left[\frac{m}{2}\right],-\left[\frac{n}{2}\right];\left(1-\frac{(-1)^m}{2}\right);\frac{-1}{\sinh^2(\omega\Delta)})\right)^2 \\ \times \frac{(m!)(n!)\left(\frac{1}{2}\tanh(\omega\Delta)\right)^{2(\left[\frac{m}{2}\right]+\left[\frac{n}{2}\right])}}{\left(\left[\frac{m}{2}\right]!\left[\frac{n}{2}\right]!\right)^2 \left(\cosh(\omega\Delta)\right)^{2-(-1)^m}} \end{array} \right)$$

where ${}_2F_1\left(a,b;c;z\right)$ is the hypergeometric function, $\left[\frac{m}{2}\right]$ means the integer part of $m/2$, and (m,n) are both even or both odd. Special cases are

$$\begin{array}{l} |A_{00}|^2 = \frac{1}{\cosh(\omega\Delta)}, \quad |A_{2M,0}|^2 = \frac{(2M)!}{2^{2M}(M!)^2}\frac{\left(\tanh(\omega\Delta)\right)^{2M}}{\cosh(\omega\Delta)}, \\ |A_{11}|^2 = \frac{1}{\cosh^3(\omega\Delta)}, \; A_{2M+1,1} = \frac{(2M+1)!}{2^{2M}(M!)^2}\frac{\left(\tanh(\omega\Delta)\right)^{2M}}{\cosh^3(\omega\Delta)}. \end{array} \tag{8.47}$$

As compared to the absence of antigravity, $\Delta = 0$, when there are no transitions, we see that antigravity causes an observable effect. Clearly, these transition amplitudes are well behaved, and do not blow up for large Δ. Unitarity is obeyed: one may verify explicitly that the sum over all states is 100% probability, $\sum_m |A_{mn}|^2 = 1$, for all fixed n, and similarly $\int \frac{d^2z_f}{\pi} \; |A\left(z_f,z_i\right)|^2 = 1$ for all fixed z_i.

8.4.5 Massive scalar field with sign flipping kinetic energy

This system has some similarities to the interacting particle above but it is not quite the same. The action is

$$S = \frac{1}{2}\int d^dx \; \left[-\varepsilon\left(\left|x^0\right| - \frac{\Delta}{2}\right) \; \partial^\mu\phi\left(x\right)\partial_\mu\phi\left(x\right) - m^2\phi^2\left(x\right)\right] \tag{8.48}$$

As in the case of the massless field in section (8.4.3), the factor $\varepsilon\left(\left|x^0\right| - \frac{\Delta}{2}\right)$ can be viewed as a gravitational background field of the form, $\sqrt{-g}g^{\mu\nu}\partial_\mu\phi\partial_\nu\phi$, with $g^{\mu\nu}\left(x\right) = \varepsilon\left(\left|x^0\right| - \frac{\Delta}{2}\right)\eta^{\mu\nu}$ and $\sqrt{-g} = 1$, that spans the union of the gravity and antigravity regions, as explained in (8.6). The mass term does not flip sign. Note that, due to the non-zero mass, this is *not* a Weyl invariant action, but we shall investigate it anyway to learn about the properties of such a system.

In momentum space, using the notation $x^0 = t$, we have

$$\phi\left(\vec{x},t\right) = \int \frac{d^{d-1}p}{\left(2\pi\right)^{(d-1)/2}}\phi_p\left(t\right)e^{i\vec{p}\cdot\vec{x}} \tag{8.49}$$

We rewrite the action in momentum space as

$$S = \frac{1}{2}\int dt \int d^{d-1}p \; \left[\begin{array}{c} \varepsilon\left(|t| - \frac{\Delta}{2}\right)\left[\begin{array}{c} \dot{\phi}_p\left(t\right)\dot{\phi}_{-p}\left(t\right) \\ -\vec{p}^2\phi_p\left(t\right)\phi_{-p}\left(t\right) \end{array} \right] \\ -m^2\phi_p\left(t\right)\phi_{-p}\left(t\right) \end{array} \right] \tag{8.50}$$

The equation of motion is

$$\partial_t \left(\varepsilon \left(|t| - \frac{\Delta}{2} \right) \partial_t \phi_p \left(t \right) \right) + \left[\varepsilon \left(|t| - \frac{\Delta}{2} \right) \vec{p}^2 + m^2 \right] \phi_p \left(t \right) = 0 \tag{8.51}$$

The solutions in separate regions of time are (similar to (8.27))

$$\begin{array}{c} t < -\frac{\Delta}{2} : \ \phi_p^A \left(t \right) = \left(\begin{array}{c} A_p^+ e^{-i\sqrt{\vec{p}^2+m^2}\left(t+\frac{\Delta}{2}\right)} \\ +A_p^- \ e^{i\sqrt{\vec{p}^2+m^2}\left(t+\frac{\Delta}{2}\right)} \end{array} \right) \\ -\frac{\Delta}{2} < t < \frac{\Delta}{2} : \phi_p^B \left(t \right) = \left(\begin{array}{c} B_p^+ \ e^{-i\sqrt{\vec{p}^2-m^2}\left(t+\frac{\Delta}{2}\right)} \\ +B_p^- e^{i\sqrt{\vec{p}^2-m^2}\left(t+\frac{\Delta}{2}\right)} \end{array} \right) \\ t > \frac{\Delta}{2} : \ \phi_p^C \left(t \right) = \left(\begin{array}{c} C_p^+ \ e^{-i\sqrt{\vec{p}^2+m^2}\left(t-\frac{\Delta}{2}\right)} \\ +C_p^- e^{i\sqrt{\vec{p}^2+m^2}\left(t-\frac{\Delta}{2}\right)} \end{array} \right) \end{array} \tag{8.52}$$

We need to match the field $\phi_p \left(t \right)$ and its canonical momentum, $\varepsilon \left(|t| - \frac{\Delta}{2} \right) \partial_t \phi_p \left(t \right)$, at each boundary $t = \pm\Delta/2$

$$\begin{array}{l} \phi_p^A \left(-\frac{\Delta}{2} \right) = \phi_p^B \left(-\frac{\Delta}{2} \right), \text{ and } \dot{\phi}_p^A \left(-\frac{\Delta}{2} \right) = -\dot{\phi}_p^B \left(-\frac{\Delta}{2} \right), \\ \phi_p^C \left(+\frac{\Delta}{2} \right) = \phi_p^B \left(+\frac{\Delta}{2} \right), \text{ and } \dot{\phi}_p^C \left(+\frac{\Delta}{2} \right) = -\dot{\phi}_p^B \left(+\frac{\Delta}{2} \right), \end{array} \tag{8.53}$$

Note the sign flip of $\dot{\phi}$ at $t = \pm\Delta/2$ although the canonical momentum does not flip. This gives four equations to relate $C_p^\pm$ and $B_p^\pm$ to $A_p^\pm$ as follows

$$\begin{array}{l} A_p^+ + A_p^- = B_p^+ + B_p^- \\ A_p^+ - A_p^- = -\left(B_p^+ \ - B_p^- \right) \frac{\sqrt{\vec{p}^2-m^2}}{\sqrt{\vec{p}^2+m^2}} \\ C_p^+ + C_p^- = B_p^+ e^{-i\sqrt{\vec{p}^2-m^2}\Delta} + B_p^- e^{i\sqrt{\vec{p}^2-m^2}\Delta} \\ C_p^+ - C_p^- = -\left(\begin{array}{c} B_p^+ e^{-i\sqrt{\vec{p}^2-m^2}\Delta} \\ -B_p^- e^{i\sqrt{\vec{p}^2-m^2}\Delta} \end{array} \right) \frac{\sqrt{\vec{p}^2-m^2}}{\sqrt{\vec{p}^2+m^2}} \end{array} \tag{8.54}$$

The solution determines $B_p^\pm$ and $C_p^\pm$ in terms of $A_p^\pm$,

$$\left(\begin{array}{c} C_p^+ \\ C_p^- \end{array} \right) = \left(\begin{array}{cc} \alpha & \beta^* \\ \beta & \alpha^* \end{array} \right) \left(\begin{array}{c} A_p^+ \\ A_p^- \end{array} \right) \tag{8.55}$$

$$\left(\begin{array}{c} B_p^+ \\ B_p^- \end{array} \right) = \left(\begin{array}{cc} \frac{1}{2} - \frac{\sqrt{\vec{p}^2+m^2}}{2\sqrt{\vec{p}^2-m^2}} & \frac{1}{2} + \frac{\sqrt{\vec{p}^2+m^2}}{2\sqrt{\vec{p}^2-m^2}} \\ \frac{1}{2} + \frac{\sqrt{\vec{p}^2+m^2}}{2\sqrt{\vec{p}^2-m^2}} & \frac{1}{2} - \frac{\sqrt{\vec{p}^2+m^2}}{2\sqrt{\vec{p}^2-m^2}} \end{array} \right) \left(\begin{array}{c} A_p^+ \\ A_p^- \end{array} \right) \tag{8.56}$$

where (α, β) are the parameters of a Bogoliubov transformation (an SU$(1,1)$ group transformation)

$$\begin{array}{l} \alpha = \cos\left(\Delta\sqrt{\vec{p}^2 - m^2}\right) + i\frac{\vec{p}^2 \sin\left(\Delta\sqrt{\vec{p}^2 - m^2}\right)}{\sqrt{\left(\vec{p}^2\right)^2 - m^4}}, \\ \beta = i\frac{m^2 \sin\left(\Delta\sqrt{\vec{p}^2 - m^2}\right)}{\sqrt{\left(p^2\right)^2 - m^4}}, \\ |\alpha|^2 - |\beta|^2 = 1. \end{array} \tag{8.57}$$

Assume the incoming state $\phi_p^A(t)$ has only positive frequency, meaning $A_p^- = 0$. Then we see that (unlike the massless case in section (8.4.3)) negative frequency fluctuations are produced in the final state $\phi_p^C(t)$ since according to (8.55), $C_p^- = \beta A_p^+$. The corresponding probability amplitude for particle production is

$$\left(C_p^- / A_p^+\right) = \beta = i\frac{\sin\left(m\Delta\sqrt{\vec{p}^2/m^2 - 1}\right)}{\sqrt{\left(\vec{p}^2/m^2\right)^2 - 1}}. \tag{8.58}$$

The produced particle number density (particles per unit volume) is the integral of $|\beta|^2$ over all momenta

$$\begin{array}{l} n(m,\Delta) = \int d^{d-1}p\,|\beta|^2 = \int d^{d-1}p \frac{\sin^2\left(m\Delta\sqrt{(\vec{p}^2/m^2)-1}\right)}{\left|(\vec{p}^2/m^2)^2 - 1\right|}, \\ = m^{d-1}\Omega_{d-1}\int_0^\infty \frac{x^{d-2}\sin^2\left((m\Delta)\sqrt{x^2-1}\right)}{|x^4-1|}dx, \end{array} \tag{8.59}$$

where $x^2 = \vec{p}^2/m^2$, while Ω_{d-1} is the volume of the solid angle in $d-1$ dimensions, $\Omega_2 = 2\pi$, $\Omega_3 = 4\pi$, etc.. This is a convergent integral for $d < (5-\varepsilon)$ dimensions, hence $n(m,\Delta)$ is finite for $d = 1,2,3,4$ dimensions. We note that the number density $n(m,\Delta)$ increases monotonically at fixed m as Δ increases. The energy density per unit volume for the produced particles for all momenta is

$$\begin{array}{l} \rho(m,\Delta) = \int \frac{d^{d-1}p}{(2\pi)^{d-1}}\sqrt{\vec{p}^2 + m^2}\,|\beta|^2 \\ = \frac{m^d\Omega_{d-1}}{(2\pi)^{d-1}}\int_0^\infty \frac{x^{d-2}\sqrt{x^2+1}\sin^2\left((m\Delta)\sqrt{x^2-1}\right)}{|x^4-1|}dx \end{array} \tag{8.60}$$

$\rho(m,\Delta)$ is convergent for $d < (4-\varepsilon)$ dimensions, and is logarithmically divergent at $d = 4$ despite the rapid oscillations at the ultraviolet limit.

Recall that the massive field is not a scale invariant model. In the Weyl symmetric limit, $m \to 0$, there is no particle production at all in any dimension. In the scale invariant theory masses for fields must come from interactions, such as interactions with the Higgs field. In a cosmological context the Higgs field is not just a constant, and therefore in the type of investigation above, the parameter m should be replaced by the cosmological behaviour of the Higgs field (see [73] for an example). This very different behaviour in a Weyl invariant theory should be the more serious approach for investigating effectively

massive fields to answer the type of questions discussed in this section.

8.5 Conformally exact sign-flipping backgrounds in string theory

We consider the worldsheet formulation of the relativistic string, but we make string theory consistent with target space Weyl symmetry as suggested in [84]. This requires promoting the string tension to a dynamical field, $(2\pi\alpha')^{-1} \to T\left(X^{\mu}\left(\tau,\sigma\right)\right)$. The background field $T\left(X\right)$, along with any other additional background fields, must be restricted to satisfy exact worldsheet conformal symmetry at the quantum level. In the worldsheet formalism, typically the tension appears together with the metric $g_{\mu\nu}\left(X\left(\tau,\sigma\right)\right)$ or antisymmetric tensor $b_{\mu\nu}\left(X\left(\tau,\sigma\right)\right)$ in the Weyl invariant combination, $Tg_{\mu\nu}$ or $Tb_{\mu\nu}$. The requirement of exact *worldsheet* conformal symmetry constrains these target-space Weyl invariant combinations. Perturbative worldsheet conformal symmetry (vanishing beta functions) is captured by the properties of the low energy effective string action. From the study of the Weyl invariant and geodesically complete formalism of the low energy string action [84] we have learned that the tension (closely connected to the gravitational constant) switches sign generically near the singularities in the classical solutions of this theory.

If we fix the target space Weyl symmetry by choosing the string gauge as in (8.4), then in those generic solutions, the tension becomes $T\left(X^{\mu}\left(\tau,\sigma\right)\right) = \pm\left(2\pi\alpha'\right)^{-1}$ on the two sides of the singularity as it appears *in the string gauge*. Those two sides are identified as the gravity/antigravity sectors of the low energy theory as discussed in section (8.2). From the perspective of the worldsheet string theory these observations lead to a simple prescription to capture all these effects in the string gauge, namely replace the Weyl invariant structures $(Tg_{\mu\nu}, Tb_{\mu\nu})$ by $\left(\pm\left(2\pi\alpha'\right)^{-1} G^{\pm}_{\mu\nu}, \pm\left(2\pi\alpha'\right)^{-1} B^{\pm}_{\mu\nu}\right)$, where the capital $\left(G^{\pm}_{\mu\nu}\left(X\right), B^{\pm}_{\mu\nu}\left(X\right)\right)$ are the background fields on the gravity/antigravity patches that are joined at the singularities *as they appear in the string gauge*. We may absorb the overall $\pm$ due to the signs of the tension into a redefinition of the background fields, and as we did for the Einstein gauge in (8.6), define

$$\left(\hat{G}_{\mu\nu}\left(X\right), \hat{B}_{\mu\nu}\left(X\right)\right) = \left(\pm G^{\pm}_{\mu\nu}\left(X\right), \pm B^{\pm}_{\mu\nu}\left(X\right)\right), \tag{8.61}$$

as the full set of background fields in the union of the gravity/antigravity sectors of the worldsheet string theory. Of course, $\left(\hat{G}_{\mu\nu}\left(X\right), \hat{B}_{\mu\nu}\left(X\right)\right)$ are required to satisfy worldsheet conformal invariance at the quantum level as usual. What is new is the geodesic completeness of the background fields $\left(\hat{G}_{\mu\nu}\left(X\right), \hat{B}_{\mu\nu}\left(X\right)\right)$ which is achieved by the sign flipping tension and the union of the corresponding gravity/antigravity sectors.

8.5.1 String in flat background with tension that flips sign

A simple example of a conformally exact worldsheet CFT, that includes a dynamical string tension that flips signs, is the flat string background $\eta_{\mu\nu}$ modified only by a time dependent string tension $T(X) = \frac{1}{2\pi\alpha'}\text{Sign}\left(\left|X^0(\tau,\sigma)\right| - \frac{\Delta}{2}\right)$. This can also be presented in the string gauge by absorbing the sign of the tension into a redefined metric

$$\hat{G}_{\mu\nu}(X) = \eta_{\mu\nu}\text{Sign}\left(\left|X^0(\tau,\sigma)\right| - \frac{\Delta}{2}\right), \quad \hat{B}_{\mu\nu}(X) = 0, \tag{8.62}$$

where Δ is a constant. Note the similarity to (8.26) or sections (8.4.3,8.4.5). Thus the tension is positive when $\left|X^0(\tau,\sigma)\right| > \frac{\Delta}{2}$ and negative when $-\frac{\Delta}{2} < X^0(\tau,\sigma) < \frac{\Delta}{2}$. This is also similar to the cosmological example with an antigravity loop given in [84], but we have greatly simplified it here by keeping only the signs but not the magnitude of the tension, thus defining a conformally exact rather than a conformally approximate CFT on the worldsheet. The corresponding worldsheet string model is

$$S = -\frac{1}{4\pi\alpha'}\int d^2\sigma\sqrt{-h}h^{ab}\partial_a X^\mu \partial_b X^\nu \eta_{\mu\nu}\text{Sign}\left(\left|X^0(\tau,\sigma)\right| - \frac{\Delta}{2}\right). \tag{8.63}$$

We should mention that it is also possible to consider a model, at least at the classical level, by inserting in the action (8.63) the inverse of the Sign function $\left(\text{Sign}\left(\left|X^0(\tau,\sigma)\right| - \frac{\Delta}{2}\right)\right)^{-1}$. In this case the tension flips sign when it is infinite rather than zero. Both of these possibilities occur smoothly rather than suddenly in cosmological backgrounds in string theory (see (30) in [84] or its generalizations). Both behaviours are significant from the perspective of string theory because perturbative versus non-perturbative methods would be needed to understand fully the physics in the vicinity of the gravity/antigravity transitions. Namely, when the tension at the transition is large the string would be close to being pointlike, so the stringy corrections would be small and perturbative in the vicinity of the gravity/antigravity transitions; by contrast when the tension at the transition is small the string would be floppy so stringy corrections could be significant. In the latter case, high spin fields [90] may be an interesting tool to investigate the gravity/antigravity transition in our setting.

From the form of the action in (8.63) it is evident that the string action is invariant under reparametrizations of the worldsheet at the classical level. We will use this symmetry to choose a gauge to perform the classical analysis below. But eventually we also need to know if this symmetry is valid also at the quantum level. The generator of this gauge symmetry is the stress tensor, so the stress tensor vanishes as a constraint to impose the gauge invariance. At the classical level the stress tensor does vanish as part of the solution of the classical equations and constraints (see below). At the quantum level, in "'covariant quantization", the stress tensor does not vanish on all states but only on the gauge invariant physical states. For consistency of covariant quantization

one must verify that the constraints form a set of first class constraints that close under quantum operator products. In our case the stress tensor derived from (8.63) has the form $T_{\pm\pm} = (\text{Sign}) \times T^0_{\pm\pm}$, where $T^0_{\pm\pm}$ is the usual worldsheet stress tensor in the flat background $\eta_{\mu\nu}$, while the sign factor switches signs at the kinks $\left|X^0(\tau,\sigma)\right| = \frac{\Delta}{2}$. In the positive (gravity, Sign=+) region, we have symbolically the operator products, $T^0_{\pm\pm} \times T^0_{\pm\pm} \sim T^0_{\pm\pm}$, where the standard CFT result on the right hand side is computed exactly for the flat string. Similarly, in the negative (antigravity, Sign=−) region we have, $\left(-T^0_{\pm\pm}\right) \times \left(-T^0_{\pm\pm}\right) \sim -\left(-T^0_{\pm\pm}\right)$. So the algebra is closed like the standard CFT locally in the positive and negative regions away from the kinks. There remains analyzing the operator products at the kinks $\left|X^0(\tau,\sigma)\right| = \frac{\Delta}{2}$ (worldsheet analogs of the kinks in Fig. 8.1).

The operator products involving the Sign factor non-trivially introduce delta functions and derivatives of delta functions multiplied by the sign factor or its derivatives that have support only at the kinks. At one contraction (order $\hbar$ effects) the coefficient of the delta function includes the flat $T^0_{\pm\pm}$ or its derivatives evaluated at the kinks. Since $T^0_{\pm\pm}$ or its derivatives are in the list of first class constraints (Virasoro operators), this is still a closed algebra of first class constraints all of which vanish on physical states. At two contractions (order $\hbar^2$ in quantum effects) there are again some terms that contain $T^0_{\pm\pm}$ or its derivatives, which again are of no concern since these still vanish on physical states. However, there are also additional operators of the form of $\left(\partial X^0\right)$ multiplying products of the sign function, delta function, or its derivatives, all evaluated at the kinks. We have analyzed these complicated distributions and found that they vanish when integrated with $\left(\partial X^0\right)$, so they do not seem to contribute. Similarly we can drop several similar terms due to the properties of the distributions. The analysis at the kinks becomes harder at higher contractions ($\hbar^3$ and beyond in quantum effects), and we leave this for future analysis to be reported at a later stage.

The main point is that if there are additional constraints that must be imposed at the kinks they will show up in this type of operator product analysis. So far, we have not found new constraints up to two contractions in the operator products. Thus, the algebra of the operator products is basically the standard algebra of a conformal field theory (CFT) locally in the positive and negative regions away from the kinks. The modification of the CFT algebra at the kinks with terms that are proportional to Virasoro operators does not change the validity of the gauge symmetry at the quantum level, since those terms vanish on physical states anyway. Although we have not yet found other operator modifications of the algebra at the kinks, conceptually it is possible that such terms may arise at higher contractions or in other models that include gravity/antigravity transitions. When and if such terms appear, they must be included in an enlarged list of constraints that should form a closed algebra under operator products, then this will define the proper quantum theory.

In this chapter our aim is to first understand the classical theory of a string described by the action in (8.63), so we do not need to be concerned here about the subtleties described in the previous paragraph. In fact, the classical analysis that we give below is helpful in further developing the right approach for the quantum theory. Thus, setting aside temporarily the possible stringy corrections, we are at first interested in the classical behaviour of strings as they propagate in the union of the gravity/antigravity regions, and later try to figure out the possible additional effects due to interactions at those transitions by using more sophisticated methods, such as string field theory, or others, as outlined in section 8.6.

8.5.2 General string propagating classically through antigravity

In this section we shall discuss the properties of the model in (8.63). The main objective is to show that there are no problems due to the negative tension during antigravity from the point of view of fundamental principles, such as unitarity or possible instability due to negative kinetic energy. The unitarity of this string model was already established in [84] more generally for any time dependent tension $T\left(X^0\right)$, and more general metric, so we shall not repeat it here. We will concentrate on the effect of the antigravity period on the propagation of the string and the corresponding signals that observers in gravity may detect. As we shall demonstrate, as compared to the complete absence of antigravity, the presence of an antigravity period for a certain amount of time causes only a time delay in the propagation of an open or closed free string of any configuration. This may seem surprising since, at first thought, one may think that string bits would fly apart under an instability caused by a negative string tension. In fact, this does not happen because a negative tension is simply an overall sign in the action of a free string, and this does not change the equations of motion and constraints of a free string during antigravity.

We work in the conformal gauge at the classical level. There is a remaining reparametrization symmetry that permits the further choice of the following time-like gauge

$$X^0(\tau,\sigma) = |H|\,\tau, \tag{8.64}$$

where H is the total time dependent Hamiltonian of the string while $|H|$ is time independent. This is similar to the massless free field in section (8.4.3). In this gauge the remaining degrees of freedom satisfy the following equations of motion and constraints

$$\begin{aligned} &\left(\partial_\tau^2 - \partial_\sigma^2\right)\vec{X}(\tau,\sigma) = 0, \\ &H^2 = \left(\partial_\tau \vec{X} \pm \partial_\sigma \vec{X}\right)^2, \end{aligned} \tag{8.65}$$

to be solved in each time region A, B, C defined by

$$A:\ \tau\,|H| < -\Delta/2,\ B: -\Delta/2 < \tau\,|H| < \Delta/2,\ \ C: \tau\,|H| > \Delta/2. \tag{8.66}$$

Furthermore, the solutions for $\vec{X}_{A,B,C}(\tau,\sigma)$ and the canonical momenta $\vec{P}_{A,B,C}(\tau,\sigma) = \partial_\tau \vec{X}_{A,B,C}(\tau,\sigma) \times \text{Sign}\left(|H\tau| - \frac{\Delta}{2}\right)$ should be continuous at the boundaries $\tau|H| = \pm\Delta/2$. The method of solution follows the simple model in (8.27) or the massive field in (8.4.5).

We will discuss the case of an open string; the closed string is treated similarly. The general solution in each region is given in terms of the center of mass $(\vec{q},\vec{p})$ and oscillator $(\vec{\alpha}_n, n = \pm1, \pm2, \cdots)$ degrees of freedom. The general configuration of the string in the positive tension region A, at a time $\tau < -\Delta/2$, is a general solution $\vec{X}_A(\tau,\sigma)$ given by

$$\vec{X}_A(\tau,\sigma) = \vec{q}_0 + \vec{p}\tau + \sum_{n=-\infty,\neq 0}^{\infty} \frac{i}{n}\vec{\alpha}_n \cos n\sigma \; e^{-in\tau}. \tag{8.67}$$

The time independent parameters $(\vec{q}_0,\vec{p})$ and $(\vec{\alpha}_n, n = \pm1, \pm2, \cdots)$ determine the initial configuration of the string at the time $\tau = \tau_0$. From the constraint equations we compute the time independent $|H|$ and the remaining constraint

$$\begin{array}{c} |H| = \sqrt{\vec{p}^2 + \sum_{n=1}^{\infty} \vec{\alpha}_{-n}\cdot\vec{\alpha}_n} \\ 0 = \vec{p}\cdot\vec{\alpha}_n + \frac{1}{2}\sum_{m=-\infty,\neq 0}^{\infty} \vec{\alpha}_{-m}\cdot\vec{\alpha}_{n+m} \end{array} \tag{8.68}$$

Thus the time dependent Hamiltonian that switches sign is

$$H(\tau) = \text{Sign}\left(|H|\,|\tau| - \frac{\Delta}{2}\right)\sqrt{\vec{p}^2 + \sum_{n=1}^{\infty}\vec{\alpha}_{-n}\cdot\vec{\alpha}_n}. \tag{8.69}$$

Assuming the constraints (8.68) are satisfied at the classical level by some set of parameters $(\vec{\alpha}_n,\vec{p})$, the momentum, $\overrightarrow{P}_A = \overrightarrow{\dot{X}}_A$, in region A is

$$\overrightarrow{P}_A(\tau,\sigma) = \vec{p} + \sum_{n=-\infty,\neq 0}^{\infty} \vec{\alpha}_n \cos n\sigma \; e^{-in\tau}. \tag{8.70}$$

In region B, $-\frac{\Delta}{2} < \tau|H| < \frac{\Delta}{2}$, the solution $\left(\vec{X}_B,\vec{P}_B\right)$ takes the same form as above, but with a new set of parameters $(\vec{q}_B,\vec{p}_B,\vec{\alpha}_{nB})$. Note that in this region there is a non-trivial minus sign in the relation between momentum and velocity, $\vec{P}_B(\tau,\sigma) = -\partial_\tau \vec{X}_B(\tau,\sigma)$. At the transition time, $\tau_* \equiv -\frac{\Delta}{2|H|}$, we must match the position and momentum, therefore $\vec{X}_A(\tau_*,\sigma) = \vec{X}_B(\tau_*,\sigma)$ and $\partial_\tau\vec{X}_A(\tau_*,\sigma) = -\partial_\tau\vec{X}_B(\tau_*,\sigma)$, noting the negative sign in the case of velocities. Because the matching is for every value of σ we find that all the parameters $(\vec{q}_B,\vec{p}_B,\vec{\alpha}_{nB})$ are uniquely determined in terms of the initial parameters $(\vec{q}_0,\vec{p},\vec{\alpha}_n)$ in region A. So the solution in region B is

$$\vec{X}_B(\tau,\sigma) = \begin{pmatrix} \vec{q}_0 + \vec{p}\left(-\tau - \frac{\Delta}{|H|}\right) \\ +\sum_{n=-\infty,\neq 0}^{\infty} \frac{i}{n}\vec{\alpha}_n \cos n\sigma \; e^{-in\left(-\tau-\frac{\Delta}{|H|}\right)} \end{pmatrix} \tag{8.71}$$

$$\vec{P}_B(\tau,\sigma) = -\overrightarrow{X}_B(\tau,\sigma) = \vec{p} + \sum_{n=-\infty,\neq 0}^{\infty} \vec{\alpha}_n \cos n\sigma \; e^{-in\left(-\tau-\frac{\Delta}{|H|}\right)} \tag{8.72}$$

There are no new constraints beyond those that are already assumed to have been satisfied in region A by the parameters $(\vec{\alpha}_n, \vec{p})$. Note the structure $(-\tau - \frac{\Delta}{|H|})$ that indicates a backward propagation similar to Fig.1 as τ increases beyond τ_*.

At the next transition time, $\tau_{**} \equiv +\frac{\Delta}{2|H|}$, we must connect the solution $\left(\vec{X}_B, \vec{P}_B\right)$ above to the solution $\left(\vec{X}_C, \vec{P}_C\right)$ in region C, $\tau > \tau_{**}$, which is given in terms of a new set of parameters $(\vec{q}_C, \vec{p}_C, \vec{\alpha}_{nC})$. Using the matching conditions $\vec{X}_C(\tau_*,\sigma) = \vec{X}_B(\tau_*,\sigma)$ and $\overrightarrow{X}_C(\tau_*,\sigma) = -\overrightarrow{X}_B(\tau_*,\sigma)$ that include the extra minus sign for velocities (as discussed above), we find that $(\vec{q}_C, \vec{p}_C, \vec{\alpha}_{nC})$ are all determined again uniquely in terms of the initial parameters $(\vec{q}_0, \vec{p}, \vec{\alpha}_n)$ introduced in region A.

$$\begin{array}{c} \vec{X}_C(\tau,\sigma) = \left(\begin{array}{c} \vec{q}_0 + \vec{p}\left(\tau - 2\frac{\Delta}{|H|}\right) \\ + \sum_{n=-\infty,\neq 0}^{\infty} \frac{i}{n}\vec{\alpha}_n \cos n\sigma \; e^{-in\left(\tau-2\frac{\Delta}{|H|}\right)} \end{array} \right) \\ \vec{P}_C(\tau,\sigma) = \vec{p} + \sum_{n=-\infty,\neq 0}^{\infty} \vec{\alpha}_n \cos n\sigma \; e^{-in\left(\tau-2\frac{\Delta}{|H|}\right)} \end{array} \tag{8.73}$$

For closed strings we find a similar result but with some additional information for region B. Namely, given some solution in region A that satisfies the string equations of motion and constraints, then the solution in regions B, C are obtained by the following substitutions of τ and σ

$$\begin{array}{l} \vec{X}_B(\tau,\sigma) = \vec{X}_A\left(-\tau - \frac{\Delta}{|H|},\; -\sigma\right) \\ \vec{X}_C(\tau,\sigma) = \vec{X}_A\left(\tau - 2\frac{\Delta}{|H|},\; \sigma\right) \end{array} \tag{8.74}$$

Note the extra minus sign in $\sigma \to -\sigma$ in region B. Namely, for the closed string the left and right movers get scrambled during antigravity. For the open string with Neumann boundary conditions discussed above, the sign flip $\sigma \to -\sigma$ in region B has no effect since $\cos(-n\sigma) = +\cos(n\sigma)$, but if the open string had Dirichlet boundary conditions then $\sin(-n\sigma) = -\sin(n\sigma)$ would induce an overall sign flip of the oscillations during the antigravity period.

Putting it all together, we see that after the antigravity period, the emergent string experiences only a time delay $2\Delta/|H|$ as compared to the string that propagates in the complete absence of antigravity. This is the same conclusion that was reached for the free particle or the free massless field.

Rotating rod propagating through antigravity

As a concrete example of a string configuration that satisfies all the constraints, we present the rotating rod solution that is modified by a tension that flips sign during antigravity

as in (8.63). We begin with a straight string lying along the $\hat{x}$ axis with its center of mass located at $\vec{q}_0$, as given by, $\vec{X}_0(\sigma) = \vec{q}_0 + \hat{x}\ R_0 \cos\sigma$. Let this string rotate in the $(\hat{x}, \hat{y})$ plane and translate in the $\hat{z}$ direction as follows

$$\vec{X}_A(\tau, \sigma) = \vec{q}_0 + \hat{z}p\tau + R_0 \cos\sigma\ \ (\hat{x}\cos\tau + \hat{y}\sin\tau)\,. \tag{8.75}$$

This satisfies the constraints in (8.68), since $\partial_\tau \vec{X} \cdot \partial_\sigma \vec{X} = 0$, and gives $|H| = \left(p^2 + R_0^2\right)^{1/2}$. Following the steps above we compute the matching string configuration during the antigravity period $-\frac{\Delta}{2|H|} < \tau < \frac{\Delta}{2|H|}$

$$\vec{X}_B(\tau, \sigma) = \begin{pmatrix} \vec{q}_0 + \hat{z}p\,(-\tau - \theta) \\ +R_0 \cos\sigma \begin{pmatrix} \hat{x}\ \cos(-\tau - \theta) \\ +\hat{y}\ \sin(-\tau - \theta) \end{pmatrix} \end{pmatrix} \tag{8.76}$$

where $\theta = \Delta\left(p^2 + R_0^2\right)^{-1/2}$, noting that this describes a backward propagation similar to Fig.1. Finally the matching string configuration in the time period $\tau > \frac{\Delta}{2|H|}$ is

$$\vec{X}_C(\tau, \sigma) = \begin{pmatrix} \vec{q}_0 + \hat{z}p\,(\tau - 2\theta) \\ +R_0 \cos\sigma\ \ (\hat{x}\cos(\tau - 2\theta) + \hat{y}\sin(\tau - 2\theta)) \end{pmatrix}. \tag{8.77}$$

As promised, as compared to the complete absence of antigravity, the presence of an antigravity period for a certain amount of time causes only a time delay in the propagation of a string of any configuration. The string bits of a freely propagating string do not fly apart during antigravity when the string tension is negative!

8.5.3 2D black hole including antigravity

Another simple example is the 2-dimensional black hole [78] based on the $\mathrm{SL}(2,R)/\mathrm{R}$ gauged WZW model [79]. The well known string background metric in this case is, $ds^2 = -2(1-uv)^{-1}\,dudv$, with $uv < 1$, where (u, v) are the string coordinates $X^\mu(\tau, \sigma)$ in the Kruskal-Szekeres basis. This space is geodesically incomplete similar to the case of the four dimensional Schwarzschild blackhole [4].

The geodesically complete modification consists of allowing the string tension to flip sign precisely at the singularity, namely $T(X) = (2\pi\alpha')^{-1}\mathrm{Sign}(1-uv)$. Then the new geodesically complete 2D-blackhole action is

$$S = \frac{1}{2\pi\alpha'} \int d^2\sigma \sqrt{-h} h^{ab} \frac{\partial_a u \partial_b v}{|1-uv|}. \tag{8.78}$$

This differs from the old 2D black hole action by the absolute value sign, and includes the antigravity region $uv > 1$ just as in the 4-dimensional case [4]. Despite the extra sign, this model is an exact CFT on the worldsheet as can be argued in the same way following

(8.63). Properties of the new 2D black hole, including the related dilaton and all orders quantum corrections in powers of α', was investigated in detail in a separate paper [91] by Bars and Araya.

8.6 String field theory with antigravity

In the neighborhood of the gravity/antigravity transition, which occurs typically at a gravitational singularity, a proper understanding of the physics would be incomplete without the input of quantum gravity that may possibly contribute large quantum effects. How should we estimate the effects of quantum gravity?

We first point out that attempting to use an effective low energy field theory that includes higher powers of curvature, such as those computed from string theory, may not be the most fruitful approach. Higher powers of curvature capture approximations to quantum gravity that are valid at momenta much smaller than the Planck scale; those cannot be used to investigate the phenomena of interest that are at the Planck scale close to the singularity. For investigating the gravity/antigravity transition more closely, we do not see an alternative to using directly an appropriate theory of quantum gravity that can incorporate the geodesically complete spacetime that includes both gravity and antigravity regions. Hence we first need to define the proper theory of quantum gravity that is consistent with geodesic completeness. As far as we know, this notion of quantum gravity was first considered in [84].

Assuming that quantum string theory is a suitable approach to quantum gravity, we outline here how string field theory may be modified to take into account geodesic completeness and the presence of an antigravity sector, so that it can be used as a proper tool to answer the relevant questions.

Open and closed string field theory (SFT) is a formalism for computing string-string interactions, including those that involve stringy gravitons. As in standard field theory, in principle the SFT formalism is suitable for both perturbative and non-perturbative computations. Technically SFT is hard to compute with, but it has the advantage of being a self consistent and conceptually complete definition of quantum gravity and the interactions with matter. It is therefore crucial to see how antigravity fits in SFT and therefore how the pertinent questions involving antigravity can be addressed in a self consistent manner.

In the context of SFT, gravitational and other backgrounds in which strings propagate are incorporated through the BRST operator Q_B that appears in the quadratic part of the action [78]

$$S_{open} = Tr\left[\frac{1}{2}A * Q_B A + \frac{g_o}{3}A * A * A\right]. \tag{8.79}$$

The complete SFT action must also include closed strings, S_{closed} and the supersymmetric versions of these. Here $A(X)$ is the string field, the product $*$ describes string joining or splitting, and the BRST operator Q_B is given by

$$Q_B = \int d\sigma \sum_{\pm} \{c_{\pm}\, T_{\pm\pm}(X) + b_{\pm} c_{\pm} \partial c_{\pm}\}\,. \tag{8.80}$$

where $(b_{\pm}, c_{\pm})$ are the Faddeev-Popov ghosts, which is a device of "covariant quantization", while $T_{\pm\pm}(X(\sigma))$ is the stress tensor for left/right moving strings, associated to any conformal field theory (CFT) on the worldsheet that is conformally exact at the quantum level.

The gravitational and other backgrounds, including a dynamical tension that flips signs (i.e. incorporating antigravity) of the type we discussed in the previous sections, are included in the stress tensor $T_{\pm\pm}(X)$. If these backgrounds are not geodesically complete we expect that the SFT theory is incomplete since even at the classical level on the worldsheet there would be string solutions that would be incomplete just like particle geodesics that would be incomplete. Thus for a geodesically complete SFT we need to make sure that $T_{\pm\pm}(X)$ belongs to a geodesically complete worldsheet string model as described in the previous section. Examples of such string models were provided in sections (8.5.1,8.5.3). Similarly one can construct many more geodesically complete backgrounds by allowing the string tension to change sign at singularities (and perhaps more generally) as long as the CFT conditions, that amount to $Q^2 = 0$, are satisfied.

If the interactions in the SFT action (8.79) are neglected we do not expect dramatic effects due to the presence of antigravity since we have seen in the previous section the effect is only a time delay as compared to the complete absence of antigravity (as in sections 8.28,8.4.3,8.5.1). By including the interactions either perturbatively or non-perturbatively we can explore the effects of antigravity in the context of the quantum theory. In the previous sections, we have obtained a glimpse of the phenomena that could happen, including particle (or string) production (as in section 8.4.5), excitations of various string states (as in section 8.4.4), and more dramatic phenomena that remain to be explored.

From the discussion in the first part of section (8.5.1) one may gather that we are still in the process of addressing some technicalities in the construction of the BRST operator Q_B for the simple model in that section. So we are not yet in a position to perform explicit computations, but we hope we have provided an outline of how one may formulate an appropriate theory to address and answer the relevant questions.

There may be alternative formalisms that could provide answers more easily than SFTs—such as the gauge-gravity dualities—and of course those should be explored, but the advantage of SFTs for being a conceptually complete and self consistent definition of the system, including the presence of antigravity as outlined above, is likely to remain as

an important feature of this approach because of the overall perspective that it provides.

8.7 Comments and conclusions

We have argued that a fundamental theory that could address the physical phenomena close to gravitational singularities, either in the form of field theory or string theory, is unlikely to be complete without incorporating geodesic completeness. The Weyl symmetric approach to the standard model coupled to gravity in (8.1), and the similar treatment of string theory [84], generally solves this problem and naturally requires that antigravity regions of spacetime should appear on the "other side" of gravitational singularities as integral parts of the spacetime described by a fundamental theory. There are other views that the notion of spacetime may not even exist at the extremes close to singularities. While acknowledging that there may be other scenarios that require more understanding at this time, we believe that our concrete proposal merits further investigation.

While emphasizing that there are nicer Weyl gauges, we have shown how gravitational theories and string theories can be formulated in their traditional Einstein or string frames to include effects of a Weyl symmetry that renders them geodesically complete. A prediction of the Weyl symmetry is to naturally include an antigravity region of field space and spacetime that is geodesically connected to the traditional gravity spacetime at gravitational singularities. Precisely at the singularities that appear in the Einstein or string frames the gravitational constant or string tension flip sign suddenly (but smoothly in nicer Weyl gauges). As shown in section (8.2), this sign can be absorbed into a redefinition of the metric in the Einstein or string frame, $\hat{g}_{\mu\nu} = \pm g^{\pm}_{\mu\nu}$, where $\hat{g}_{\mu\nu}$ describes the spacetime in the union of the gravity and antigravity regions. This definition of the complete spacetime may then be used to perform computations in the geodesically complete theory.

The appearance of negative kinetic energy terms for some degrees of freedom during antigravity was a source of concern. The arguments presented here show that this was a false alarm. We argued that unitarity is not an issue either in gravity or antigravity and that negative energy does not imply an instability of the theory as seen by observers in the gravity region (namely, observers like us, analyzing the universe). We made this point by studying many simple examples and we showed that observers in the gravity sector can deduce the existence and at least some properties of antigravity.

We have thus eliminated the initial concerns regarding unitarity or instability of the complete theory when there is an antigravity sector with negative kinetic energy. We have also demonstrated in this chapter that there are very interesting physical phenomena associated with antigravity that remain to be explored concerning fundamental physics at the extremities of spacetime. These will have applications in cosmology as in [62, 63, 75, 84] and black hole physics as discussed in the next chapter and in [4, 91].

Chapter 9

Journey beyond the Schwarzschild black hole singularity

The Schwarzschild black hole is a spherically symmetric solution to the vacuum Einstein equations $R_{\mu\nu}(g) = 0$

$$ds^2 = -\left(1 - \frac{r_0}{r}\right) dt^2 + \left(1 - \frac{r_0}{r}\right)^{-1} dr^2 + r^2 d\Omega^2. \tag{9.1}$$

Here, $r_0 \equiv 2G_N M$, is the radius of the horizon, G_N is the gravitational constant, and M is the ADM mass of the black hole. Although the Ricci and scalar curvatures are zero, the curvature tensor $R_{\mu\nu\lambda\sigma}$ blows up at the $r = 0$ singularity. The spacetime is better described in terms of the Kruskal-Szekeres coordinates,

$$\begin{aligned} u &= \pm \left|1 - \tfrac{r}{r_0}\right|^{\frac{1}{2}} e^{(r+t)/2r_0}, \\ v &= \pm \left|1 - \tfrac{r}{r_0}\right|^{\frac{1}{2}} \text{Sign}\left(1 - \tfrac{r}{r_0}\right) e^{(r-t)/2r_0}, \end{aligned} \tag{9.2}$$

that satisfy the following properties (+ corresponds to regions I&II and − to regions III&IV in Fig. 9.1)

$$\begin{aligned} &\text{when } uv < 1 \text{ or } r > 0, \\ uv = \left(1 - \tfrac{r}{r_0}\right) e^{r/r_0}, \;\; \tfrac{u}{v} &= \text{Sign}\left(1 - \tfrac{r}{r_0}\right) e^{t/r_0}, \\ r = r_0 R_+(uv), \; t &= r_0 \ln\left|\tfrac{u}{v}\right|, \\ R_+(uv) &\equiv 1 + \text{ProductLog}[0, \tfrac{-uv}{e}], \\ ds^2 = r_0^2 \left(2\tfrac{e^{-R_+(uv)}}{R_+(uv)}(-2dudv) + R_+^2(uv)\, d\Omega^2\right). & \end{aligned} \tag{9.3}$$

The spacetime $uv < 1$ is geodesically incomplete because an observer that starts a journey in region I on a geodesic that crosses the horizon into region II, reaches the black hole singularity in a finite amount of *proper time*. Such geodesics are artificially stopped at the $r = 0$ singularity because in conventional general relativity it is assumed there does not exist a spacetime beyond this point. This indicates that the theory is incomplete

since it cannot answer the question of what happens as proper time continues to tick. The geodesic incompleteness is a general problem that occurs at every gravitational singularity, not only at the Schwarzschild black hole.

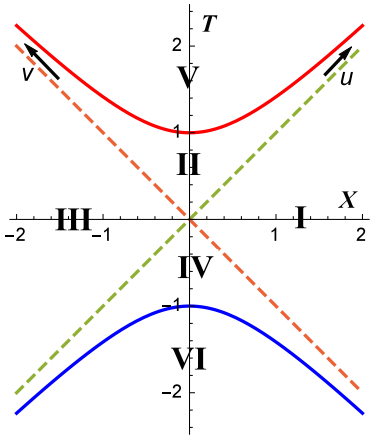

Figure 9.1: Kruskal diagram in the lightcone coordinates for the Schwarzschild black hole indicating the distinct spacetime regions I to VI.

The problem occurs both in the Einstein frame and in the string frame of general relativity, as well as in string theory when it uses geodesically incomplete background geometries in the worldsheet formulation (there would be incomplete string solutions similar to particle geodesics). Usually an appeal is made to "quantum gravity", such as string theory, to resolve the problems at singularities. However if the worldsheet formalism of strings is already geodesically incomplete we may expect that such an incomplete version of string theory would also be subject to similar problems in its classical and quantum versions. Therefore we believe that a healthier approach is to first understand and improve the geodesic completeness of gravitational and string theories at the classical level and then study the quantum effects using the improved theories. Later in this chapter we will connect to the general approach [62, 84] to construct geodesically complete gravitational and string theories.

9.1 The setup

We propose a geodesic completion of the Schwarzschild blackhole geometry as follows. We note that there is another solution of $R_{\mu\nu}(g) = 0$ which looks just like Eq.(9.1) except for replacing r_0 by $-r_0$. This solution has no horizon and corresponds to a bare singularity and is usually discarded as being too unphysical. We propose a new interpretation of this solution. We attribute the flip of sign of r_0 to be due to the flip of sign of the gravitational constant exactly at the singularity, $G_N \to -G_N$. This flip naturally occurs in general relativity interacting with matter improved with local scale (Weyl) invariance [62] as well as in the related improved string theory [84]. We therefore suggest, consistently with

[62, 84], that this solution must belong to regions V and VI that are behind the black or white hole singularities, and claim that those are antigravity regions where gravity is repulsive rather than attractive. We will show that the gravity regions (I, II, III, IV) and the antigravity regions (V, VI) are geodesically connected by exhibiting the metric $g_{\mu\nu}$ that spans the union of all regions and by displaying the complete set of geodesics in this geometry that go through the black/white hole singularity. To begin, we use new Kruskal-Szekeres coordinates to rewrite the solution

$$ds^2 = -\left[-\left(1+\frac{r_0}{r}\right)dt^2 + \left(1+\frac{r_0}{r}\right)^{-1} dr^2 + r^2 d\Omega^2\right]. \tag{9.4}$$

The unusual overall minus sign is needed for the continuity of the metrics in Eqs.(9.1,9.4) at $r = 0$. The extra sign is typical of antigravity as explained in Eq.(9.20). See the discussion following Eq.(9.20) to address any concerns about ghosts. So, in regions $V\&VI$,

$$\begin{gathered}
\text{when } uv > 1, \text{ and } r > 0, \\
u = \pm\left(1+\tfrac{r}{r_0}\right)^{-\frac{1}{2}} e^{(r+t)/2r_0}, \\
v = \pm\left(1+\tfrac{r}{r_0}\right)^{-\frac{1}{2}} e^{(r-t)/2r_0}, \\
uv = \left(1+\tfrac{r}{r_0}\right)^{-1} e^{r/r_0},\ \tfrac{u}{v} = e^{t/r_0}, \\
r = r_0 R_-(uv)\,,\ t = r_0 \ln\left|\tfrac{u}{v}\right|, \\
R_-(uv) = \left(-1 - \text{ProductLog}[-1, \tfrac{-1}{euv}]\right), \\
\tfrac{ds^2}{r_0^2} = 2\tfrac{e^{-R_-}}{R_-}\left(1+R_-\right)^2(-2dudv) - R_-^2 d\Omega^2.
\end{gathered} \tag{9.5}$$

The function ProductLog[k,z] corresponds to branches of the Lambert function in the complex plane. For $k = -1$ our $R_-(uv)$ is always real and positive when $uv > 1$.

The union of the $uv \lessgtr 1$ regions is the metric

$$\begin{gathered}
ds^2 = r_0^2\left[-2sR'(uv)(-2dudv) + sR^2(uv)\,d\Omega^2\right], \\
R(uv) \equiv s\left(1 + \text{ProductLog}\left[\tfrac{s-1}{2}, \tfrac{(-uv)^s}{e}\right]\right), \\
s \equiv \text{Sign}(1-uv).
\end{gathered} \tag{9.6}$$

In this metric *space and time, (X,T) in Fig. 9.1, do not switch roles on the other side of the singularity.* We will show that this is a geodesically complete spacetime of gravity and antigravity regions, noting that the effective gravitational constant switches sign at $uv = 1$

$$G_N\ \text{Sign}(1-uv). \tag{9.7}$$

The expression for $R(uv)$ given in Eq.(9.6) is the unique *real* and *positive* R solution for the following equation

$$(1-sR)^s e^R = uv. \tag{9.8}$$

A plot of $R\,(uv)$ and its derivative $R'\,(uv)$ is given in Fig. 9.2, showing that R is positive for all uv, vanishes at the singularity $uv = 1$, and approaches an infinite slope $R' \to \pm\infty$ at that point. Generally Eq.(9.8) has many solutions in the complex R plane. These are

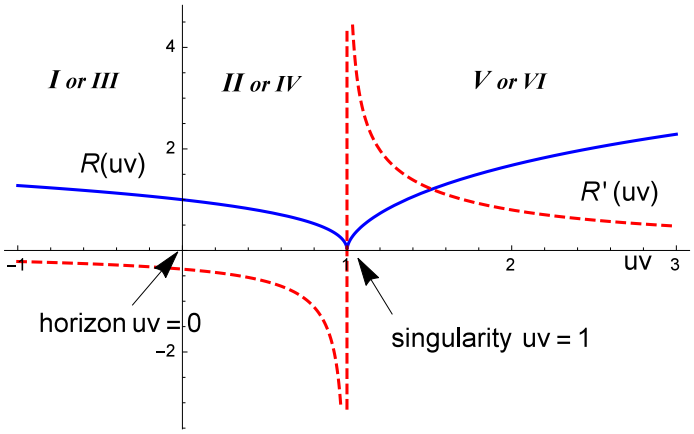

Figure 9.2: $R\,(uv)$ solid, $R'\,(uv)$ dashed.

expressed in terms of the many branches of the well documented function ProductLog[k,z]. The branch in Eq.(9.6) is real and positive for all real values of uv. We now show that the derivative $R'\,(uv)$ for all uv, including $uv = 1$, is given by

$$sR' = \frac{e^{-R}}{-R}\,(1 - sR)^{1-s} = \frac{1 - sR}{-uv\ R}. \tag{9.9}$$

With this form of R' the generalized metric in Eq.(9.6) agrees with the metrics in Eqs.(9.3,9.5) for $uv < 1$ and $uv > 1$, and also defines the new metric at the singularity $uv = 1$. Some care is needed to verify Eq.(9.9) since the derivative of s is a delta function $s' = -2\delta\,(1 - uv)$. The simplest approach is to formally take the derivative of both sides of Eq.(9.8) for any $R\,(uv)$ and $s\,(uv)$,

$$\left[\begin{array}{c} \frac{1-s^2-sR}{1-sR}R' \\ +\left(\ln\,(1 - sR) - \frac{sR}{1-sR}\right)s' \end{array}\right](1 - sR)^s\,e^R = 1. \tag{9.10}$$

Near the singularity, for small R and well behaved s, the coefficient of s' in Eq.(9.10) has an expansion such that the s' term becomes, $\left(s^2\right)'(-R)\left(1 + \frac{3}{4}sR + O\left((sR)^2\right)\right)$. With our $s\,(uv)$ Eq.(9.6), and $\left(s^2\right)'R\,(uv) \to 0$, the s' term in Eq.(9.10) vanishes for all uv, including $uv = 1$. The remaining R' term in Eq.(9.10) shows that $R'\,(uv)$ is given by Eq.(9.9) for all uv. We record here the behavior of R and R' near the singularity and far

away from it

$$\begin{aligned} uv \simeq 1: & \begin{cases} R \simeq (2\,|1-uv|)^{1/2}, \\ sR' \simeq -(2\,|1-uv|)^{-1/2}. \end{cases} \\ |uv| \simeq \infty: & \begin{cases} R \simeq \ln\left(|uv|\,(\ln|uv|)^{\mathrm{Sign}(uv)}\right). \\ sR' \simeq \frac{1}{|uv|} + \frac{1}{uv\ln|uv|}. \end{cases} \end{aligned} \tag{9.11}$$

noting that these are consistent with the plots in Fig. 9.2.

Remarkably, the metric in Eq.(9.6) is a solution of the vacuum Einstein equations, $R_{\mu\nu}\left(g\left(u,v,\Omega\right)\right)=0$, for all (u,v). By construction, we knew that we have a solution when $uv\neq 1$. We remark that for a metric of the form (9.6) which is fully specified by a single function $R\left(uv\right)$, the Ricci tensor vanishes automatically for any $R\left(uv\right)$. In our case, for the specific form of $R\left(uv\right)$ given in Eqs.(9.6,9.9), we obtain $R_{\mu\nu}=0$ for all (u,v) including at the black and white hole singularities at $uv=1$.

9.2 Geodesic probes of the modified background

To study the geodesics we now consider a test particle of mass m moving in this improved black hole background. The worldline Lagrangian has the form $\mathcal{L}=\frac{1}{2e}g_{\mu\nu}\left(x\right)\dot{x}^{\mu}\dot{x}^{\nu}-e\frac{m^2}{2}$, where $e\left(\tau\right)$ is the einbein. The constraint due to τ-reparametrization is the equation of motion with respect to $e\left(\tau\right)$. After choosing the gauge $e\left(\tau\right)=r_0^2$, which corresponds to interpreting τ as a dimensionless *proper time*, the constraint takes the form

$$\left[-2sR'\left(uv\right)\left(-2\dot{u}\dot{v}\right)+sR^2\left(uv\right)\dot{\Omega}^2\right]+m^2r_0^2=0. \tag{9.12}$$

This is the $g^{\mu\nu}p_\mu p_\nu+m^2=0$ constraint for our new extended black hole metric. The canonical conjugate to the solid angle $\vec{\Omega}$ (a unit vector) is related to angular momentum $\vec{L}$, which is conserved due to rotational symmetry in the Lagrangian or the metric (9.6). Furthermore, there is also a symmetry under opposite global rescalings of $(u,v)\to\left(\lambda u,\lambda^{-1}v\right)$. This amounts to translations of the time coordinate, $t/r_0\to\left(t/r_0+\ln\lambda^2\right)$, as seen from Eqs.(9.3,9.5). Hence, there is an additional conserved quantity, that amounts to the canonical conjugate to t/r_0, which is (up to a rescaling by r_0) a dimensionless energy parameter E. Taking the conserved quantities $\left(E,\vec{L}\right)$ into account, we rewrite the constraint in Eq.(9.12) as follows (see derivation below)

$$s\left(\frac{-E^2}{uvR'}+\frac{R'\left(\partial_\tau\left(uv\right)\right)^2}{uv}+\frac{\vec{L}^2}{R^2}\right)+m^2r_0^2=0. \tag{9.13}$$

This equation now involves a single time-dependent degree of freedom, namely $\left(uv\right)\left(\tau\right)$, whose solution as a function of proper time τ would determine all geodesics. The second order equations derived from the worldline Lagrangian (geodesics) are automatically

solved by the solutions of this first order differential equation because they must obey the constraint (9.13). Hence this determines *all geodesics for all possible initial conditions* $\left(E, \vec{L}\right)$ for a test particle of small mass m.

To see how Eq.(9.13) is derived from the constraint Eq.(9.12), we need to clearly identify the canonical conjugate to $t(\tau)$. For this purpose it is useful to transform to yet another set of coordinates (ρ, t) instead of (u, v) that still cover the entire (u, v) plane. We leave t unchanged as in Eqs.(9.3,9.5) and introduce, $\rho = 1 - uv$, in the range $-\infty < \rho < \infty$. Thus, the coordinate transformation and its inverse is

$$\begin{gathered}\rho = 1 - uv, \;\; \tfrac{t}{r_0} = \ln\left|\tfrac{u}{v}\right| \equiv \tilde{t}, \\ u = \pm\sqrt{|1-\rho|}e^{\frac{t}{2r_0}}, \; v = \pm \text{Sign}\,(1-\rho)\sqrt{|1-\rho|}e^{-\frac{t}{2r_0}}.\end{gathered}$$

After this change of coordinates the metric (9.6) becomes

$$ds^2 = r_0^2\left[-sR'\left(-d\tilde{t}^2\,(\rho-1) + d\rho^2\,(\rho-1)^{-1}\right) + sR^2 d\Omega^2\right].$$

From the corresponding worldline Lagrangian we compute, E, the canonical conjugate to $\tilde{t}(\tau)$, and express the conserved angular momentum, $\vec{L}$, in terms of the angular velocity $\partial_\tau \vec{\Omega}(\tau)$

$$E = (\rho-1)\,sR'\partial_\tau \tilde{t}, \;\; \vec{L} = sR^2\partial_\tau\vec{\Omega}. \tag{9.14}$$

After rewriting $\left(\dot{u}, \dot{v}, \dot{\Omega}\right)$ in terms of $\left(\dot{t}, \dot{\rho}, \vec{L}\right)$, the constraint (9.12) takes the form of Eq.(9.13).

Now, it is easy to get an intuitive understanding of the time development of $(uv)(\tau)$, or equivalently $\rho(\tau) = 1 - (uv)(\tau)$, by rewriting the constraint (9.13) in the form of a non-relativistic "Hamiltonian" $\mathcal{H}$ (i.e. kinetic energy + potential energy) for one degree of freedom, subject to the condition that the corresponding "energy" level is zero, namely $\mathcal{H} = 0$ (the constraint), as follows

$$\mathcal{H} \equiv \frac{1}{2}\left(\partial_\tau\,(uv)\right)^2 + V\,(uv) = 0. \tag{9.15}$$

This exercice identifies the potential $V(uv)$

$$V\,(uv) \equiv \frac{uv}{2R'}\left(\frac{\vec{L}^2}{R^2} + sm^2r_0^2\right) - \frac{E^2}{2R'^2}. \tag{9.16}$$

Plots of $V(uv)$ for small $\left|m^2\right| r_0^2$ are given in Figs. (9.3, 9.4). The features of the plots follow from the approximate behavior near to and far from the singularity

$$\begin{gathered}uv \simeq 1 : V \simeq -\left[\frac{uv\;\left(\;s\vec{L}^2 + 2|1-uv|\;m^2r_0^2\right)}{2\sqrt{2}\sqrt{|1-uv|}} + E^2\,|1-uv|\right], \\ uv \simeq \pm\infty : V \simeq \frac{(uv)^2}{2}\left[-E^2 + sm^2r_0^2 + \frac{L^2}{(\ln|uv|)^2}\right].\end{gathered}$$

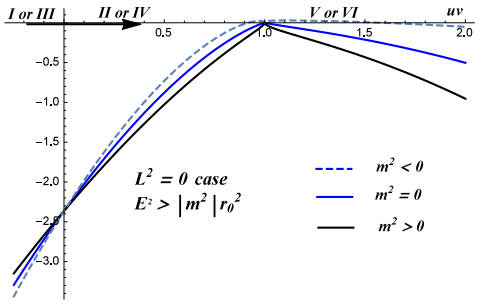

Figure 9.3: $V\,(uv)$ for $L = 0$. Middle curve for $m = 0$.

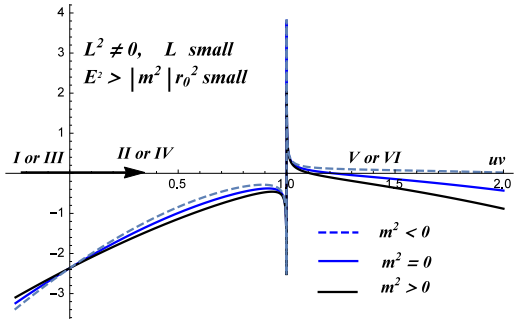

Figure 9.4: $V\,(uv)$ for $L \neq 0$. Middle curve for $m = 0$.

In this potential, the dimensionless parameters $(E^2, \vec{L}^2)$ may be considered as initial conditions for the particle of dimensionless mass $m^2 r_0^2$. We omit the discussion of particles trapped in orbits around the black hole, that would occur when $E^2 < m^2 r_0^2$, as this does not change our main points. Then, the asymptotic form of Eq.(9.13) for large $|uv|$ is, $-E^2 + \vec{p}^2 + m^2 r_0^2 = 0$, indicating that E must satisfy $E^2 > m^2 r_0^2$. We consider small values of $\left|m^2 r_0^2\right|$ since huge masses would violate the spirit that m represents a small probe for which the back reaction of the black hole can be neglected.

The constraint (9.15) is equivalent to a first order differential equation, $\partial_\tau\,(uv) = \pm\sqrt{-2V\,(uv)}$, for the single variable uv whose solution is

$$(\tau - \tau_0) = \pm \int_{u_0 v_0}^{uv} dx/\sqrt{-2V\,(x)}, \tag{9.17}$$

where the $\pm$ signs are chosen according to whether the initial velocity is toward or away from the black hole. This expression can in principle be solved for uv as a function of τ, yielding the desired solution $(uv)\,(\tau) = F\,(\tau)$ where $F\,(\tau)$ is fully determined. Although this appears to be complicated we note that from the plots of $V\,(uv)$ alone we can easily obtain an intuitive feeling of all possible motions that $(uv)\,(\tau)$ can perform.

Consider the case of zero angular momentum ($\vec{L} = 0$, Fig. 9.3). A particle that obeys the constraint in Eq.(9.15) has the same $\mathcal{H}$-energy level as the summit of the "mountain". Such a particle that comes from region I where $uv < 0$ (approaching from the left in

Fig. 9.3) will keep climbing the $V(uv)$ mountain, passing into region II at the horizon at $uv = 0$, and (in the case of $m^2 \geq 0$) reaching the peak of the mountain where it slows down and stops momentarily at the $uv = 1$ singularity. Note that at the peak the potential vanishes, $V(uv = 1)|_{L=0} = 0$, and therefore $\partial_\tau (uv) = 0$ to satisfy the constraint (9.15). In fact, at the singularity, $\dot{u} = \dot{v} = 0$ when we examine the rest of the equations of motion that follow from the worldline Lagrangian $\mathcal{L}$, so the particle stops temporarily at the summit of the mountain in Fig. 9.3. This journey takes a finite amount of proper time τ because the integral in Eq.(9.17) is finite. Clearly the summit is an unstable point, so at the subsequent moment in proper time, the particle will either slide forward to $uv > 1$ down the mountain into region V where there is antigravity, or slide back to $uv < 1$ into region II and then III where there is gravity. It will not slide back into regions II and then I because this would cause closed timelike curves, and indeed this can be deduced from analytic investigations. Forward uv or backward uv at $uv = 1$ are allowed solutions of the geodesic equations of motion, so both of them will happen. In either case *the particle moves on to another world* that is geodesically connected to the original starting point in region I. This shows that particles that fall into the black hole (beyond the horizon) will inevitably end up in a new universe according to this classical analysis. Note that gravity observers in region III will interpret that the particle comes out of a white hole, while those in the antigravity region V will interpret it as coming out of a naked singularity.

A quantum analysis that treats a small probe in a static black hole (as in the present case) will reach the same conclusion and provide non-vanishing probability amplitudes[1] for transmission to regions III and V (for tachyons as well). The computation may be performed in a WKB approximation just as in non-relativistic potential theory as presented elsewhere.

Next we consider non-zero angular momentum ($L^2 \neq 0$, Fig. 9.4). In this case the particle coming from regions $I\&II$ hits an angular momentum barrier at $uv = 1$, so classically it can only bounce back to regions $II\&III$. However, quantum mechanically there will be a non-zero transmission probability to also tunnel into region V.

To be fully convinced of our intuitive analysis it is useful to have some analytic expressions for the geodesics. This looks complicated in 4-dimensions although there is no problem numerically. However, for the closely related 2-dimensional stringy black hole, after geodesically completing its space-time as we did above, we have explicitly constructed the full set of geodesics of the type $L = 0$ discussed above. This classical result fully supports the intuitive discussion. This work, together with the corresponding quantum computation, is presented in [91]. In a very similar manner we can also discuss the geodesics whose initial conditions begin in the regions V or VI.

[1] We assume that there would be a canonical way to construct the Hilbert space for doing perturbation theory in this background.

9.3 Connection to Weyl symmetric gravity

We now give a short description of how our geodesically complete black hole spacetime in Eq.(9.6) fits perfectly with the Weyl symmetric re-formulation of geodesically complete gravity (SM+GR) [62] and string theory [84]. We concentrate only on the basic consequence of the Weyl symmetry, which is that dimensionful parameters are not allowed. All dimensionful constants of phenomenological significance, including the Newton constant (and therefore the string tension) emerge from Weyl-gauge fixing of some gauge degrees of freedom [62, 84]. As an illustration, consider the case of the SM+GR which contains the SU(2) ×U(1) Higgs doublet H and an additional singlet scalar ϕ required by the Weyl-symmetric approach. ϕ is compensated by the Weyl symmetry, so ϕ is not a true additional degree of freedom, but participates in an important structure of the symmetry that has physical consequences. In order to have the symmetry all scalars are "conformally coupled", implying the special non-minimal coupling to the curvature

$$\frac{1}{12}\left(\phi^2 - s^2\right) R\left(g\right), \text{ with } s^2 \equiv 2H^\dagger H. \tag{9.18}$$

This structure is the same in low energy string theory [84] but with a different interpretation of s. The relative minus sign in Eq.(9.18) is obligatory. Weyl symmetry requires that, with the signs above, ϕ has the wrong sign kinetic energy while H has the correct sign. So, ϕ is a ghost but, since it can be removed by a Weyl gauge choice, this is not a problem. If ϕ were not a ghost then the curvature term would have a purely negative coefficient, $-\frac{1}{12}\left(\phi^2 + s^2\right)$, which leads to only a purely negative gravitational constant, so there are no alternatives to (9.18). Therefore, the effective Planck mass $\frac{1}{12}\left(\phi^2 - s^2\right)$ (or the Newton constant) is not positive definite. At the outset of this approach in 2008 the immediate question was whether the dynamics would allow $\left(\phi^2 - s^2\right)$ to remain always positive. It was eventually determined in 2010-2011 (references in [62, 84]) that the solutions of the field equations that do not switch sign for this quantity are non-generic and of measure zero in the phase space of initial conditions for the fields (ϕ, s). So, according to the dynamics, it is untenable to insist on a limited patch of field space. By contrast, it was found that the theory becomes geodesically complete when all field configurations are included, thus doing away generally with the basic problem of geodesic incompleteness.

With a gauge choice, the redundant Weyl gauge degrees of freedom can be eliminated, but one can err by choosing an illegitimate gauge that corresponds to a geodesically incomplete patch. Indeed this is what happens in the "Einstein gauge" (E) and in the "string gauge" (s) [62, 84]:

$$\begin{array}{l} \text{E-gauge: } \frac{1}{12}\left(\phi_{E+}^2 - s_{E+}^2\right) = \frac{+1}{16\pi G_N}, \\ \text{s-gauge: } \frac{d-2}{8(d-1)}\left(\phi_{s+}^2 - s_{s+}^2\right) = \frac{+1}{2\kappa_d^2} e^{-2\Phi},\ \Phi = \text{dilaton}. \end{array} \tag{9.19}$$

Conventional general relativity and string theory are geodesically incomplete because the gauge choices just shown are valid only in the field patch in which $|\phi| > |s|$. The dynamics contradict the assumption of gauge fixing to only the positive patch. In the negative regions one may choose again the Einstein or string gauge, but now with a negative gravitational constant, $\frac{1}{12}\left(\phi_{E-}^2 - s_{E-}^2\right) = \frac{-1}{16\pi G_N}$, or $\frac{d-2}{8(d-1)}\left(\phi_{s-}^2 - s_{s-}^2\right) = \frac{-1}{2\kappa_d^2}e^{-2\Phi}$; in those spacetime regions gravity is repulsive (antigravity). In the corresponding worldsheet formulation of string theory the string tension also switches sign [84]. Thus the Weyl symmetric (SM+GR) or string theory predict that, in the Einstein or string gauges, one should expect a sudden sign switch of the effective Planck mass $\frac{1}{12}\left(\phi^2 - s^2\right)$ at certain spacetime points that typically correspond to singularities (e.g. big bang, black holes) encountered in the Einstein or string frames. As shown in [62, 84] one may choose better Weyl gauges (e.g. "γ-gauge", choose $\det(-g) \to 1$, or "c-gauge", choose $\phi \to$constant) that cover globally all the positive and negative patches. Then the sign switch of the effective Planck mass $\frac{1}{12}\left(\phi^2 - s^2\right)$ is smooth rather than abrupt. However, if one wishes to work in the Einstein or string frames, as we did in this chapter, to recover the geodesically complete theory one must allow for the gravitational constant to switch sign at singularities, as in Eq.(9.7), and connect solutions for fields across gravity/antigravity patches. In the $\pm$ Einstein gauges Eq.(9.18) becomes

$$\frac{\left(\phi_{E\pm}^2 - s_{E\pm}^2\right) R\left(g_{E\pm}\right)}{12} = \frac{R\left(g_{E\pm}\right)}{\pm 16\pi G_N} = \frac{R\left(\pm g_{E\pm}\right)}{16\pi G_N}. \tag{9.20}$$

where the $\pm$ for the gravity/antigravity regions can be absorbed into a redefinition of the signature of the metric, $\tilde{g}_{\mu\nu}^E = \pm g_{\mu\nu}^{E\pm}$ [84]. Our new black hole in Eq.(9.6) is for the *continuous* $\tilde{g}_{\mu\nu}^E$ in the *union* of the gravity/antigravity patches. This explains the extra minus sign in Eq.(9.4) and connects it to the underlying Weyl symmetric theory.

One may be worried that the sign switches of the gravitational constant or the string tension may lead to problems like unitarity or negative kinetic energy ghosts. For example, in the SM + GR action in the $\pm$ Einstein gauge, some terms in the antigravity sector flip sign and some don't [84] when $g_{\mu\nu}^{E-} \to -g_{\mu\nu}^{E-}$ (e.g. $F_{\mu\nu}F^{\mu\nu}$ does not, but $R(g)$ does as in (9.20)). We should mention that Ref.[84] has already settled that there are no unitarity problems due to sign flips in field/string theories. As to the negative kinetic energy concerns in antigravity (as in $-R_-^2\,(uv)\,\dot{\Omega}^2$ in (9.5)), this apparent instability is rendered harmless by insisting that the only reasonable interpretation of the theory is by *observers in the gravity sector* . Such observers cannot experience the negative kinetic energy in antigravity directly, but can only detect "in" and "out" signals that interact with the antigravity region. This is no different than a closed spacetime box for which the information about its interior is encoded in terms of scattering amplitudes for in/out states at its exterior. An analogous situation for a cosmological singularity [62, 84] is treated in detail in [85]. So, there are no issues of fundamental principles.

9.4 Outlook

We have demonstrated in this chapter that the Schwarzschild blackhole has a geodesic completion, and that proper observers can in principle travel through the singularity. These results generalize to black holes in other dimensions as well. A similar result that was first obtained for cosmological singularities has been applied to develop a completely new perspective for the role of antigravity just before the big bang (see [62, 84] and references there in). Similarly, our findings may have implications for our understanding of black holes (see the treatment in [91]), the role of the geodesically complete spacetime in their formation and evaporation, the information loss problem, and for investigating how new physics beyond singularities in classical and quantum gravity/string theory impacts observations in our own universe.

Chapter 10

Conclusions and future directions

In the second part of this thesis, we have explored the implications of spacetime backgrounds with regions of antigravity using some simple models that allow for negative kinetic energy states, and a modified blackhole background. By considering kinetic terms with a discontinuous sign flip $\mathrm{sgn}(x^0 - \Delta/2)$, as a function of the timelike coordinate, we found that the models capture the essential physics of such systems. The new physics is primarily encoded in the structure of the propagator and the transition amplitudes which are demonstrated to be regular and non-singular. We have thus resolved some important consistency questions pertaining to the system stability for the case of particles, fields and strings.

Yet another application was in examining the modified Schwarzschild solutions from conventional general relativity. We have shown that one can connect geodesics across the spacelike singularity for the Schwarzschild geometry when the beyond singularity region is one of antigravity. The trajectories were described in terms of the global (u, v) coordinates in the Kruskal-Szekeres parametrization. This suggests that the field dynamics would also be altered in the new background; see [91] for a recent treatment of the propagators in the modified $2d$ black hole background.

It would be of interest to generalize the results presented here in several directions. It is conceivable that other conformal frames for gauge fixing could prove insightful and some of the symmetry assumptions for the backgrounds may be relaxed, like in the case of cosmology. To make the arguments somewhat less formal and to circumvent order of limits issues, it could be helpful to restrict to non-generalized functions while seeking solutions. As we mentioned, the models considered are not necessarily solutions of the equations of motion and it would be interesting to perform similar calculations with a broader class of consistent backgrounds.

Perhaps doing a first principles analysis of the world-line for a detector moving in the modified backgrounds may also be a helpful exercice towards gathering mathematically well-posed questions. Since Poincaré symmetry is broken by our backgrounds, one expects modifications to the validity of standard QFT procedures such as LSZ reduction [92] for Green function computations. Specifying alternate boundary conditions at asymptotic

infinities [93, 94] could also lead to a classification of concrete observables [68, 95–97] consistent with relativistic notions [76, §14,§10]. Finally, higher point correlators (N-point functions) in the background may also be used for probing the signatures of the antigravity patch and such computations also merit further investigation.

Appendix A

Weyl ordered polynomials and the Moyal product

We start with the Heisenberg algebra $\mathfrak{h}_N$ generated by the N pairs of phase space operators X^i, P_j and a central element $C =: i\theta$, satisfying the canonical commutation relations:

$$[X^i, P_j] = C\,\delta^i{}_j, \qquad [C, X^i] = 0 = [C, P_j], \tag{A.1}$$

and is hence a $2N+1$ dimensional Lie algebra. It is also an associative algebra as may be seen from the Jacobi identity. A very useful construction out of this is its universal enveloping algebra[1], which is the Weyl algebra $A_N \cong \mathcal{U}(\mathfrak{h}_N)$. Its elements are the formal polynomials in X^i and P_j modulo the canonical commutation relations.

Let us denote the generators of $\mathfrak{h}_N$ by T_i. Then, a natural basis for A_N is the collection of all distinct *Weyl-ordered* formal homogeneous polynomials

$$T_{i_1} \dots T_{i_k} + \text{ permutations}, \tag{A.2}$$

which makes it isomorphic to the symmetric algebra $\odot(\mathfrak{h}_N)$. This naturally leads one to consider an association with variable t_i (that would become the Moyal coordinates x^μ_{2n}, p^μ_{2n} later) and an identification with the polynomial algebra $\mathbb{K}[t_i]$ with elements

$$P(\vec{t}) = \sum_{k=0} \Pi^{i_1 \dots i_k} t_{i_1} \dots t_{i_k} \tag{A.3}$$

with symmetric coefficients $\Pi^{i_1 \dots i_k}$ valued in the field $\mathbb{K}$ (which will be taken as $\mathbb{C}$ for OSFT).

The non-commutativity of $\mathcal{U}(\mathfrak{h}_N)$ means that the product of two Weyl ordered polynomials would require further reordering. This induces a deformation of the usual commutative product in $\mathbb{K}[t_i]$ and results in a $*$ algebra. The Lie bracket in $\mathfrak{h}_N$ (or the algebra $\mathfrak{g}$ in general) uniquely fixes this product and using the BCH formula, an explicit representation in terms of a *bidifferential* operator may be obtained (see [25, §2.3]). This would

[1] We closely follow [25, §2] in this discussion to motivate the Moyal product.

then be the Moyal product for the $*$ algebra which for the ghost sector of OSFT is given by (2.39) or (2.47) for brevity.

The generalization to OSFT requires an infinite number of modes (to realize the Virasoro algebra that guarantees its consistency) and hence we are essentially considering $\mathcal{U}(\mathfrak{h}_\infty)$. For physically interesting string configurations, one also needs to enlarge from the space of polynomials to exponential functions (§2.2.3). Hence, convergence properties with these differential operators become more challenging in these limits. See [98] for some relevant treatment.

Appendix B

Determinant factors

In order to compute the divergent part of the tadpole integrand, we must include the matter contribution as well. Here we present this computation; we will use this combined result in the following to look at the convergence properties of the finite N regularization for the simplest loop amplitude.

B.1 Matter sector Gaussian integrals

Similar to the ghost sector, we evaluate the matter sector integrand by performing the state sum over matter degrees of freedom by choosing a Fourier basis: $e^{-i\xi^\top\eta}e^{ip\bar{x}}$. Here, however, the presence of the matter zero mode results in additional terms which were absent in the ghost sector by virtue of the Feynman-Siegel gauge.
The matter contribution to the integrand is given by:

$$\mathcal{I}_e^X(q) = \int d^d\bar{x} \int \frac{d^dp}{(2\pi)^d} \frac{(d\eta)}{(2\pi)^{2dN}} \mathrm{Tr}\left[A_e * e^{-i\xi^\top\eta - ip\bar{x}} * (q^{\hat{L}_0^X - 1} e^{i\xi^\top\eta + ip\bar{x}})\right] \tag{B.1}$$

Once again, we choose the monoid elements appropriate for excitations on the perturbative vacuum:

$$\begin{aligned} A_1(\xi,\lambda) &= \mathcal{N}_0^X e^{-\xi^\top M_0^X \xi - \xi^\top\lambda}, \\ A_2(\xi,\eta,p) &= e^{-i\xi^\top\eta} e^{-ip\bar{x}}, \\ A_3(\xi,\eta,p) &= e^{+i\xi^\top\eta} e^{+ip\bar{x}}, \end{aligned} \tag{B.2}$$

where we have assumed Lorentz symmetry over all the matter indices in ξ^μ. Note the extra factors of i as compared to the ghost sector and the loop momentum p^μ. The monoid $A_1(\xi)$, which serves as a generating functional, is chosen to have zero momentum since this is the one-point function for the $D25$ brane case. We recall for convenience that the matrix M_0^X and the normalization factor used in defining the matter vacuum are given by

$$M_0^X = \begin{bmatrix} \frac{1}{4}\kappa_e & \mathbb{0} \\ \mathbb{0} & 4T\kappa_o^{-1}T^\top \end{bmatrix}, \qquad \mathcal{N}_0^X = \det(4\sigma M_0^X)^{d/4} = 2^{Nd}(1 + w^\top w)^{d/8}. \tag{B.3}$$

As before, we sequentially apply the monoid algebra rules for doing the string products. The rules in the matter sector [19, 26] are identical to the ghost sector with the choice of basis we are using, including the signs in the exponentials from Gaussian integrations. Then we obtain the parameters for the monoids $A_{12} \coloneqq A_1 * A_2$:

$A_{12}(\xi, p)$:

$$\begin{aligned} M_{12} &= M_0^X, & \lambda_{12} &= (1 - m_0^X)(i\eta) + \lambda, \\ \mathcal{N}_{12} &= \mathcal{N}_0 \exp\left(-\frac{1}{4}\eta^\top \sigma m_0 \eta + \frac{i}{2}\lambda^\top \sigma \eta\right), & p_{12} &= -p. \end{aligned} \tag{B.4}$$

For the propagator rules[21], there are extra terms from the momentum p as given in (2.67) which we provide here again for convenience:

$$M(t) = \left[\sinh t\tilde{\kappa} + (\sinh t\tilde{\kappa} + M_0^X M^{-1} \cosh(t\tilde{\kappa}))^{-1}\right] (\cosh(t\tilde{\kappa}))^{-1} M_0^X, \tag{B.5a}$$

$$\lambda(t) = \left[(\cosh(t\tilde{\kappa}) + M M_0^{X-1} \sinh t\tilde{\kappa})^{-1}(\lambda + iwp)\right] - iwp, \tag{B.5b}$$

$$\mathcal{N}(t) = \frac{\mathcal{N} e^{-p^2 t} \exp\left[\frac{1}{4}(\lambda + ipw)^\top (M + \coth t\tilde{\kappa} M_0^X)^{-1}(\lambda + iwp)\right]}{\det\left(\frac{1}{2}(1 + M M_0^{X-1}) + \frac{1}{2}(1 - M M_0^{X-1}) e^{-2t\tilde{\kappa}}\right)^{d/2}}. \tag{B.5c}$$

Applying this to A_3 in (B.2) and rewriting the hyperbolic functions in terms of the functions $f_i(\tilde{\kappa}; q)$, we have the parameters for

$A_3(\xi, p, q)$:

$$\begin{aligned} M_3(q) &= \frac{f_3(q)}{f_2(q)} M_0, \qquad \lambda_3(q) = \frac{2q^{\tilde{\kappa}}}{f_2(q)}(-i\eta + iwp) - iwp, \\ \mathcal{N}_3(q) &= \frac{2^{dN} q^{p^2}}{\det(f_2(q))^{d/2}} \exp\left[-\frac{1}{4}(\eta - wp)^\top M_0^{-1} \frac{f_3(q)}{f_2(q)}(\eta - wp)\right], \qquad p_3 = +p. \end{aligned} \tag{B.6}$$

As before one may now remove the remaining $*$ product in the trace and simply set $A_{12}A_3(q) =: A_{123}(q)$ with parameters:

$$\begin{aligned} M_{123}(q) &= \frac{2}{f_2(q)} M_0, \\ \lambda_{123}(q) &= i\left(\frac{f_1(q)}{f_2(q)} - m_0\right)\eta - i\frac{f_1(q)}{f_2(q)} wp + \lambda, \\ \mathcal{N}_{123}(q) &= \mathcal{N}_{12}\mathcal{N}_3(q), \qquad p_{123} = 0. \end{aligned} \tag{B.7}$$

The trace operation is simply a functional Gaussian integral[1] and produces

$$\begin{aligned}\mathrm{Tr}[A_{123}(q)] &= \frac{\mathcal{N}_{123}(q)}{\det(2M_{123}(q)\sigma)^{d/2}} \exp\left(\frac{1}{4}\lambda_{123}^{\top} M_{123}^{-1}\lambda_{123}\right) \\ &\coloneqq \mathcal{C}_\eta \exp\left[-\eta^{\top}\mathcal{Q}_\eta\eta + \mathcal{L}_\eta^{\top}\eta\right], \end{aligned} \tag{B.8}$$

where we suppress the q dependence for typographical simplicity. Collecting the η dependence from the various factors, the coefficient matrices which appear in the quadratic exponential above are the following

$$\begin{aligned}
&\mathcal{Q}_\eta = \mathcal{Q}_{\eta|1} + \mathcal{Q}_{\eta|2} + \mathcal{Q}_{\eta|3}, \quad \text{with} \\
&\mathcal{Q}_{\eta|1} = \frac{1}{4}\sigma m_0, \qquad \mathcal{Q}_{\eta|2} = \frac{1}{4}M_0^{-1}\frac{f_3(q)}{f_2(q)}, \qquad \mathcal{Q}_{\eta|3} = \frac{1}{8}\left(\frac{f_1}{f_2} - m_0\right)^{\top} M_0^{-1} f_2 \left(\frac{f_1}{f_2} - m_0\right), \\
&\mathcal{L}_\eta = \mathcal{L}_{\eta|1} + \mathcal{L}_{\eta|2} + \mathcal{L}_{\eta|3}, \quad \text{with} \\
&\mathcal{L}_{\eta|1}^{\top} = \frac{i}{2}\lambda^{\top}\sigma, \qquad \mathcal{L}_{\eta|2}^{\top} = \frac{p}{2}w^{\top}M_0^{-1}\frac{f_3}{f_2}, \qquad \mathcal{L}_{\eta|3}^{\top} = \frac{i}{4}\left(\lambda - i\frac{f_1(q)}{f_2(q)}wp\right)^{\top} M_0^{-1} f_2(q)\left(\frac{f_1(q)}{f_2(q)} - m_0\right), \quad \text{and} \\
&\mathcal{C}_\eta = \mathcal{C}_{\eta|1}\cdot\mathcal{C}_{\eta|2}\cdot\mathcal{C}_{\eta|3}, \quad \text{with} \\
&\mathcal{C}_{\eta|1} = \mathcal{N}_0, \qquad \mathcal{C}_{\eta|2} = \frac{2^{dN}q^{p^2}}{\det(f_2(q))^{d/2}} \exp\left[-\frac{p^2}{4}w^{\top}M_0^{-1}\frac{f_3}{f_2}w\right], \\
&\mathcal{C}_{\eta|3} = \det\left(\frac{1}{4}M_0^{-1}f_2(q)\right)^{d/2} \exp\left[\frac{1}{8}\left(\lambda - i\frac{f_1}{f_2}wp\right)^{\top} M_0^{-1} f_2 \left(\lambda - i\frac{f_1}{f_2}wp\right)\right].
\end{aligned} \tag{B.9}$$

We can rewrite the above expressions for the *symmetric* matrix $\mathcal{Q}_\eta$ after some matrix algebra as:

$$\mathcal{Q}_\eta^X = \frac{1}{8}\left[M_0^{-1}f_4(q) + \sigma f_3(q) M_0\sigma + \sigma f_1(q) - f_1(q)^{\top}\sigma\right] \tag{B.10}$$

where we remind the reader that $f_4(q) \coloneqq \dfrac{f_1^2 + 2f_3}{f_2}$.

Combining the four terms, we have the block matrix form:

$$\mathcal{Q}_\eta^X(q) = \frac{1}{2}\begin{bmatrix} \kappa_e^{-1}f_4 + T\kappa_o^{-1}f_3(q;\kappa_o)T^{\top} & -\frac{i}{4}(f_1(\kappa_e) - Tf_1(\kappa_o)R) \\ -\frac{i}{4}(f_1(\kappa_e) - Tf_1(\kappa_o)R)^{\top} & \frac{1}{16}\left(\kappa_e f_3 + R^{\top}\kappa_o f_4 R\right) \end{bmatrix}$$

Performing the Gaussian integration of (B.8) over η gives

$$\frac{1}{(2\pi)^{dN}}\mathcal{C}_\eta \left(\det 2Q_\eta\right)^{-d/2} \exp\left[\frac{1}{4}\mathcal{L}_\eta^{\top}\mathcal{Q}_\eta^{-1}\mathcal{L}_\eta\right] \tag{B.11}$$

Now rewriting

$$\mathcal{L}_\eta^{\top} = \frac{i}{2}\lambda^{\top}\alpha^{\top} + \frac{p}{2}w^{\top}\beta^{\top},$$

[1] with the appropriate factors of 2π and i s inserted in the measure.

for compactness using a little algebra in terms of

$$\alpha^\top(q) \coloneqq \frac{1}{2}\left(M_0^{-1} f_1 + f_3^\top \sigma\right) \tag{B.12a}$$

$$\beta^\top(q) \coloneqq \frac{1}{2}\left(M_0^{-1} f_4 - f_1^\top \sigma\right) \tag{B.12b}$$

the argument of the exponential factor involving $\mathcal{Q}_\eta^{-1}$ becomes:

$$\frac{1}{16}\left\{-\lambda^\top \alpha^\top \mathcal{Q}_\eta^{-1} \alpha\lambda + p^2 w^\top \beta^\top \mathcal{Q}_\eta^{-1} \beta w + 2ipw^\top \beta^\top \mathcal{Q}_\eta^{-1} \alpha\lambda\right\}$$

where the Lorentz contraction with λ is understood. Then identifying the quadratic and linear pieces in the centre of mass momentum p (conjugate to the *matter* zero mode) as follows:

$$\mathcal{Q}_p = -\ln q + \frac{1}{8} w^\top M_0^{-1} f_4 w - \frac{1}{16} w^\top \beta^\top \mathcal{Q}_\eta^{-1} \beta w \tag{B.13a}$$

$$\mathcal{L}_p = -\frac{i}{4} w^\top M_0^{-1} f_1 \lambda + \frac{i}{8} w^\top \beta^\top \mathcal{Q}_\eta^{-1} \alpha\lambda \tag{B.13b}$$

we can finally perform the integration over p, to yield the matter contribution to the generating functional:

$$\mathcal{W}^X(t,\lambda) = \frac{(1+w^\top w)^{d/8}}{(4\pi)^{d(N+1/2)}} \frac{1}{|\det(\mathcal{Q}_\eta)\mathcal{Q}_p|^{d/2}} \exp\left[-\lambda^\top \mathcal{Q}_\lambda^X \lambda\right] \qquad \text{where,} \tag{B.14}$$

$$\mathcal{Q}_\lambda^X = \frac{1}{4}\left\{\alpha^\top \mathcal{Q}_\eta^{-1} \alpha - \frac{1}{2} M_0^{X-1} f_2(q) + \frac{1}{16} \frac{\alpha^\top \mathcal{Q}_\eta^{-1} \beta w w^\top \beta^\top \mathcal{Q}_\eta^{-1} \alpha}{\mathcal{Q}_p}\right\}, \tag{B.15}$$

where $d = 26$ is required for having $c = 0$ for the BCFT.

Combined integration over η, p

Another equivalent form that would be more suitable for numerical calculations of the determinant factor is obtained by performing the integration over η and p after combining them into a single $(2N+1) \times 1$ vector ψ:

$$\psi \coloneqq \begin{pmatrix} \eta \\ p \end{pmatrix} \tag{B.16}$$

Now, we can trade using the inverse $\mathcal{Q}_\eta^{-1}$, which is numerically extensive, in favour of working with a larger size matrix while evaluating determinants. In terms of ψ, we can write the expression obtained by taking the trace over ξ (B.8) as

$$\mathrm{Tr}(A_{123}(q)) = \Gamma_\psi \exp\left[-\psi^\top \mathcal{Q}_\psi \psi + \mathcal{L}_\psi^\top \psi\right], \tag{B.17}$$

where the matrix $\mathcal{Q}_\psi$ would now be $(2N+1)\times(2N+1)$ dimensional and can be written as:

$$\begin{aligned}
\mathcal{Q}_\psi &= \begin{bmatrix} \mathbf{A} & \mathbf{B} \\ \mathbf{B}^\top & \mathbf{C} \end{bmatrix}, \text{ where} \\
\mathbf{A} &= \mathcal{Q}_\eta^X, \text{ above in (B.11)}, \\
\mathbf{B} &= \frac{1}{8}(M_0^{-1} f_4 + \sigma f_1) w, \quad \text{a } 2N\times 1 \text{ column vector}, \\
\mathbf{C} &= -\ln q + \frac{1}{8} w^\top M_0^{-1} f_4 w, \text{a scalar}
\end{aligned} \tag{B.18}$$

and the $(2N+1)\times 1$ column vector $\mathcal{L}_\psi$ would simply be of the form:

$$\begin{aligned}
\mathcal{L}_\psi &= \frac{i}{4}\begin{bmatrix} \left(M_0^{-1} f_1 - \sigma f_3\right)\lambda \\ -w^\top M_0^{-1} f_1 \lambda \end{bmatrix} \\
&= \frac{i}{4}\begin{bmatrix} \left(M_0^{-1} f_1 - \sigma f_3\right) & \mathbb{0} \\ -w^\top M_0^{-1} f_1 & 0 \end{bmatrix}\begin{bmatrix} \lambda \\ 0 \end{bmatrix} =: \hat{\mathcal{L}}_\psi \begin{bmatrix} \lambda \\ 0 \end{bmatrix}.
\end{aligned} \tag{B.19}$$

The remaining factor Γ_ψ is then given by:

$$\mathcal{C}_\psi = (1 + w^\top w)^{d/8} \exp\left[\frac{1}{4}\lambda^\top M_{123}^{-1}\lambda\right] \tag{B.20}$$

Now, performing the Gaussian integration over ψ as

$$\begin{aligned}
\int \frac{(d\psi)}{(2\pi)^{(2N+1)d}}\, \mathcal{C}_\psi \exp\left[-\psi^\top \mathcal{Q}_\psi \psi + \mathcal{L}_\eta^\top \psi\right] &= \frac{(1+w^\top w)^{d/8}}{(4\pi)^{d(N+1/2)}} \det(\mathcal{Q}_\psi)^{-d/2} \\
&\times \exp\left\{\frac{1}{4}\lambda^\top \left[\left(\hat{\mathcal{L}}_\psi \mathcal{Q}_\psi^{-1} \hat{\mathcal{L}}_\psi\right)_{2N\times 2N} + \frac{1}{2} M_0^{-1} f_2(q)\right]\lambda\right\}.
\end{aligned} \tag{B.21}$$

Here, the first term in the exponential $\left(\hat{\mathcal{L}}_\psi \mathcal{Q}_\psi^{-1} \hat{\mathcal{L}}_\psi\right)_{2N\times 2N}$ denotes the first $2N\times 2N$ square block in the $(2N+1)\times(2N+1)$ matrix $\hat{\mathcal{L}}_\psi \mathcal{Q}_\psi^{-1} \hat{\mathcal{L}}_\psi$ which turns out to be the non-zero entry in that matrix. We use only the λ independent factors while numerically computing the matter contribution to the integrand next.

B.2 Some numerical results

In analogy with the analysis done in the oscillator formalism [14, §4] to study the determinant factor (the scalar part) to the one-loop tadpole, we plot $\log S_0(t)$ vs $1/t$ for various values of the finite cut-off N. This is an interesting exercice as both the oscillator and the Moyal representations have their advantages and disadvantages. In the oscillator case, we have the exact Neumann matrices and the analytical expression for the matter-ghost

determinant involves lesser number of inverses and matrix multiplications (which makes a numerical analysis more reliable). However, the level truncated Neumann matrices do not satisfy the Gross-Jevicki non-linear identities and so wouldn't be fully internally consistent. For the Moyal representation, the finite N deformation is in a sense consistent since the matrices satisfy identical algebraic relations as the open-string ($N \to \infty$) limit whenever they do not lead to associativity anomalies. But associativity anomalies are essential to obtain the correct closed string physics in OSFT and hence we examine the convergence rate in the Moyal formalism as well.

We use the finite N versions of the matrices and vectors given in [26] and (2.52) for our analysis: Now, in addition to the matter-ghost contribution we have, we need to insert the extra factors which relate the Witten vertex and the Moyal star. Hence, while doing the numerical analysis we have multiplied by the additional factor $-\mu_3^{-1}K^3$, where $K = \frac{3\sqrt{3}}{4}$ and μ_3 is given in (2.86). We find that the results are comparable although the

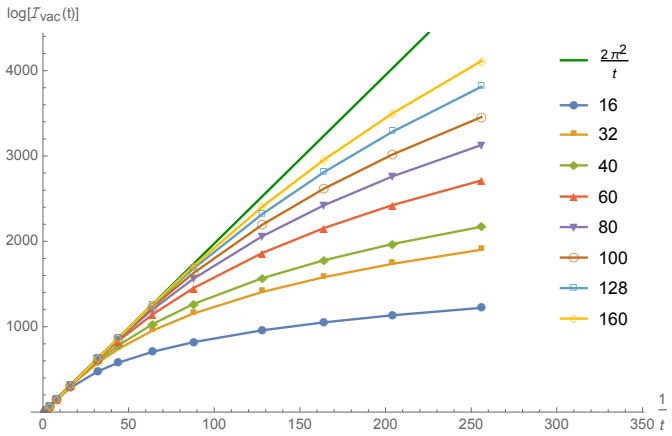

Figure B.1: The log of the overlap amplitude with the perturbative vacuum plotted against $1/t$ for various values of the matrix size N. The green line is the expected infinite N behaviour with slope $2\pi^2$. We see that the result steadily approaches this line as N increases.

convergence rate is not as good. This was to be expected as because of the substructure of the Neumann matrices, more number of inverses and matrix multiplications are required which also affects the convergence rate. However, the relation between the size of the matrices L and $2N$ in the two regularizations is not direct as in the latter, the matrix identities are satisfied even when $N < \infty$. Therefore, there is no analogue of the UV cut-off seen in the level truncation approach as the determinant is still singular for finite N as $t \to 0$.

Bibliography

[1] Gerard 't Hooft. "Under the spell of the gauge principle". *Adv. Ser. Math. Phys.* 19 (1994), pp. 1–683.

[2] Albin James. "Concerning the ghost contribution to the one-loop integrands in open string field theory" (2018). arXiv: 1803.02530 [hep-th].

[3] Itzhak Bars and Albin James. "Physical Interpretation of Antigravity". *Phys. Rev.* D93.4 (2016), p. 044029. DOI: 10.1103/PhysRevD.93.044029. arXiv: 1511.05128 [hep-th].

[4] Ignacio J. Araya, Itzhak Bars, and Albin James. "Journey Beyond the Schwarzschild Black Hole Singularity" (2015). arXiv: 1510.03396 [hep-th].

[5] Daniel Friedan, Emil J. Martinec, and Stephen H. Shenker. "Conformal Invariance, Supersymmetry and String Theory". *Nucl. Phys.* B271 (1986), pp. 93–165. DOI: 10.1016/0550-3213(86)90356-1,10.1016/S0550-3213(86)80006-2.

[6] D. Gross, A. Neveu, Joel Scherk, and J. H. Schwarz. "Renormalization and unitary in the dual-resonance model". *Phys. Rev.* D2 (1970), pp. 697–710. DOI: 10.1103/PhysRevD.2.697.

[7] B. P. Abbott et al. "Observation of Gravitational Waves from a Binary Black Hole Merger". *Phys. Rev. Lett.* 116.6 (2016), p. 061102. DOI: 10.1103/PhysRevLett.116.061102. arXiv: 1602.03837 [gr-qc].

[8] Edward Witten. "Noncommutative Geometry and String Field Theory". *Nucl. Phys.* B268 (1986), pp. 253–294. DOI: 10.1016/0550-3213(86)90155-0.

[9] Matthias R. Gaberdiel and Barton Zwiebach. "Tensor constructions of open string theories. 1: Foundations". *Nucl. Phys.* B505 (1997), pp. 569–624. DOI: 10.1016/S0550-3213(97)00580-4. arXiv: hep-th/9705038 [hep-th];
Sebastian Johann Hermann Konopka. "On the construction of classical superstring field theories". PhD thesis. lmu, 2016.

[10] Charles B. Thorn. "String Field Theory". *Phys. Rept.* 175 (1989), pp. 1–101. DOI: 10.1016/0370-1573(89)90015-X.

[11] Washington Taylor and Barton Zwiebach. "D-branes, tachyons, and string field theory". *Strings, Branes and Extra Dimensions: TASI 2001: Proceedings.* 2003, pp. 641–759. DOI: 10.1142/9789812702821_0012. arXiv: hep-th/0311017 [hep-th];

Yuji Okawa. "Analytic methods in open string field theory". *Prog. Theor. Phys.* 128 (2012), pp. 1001–1060. DOI: 10.1143/PTP.128.1001 ;
Kazuki Ohmori. "A Review on tachyon condensation in open string field theories". PhD thesis. Tokyo U., 2001. arXiv: hep-th/0102085 [hep-th] ;
Leonardo Rastelli and Barton Zwiebach. "Tachyon potentials, star products and universality". *JHEP* 09 (2001), p. 038. DOI: 10.1088/1126-6708/2001/09/038. arXiv: hep-th/0006240 [hep-th].

[12] Charles B. Thorn. "Perturbation Theory for Quantized String Fields". *Nucl. Phys.* B287 (1987), pp. 61–92. DOI: 10.1016/0550-3213(87)90096-4;
Joaquim Gomis, Jordi Paris, and Stuart Samuel. "Antibracket, antifields and gauge theory quantization". *Phys. Rept.* 259 (1995), pp. 1–145. DOI: 10.1016/0370-1573(94)00112-G. arXiv: hep-th/9412228 [hep-th].

[13] Robert Bluhm and Stuart Samuel. "Off-shell Conformal Field Theory at the One Loop Level". *Nucl. Phys.* B325 (1989), pp. 275–328. DOI: 10.1016/0550-3213(89)90458-6;
Stuart Samuel. "COVARIANT OFF-SHELL STRING AMPLITUDES". *Nucl. Phys.* B308 (1988), pp. 285–316. DOI: 10.1016/0550-3213(88)90566-4 ;
Stuart Samuel. "Solving the Open Bosonic String in Perturbation Theory". *Nucl. Phys.* B341 (1990), pp. 513–610. DOI: 10.1016/0550-3213(90)90541-K ;
Daniel Z. Freedman, Steven B. Giddings, Joel A. Shapiro, and Charles B. Thorn. "The Nonplanar One Loop Amplitude in Witten's String Field Theory". *Nucl. Phys.* B298 (1988), p. 253. DOI: 10.1016/0550-3213(88)90268-4.

[14] Ian Ellwood, Jessie Shelton, and Washington Taylor. "Tadpoles and closed string backgrounds in open string field theory". *JHEP* 07 (2003), p. 059. DOI: 10.1088/1126-6708/2003/07/059. arXiv: hep-th/0304259 [hep-th].

[15] Ian Ellwood. "The Closed string tadpole in open string field theory". *JHEP* 08 (2008), p. 063. DOI: 10.1088/1126-6708/2008/08/063. arXiv: 0804.1131 [hep-th].

[16] Sebastian Konopka. "The S-Matrix of superstring field theory". *JHEP* 11 (2015), p. 187. DOI: 10.1007/JHEP11(2015)187. arXiv: 1507.08250 [hep-th].

[17] Korbinian Munster and Ivo Sachs. "Quantum Open-Closed Homotopy Algebra and String Field Theory". *Commun. Math. Phys.* 321 (2013), pp. 769–801. DOI: 10.1007/s00220-012-1654-1. arXiv: 1109.4101 [hep-th];
Hiroshige Kajiura. "Noncommutative homotopy algebras associated with open strings". *Rev. Math. Phys.* 19 (2007), pp. 1–99. DOI: 10.1142/S0129055X07002912. arXiv: math/0306332 [math-qa] ;
Bruno Vallette. "Algebra + homotopy = operad". *arXiv preprint 1202.3245* (2012). URL: https://arxiv.org/abs/1202.3245 ;

Korbinian Muenster. "String field theory: algebraic structure, deformation properties and superstrings". PhD thesis. Munich U., 2013. URL: https://edoc.ub.uni-muenchen.de/16096/.

[18] V. Alan Kostelecky and Robertus Potting. "Analytical construction of a nonperturbative vacuum for the open bosonic string". *Phys. Rev.* D63 (2001), p. 046007. DOI: 10.1103/PhysRevD.63.046007. arXiv: hep-th/0008252 [hep-th].

[19] Itzhak Bars. "Map of Witten's * to Moyal's *". *Phys. Lett.* B517 (2001), pp. 436–444. DOI: 10.1016/S0370-2693(01)00908-X. arXiv: hep-th/0106157 [hep-th];
Itzhak Bars. "MSFT: Moyal star formulation of string field theory". *3rd International Sakharov Conference on Physics Moscow, Russia, June 24-29, 2002*. 2002. arXiv: hep-th/0211238 [hep-th].

[20] I. Bars, I. Kishimoto, and Y. Matsuo. "Fermionic ghosts in Moyal string field theory". *JHEP* 07 (2003), p. 027. DOI: 10.1088/1126-6708/2003/07/027. arXiv: hep-th/0304005 [hep-th].

[21] I. Bars, I. Kishimoto, and Y. Matsuo. "String amplitudes from Moyal string field theory". *Phys. Rev.* D67 (2003), p. 066002. DOI: 10.1103/PhysRevD.67.066002. arXiv: hep-th/0211131 [hep-th].

[22] Itzhak Bars and Yutaka Matsuo. "Associativity anomaly in string field theory". *Phys. Rev.* D65 (2002), p. 126006. DOI: 10.1103/PhysRevD.65.126006. arXiv: hep-th/0202030 [hep-th].

[23] Theodore Erler. "A Fresh look at midpoint singularities in the algebra of string fields". *JHEP* 03 (2005), p. 042. DOI: 10.1088/1126-6708/2005/03/042. arXiv: hep-th/0304044 [hep-th].

[24] Leonardo Rastelli, Ashoke Sen, and Barton Zwiebach. "Star algebra spectroscopy". *JHEP* 03 (2002), p. 029. DOI: 10.1088/1126-6708/2002/03/029. arXiv: hep-th/0111281 [hep-th];
D. M. Belov and C. Lovelace. "Witten's vertex made simple". *Phys. Rev.* D68 (2003), p. 066003. DOI: 10.1103/PhysRevD.68.066003. arXiv: hep-th/0304158 [hep-th];
Michael R. Douglas, Hong Liu, Gregory W. Moore, and Barton Zwiebach. "Open string star as a continuous Moyal product". *JHEP* 04 (2002), p. 022. DOI: 10.1088/1126-6708/2002/04/022. arXiv: hep-th/0202087 [hep-th].

[25] Xavier Bekaert. *Universal enveloping algebras and some applications in physics*. Tech. rep. 2005. URL: http://preprints.ihes.fr/2005/P/P-05-26.pdf.

[26] Itzhak Bars and Yutaka Matsuo. "Computing in string field theory using the Moyal star product". *Phys. Rev.* D66 (2002), p. 066003. DOI: 10.1103/PhysRevD.66.066003. arXiv: hep-th/0204260 [hep-th];

Itzhak Bars and I. Y. Park. "Improved off-shell scattering amplitudes in string field theory and new computational methods". *Phys. Rev.* D69 (2004), p. 086007. DOI: 10.1103/PhysRevD.69.086007. arXiv: hep-th/0311264 [hep-th].

[27] Barton Zwiebach. "Trimming the tachyon string field with SU(1,1)" (2000). arXiv: hep-th/0010190 [hep-th];
Warren Siegel and Barton Zwiebach. "Gauge String Fields". *Nucl. Phys.* B263 (1986), pp. 105–128. DOI: 10.1016/0550-3213(86)90030-1 ;
Hiroyuki Hata and Shun'ichi Shinohara. "BRST invariance of the nonperturbative vacuum in bosonic open string field theory". *JHEP* 09 (2000), p. 035. DOI: 10.1088/1126-6708/2000/09/035. arXiv: hep-th/0009105 [hep-th].

[28] *Non Commutative Algebra package (NCAlgebra).* URL: http://math.ucsd.edu/~ncalg/.

[29] Barton Zwiebach. "Oriented open - closed string theory revisited". *Annals Phys.* 267 (1998), pp. 193–248. DOI: 10.1006/aphy.1998.5803. arXiv: hep-th/9705241 [hep-th].

[30] Martin Schnabl. "Wedge states in string field theory". *JHEP* 01 (2003), p. 004. DOI: 10.1088/1126-6708/2003/01/004. arXiv: hep-th/0201095 [hep-th];
Martin Schnabl. "Analytic solution for tachyon condensation in open string field theory". *Adv. Theor. Math. Phys.* 10.4 (2006), pp. 433–501. DOI: 10.4310/ATMP.2006.v10.n4.a1. arXiv: hep-th/0511286 [hep-th] ;
Theodore Erler and Carlo Maccaferri. "String Field Theory Solution for Any Open String Background". *JHEP* 10 (2014), p. 029. DOI: 10.1007/JHEP10(2014)029. arXiv: 1406.3021 [hep-th].

[31] Michael Kiermaier and Barton Zwiebach. "One-Loop Riemann Surfaces in Schnabl Gauge". *JHEP* 07 (2008), p. 063. DOI: 10.1088/1126-6708/2008/07/063. arXiv: 0805.3701 [hep-th].

[32] Barton Zwiebach. "A Proof that Witten's open string theory gives a single cover of moduli space". *Commun. Math. Phys.* 142 (1991), pp. 193–216. DOI: 10.1007/BF02099176;
Steven B. Giddings, Emil J. Martinec, and Edward Witten. "Modular Invariance in String Field Theory". *Phys. Lett.* B176 (1986), pp. 362–368. DOI: 10.1016/0370-2693(86)90179-6.

[33] Andre LeClair, Michael E. Peskin, and C. R. Preitschopf. "String Field Theory on the Conformal Plane. 1. Kinematical Principles". *Nucl. Phys.* B317 (1989), pp. 411–463. DOI: 10.1016/0550-3213(89)90075-8;
Andre LeClair, Michael E. Peskin, and C. R. Preitschopf. "String Field Theory on the Conformal Plane. 2. Generalized Gluing". *Nucl. Phys.* B317 (1989), pp. 464–508. DOI: 10.1016/0550-3213(89)90076-X ;

Steven B. Giddings and Emil J. Martinec. "Conformal Geometry and String Field Theory". *Nucl. Phys.* B278 (1986), pp. 91–120. DOI: 10.1016/0550-3213(86)90108-2 ;
V. Alan Kostelecky, Olaf Lechtenfeld, Wolfgang Lerche, Stuart Samuel, and Satoshi Watamura. "Conformal Techniques, Bosonization and Tree Level String Amplitudes". *Nucl. Phys.* B288 (1987), pp. 173–232. DOI: 10.1016/0550-3213(87)90213-6.

[34] David J. Gross and Antal Jevicki. "Operator Formulation of Interacting String Field Theory. 2." *Nucl. Phys.* B287 (1987), pp. 225–250. DOI: 10.1016/0550-3213(87)90104-0;
David J. Gross and Antal Jevicki. "Operator Formulation of Interacting String Field Theory". *Nucl. Phys.* B283 (1987), pp. 1–49. DOI: 10.1016/0550-3213(87)90260-4 ;
Isao Kishimoto. "Some properties of string field algebra". *JHEP* 12 (2001), p. 007. DOI: 10.1088/1126-6708/2001/12/007. arXiv: hep-th/0110124 [hep-th].

[35] J. E. Moyal. "Quantum mechanics as a statistical theory". *Proc. Cambridge Phil. Soc.* 45 (1949), pp. 99–124. DOI: 10.1017/S0305004100000487;
Eugene P. Wigner. "On the quantum correction for thermodynamic equilibrium". *Phys. Rev.* 40 (1932), pp. 749–760. DOI: 10.1103/PhysRev.40.749.

[36] Michael R. Douglas and Nikita A. Nekrasov. "Noncommutative field theory". *Rev. Mod. Phys.* 73 (2001), pp. 977–1029. DOI: 10.1103/RevModPhys.73.977. arXiv: hep-th/0106048 [hep-th].

[37] David J. Gross and Washington Taylor. "Split string field theory. 1." *JHEP* 08 (2001), p. 009. DOI: 10.1088/1126-6708/2001/08/009. arXiv: hep-th/0105059 [hep-th].

[38] J. Bordes, Hong-Mo Chan, Lukas Nellen, and Sheung Tsun Tsou. "HALF STRING OSCILLATOR APPROACH TO STRING FIELD THEORY". *Nucl. Phys.* B351 (1991), pp. 441–473. DOI: 10.1016/0550-3213(91)90097-H.

[39] A. Abdurrahman and J. Bordes. "The Relationship between the comma theory and Witten's string field theory. 1." *Phys. Rev.* D58 (1998), p. 086003. DOI: 10.1103/PhysRevD.58.086003.

[40] Itzhak Bars and Dmitry Rychkov. "Background Independent String Field Theory" (2014). arXiv: 1407.4699 [hep-th].

[41] J. Polchinski. *String theory. Vol. 1: An introduction to the bosonic string.* Cambridge University Press, 2007.

[42] I. Bars, I. Kishimoto, and Y. Matsuo. "Analytic study of nonperturbative solutions in open string field theory". *Phys. Rev.* D67 (2003), p. 126007. DOI: 10.1103/PhysRevD.67.126007. arXiv: hep-th/0302151 [hep-th].

[43] Michel Laurent Lapidus. *In Search of the Riemann Zeros: Strings, fractal membranes and noncommutative spacetimes*. American Mathematical Soc., 2008.

[44] Joseph Polchinski. "Factorization of Bosonic String Amplitudes". *Nucl. Phys.* B307 (1988), pp. 61–92. DOI: 10.1016/0550-3213(88)90522-6.

[45] Stuart Samuel. "The Ghost Vertex in E. Witten's String Field Theory". *Phys. Lett.* B181 (1986), pp. 255–262. DOI: 10.1016/0370-2693(86)90042-0;
Eugene Cremmer, Adam Schwimmer, and Charles B. Thorn. "The Vertex Function in Witten's Formulation of String Field Theory". *Phys. Lett.* B179 (1986), pp. 57–65. DOI: 10.1016/0370-2693(86)90435-1.

[46] Washington Taylor. "Perturbative diagrams in string field theory" (2002). arXiv: hep-th/0207132 [hep-th].

[47] Harry Bateman, Arthur Erdelyi, et al. *Higher transcendental functions*. Vol. 1. 2. McGraw-Hill New York, 1953.

[48] Akikazu Hashimoto and N. Itzhaki. "Observables of string field theory". *JHEP* 01 (2002), p. 028. DOI: 10.1088/1126-6708/2002/01/028. arXiv: hep-th/0111092 [hep-th].

[49] Davide Gaiotto, Leonardo Rastelli, Ashoke Sen, and Barton Zwiebach. "Ghost structure and closed strings in vacuum string field theory". *Adv. Theor. Math. Phys.* 6 (2003), pp. 403–456. arXiv: hep-th/0111129 [hep-th].

[50] Yuji Okawa. "Some exact computations on the twisted butterfly state in string field theory". *JHEP* 01 (2004), p. 066. DOI: 10.1088/1126-6708/2004/01/066. arXiv: hep-th/0310264 [hep-th];
Martin Schnabl. "Anomalous reparametrizations and butterfly states in string field theory". *Nucl. Phys.* B649 (2003), pp. 101–129. DOI: 10.1016/S0550-3213(02)01018-0. arXiv: hep-th/0202139 [hep-th].

[51] Yuji Okawa, Leonardo Rastelli, and Barton Zwiebach. "Analytic Solutions for Tachyon Condensation with General Projectors" (2006). arXiv: hep-th/0611110 [hep-th];
Leonardo Rastelli and Barton Zwiebach. "Solving Open String Field Theory with Special Projectors". *JHEP* 01 (2008), p. 020. DOI: 10.1088/1126-6708/2008/01/020. arXiv: hep-th/0606131 [hep-th] ;
Davide Gaiotto, Leonardo Rastelli, Ashoke Sen, and Barton Zwiebach. "Star algebra projectors". *JHEP* 04 (2002), p. 060. DOI: 10.1088/1126-6708/2002/04/060. arXiv: hep-th/0202151 [hep-th] ;

Leonardo Rastelli, Ashoke Sen, and Barton Zwiebach. "Half strings, projectors, and multiple D-branes in vacuum string field theory". *JHEP* 11 (2001), p. 035. DOI: 10.1088/1126-6708/2001/11/035. arXiv: hep-th/0105058 [hep-th].

[52] Nicolas Bourbaki and Philip Spain. *Elements of Mathematics Functions of a Real Variable: Elementary Theory*. Springer Berlin, 2004.

[53] John R Shackell. *Symbolic asymptotics*. Vol. 12. Springer Science & Business Media, 2013.

[54] Reinhold Remmert. *Theory of complex functions*. Vol. 122. Springer Science & Business Media, 2012.

[55] *The On-Line Encyclopedia of Integer Sequences (OEIS)/Sloane's*. URL: https://oeis.org/.

[56] Hiroaki S Yamada and Kensuke S Ikeda. "A numerical test of Padé approximation for some functions with singularity". *International Journal of Computational Mathematics* 2014 (2014);
George A Baker and Peter Graves-Morris. *Padé approximants*. Vol. 59. Cambridge University Press, 1996 ;
Walter Van Assche. "Padé and Hermite-Padé approximation and orthogonality". *Surveys in Approximation Theory* 2 (2006), pp. 61–91.

[57] Theodore Erler and Martin Schnabl. "A Simple Analytic Solution for Tachyon Condensation". *JHEP* 10 (2009), p. 066. DOI: 10.1088/1126-6708/2009/10/066. arXiv: 0906.0979 [hep-th].

[58] Hiroshi Kunitomo and Yuji Okawa. "Complete action for open superstring field theory". *PTEP* 2016.2 (2016), 023B01. DOI: 10.1093/ptep/ptv189. arXiv: 1508.00366 [hep-th];
Theodore Erler. "Supersymmetry in Open Superstring Field Theory". *JHEP* 05 (2017), p. 113. DOI: 10.1007/JHEP05(2017)113. arXiv: 1610.03251 [hep-th] ;
Theodore Erler, Yuji Okawa, and Tomoyuki Takezaki. "Complete Action for Open Superstring Field Theory with Cyclic A_∞ Structure". *JHEP* 08 (2016), p. 012. DOI: 10.1007/JHEP08(2016)012. arXiv: 1602.02582 [hep-th].

[59] Theodore Erler, Sebastian Konopka, and Ivo Sachs. "One Loop Tadpole in Heterotic String Field Theory". *JHEP* 11 (2017), p. 056. DOI: 10.1007/JHEP11(2017)056. arXiv: 1704.01210 [hep-th].

[60] Hiroshi Kunitomo, Yuji Okawa, Hiroki Sukeno, and Tomoyuki Takezaki. "Fermion scattering amplitudes from gauge-invariant actions for open superstring field theory" (2016). arXiv: 1612.00777 [hep-th].

[61] Hiroaki Matsunaga. "Comments on complete actions for open superstring field theory". *JHEP* 11 (2016), p. 115. DOI: 10.1007/JHEP11(2016)115. arXiv: 1510.06023 [hep-th];
Hiroaki Matsunaga. "Notes on the Wess-Zumino-Witten-like structure: L_∞ triplet and NS-NS superstring field theory". *JHEP* 05 (2017), p. 095. DOI: 10.1007/JHEP05(2017)095. arXiv: 1612.08827 [hep-th] ;
Hiroaki Matsunaga and Mitsuru Nomura. "On the BV formalism of open superstring field theory in the large Hilbert space" (2018). arXiv: 1802.04171 [hep-th] ;
Keiyu Goto and Hiroaki Matsunaga. "On-shell equivalence of two formulations for superstring field theory" (2015). arXiv: 1506.06657 [hep-th].

[62] Itzhak Bars, Paul Steinhardt, and Neil Turok. "Local Conformal Symmetry in Physics and Cosmology". *Phys. Rev.* D89.4 (2014), p. 043515. DOI: 10.1103/PhysRevD.89.043515. arXiv: 1307.1848 [hep-th].

[63] Itzhak Bars, Paul J. Steinhardt, and Neil Turok. "Cyclic Cosmology, Conformal Symmetry and the Metastability of the Higgs". *Phys. Lett.* B726 (2013), pp. 50–55. DOI: 10.1016/j.physletb.2013.08.071. arXiv: 1307.8106 [gr-qc].

[64] F. Englert, E. Gunzig, C. Truffin, and Paul Windey. "Conformal Invariant General Relativity with Dynamical Symmetry Breakdown". *Phys. Lett.* 57B (1975), pp. 73–77. DOI: 10.1016/0370-2693(75)90247-6.

[65] François Englert, C Truffin, and Raymond Gastmans. "Conformal invariance in quantum gravity". *Nuclear physics B* 117.2 (1976), pp. 407–432.

[66] Stanley Deser. "Scale invariance and gravitational coupling". *Annals of Physics* 59.1 (1970), pp. 248–253;
Andrei D. Linde. "Gauge theory and the variability of the gravitational constant in the early universe (in Russian)." *Pisma Zh. Eksp. Teor. Fiz.* 30 (1979). [Phys. Lett.93B,394(1980)], pp. 479–482. DOI: 10.1016/0370-2693(80)90350-0 ;
AA Starobinskii. "Can the effective gravitational constant become negative". *Sov. Astron. Lett.(Engl. Transl.);(United States)* 7.1 (1981) ;
Atish Dabholkar. "Quantum Weyl invariance and cosmology". *Physics Letters B* 760 (2016), pp. 31–35.

[67] Stanley Deser. "Improvement Versus Stability in Gravity Scalar Coupling". *Phys. Lett.* 134B (1984), pp. 419–421. DOI: 10.1016/0370-2693(84)91375-3.

[68] S. A. Fulling. "Aspects of Quantum Field Theory in Curved Space-time". *London Math. Soc. Student Texts* 17 (1989), pp. 1–315.

[69] Itzhak Bars and Costas Kounnas. "Theories with two times". *Phys. Lett.* B402 (1997), pp. 25–32. DOI: 10.1016/S0370-2693(97)00452-8. arXiv: hep-th/9703060 [hep-th];

Itzhak Bars. "The Standard Model of Particles and Forces in the Framework of 2T-physics". *Phys. Rev.* D74 (2006), p. 085019. DOI: 10.1103/PhysRevD.74.085019. arXiv: hep-th/0606045 [hep-th] ;
Itzhak Bars. "Gravity in 2T-Physics". *Phys. Rev.* D77 (2008). see last part of Sec.(8), p. 125027. DOI: 10.1103/PhysRevD.77.125027. arXiv: 0804.1585 [hep-th] ;
Itzhak Bars. "Gauge Symmetry in Phase Space, Consequences for Physics and Spacetime". *Int. J. Mod. Phys.* A25 (2010). [,297(2010)], pp. 5235–5252. DOI: 10.1142/9789814335614_0026, 10.1142/S0217751X10051128. arXiv: 1004.0688 [hep-th].

[70] Itzhak Bars and Soo-Jong Rey. "Noncommutative Sp(2,R) gauge theories: A Field theory approach to two time physics". *Phys. Rev.* D64 (2001), p. 046005. DOI: 10.1103/PhysRevD.64.046005. arXiv: hep-th/0104135 [hep-th];
Itzhak Bars. "U*(1,1) noncommutative gauge theory as the foundation of 2T-physics in field theory". *Phys. Rev.* D64 (2001), p. 126001. DOI: 10.1103/PhysRevD.64.126001. arXiv: hep-th/0106013 [hep-th] ;
Itzhak Bars and Yueh-Cheng Kuo. "Supersymmetric Field Theory in 2T-physics". *Phys. Rev.* D76 (2007), p. 105028. DOI: 10.1103/PhysRevD.76.105028. arXiv: hep-th/0703002 [HEP-TH] ;
Itzhak Bars. "Twistor superstring in 2T-physics". *Phys. Rev.* D70 (2004), p. 104022. DOI: 10.1103/PhysRevD.70.104022. arXiv: hep-th/0407239 [hep-th].

[71] R. Jackiw and So-Young Pi. "Fake Conformal Symmetry in Conformal Cosmological Models". *Phys. Rev.* D91.6 (2015), p. 067501. DOI: 10.1103/PhysRevD.91.067501. arXiv: 1407.8545 [gr-qc].

[72] Itzhak Bars. "Traversing Cosmological Singularities, Complete Journeys Through Spacetime Including Antigravity" (2012). arXiv: 1209.1068 [hep-th].

[73] Itzhak Bars, Paul Steinhardt, and Neil Turok. "Sailing through the big crunch-big bang transition". *Phys. Rev.* D89.6 (2014), p. 061302. DOI: 10.1103/PhysRevD.89.061302. arXiv: 1312.0739 [hep-th].

[74] Itzhak Bars. "Constraints on Interacting Scalars in 2T Field Theory and No Scale Models in 1T Field Theory". *Phys. Rev.* D82 (2010), p. 125025. DOI: 10.1103/PhysRevD.82.125025. arXiv: 1008.1540 [hep-th].

[75] Itzhak Bars, Shih-Hung Chen, Paul J. Steinhardt, and Neil Turok. "Antigravity and the Big Crunch/Big Bang Transition". *Phys. Lett.* B715 (2012), pp. 278–281. DOI: 10.1016/j.physletb.2012.07.071. arXiv: 1112.2470 [hep-th].

[76] Robert M. Wald. *General Relativity*. Chicago, USA: Chicago Univ. Pr., 1984. DOI: 10.7208/chicago/9780226870373.001.0001.

[77] D. Cangemi, R. Jackiw, and B. Zwiebach. "Physical states in matter coupled dilaton gravity". *Annals Phys.* 245 (1996), pp. 408–444. DOI: 10.1006/aphy.1996.0015. arXiv: hep-th/9505161 [hep-th].

[78] Edward Witten. "On string theory and black holes". *Phys. Rev.* D44 (1991), pp. 314–324. DOI: 10.1103/PhysRevD.44.314.

[79] Itzhak Bars and Dennis Nemeschansky. "String Propagation in Backgrounds With Curved Space-time". *Nucl. Phys.* B348 (1991), pp. 89–107. DOI: 10.1016/0550-3213(91)90223-K.

[80] Curtis G. Callan Jr., Steven B. Giddings, Jeffrey A. Harvey, and Andrew Strominger. "Evanescent black holes". *Phys. Rev.* D45.4 (1992), R1005. DOI: 10.1103/PhysRevD.45.R1005. arXiv: hep-th/9111056 [hep-th].

[81] A. Codello, G. D'Odorico, C. Pagani, and R. Percacci. "The Renormalization Group and Weyl-invariance". *Class. Quant. Grav.* 30 (2013), p. 115015. DOI: 10.1088/0264-9381/30/11/115015. arXiv: 1210.3284 [hep-th].

[82] Steven Weinberg. *The quantum theory of fields. Vol. 3: Supersymmetry.* Cambridge University Press, 2013, p. 351. ISBN: 9780521670555, 9781139632638, 9780521670555.

[83] Sergio Ferrara, Renata Kallosh, Andrei Linde, Alessio Marrani, and Antoine Van Proeyen. "Superconformal Symmetry, NMSSM, and Inflation". *Phys. Rev.* D83 (2011), p. 025008. DOI: 10.1103/PhysRevD.83.025008. arXiv: 1008.2942 [hep-th];
Renata Kallosh and Andrei Linde. "Superconformal generalization of the chaotic inflation model $\frac{\lambda}{4}\phi^4 - \frac{\xi}{2}\phi^2 R$". *JCAP* 1306 (2013), p. 027. DOI: 10.1088/1475-7516/2013/06/027. arXiv: 1306.3211 [hep-th] ;
Renata Kallosh and Andrei Linde. "Superconformal generalizations of the Starobinsky model". *JCAP* 1306 (2013), p. 028. DOI: 10.1088/1475-7516/2013/06/028. arXiv: 1306.3214 [hep-th].

[84] Itzhak Bars, Paul Steinhardt, and Neil Turok. "Dynamical String Tension in String Theory with Spacetime Weyl Invariance". *Fortsch. Phys.* 62 (2014), pp. 901–920. DOI: 10.1002/prop.201400059. arXiv: 1407.0992 [hep-th].

[85] Steffen Gielen and Neil Turok. "Perfect Quantum Cosmological Bounce". *Phys. Rev. Lett.* 117.2 (2016), p. 021301. DOI: 10.1103/PhysRevLett.117.021301. arXiv: 1510.00699 [hep-th].

[86] M. J. Duff and Jussi Kalkkinen. "Metric and coupling reversal in string theory". *Nucl. Phys.* B760 (2007), pp. 64–88. DOI: 10.1016/j.nuclphysb.2006.10.016. arXiv: hep-th/0605274 [hep-th].

[87] Itzhak Bars. "Relativistic Harmonic Oscillator Revisited". *Phys. Rev.* D79 (2009), p. 045009. DOI: 10.1103/PhysRevD.79.045009. arXiv: 0810.2075 [hep-th].

[88] Bryce S. DeWitt. "Quantum Theory of Gravity. 1. The Canonical Theory". *Phys. Rev.* 160 (1967), pp. 1113–1148. DOI: 10.1103/PhysRev.160.1113.

[89] Itzhak Bars. *online book on Quantum Mechanics*, p. 358.

[90] Mikhail A. Vasiliev. "Consistent equation for interacting gauge fields of all spins in (3+1)-dimensions". *Phys. Lett.* B243 (1990), pp. 378–382. DOI: 10.1016/0370-2693(90)91400-6.

[91] Ignacio J. Araya and Itzhak Bars. "Extended Rindler Spacetime and a New Multiverse Structure". *Phys. Rev.* D97.8 (2018), p. 085009. DOI: 10.1103/PhysRevD.97.085009. arXiv: 1712.01326 [gr-qc].

[92] Sidney Coleman. "Notes from Sidney Coleman's Physics 253a: Quantum Field Theory" (2011). See §14 and §15. arXiv: 1110.5013 [physics.ed-ph].

[93] R. Penrose. "Conformal treatment of infinity". *Gen. Rel. Grav.* 43 (2011). [,565(1964)], pp. 901–922. DOI: 10.1007/s10714-010-1110-5.

[94] S. A. Fulling. "Alternative Vacuum States in Static Space-Times with Horizons". *J. Phys.* A10 (1977), pp. 917–951. DOI: 10.1088/0305-4470/10/6/014;
Stephen A Fulling and Simon Norbertus Maria Ruijsenaars. "Temperature, periodicity and horizons". *Physics reports* 152.3 (1987), pp. 135–176 ;
Stephen A. Fulling. "Nonuniqueness of canonical field quantization in Riemannian space-time". *Phys. Rev.* D7 (1973), pp. 2850–2862. DOI: 10.1103/PhysRevD.7.2850 ;
S. A. Fulling, B. G. Englert, and M. D. Pilloff. "Interacting bosons at finite temperature: How Bogolyubov visited a black hole and came home again". *Found. Phys.* 33 (2003), pp. 87–110. DOI: 10.1023/A:1022819825765. arXiv: gr-qc/0207032 [gr-qc].

[95] Sidney R. Coleman and Erick J. Weinberg. "Radiative Corrections as the Origin of Spontaneous Symmetry Breaking". *Phys. Rev.* D7 (1973), pp. 1888–1910. DOI: 10.1103/PhysRevD.7.1888;
Sidney R. Coleman and Roman Jackiw. "Why dilatation generators do not generate dilatations?" *Annals Phys.* 67 (1971), pp. 552–598. DOI: 10.1016/0003-4916(71)90153-9 ;
Joseph Polchinski. "Scale and Conformal Invariance in Quantum Field Theory". *Nucl. Phys.* B303 (1988), pp. 226–236. DOI: 10.1016/0550-3213(88)90179-4.

[96] Kara Farnsworth, Markus A. Luty, and Valentina Prilepina. "Weyl versus Conformal Invariance in Quantum Field Theory". *JHEP* 10 (2017), p. 170. DOI: 10.1007/JHEP10(2017)170. arXiv: 1702.07079 [hep-th];
Mario Herrero Valea. "Weyl Invariance in the gravitational sector". PhD thesis. Madrid, Autonoma U., 2016. URL: http://inspirehep.net/record/1592477/files/herrero_valea_mario.pdf.

[97] Edward Witten. "Notes on Some Entanglement Properties of Quantum Field Theory" (2018). arXiv: 1803.04993 [hep-th];
Kazumi Okuyama. "$\mathcal{N} = 4$ SYM on $\mathbb{R} \times \mathbb{S}^3$ and PP wave". *JHEP* 11 (2002), p. 043. DOI: 10.1088/1126-6708/2002/11/043. arXiv: hep-th/0207067 [hep-th] ;
Goro Ishiki, Yastoshi Takayama, and Asato Tsuchiya. "$\mathcal{N} = 4$ SYM on $\mathbb{R} \times \mathbb{S}^3$ and theories with 16 supercharges". *JHEP* 10 (2006), p. 007. DOI: 10.1088/1126-6708/2006/10/007. arXiv: hep-th/0605163 [hep-th].

[98] Hideki Omori, Yoshiaki Maeda, Naoya Miyazaki, and Akira Yoshioka. "Singular systems of exponential functions". *Noncommutative Differential Geometry and Its Applications to Physics*. Springer, 2001, pp. 169–186.